frontiers | Research Topics

Estrogen effects on fertility and neurodegeneration – classical versus non-classical actions

Edited by
Zsuzsanna Nagy, Allan Herbison, Andrea Kwakowsky, Gergely Kovacs and Klaudia Barabas

Published in
Frontiers in Endocrinology
Frontiers in Neuroinformatics

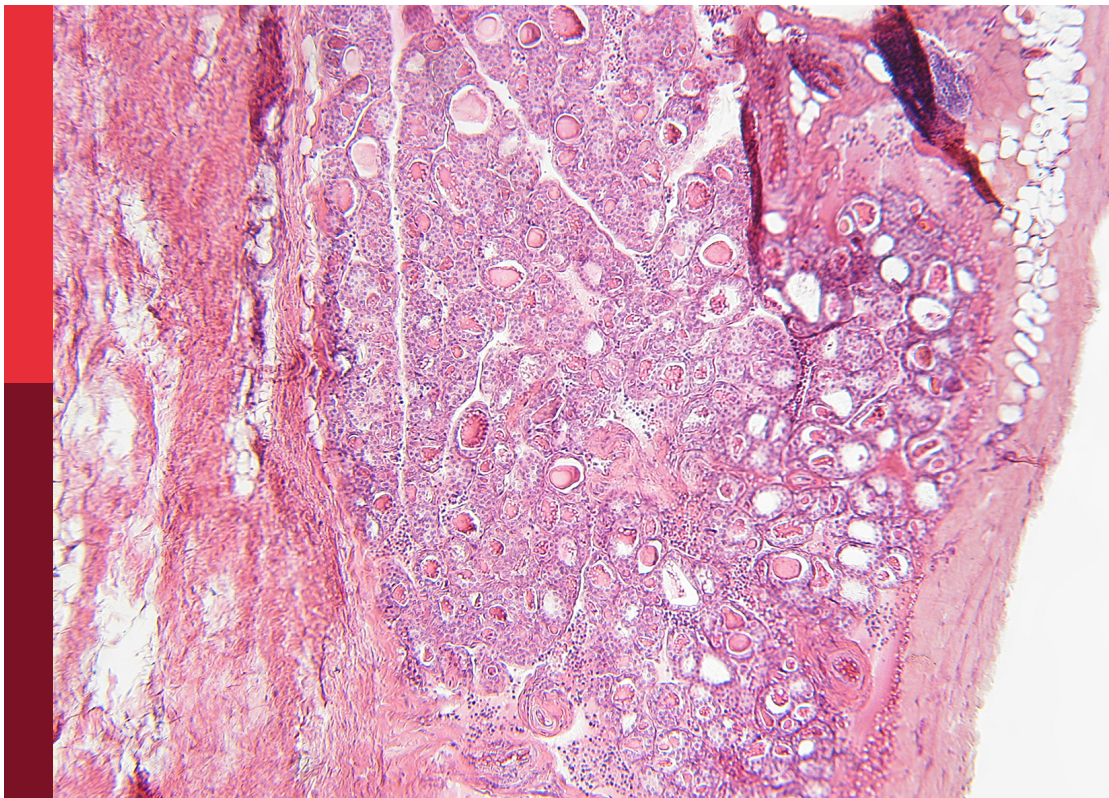

ISSN 1664-8714
ISBN 978-2-8325-3150-1
DOI 10.3389/978-2-8325-3150-1

About Frontiers

Frontiers is more than just an open access publisher of scholarly articles: it is a pioneering approach to the world of academia, radically improving the way scholarly research is managed. The grand vision of Frontiers is a world where all people have an equal opportunity to seek, share and generate knowledge. Frontiers provides immediate and permanent online open access to all its publications, but this alone is not enough to realize our grand goals.

Frontiers journal series

The Frontiers journal series is a multi-tier and interdisciplinary set of open-access, online journals, promising a paradigm shift from the current review, selection and dissemination processes in academic publishing. All Frontiers journals are driven by researchers for researchers; therefore, they constitute a service to the scholarly community. At the same time, the *Frontiers journal series* operates on a revolutionary invention, the tiered publishing system, initially addressing specific communities of scholars, and gradually climbing up to broader public understanding, thus serving the interests of the lay society, too.

Dedication to quality

Each Frontiers article is a landmark of the highest quality, thanks to genuinely collaborative interactions between authors and review editors, who include some of the world's best academicians. Research must be certified by peers before entering a stream of knowledge that may eventually reach the public - and shape society; therefore, Frontiers only applies the most rigorous and unbiased reviews. Frontiers revolutionizes research publishing by freely delivering the most outstanding research, evaluated with no bias from both the academic and social point of view. By applying the most advanced information technologies, Frontiers is catapulting scholarly publishing into a new generation.

What are Frontiers Research Topics?

Frontiers Research Topics are very popular trademarks of the *Frontiers journals series*: they are collections of at least ten articles, all centered on a particular subject. With their unique mix of varied contributions from Original Research to Review Articles, Frontiers Research Topics unify the most influential researchers, the latest key findings and historical advances in a hot research area.

Find out more on how to host your own Frontiers Research Topic or contribute to one as an author by contacting the Frontiers editorial office: frontiersin.org/about/contact

Estrogen effects on fertility and neurodegeneration – classical versus non-classical actions

Topic editors

Zsuzsanna Nagy — University of Pécs, Hungary
Allan Herbison — University of Cambridge, United Kingdom
Andrea Kwakowsky — University of Galway, Ireland
Gergely Kovacs — University of Pécs, Hungary
Klaudia Barabas — University of Pécs, Hungary

Citation

Nagy, Z., Herbison, A., Kwakowsky, A., Kovacs, G., Barabas, K., eds. (2023). *Estrogen effects on fertility and neurodegeneration – classical versus non-classical actions*. Lausanne: Frontiers Media SA.
doi: 10.3389/978-2-8325-3150-1

Table of contents

frontiers | Frontiers in Endocrinology

TYPE Editorial
PUBLISHED 17 April 2023
DOI 10.3389/fendo.2023.1192671

OPEN ACCESS

EDITED AND REVIEWED BY
Richard Ivell,
University of Nottingham, United Kingdom

*CORRESPONDENCE
Zsuzsanna Nagy
zsuzsanna.nagy69@gmail.com

SPECIALTY SECTION
This article was submitted to Reproduction, a section of the journal Frontiers in Endocrinology

RECEIVED 23 March 2023
ACCEPTED 30 March 2023
PUBLISHED 17 April 2023

CITATION
Nagy Z, Herbison A, Kwakowsky A, Kovacs G and Barabas K (2023) Editorial: Estrogen effects on fertility and neurodegeneration – classical versus non-classical actions.
Front. Endocrinol. 14:1192671.
doi: 10.3389/fendo.2023.1192671

Editorial: Estrogen effects on fertility and neurodegeneration – classical versus non-classical actions

Zsuzsanna Nagy[1]*, Allan Herbison[2], Andrea Kwakowsky[3], Gergely Kovacs[1] and Klaudia Barabas[1]

[1]Institute of Physiology, Medical School, University of Pécs, Pécs, Hungary, [2]Department of Physiology, Development and Neuroscience, University of Cambridge, Cambridge, United Kingdom, [3]Pharmacology and Therapeutics, School of Medicine, Galway Neuroscience Centre, University of Galway, Galway, Ireland

KEYWORDS

estrogen, estrogen receptor, GnRH, neurodegeneration, classical and non-classical actions

Editorial on the Research Topic
Estrogen effects on fertility and neurodegeneration – classical versus non-classical actions

The gonadal steroid 17β-estradiol (E2) is the most potent form of estrogen with a broad spectrum of biological actions from fertility to neuroprotection. Studies during the last decades have provided a vast amount of data that have extended our understanding of the physiological importance of E2 in regulating a variety of tissues and organs, but many pieces of this intriguing puzzle remained to be elucidated (1). According to the classic paradigm, the cellular effects of E2 occur slowly: upon ligand binding cytoplasmic estrogen receptors (ERs) are translocated to the nucleus and regulate expression of target genes by binding to DNA sequences within hours or days (2). However, E2 can also exert rapid, non-classical effects in different types of cells including neurons. In response to their ligands, plasma membrane-bound estrogen receptors (ERs) are activated and E2 can change various cellular functions or modulate the transcription of several genes directly or indirectly by rapidly altering the activity of multiple signal transduction cascades (3).

This special issue is a collection of reviews and original research papers focusing on various aspects of the engagement of the hypothalamus-pituitary-gonadal axis in female reproductive functions and neurodegenerative diseases. The main female gonadal hormone E2 is a controversial molecule with the potential to have both beneficial and detrimental impacts on specific tissues. Non-classical actions of E2 in the brain are associated with advantageous effects like neuroprotection and enhanced cognitive functions, hence it is critical to explore further these mechanisms.

The article by Johnson et al. reviews the rapid, membrane-initiated estrogen signaling in female reproduction with a special focus on the interaction between the membrane-bound estrogen receptors (mERs) and the metabotropic glutamate receptors (mGluRs).

The study by Koppan et al. highlights the role of PACAP in the regulation of female reproductive functions including the GnRH-kisspeptin neuronal network, gonadal hormone

production, follicular development, fertilization, embryonic/placental development, and maternal behavior. Results published by Barabás et al shed light on new angles of the GnRH-kisspeptin neural network in the modulatory effect of PACAP on the integrity of estrus cycle.

The article by Göcz et al. compares the estrogen-driven transcriptional responses of the two functionally different kisspeptin neuron populations that mediate the positive and negative feedback effects of estrogen. The RNA sequencing analysis uncovered new neuropeptides and mechanisms involved in the regulation of estrogen feedback.

Another study by Barabás et al based on a survey in Hungary observed the impact of COVID-19 pandemic and vaccination on the menstrual cycle but found no proof that the SARS-CoV-2 infection or vaccination were associated with menstrual cycle changes. The results, however, implicate that the increased levels of depression may cause the reported menstrual cycle abnormalities.

The paper by Rijal et al. investigates another aspect of the regulation of fertility. Their results show that the reactive oxygen species (ROS) acting as a signaling molecule affect fertility by directly modulating the excitability of gonadotropin-releasing hormone (GnRH) neurons.

Three articles in this Research Topic focus on the role of estrogen in neurodegeneration. As estrogen has been shown to have beneficial effects in the treatment of neurodegenerative diseases, two papers aimed to explore the mechanisms underlying the neuroprotective effects of estrogen. Farkas et al. demonstrated that female hormone depletion exacerbated the progression of Alzheimer's disease-associated changes in the brain of a triple transgenic mouse model of Alzheimer's disorder without causing cognitive behavioral symptoms. Kövesdi et al. analyzed the effect of estrogen on the activity of striatal cholinergic neurons that play a pivotal role in neurological disorders such as Parkinson's and Huntington's diseases. However, no evidence was found that estrogen alters the intrinsic properties of the striatal cholinergic neurons. The third article by Koszegi and Cheong is a mini review summarizing data collected on the potential use of estrogen analogues activating the non-classical pathways in the treatment of neurodegenerative diseases.

Finally, Makkai et al. contributes to the field of estradiol research by providing a deeper understanding of non-classical estradiol actions through investigation of receptor dynamics. By comparing two methods of calculating diffusion coefficients, the study suggests that Maximum likelihood-based estimation is a more reliable method for determining receptor movement, especially for cases with large localization errors or slow movements. This finding may have important implications for future research on membrane receptors and their function.

Overall, these articles provide new insights into the diverse effects of E2, illustrating the complexity of its actions and highlighting the many areas still to be explored in the field of neuroendocrine research.

Author contributions

All authors listed have made a substantial, direct, and intellectual contribution to the work and approved it for publication.

Conflict of interest

The authors declare that the research was conducted in the absence of any commercial or financial relationships that could be construed as a potential conflict of interest.

Publisher's note

frontiers | Frontiers in Endocrinology

TYPE Original Research
PUBLISHED 25 August 2022
DOI 10.3389/fendo.2022.960769

OPEN ACCESS

EDITED BY
Zsuzsanna Nagy,
University of Pécs, Hungary

REVIEWED BY
Michael Candlish,
Goethe University Frankfurt, Germany
Richard Piet,
Kent State University, United States
Shannon Brooke Zoe Stephens,
Albany Medical College, United States

*CORRESPONDENCE
Erik Hrabovszky
hrabovszky.erik@koki.hu
Miklós Sárvári
sarvari.miklos@koki.hu
Balázs Göcz
gocz.balazs@koki.hu

SPECIALTY SECTION
This article was submitted to Reproduction, a section of the journal Frontiers in Endocrinology

RECEIVED 03 June 2022
ACCEPTED 28 July 2022
PUBLISHED 25 August 2022

CITATION
Göcz B, Takács S, Skrapits K, Rumpler É, Solymosi N, Póliska S, Colledge WH, Hrabovszky E and Sárvári M (2022) Estrogen differentially regulates transcriptional landscapes of preoptic and arcuate kisspeptin neuron populations.
Front. Endocrinol. 13:960769.
doi: 10.3389/fendo.2022.960769

Estrogen differentially regulates transcriptional landscapes of preoptic and arcuate kisspeptin neuron populations

Balázs Göcz[1,2]*, Szabolcs Takács[1], Katalin Skrapits[1], Éva Rumpler[1], Norbert Solymosi[3], Szilárd Póliska[4], William H. Colledge[5], Erik Hrabovszky[1]* and Miklós Sárvári[1]*

[1]Laboratory of Reproductive Neurobiology, Institute of Experimental Medicine, Budapest, Hungary, [2]János Szentágothai Doctoral School of Neurosciences, Semmelweis University, Budapest, Hungary, [3]Centre for Bioinformatics, University of Veterinary Medicine, Budapest, Hungary, [4]Department of Biochemistry and Molecular Biology, Faculty of Medicine, University of Debrecen, Debrecen, Hungary, [5]Department of Physiology, Development and Neuroscience, University of Cambridge, Cambridge, United Kingdom

Kisspeptin neurons residing in the rostral periventricular area of the third ventricle (KP^{RP3V}) and the arcuate nucleus (KP^{ARC}) mediate positive and negative estrogen feedback, respectively. Here, we aim to compare transcriptional responses of KP^{RP3V} and KP^{ARC} neurons to estrogen. Transgenic mice were ovariectomized and supplemented with either 17β-estradiol (E2) or vehicle. Fluorescently tagged KP^{RP3V} neurons collected by laser-capture microdissection were subjected to RNA-seq. Bioinformatics identified 222 E2-dependent genes. Four genes encoding neuropeptide precursors (*Nmb, Kiss1, Nts, Penk*) were robustly, and *Cartpt* was subsignificantly upregulated, suggesting putative contribution of multiple neuropeptides to estrogen feedback mechanisms. Using overrepresentation analysis, the most affected KEGG pathways were neuroactive ligand-receptor interaction and dopaminergic synapse. Next, we re-analyzed our previously obtained KP^{ARC} neuron RNA-seq data from the same animals using identical bioinformatic criteria. The identified 1583 E2-induced changes included suppression of many neuropeptide precursors, granins, protein processing enzymes, and other genes related to the secretory pathway. In addition to distinct regulatory responses, KP^{RP3V} and KP^{ARC} neurons exhibited sixty-two common changes in genes encoding three hormone receptors (*Ghsr, Pgr, Npr2*), GAD-65 (*Gad2*), calmodulin and its regulator (*Calm1, Pcp4*), among others. Thirty-four oppositely regulated genes (*Kiss1, Vgf, Chrna7, Tmem35a*) were also identified. The strikingly different transcriptional responses in the two neuron populations prompted us to explore the transcriptional mechanism further. We identified ten E2-dependent transcription factors in KP^{RP3V} and seventy in KP^{ARC} neurons. While none of the ten transcription factors interacted with estrogen receptor-α, eight of the seventy did. We propose that an intricate, multi-layered transcriptional mechanism exists in KP^{ARC} neurons

and a less complex one in KP^{RP3V} neurons. These results shed new light on the complexity of estrogen-dependent regulatory mechanisms acting in the two functionally distinct kisspeptin neuron populations and implicate additional neuropeptides and mechanisms in estrogen feedback.

KEYWORDS

fertility, kisspeptin neuron, RNA-seq, neuropeptides, dense-core vesicle, transcription factors, reproduction

Introduction

The kisspeptin neuropeptide family includes hormones of varying amino acid length released from the prohormone product of the *Kiss1* gene. Kisspeptin producing neurons mediate the effect of estrogens to GnRH neurons *via* the KiSS-1 receptor and play indispensable role in the regulation of GnRH/LH pulsatility and estrogen feedback mechanisms. Inactivating mutations of *KISS1R*, which encodes the KiSS-1 receptor (1, 2) or *KISS1* itself (3), cause hypogonadotropic hypogonadism in humans. These reproductive defects can be replicated in knockout mouse models (2, 4, 5).

Most kisspeptin producing neurons reside in two areas of the rodents' hypothalamus. One population, KP^{ARC} neurons, are localized in the arcuate nucleus (ARC). Their majority co-express neurokinin B and dynorphin, and are, therefore, called KNDy neurons. KP^{RP3V} neurons are mainly located in the anteroventral periventricular nucleus (AVPV) and the periventricular nucleus (PeN) of the preoptic area, and co-express galanin (6, 7), met-enkephalin (6) and some markers for dopamine (8, 9), GABA (10) and glutamate (10) phenotypes. The two kisspeptin neuron populations innervate different cellular domains of GnRH neurons (11). KP^{ARC} neurons innervate distal dendrons at the median eminence while KP^{RP3V} neurons contact the soma and proximal dendrites in the preoptic area. Kisspeptin exerts stimulatory effects on GnRH neurons and triggers GnRH secretion into the portal circulation at the median eminence, which in turn, increases the synthesis and secretion of gonadotropins in the anterior pituitary (12). In females, KP^{ARC} and KP^{RP3V} neurons mediate the negative and positive estrogen feedback, respectively, on gonadotropin secretion. Earlier transcriptomic studies provided partial insight into the molecular phenotype of KP^{ARC} and KP^{RP3V} neurons. In these Drop-seq studies, cells of the ARC (13) and the preoptic area (14) have been categorized based on their transcriptional profile. KP^{ARC} neurons have been described as KISS1/TAC2 while KP^{RP3V} neurons as dopaminergic cells, suggesting that the two populations display distinct molecular phenotypes.

Hypothalamic kisspeptin neurons express nuclear hormone receptors including estrogen receptor α (ERα), which enable them to respond to changes in circulating estrogen levels. Estrogens are robust transcriptional regulators of *Kiss1* (15). In KP^{ARC} neurons, E2 inhibits *Kiss1* expression through a non-classical estrogen receptor mechanism, whereas in KP^{RP3V} neurons, E2 activates *Kiss1* transcription *via* the classic mode of action (16). In a recent study, we dissected the genome-wide transcriptional responses of KP^{ARC} neurons to E2 (17) and identified thousands of E2-dependent genes. Here, we used the same animals as in the case of KP^{ARC} neurons with surgical ovariectomy model with or without E2 replacement. From each, we collected three hundred pooled, fluorescently labelled KP^{RP3V} neurons by laser-capture microdissection (LCM). Transcriptomes of KP^{RP3V} neurons were determined by Illumina-based RNA-seq in the same way as in our recent KP^{ARC} neuron study (17) and then, bioinformatic analysis was performed using stringent criteria to generate the list of E2-regulated genes without low expressing and statistically non-significant genes. The detailed E2-dependent transcriptome of KP^{ARC} neurons has been published recently from our laboratory. Sequencing files, placed in a public repository (BioProject with the accession number of PRJNA686688), were re-analyzed with the same criteria to compare the KP^{RP3V} and KP^{ARC} neuron transcriptomes. The comparative analysis focused on neuropeptides, granins and genes of the secretory pathway, because of the presence of a large number of changes in these categories. Finally, the markedly different E2-driven responses of the two cell types were attributed to different transcriptional mechanisms revealed in KP^{RP3V} and KP^{ARC} neurons.

Materials and methods

Animals

Animal experiments were carried out in accordance with the Institutional Ethical Codex, Hungarian Act of Animal Care and Experimentation (1998, XXVIII, section 243/1998) and the

European Union guidelines (directive 2010/63/EU). All efforts were made to minimize potential pain or suffering, and to reduce the number of animals used. Procedures were approved by the Institutional Animal Care and Use Committee. Young adult (day 60-80) female mice (n=6) were housed under standard conditions (lights on between 06:00 and 18:00 h, temperature 22 ± 1°C, chow and water *ad libitum*) in the animal facility of the Institute of Experimental Medicine. The E2-dependent transcripts of KP^{RP3V} neurons were identified in KP-Cre/ZsGreen mice generated by crossing Kiss1-Cre (18) males with females of the Ai6(RCL-ZsGreen) indicator strain (The Jackson Laboratory, JAX No. 007906) as described previously (17). The paper which reported generation of the Kiss1-Cre transgenic mouse provided evidence that 80-90% of fluorescently labelled cells expressed kisspeptin in the ARC (18).

Surgical ovariectomy and subsequent E2 replacement

We have recently published a detailed protocol for the dissection of KP^{ARC} neurons (17). The same protocol was used here to dissect KP^{RP3V} neurons from the preoptic area. In brief, all mice were first anesthetized and ovariectomized (OVX) bilaterally. On post-ovariectomy day 9, the animals were implanted subcutaneously with a single silastic capsule (Sanitech, Havant, UK; l=10 mm; id=1.57 mm; od=3.18 mm) containing either 100 µg/ml E2 (Sigma Chemical Co., St Louis, MO) in sunflower oil (OVX+E2 group, n=3) or oil vehicle (OVX+Veh group, n=3) (19). Four days later, mice were sacrificed between 09:00-11:00 am. We have recently established that this E2 regimen resulted in 7.59 pg/mL serum E2 levels (high diestrus/proestrus range) and 7.58-fold uterine hypertrophy (17).

LCM-assisted dissection of KP^{RP3V} neurons

We followed our recently published protocol for LCM-assisted dissection of fluorescent neurons. In brief, treated KP-Cre/ZsGreen mice (n=6) were perfused transcardially with 0.5% formaldehyde, followed by 20% sucrose. Brains were snap-frozen and tissue blocks containing the preoptic area were dissected. Then, coronal sections were cut from the preoptic area, collected onto PEN slides (Membrane Slide 1.0 PEN, Carl Zeiss, Göttingen, Germany) and air-dried in the cryostat chamber. Formaldehyde-fixed sections, containing fluorescent KP^{RP3V} neurons were treated sequentially with 50% EtOH, n-butanol:EtOH and xylene substitution:n-butanol. Three hundred KP-Cre/ZsGreen neurons were microdissected from 12-µm-thick preoptic sections of each mouse. Microdissected cells were pressure-catapulted into 0.5 ml tube caps (Adhesive Cap 200, Carl Zeiss), pooled and were stored at -80 °C until RNA extraction.

RNA sequencing

Total RNA samples from KP^{RP3V} neurons were prepared with the Arcturus Paradise Plus RNA Extraction and Isolation Kit (Applied Biosystems, Waltham, MA, USA), and converted into RNA-seq libraries with the TrueSeq Stranded Total RNA Library Preparation Gold kit (Illumina, San Diego, CA, USA). Although the TrueSeq Stranded kit was optimized for 100 ng input RNA, a recent study found that it generates reliable libraries from as little as ng amounts of RNA (20). Total RNA extracted from 300 KP^{ARC} neurons provided sufficient amount of cDNA input for sequencing (17). For DNA fragment enrichment, our protocol used 16, instead of 15 cycles recommended by the manufacturer. Sequencing was performed on Illumina NextSeq500 instrument using the NextSeq500/550 High Output v2.5 kit (75 cycles). Sequencing files were deposited to BioProject with accession number of PRJNA847063.

Bioinformatics

Following FastQC quality control, sequencing reads with low quality bases were removed using Trimmomatic 0.39 (settings: LEADING:3, TRAILING:3, SLIDINGWINDOW:4:30, MINLEN:50). Sequencing reads were mapped to the mm100 mouse reference genome using STAR (v 2.7.3a) (21), which resulted in an average overall alignment rate of 74.9 ± 3.5%. Read summarization and gene level quantification were performed by featureCounts (subread v 2.0.0) (22). Raw read counts were normalized and processed further with the packages of edgeR (23) and DESeq2 (24). EdgeR and DESeq2 calculated count per million (cpm) values and identified differentially expressed genes, respectively. Changes in mRNA expression were quantified by log2 fold change (log_2FC). P values were corrected by the method of Benjamini (25) to take multiple testing into account. In differential expression analysis with DESeq2 we applied the basemean>20, p.adj<0.05 cutoffs to generate the list of E2-regulated genes without low-expressing and statistically non-significant genes. Genes were assigned to KEGG (26) signaling pathways by the R package KEGGREST (Dan Tenenbaum (2019): KEGGREST: Client-side REST access to KEGG., R package version 1.26.1). Overrepresentation analysis (ORA) (27) was performed by the clusterProfiler (28) R packages. All program packages for differential expression analysis and pathway analysis were run in the R environment (R2020). E2-dependent transcription factors were identified using functional classification with the Animal Transcription Factor DataBase (29). Putative transcription factors were

double-checked using UniProt (https://www.uniprot.org) website. Listed transcription factors fulfilled the criteria to have 'transcription factor activity' GO molecular function, and experimental evidence at protein level.

Results

RNA-seq of KP^{RP3V} neurons reveals 222 E2-dependent genes

To examine estrogenic regulation of KP^{RP3V} neurons, we dissected and pooled fluorescent KP^{RP3V} neurons by LCM from OVX mice substituted with either oil or E2. Illumina-based RNA-seq was performed to determine the transcriptional landscape of KP^{RP3V} neurons at high physiological (7.59 pg/mL) and gonadectomy E2 levels which latter is below 0.3 pg/mL (30). Initial DESeq2 analysis identified 203 E2-regulated genes in KP^{RP3V} neurons with the p.adj<0.05 cutoff. P.adj values are highly sensitive to the number of comparisons which can severely compromise the detection power for true positives (31, 32). Noisy, low-expression genes were shown to have adverse impact on the power of statistics in RNA-seq studies (32). Given that these genes likely have relatively minor effect on kisspeptin neuron biology, we improved the power of DeSeq2 analysis by filtering out low-expression genes. Using the basemean>20 and p.adj<0.05 cutoffs, we identified 10,623 transcripts, 247 of which were E2-dependent (Supplementary Table/ Table 1) including 222 protein coding genes. The 222 genes contained 45 new changes that were not included in the list unfiltered to low basemean. The heat map of E2-regulated transcripts showed disparate expression in the two experimental groups (Figure 1A). Among the 222 protein coding genes, 142 were up- and 80 were downregulated. The most robust upregulation was seen in the case of *Nmb* encoding neuromedin B (Figure 1B). Highly upregulated genes ($log_2FC>1$) comprised additional neuropeptides (*Kiss1, Nts, Penk*) and a granin (*Vgf*), among others. *Cartpt* encoding neuropeptide CART was also highly upregulated, but the change did not reach statistical significance. ORA identified enrichment in changes of the dopaminergic synapse and neuroactive ligand-receptor interaction KEGG pathways (Figure 1C). Using gene ontology (GO) terms, ORA revealed significant enrichment of changes in the regulation of membrane potential (GO:0042391), synapse organization (GO:0050808), peptide transport (GO:0015833), hormone secretion (GO:0046879) GO categories, among others (Supplementary Table/ Table 2).

Comparative analysis unveils disparate E2-driven transcriptional responses

For consistency, we re-analyzed our recently deposited RNA-seq data of KP^{ARC} neurons (17) with the same filtering which resulted in 1583 medium-to-high abundance E2-regulated genes. While 470 low-expressed genes were excluded by this filtering, the enhanced statistical power resulted in the identification of 48 newly identified genes in KP^{ARC} neurons. Compared to KP^{RP3V} neurons, the KP^{ARC} neurons showed much higher number and more robust transcriptional responses to E2. To display differences in estrogenic regulation of the two populations, we generated heat maps with the top 25 activated and top 25 suppressed genes in KP^{RP3V} neurons and illustrated in parallel expression of the same genes from KP^{ARC} neurons (Figure 2A). The top 25 activated and top 25 suppressed genes of KP^{ARC} neurons and their behavior in KP^{RP3V} neurons are shown similarly in Figure 2B. Markedly different responses of the two kisspeptin neuron populations to E2 prompted us to check the expression of major estrogen receptors. We detected abundant mRNA expression of *Esr1* encoding ERα in both KP^{RP3V} and KP^{ARC} neurons. However, we did not detect transcription of *Esr2* and *Gper1* encoding ERβ and G-protein coupled estrogen receptor, respectively.

Despite disparate regulation there are ninety-six overlapping E2 target genes

Although the E2-driven transcriptional responses were different, we found ninety-six overlapping genes with sixty-two analogous and thirty-four opposite changes in preoptic and arcuate kisspeptin neurons. The sixty-two genes, which were regulated in the same direction consisted of transcription factors, synapse associated genes and calcium signaling molecules, among others (Figure 3A). There were 25 genes that displayed $|log_2FC| >1.0$ changes in both populations representing the highly responsive, common E2-dependent genes in kisspeptin neurons. Among highly expressed genes, E2 upregulated *App, Itm2c* (inhibits APP processing), *Calm1, Eef1a1*. E2 also increased expression of some synapse-associated genes including *Cadm1, Enah, Gad2, Syt6*, and decreased *Grin2b*. In addition, E2 enhanced mRNA expression of major calcium signaling molecules (*Pcp4, Calm1*) and pacemaker channel *Hcn1* in both cell populations. Thirty-four genes including *Kiss1* were oppositely regulated (Figure 3B), and several of them, regulated in a similar fashion as *Kiss1* (*Atp1a1, Chga, Vgf, Ptprn, Ralgps2*), were associated with neuropeptide secretion. Other oppositely regulated genes encoded proteins related to translational control (*Msi2*), calcium signaling (*Cpne2, Ryr3*), protein quality control (*Clu*), synaptic plasticity (*Cct4, Chl1*), cholinergic transmission (*Chrna7, Tmem35a*), among other functions.

E2 activates neuropeptide precursor and granin genes in KP^{RP3V} neurons

In KP^{RP3V} neurons, we identified seven E2-regulated neuropeptide and granin genes. Transcriptional activation of

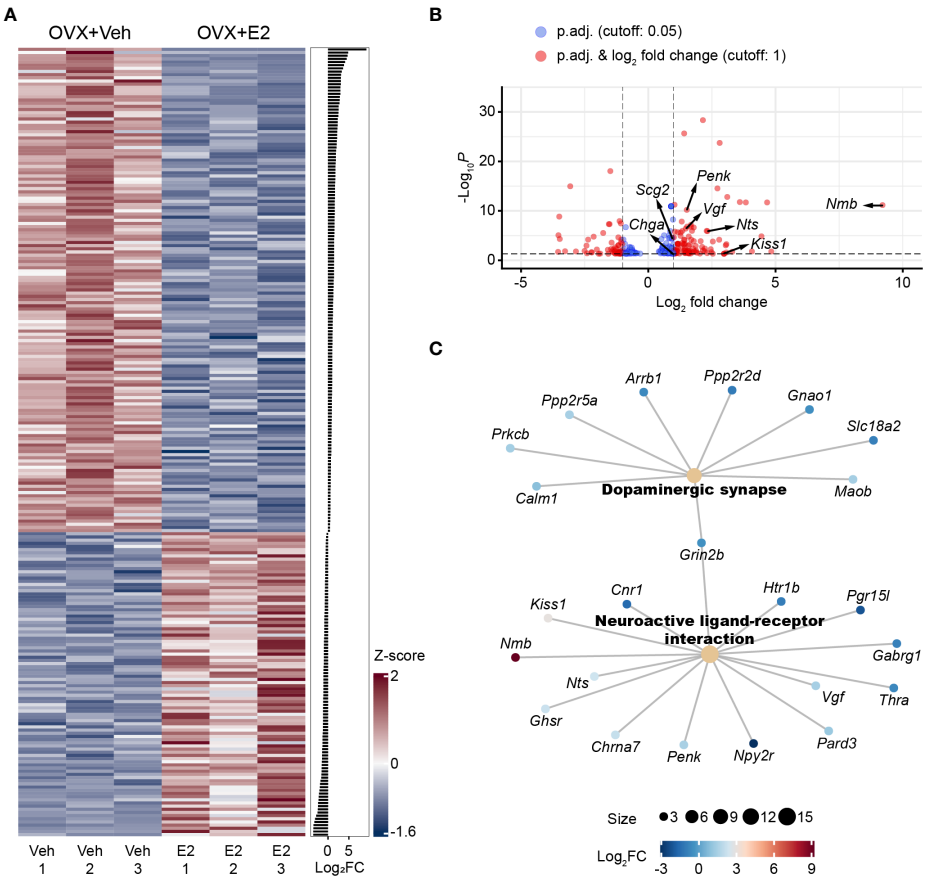

FIGURE 1
Estrogenic regulation of the KP^{RP3V} neuron transcriptome. Heat map of all E2-dependent transcripts. Transcripts were arranged by size of fold change (FC). We used z-score values to illustrate the size of transcriptional changes, and the values are color coded. z-score is calculated from the CPM value, the mean CPM and the standard deviation of CPM values in a given experimental group **(A)**. Volcano plot reveals 132 regulatory changes that exceed |log$_2$FC| 1.0. Transcriptional changes of neuropeptides (*Nmb, Kiss1, Nts, Penk*) and granins (*Chga, Scg2, Vgf*) were marked **(B)**. Overrepresentation analysis (ORA) of E2-dependent genes identified significant changes in the dopaminergic synapse and the neuroactive ligand-receptor interactions KEGG pathways. The number of genes in a given pathway is reflected in the size of the dot for the pathway. E2-induced changes of individual genes are color coded based on log$_2$FC values **(C)**.

Nmb, Kiss1, Nts and *Penk* was significant (Figure 4A), and these neuropeptide genes were ranked first, eleventh, seventeenth and fiftieth in the list of E2-regulated genes. E2-induced increase of *Pnoc, Prok2* and *Cartpt* did not reach statistical significance. KP^{RP3V} neurons highly expressed *Cartpt, Kiss1, Nmb, Nts* and *Penk*, while *Gal* was expressed moderately in OVX mice with E2 replacement. Neuropeptide precursor proteins are transported from the endoplasmic reticulum to the trans-Golgi network, where they are sorted and packed into DCVs. We showed upregulation of three granin genes, namely *Chga, Scg2, Vgf* and another gene of the secretory pathway, *Ptprn* (Figure 4A). Maturation of neuropeptides requires peptide bond cleavages in precursor molecules. E2 stimulated transcription of *Cpe, Pam* and *Pcsk2* prohormone processing enzymes, but the changes did not reach statistical significance (p.adj<0.05). Genes related to DCV translocation, transport and fusion were not regulated.

E2 inhibits neuropeptide precursors, granins, processing enzymes and multiple secretory pathway genes in KP^{ARC} neurons

In KP^{ARC} neurons, we found transcriptional inhibition of five co-expressed neuropeptide precursor genes including *Kiss1, Nms, Nxph3, Pdyn* and *Tac2* (Figure 4B). We showed downregulation of five members of the granin family including *Scg3, Chga, Chgb, Vgf, Pcsk1n/ProSAAS* and another gene, *Ptprn* (Figure 4B). Neuropeptide maturation takes place in DCVs. E2 decreased mRNA expression of six processing enzymes including *Cpe, Ctsb, Pam, Pcsk1, Pcsk2* and *Pcsk5*, whereas the protease, *Pcsk6*, showed increased expression (Figure 4B). DCV formation and cargo selection depend on ADP-ribosylation factor 1 (*Arf1*) and components of the coat machinery. In

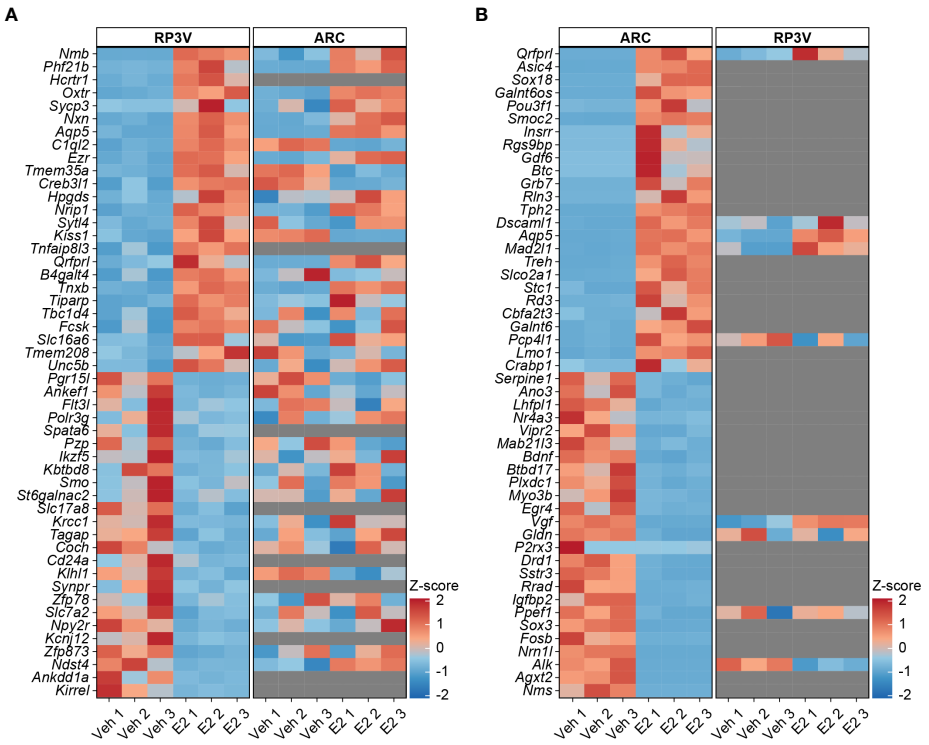

FIGURE 2
E2 differentially regulates the transcriptomes of preoptic and arcuate KP neurons. Heat map of the top 25 activated and top 25 inhibited genes in KP^{RP3V} neurons and behavior of the same genes in KP^{ARC} neurons **(A)**. Heat map of the top 25 activated and top 25 inhibited genes in KP^{ARC} neurons and their behavior in KP^{RP3V} neurons **(B)**.

KP^{ARC} neurons, E2 decreased transcription of *Arf1*, *Cltc, Ap2m1* and *Ap1s1*. From the trans-Golgi network, DCVs move towards the plasma membrane to release their content. Translocation relies upon dynamins, syntaxins, scaffolding and myosin motor proteins. In KP^{ARC} neurons, E2 downregulated mRNA expression of a large number of genes encoding dynamins (*Dnm1, Dnm3*), synaptotagmins (*Syt4, Syt5*) myosin (*Myo1b, Myo1c, Myo3b, Myo5a*) and scaffolding (*Tanc2*) proteins (Figure 4B). The SNARE complex and accessory factors are required for specific targeting and fusion of DCVs with the plasma membrane. E2 suppressed transcription of genes encoding components of the SNARE complex (*Vamp2*, *Stx1a, Stx1b*, *Snap25*) and accessory factors (*Rab15, Rab27, Rab39, Unc13a, Unc13b*). The DCV fusion machinery is linked to the Munc18-1/CASK/Mint1/Lin7b organizer complex, which binds to synaptic adhesion molecules neurexins. E2 downregulated constituents of the organizer complex [*Stxbp1* (coding Munc18-1), *Cask, Apba1* (coding Mint1), *Lin7b*] and neurexins (*Nrxn1, Nrxn2*) (Figure 4B). Cav2.1 and Cav2.2 channels orchestrate synchronous release of neuropeptides and neurotransmitters in most synapses. E2 downregulated *Cacna1a* (Cav2.1) and auxiliary Cav subunit *Cacnb1*, among others. Rab3-interacting proteins (RIMs), chief organizers of the active zone, are linked to Cav2.1 *via* RIM-binding protein encoded by *Erc1*, which was also suppressed by E2.

Transcription factors show markedly different estrogenic regulation

Strikingly different transcriptional responses to E2 in KP^{RP3V} and KP^{ARC} neurons prompted us to determine the number of E2-dependent transcription factors. In KP^{RP3V} neurons, E2 regulated ten transcription factors. Based on the result of a recent publication (33), none of them interacted with ERα. In accord, STRING predicted no protein-protein interaction among them (Figure 5A). Neither transcriptional regulators, nor lncRNAs displayed E2-dependent expression in KP^{RP3V} neurons.

In KP^{ARC} neurons, E2 regulated mRNA expression of seventy transcription factors. E2-dependent transcription factors included nuclear hormone receptors (*Pgr, Rora, Thrb, Nr1d2, Nr2c2, Nr4a2, Nr5a2, Ar, Esr1, Nr4a1, Nr4a3*), homeobox proteins (*Adnp, Cux1, Pbx1, Pknox2, Zfhx2*), subunits of the AP-1 complex (*Fos, Junb, Jdp2*) and zinc finger proteins (*Hivep1, Zfp317*), among others. Of note, eight

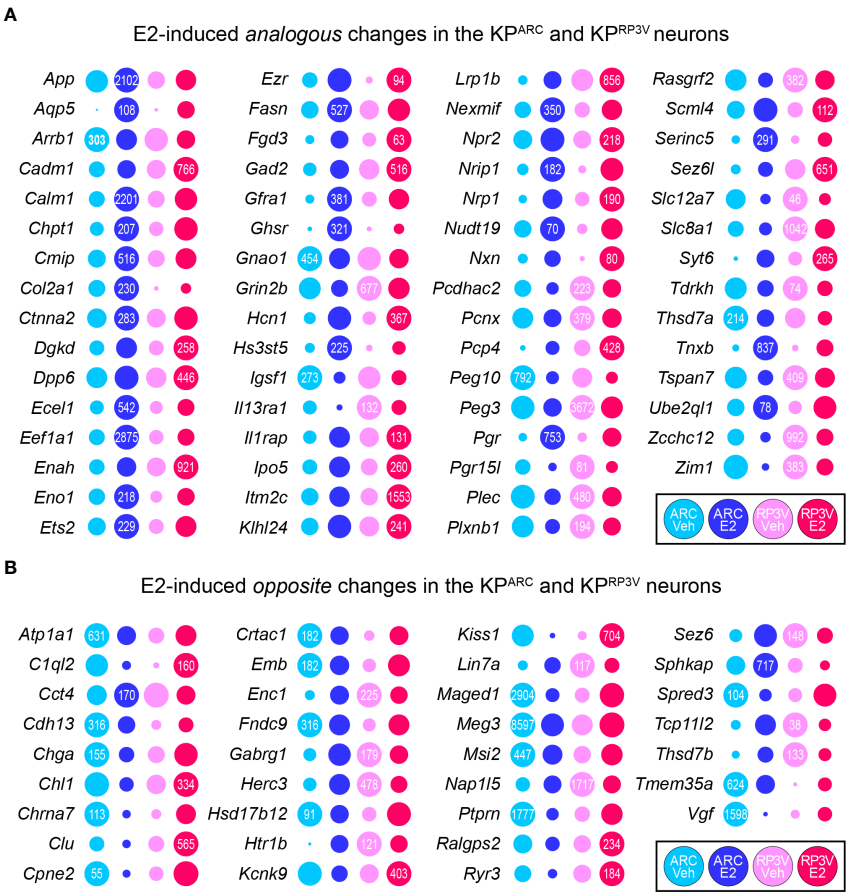

FIGURE 3
Overlapping E2 target genes in KP^{RP3V} and KP^{ARC} neurons. E2 regulated 62 genes in the same (**A**, analogous changes), and 34 genes in opposite direction (**B**, opposite changes). Numbers in the dots reflect transcript abundance in CPM units.

transcription factors including *Cebpb, Cic, Cux1, Fosl2, Gtf2i, Hivep1, Hivep2, Junb* were able to interact with ERα according to recently published data (33). To build a protein interaction map of E2-dependent transcription factors including putative interactions with ERα, we used the STRING database (34). Using strict settings (interaction source: experiment and databases, minimum required interaction score: medium confidence), STRING predicted thirty-four protein-protein interactions between thirty-one transcription factors (Figure 5B). According to STRING, five transcription factors can interact with ERα. The STRING protein interaction map predicted hubs in the network including ERα, Fos, Junb and Nfatc2.

In addition, E2 also modulated mRNA expression of genes encoding transcriptional regulators, chromatin modifiers and regulatory lncRNAs in KP^{ARC} neurons. E2 upregulated components of the SWI/SNF (*Smarca2, Smarca4, Smarcd3, Bicral*) and ATRX : DAXX (*Atrx, Daxx*) chromatin remodelling complexes, histone methyltransferases (*Kmt2e, Wdr82*) and deacetylases (*Hdac11*). E2 downregulated some transcriptional repressors (*Gatad2a, Trps1, Zfp219*), DNA methyltransferases (*Dnmt3a*) and histone deacetylases (*Hdac3, Hdac9*). Among them, one transcriptional coregulator (*Ncoa6*) and several repressors/activators (*Atrx, Gatad2a, Nrip1, Smarca2, Smarca4, Trim24, Trps1*) may interact with ERα. E2 also modified expression of numerous regulatory lncRNAs in KP^{ARC} neurons as described previously (17).

Discussion

E2 evokes different transcriptional responses in preoptic and arcuate kisspeptin neurons

To our knowledge, this is the first comprehensive study to examine and compare E2-driven transcriptional responses in KP^{ARC} and KP^{RP3V} neurons in the same animals. Here, we

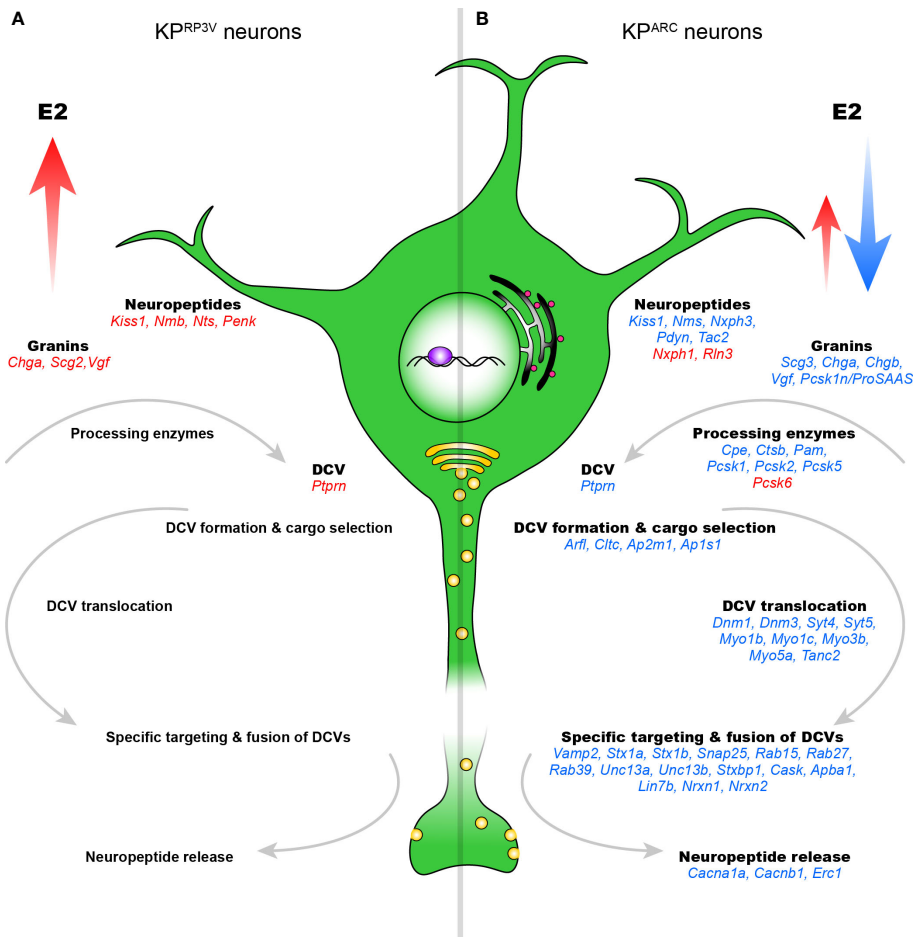

FIGURE 4
E2-dependent elements of the regulated secretory pathway in KP^{RP3V} and KP^{ARC} neurons. E2-regulated genes involved in neuropeptide secretion are shown in KP^{RP3V} **(A)** and KP^{ARC} neurons **(B)**. Genes in red and blue are up- and downregulated, respectively. DCV, dense-core vesicle.

improved the power of DeSeq2 analysis by filtering out low-expression genes using a cutoff of basemean>20. This has resulted in a list of 222 and 1583 E2-regulated genes expressed at medium or high level in KP^{RP3V} and KP^{ARC} neurons, respectively. The highly different numbers of E2-dependent genes in the two kisspeptin neuron populations suggest that KP^{ARC} neurons are much more responsive to E2 treatment than KP^{RP3V} neurons in our model.

The goal of this study was to identify E2-regulated genes in KP^{RP3V} and KP^{ARC} neurons. In our recent study on the E2-dependent genes of KP^{ARC} neurons (17), we have justified the choice of non-physiological animal models (surgical OVX, followed by E2 substitution) to achieve this goal. Treatment of OVX mice with E2 or vehicle generates two well-defined experimental groups with little biological variations and large differences in the E2-dependent transcriptome profiles. In addition, using a single transcriptome snapshot the different regulatory dynamics of E2 dependent transcripts would also cause interpretation problems, complicated further by the cyclic presence of progesterone effects we could eliminate using our non-physiological models. Transcriptional responses in KP^{ARC} and KP^{RP3V} neurons to E2 in our model allowed us to identify E2-dependent genes and to compare their changes in the two kisspeptin neuronal populations. Of course, the gene expression profile of OVX+E2 mice exposed to high levels of E2 for 4 days is unlikely to mirror physiological conditions produced by peak E2 levels. We note that OVX rodents treated with constant E2 display a late afternoon LH surge which repeats daily at the same time (35). While high levels of E2 cause negative feedback on serum LH levels in our OVX+E2 animal model killed in the morning, transcriptomic changes which take place in response to E2 in KP^{RP3V} neurons (e.g. induction of *Kiss1*) may already be relevant to E2 positive feedback on LH secretion which is expected to occur in the late afternoon and requires a circadian signal as well. Future comparison of E2-treated animals in the morning with the late afternoon surging model

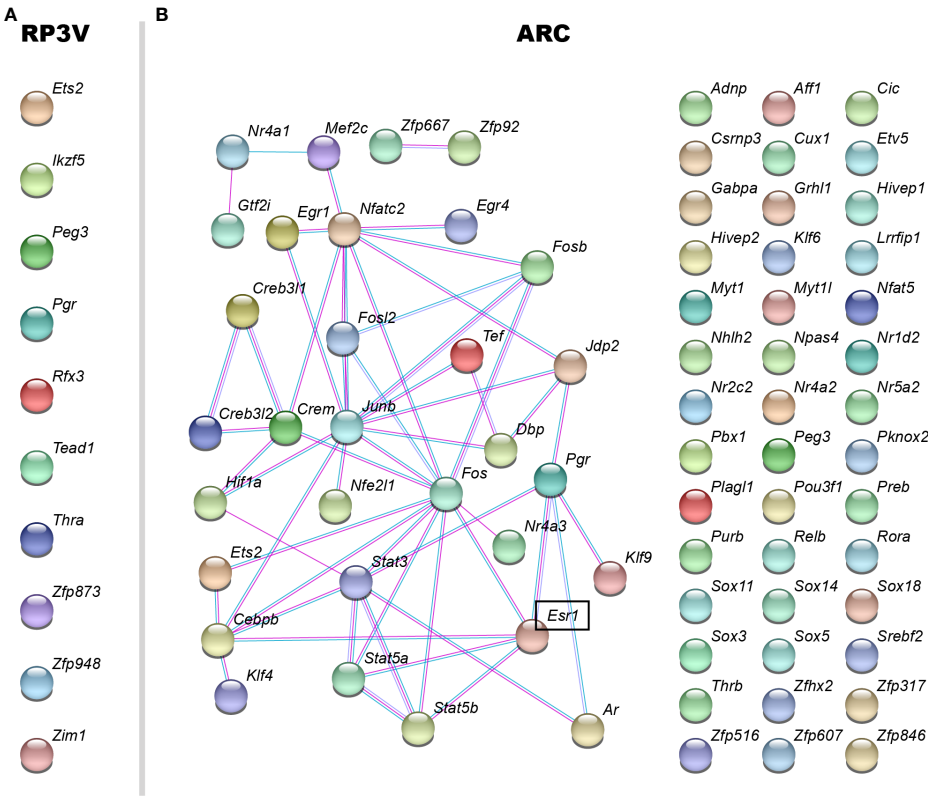

FIGURE 5
Protein interaction map of E2-dependent transcription factors in KP^{RP3V} and KP^{ARC} neurons. Based on the STRING database, protein interaction map of E2-regulated transcription factors was built using stringent settings (interaction source: experiment and databases, minimum required interaction score: medium confidence). STRING identified no potential interactions in KP^{RP3V} neurons **(A)**. In contrast, STRING found potential interactions between 31 E2-dependent transcription factors in KP^{ARC} neurons **(B)**. Genes in bold are regulated in both cell types. *Esr1*, which encodes ERα is in bold and framed.

will be particularly interesting in order to separate the activity-dependent regulatory changes from the E2-dependent ones in the transcriptome of KP^{RP3V} neurons.

We identified ninety-six overlapping E2-dependent genes including sixty-two genes with the same and thirty-four with opposite regulation. The sixty-two genes represent the common E2-dependent genes in hypothalamic kisspeptin neurons. Common upregulated genes encode three hormone receptors (*Ghsr, Pgr, Npr2*) indicating that ghrelin (and growth hormone), progesterone and natriuretic peptide may exert regulatory effects on estrogen feedback *via* acting on both kisspeptin cell populations. This notion is in accord with previously published data about the regulatory role of these hormones on kisspeptin neurons (36–38). Other common E2-dependent genes include *Gad2*, transcriptional activation of which may results in increased GABA synthesis in kisspeptin neurons. Of note, GABA exerts excitatory actions on GnRH neurons (39). The presence and estrogen-dependent regulation of *Gad2* in KP^{ARC} neurons is particularly interesting. Although the glutamatergic (Vglut2) phenotype of these neurons has been well-established (10, 40, 41), earlier *in situ* hybridization studies have already raised the possibility that a subpopulation may exhibit a mixed GABAergic/glutamatergic phenotype (10). RNAscope experiments recently revealed co-expression of vGAT and VGluT2 genes in the same cells (42), although functional studies indicate that KP^{ARC} neurons release glutamate but not GABA (43, 44). Opposite regulation by E2 characterizes a set of genes in KP^{RP3V} and KP^{ARC} neurons. This set contains *Kiss1*, *Vgf*, *Chrna7* and *Tmem35a*. So far, the role of Vgf and cholinergic transmission has not been described in estrogen feedback.

Estrogens increase transcription of a set of neuropeptides in KP^{RP3V} neurons

Peptidergic transmission plays central role in the function of KP^{RP3V} neurons. We found upregulation of four co-expressed neuropeptides including *Kiss1, Nmb, Nts* and *Penk* (p.adj<0.05). Further, highly increased expression of three additional

neuropeptides, namely *Pnoc, Prok2* and *Cartpt*, did not reach statistical significance (p.adj>0.05) in our study.

Of note, transcriptional activation of a set of neuropeptides occurs in response to E2 in KP^{RP3V} neurons. Among E2-dependent genes, *Nmb* showed the most robust response to E2 in our study. Neuromedin B stimulates GnRH release from hypothalamic extracts, and increases plasma LH level after intracerebroventricular administration (45). It has already been implicated in estrogen feedback as GnRH neurons express receptors for neuromedin B (46). Robust upregulation of *Nmb* supports the notion that neuromedin B may be an important regulator of positive estrogen feedback acting in concert with kisspeptins and other upregulated neuropeptides. We indicate that E2 also increases *Nts* expression in KP^{RP3V} neurons. According to a previous study, E2 induces *Nts* expression in the AVPV, and blockade of neurotensin signaling reduces the LH surge (47). Although GnRH neurons express *Ntsr2*, central administration of neurotensin does not induce LH surge. No co-expression of *Kiss1* and *Nts* has been detected by double-label ISH (47). We also detected expression of neurotensin receptors (*Ntsr1, Ntsr2*) in KP^{RP3V} neurons suggesting that neurotensin signaling plays a role in the communication between KP^{RP3V} neurons, in addition to signaling towards GnRH neurons. We also found that E2 enhanced *Penk* expression. In accord with this finding, a previous paper proves co-expression of kisspeptin and met-enkephalin in the AVPV (6). It is tempting to speculate that increased transcription of a set of neuropeptide genes including *Kiss1, Nmb, Nts* and *Penk* in KP^{RP3V} neurons might act in synergy to trigger the LH surge during positive feedback.

Following their synthesis, neuropeptide precursors undergo processing and transport prior to secretion. Granins, major constituents of DCV intravesicular matrix, bind Ca^{2+} and aggregate at acidic pH (48), which is considered to be the driving force of DCV biogenesis. We provide evidence that estrogens activate transcription of *Chga, Scg2*, and *Vgf*. Insulinoma-asssociated (Ia-2) protein is involved in the transcriptional control of DCV biogenesis (49). E2 activates *Ptprn* encoding Ia-2 protein, which may result in elevated DCV biogenesis.

A recent, elegant paper published the active translatome and its estrogenic regulation in AVPV kisspeptin neurons (50). The authors used the p<0.05 criterion and claimed 683 differentially expressed transcripts. Comparison of our results to the presented set of differentially expressed transcripts resulted in 52 overlapping genes in the two studies. Common E2-regulated genes included 13 genes with statistical significance (p.adj<0.05) in both studies (*Scg2, App, Maged1, Nap1l5, Itm2c, Calm1, Ptprn, Ckb, Zcchc12, Vgf, Gad2, Kiss1, Penk*) and 39 additional genes with statistical significance in our study and with marked difference without reported statistical significance in the study by Stephens and Kauffman (*C1ql2, Nmb, Sytl4, Crtac1, Tmem35a, Syt6, Fhod3, Aqp5, Maob, Brinp2, Pgr, Map3k15, Ghsr, Nxn, Nell2, Mgat1, Hcn1, Cadm1, Phyhipl, Fgd3, Pcp4, Rap1gap, Ipo5, Nts, Enah, Ptpn5, Usp48, Nrip1, Npr2, Tmcc3, Hs3st5, Hpcal1, Ngb, Flrt3, Thsd7b, Pgr15l, Peg10, Npy2r, Slc17a8)*. The four upregulated neuropeptides (*Kiss1, Nmb, Nts* and *Penk*) in our study mentioned previously were among the overlapping genes. Although our study and the paper by Stephens and Kauffman (50) used dissimilar methodologies (Kiss1-Cre/ZsGreen vs. *Kiss1*Cre/Ribotag mice, 4-day E2 treatment vs. two sequential E2 treatments with different hormone regimen) and targeted distinct RNA populations (total RNA vs. ribosome bound mRNA) for sequencing, more than fifty genes with almost identical estrogenic regulation were observed in preoptic kisspeptin neurons in the two studies.

Estrogens inhibit transcription of neuropeptide precursor, granin, processing enzyme and DCV related genes in KP^{ARC} neurons

We find that both kisspeptin neuron populations possess unique neuropeptide profiles that are highly regulated by E2. In KP^{ARC} neurons, besides *Kiss1* we show four more co-expressed neuropeptide genes including *Nms, Nxph3, Pdyn, Tac2* that are all suppressed. We demonstrate that estrogens suppress not only genes encoding neuropeptide precursors, but granins, processing enzymes and multiple elements of the regulated secretory pathway. Along with granins and their processing enzymes, neuropeptide precursors are transported from the endoplasmic reticulum to the trans-Golgi network, where they are sorted and packed into DCVs. E2 inhibits several highly expressed granin genes including *Chga, Chgb, Pcsk1n, Scg3, Vgf* and Ia-2 protein coding gene *Ptprn* that may lead to decreased DCV biogenesis. E2 inhibits six protease genes including *Cpe, Ctsb, Pam, Pcsk1, Pcsk2, Pcsk5* that can be involved in the maturation of co-expressed neuropeptides in KP^{ARC} neurons. DCVs move towards the plasma membrane to release their content. This translocation relies upon dynamins, syntaxins, scaffolding and myosin motor proteins. E2 inhibits transcription of several genes encoding dynamins, synaptotagmins, myosins and scaffolding proteins. Specific targeting and fusion of DCVs with the plasma membrane requires concerted action of SNARE proteins and accessory factors. We show that E2 inhibits transcription of genes encoding multiple components of the SNARE complex and accessory proteins. The fusion machinery is linked to the organizer complex, which binds to synaptic adhesion molecules neurexins. E2 suppresses constituents of the Munc18-1/CASK/Mint1/Lin7b organizer complex and neurexins. Cav2.1 and Cav2.2 channels, which orchestrate synchronous release of neuropeptides and neurotransmitters were also downregulated. With the above findings, we provide evidence that an intricate E2-driven transcriptional regulatory mechanism exists in KP^{ARC} neurons, which can provide coordinated suppression of multiple elements of the secretory pathway. Of note, we can't exclude the

possibility that a minor portion of fluorescently labelled cells does not express *Kiss1* at the time of sample collection. We also do not know that which set of E2-dependent genes is expressed in a given cell due to cell samples containing 300 pooled kisspeptin neurons.

Mechanisms underlying the transcriptional changes

In line with previous papers we found that the effects of estrogens are mediated solely by ERα in both arcuate and preoptic kisspeptin neurons (51). We detected abundant expression of *Esr1*, which encodes ERα. Neither *Esr2* nor *Gper1* encoding ERβ and G-protein coupled estrogen receptor, respectively, showed expression in KP^{RP3V} and KP^{ARC} neurons. Our results confirm that E2-driven transcriptional effects in kisspeptin neurons are mediated solely by ERα. Multiple ERα-driven mechanisms (52, 53) that operate in hypothalamic kisspeptin neurons were inseparable in our study. ERα can bind in *cis* (chromatin association *via* direct DNA binding at ERE) or in *trans* (chromatin association *via* binding to other transcription factors) at enhancers. Enhancer activation requires cooperative recruitment of multiple transcription factors and their cofactors. Approximately 200-300 transcription factors are expressed in each cell type (54). Expression of ten transcription factors was E2-dependent in KP^{RP3V} neurons. In contrast, expression of seventy was E2-dependent in KP^{ARC} neurons, eight of which interacted with ERα. The STRING database predicted an intricate network of transcription factors in KP^{ARC} neurons. In addition, E2 regulated several transcriptional regulators, chromatin modifiers and regulatory lncRNAs (17) adding another layer of complexity to the ERα mediated transcriptional mechanism in KP^{ARC} neurons. The complex, multi-layered transcriptional regulatory mechanism allows KP^{ARC} neurons to respond and integrate humoral and neuronal inputs that influence reproduction, potentially including metabolic, circadian and stress-related cues. The less complex estrogen-dependent mechanisms revealed in KP^{RP3V} neurons suggest a less integrative role of this population at least in our model.

Data availability statement

The data for KPRP3V neuron sequencing presented in the study are deposited in the BioProject repository, accession number of PRJNA847063. The data for KPARC neuron sequencing presented in the study have already been released: BioProject repository, accession number PRJNA686688.

Ethics statement

The animal study was reviewed and approved by Institutional Animal Care and Use Committee.

Author contributions

Conceptualization, BG, ST, KS, ER, NS, SP, WHC, EH, and MS; Methodology, BG, ST, KS, ER, NS, SP, EH, and MS; Investigation, BG, ST, KS, ER, NS, SP, WHC, EH, and MS; Writing-editing, BG, ST, KS, ER, NS, SP, WHC, EH, and MS; Funding acquisition and Supervision, KS and EH. All authors contributed to the article and approved the submitted version.

Funding

The research leading to these results has received funding from the National Science Foundation of Hungary (K128317 and 138137 to EH and PD134837 to KS) and the Hungarian Brain Research Program (2017-1.2.1-NKP-2017-00002 to EH).

Conflict of interest

The authors declare that the research was conducted in the absence of any commercial or financial relationships that could be construed as a potential conflict of interest.

Publisher's note

Supplementary material

The Supplementary Material for this article can be found online at: https://www.frontiersin.org/articles/10.3389/fendo.2022.960769/full#supplementary-material

References

1. de Roux N, Genin E, Carel JC, Matsuda F, Chaussain JL, Milgrom E, et al. Hypogonadotropic hypogonadism due to loss of function of the KiSS1-derived peptide receptor GPR54. *Proc Natl Acad Sci USA*. (2003) 100(19):10972–6. doi: 10.1073/pnas.1834399100

2. Seminara SB, Messager S, Chatzidaki EE, Thresher RR, Acierno JS Jr, Shagoury JK, et al. The GPR54 gene as a regulator of puberty. *N Engl J Med* (2003) 349(17):1614–27. doi: 10.1056/NEJMoa035322

3. Topaloglu AK, Tello JA, Kotan LD, Ozbek MN, Yilmaz MB, Erdogan S, et al. Inactivating KISS1 mutation and hypogonadotropic hypogonadism. *N Engl J Med* (2012) 366(7):629–35. doi: 10.1056/NEJMoa1111184

4. Funes S, Hedrick JA, Vassileva G, Markowitz L, Abbondanzo S, Golovko A, et al. The KiSS-1 receptor GPR54 is essential for the development of the murine reproductive system. *Biochem Biophys Res Commun* (2003) 312(4):1357–63. doi: 10.1016/j.bbrc.2003.11.066

5. d'Anglemont de Tassigny X, Fagg LA, Dixon JP, Day K, Leitch HG, Hendrick AG, et al. Hypogonadotropic hypogonadism in mice lacking a functional Kiss1 gene. *Proc Natl Acad Sci USA*. (2007) 104(25):10714–9. doi: 10.1073/pnas.0704114104

6. Porteous R, Petersen SL, Yeo SH, Bhattarai JP, Ciofi P, de Tassigny XD, et al. Kisspeptin neurons co-express met-enkephalin and galanin in the rostral periventricular region of the female mouse hypothalamus. *J Comp Neurol* (2011) 519(17):3456–69. doi: 10.1002/cne.22716

7. Kallo I, Vida B, Deli L, Molnar CS, Hrabovszky E, Caraty A, et al. Co-Localisation of kisspeptin with galanin or neurokinin b in afferents to mouse GnRH neurones. *J Neuroendocrinol* (2012) 24(3):464–76. doi: 10.1111/j.1365-2826.2011.02262.x

8. Clarkson J, Herbison AE. Dual phenotype kisspeptin-dopamine neurones of the rostral periventricular area of the third ventricle project to gonadotrophin-releasing hormone neurones. *J Neuroendocrinol* (2011) 23(4):293–301. doi: 10.1111/j.1365-2826.2011.02107.x

9. Kauffman AS, Gottsch ML, Roa J, Byquist AC, Crown A, Clifton DK, et al. Sexual differentiation of Kiss1 gene expression in the brain of the rat. *Endocrinology* (2007) 148(4):1774–83. doi: 10.1210/en.2006-1540

10. Cravo RM, Margatho LO, Osborne-Lawrence S, Donato J Jr., Atkin S, Bookout AL, et al, et al. Characterization of Kiss1 neurons using transgenic mouse models. *Neuroscience* (2011) 173:37–56. doi: 10.1016/j.neuroscience.2010.11.022

11. Herbison AE. The gonadotropin-releasing hormone pulse generator. *Endocrinology* (2018) 159(11):3723–36. doi: 10.1210/en.2018-00653

12. Sobrino V, Avendano MS, Perdices-Lopez C, Jimenez-Puyer M, Tena-Sempere M. Kisspeptins and the neuroendocrine control of reproduction: Recent progress and new frontiers in kisspeptin research. *Front Neuroendocrinol* (2022) 65:100977. doi: 10.1016/j.yfrne.2021.100977

13. Campbell JN, Macosko EZ, Fenselau H, Pers TH, Lyubetskaya A, Tenen D, et al. A molecular census of arcuate hypothalamus and median eminence cell types. *Nat Neurosci* (2017) 20(3):484–96. doi: 10.1038/nn.4495

14. Moffitt JR, Bambah-Mukku D, Eichhorn SW, Vaughn E, Shekhar K, Perez JD, et al. Molecular, spatial, and functional single-cell profiling of the hypothalamic preoptic region. *Science* (2018) 362(6416). doi: 10.1126/science.aau5324

15. Garcia-Galiano D, Pinilla L, Tena-Sempere M. Sex steroids and the control of the Kiss1 system: developmental roles and major regulatory actions. *J Neuroendocrinol* (2012) 24(1):22–33. doi: 10.1111/j.1365-2826.2011.02230.x

16. Gottsch ML, Navarro VM, Zhao Z, Glidewell-Kenney C, Weiss J, Jameson JL, et al. Regulation of Kiss1 and dynorphin gene expression in the murine brain by classical and nonclassical estrogen receptor pathways. *J Neurosci* (2009) 29 (29):9390–5. doi: 10.1523/JNEUROSCI.0763-09.2009

17. Gocz B, Rumpler E, Sarvari M, Skrapits K, Takacs S, Farkas I, et al. Transcriptome profiling of kisspeptin neurons from the mouse arcuate nucleus reveals new mechanisms in estrogenic control of fertility. *Proc Natl Acad Sci U.S.A.* (2022) 119(27):e2113749119. doi: 10.1073/pnas.2113749119

18. Yeo SH, Kyle V, Morris PG, Jackman S, Sinnett-Smith LC, Schacker M, et al. Visualisation of Kiss1 neurone distribution using a Kiss1-CRE transgenic mouse. *J Neuroendocrinol* (2016) 28(11). doi: 10.1111/jne.12435

19. Molnar CS, Kallo I, Liposits Z, Hrabovszky E. Estradiol down-regulates RF-amide-related peptide (RFRP) expression in the mouse hypothalamus. *Endocrinology* (2011) 152(4):1684–90. doi: 10.1210/en.2010-1418

20. Schuierer S, Carbone W, Knehr J, Petitjean V, Fernandez A, Sultan M, et al. A comprehensive assessment of RNA-seq protocols for degraded and low-quantity samples. *BMC Genomics* (2017) 18(1):442. doi: 10.1186/s12864-017-3827-y

21. Dobin A, Davis CA, Schlesinger F, Drenkow J, Zaleski C, Jha S, et al. STAR: ultrafast universal RNA-seq aligner. *Bioinformatics* (2013) 29(1):15–21. doi: 10.1093/bioinformatics/bts635

22. Liao Y, Smyth GK, Shi W. featureCounts: an efficient general purpose program for assigning sequence reads to genomic features. *Bioinformatics* (2014) 30(7):923–30. doi: 10.1093/bioinformatics/btt656

23. McCarthy DJ, Chen Y, Smyth GK. Differential expression analysis of multifactor RNA-seq experiments with respect to biological variation. *Nucleic Acids Res* (2012) 40(10):4288–97. doi: 10.1093/nar/gks042

24. Love MI, Huber W, Anders S. Moderated estimation of fold change and dispersion for RNA-seq data with DESeq2. *Genome Biol* (2014) 15(12):550. doi: 10.1186/s13059-014-0550-8

25. Benjamini Y, Drai D, Elmer G, Kafkafi N, Golani I. Controlling the false discovery rate in behavior genetics research. *Behav Brain Res* (2001) 125(1-2):279–84. doi: 10.1016/S0166-4328(01)00297-2

26. Kanehisa M, Goto S. KEGG: kyoto encyclopedia of genes and genomes. *Nucleic Acids Res* (2000) 28(1):27–30. doi: 10.1093/nar/28.1.27

27. Tavazoie S, Hughes JD, Campbell MJ, Cho RJ, Church GM. Systematic determination of genetic network architecture. *Nat Genet* (1999) 22(3):281–5. doi: 10.1038/10343

28. Wu T, Hu E, Xu S, Chen M, Guo P, Dai Z, et al. clusterProfiler 4.0: A universal enrichment tool for interpreting omics data. *Innovation (NY)* (2021) 2 (3):100141. doi: 10.1016/j.xinn.2021.100141

29. Hu H, Miao YR, Jia LH, Yu QY, Zhang Q, Guo AY. AnimalTFDB 3.0: a comprehensive resource for annotation and prediction of animal transcription factors. *Nucleic Acids Res* (2019) 47(D1):D33–8. doi: 10.1093/nar/gky822

30. Nilsson ME, Vandenput L, Tivesten A, Norlen AK, Lagerquist MK, Windahl SH, et al. Measurement of a comprehensive sex steroid profile in rodent serum by high-sensitive gas chromatography-tandem mass spectrometry. *Endocrinology* (2015) 156(7):2492–502. doi: 10.1210/en.2014-1890

31. Bourgon R, Gentleman R, Huber W. Independent filtering increases detection power for high-throughput experiments. *Proc Natl Acad Sci U.S.A.* (2010) 107(21):9546–51. doi: 10.1073/pnas.0914005107

32. Sha Y, Phan JH, Wang MD. (2015). Effect of low-expression gene filtering on detection of differentially expressed genes in RNA-seq data, in: *Annu Int Conf IEEE Eng Med Biol Soc*, , Vol. 2015. pp. 6461–4. doi: 10.1109/EMBC.2015.7319872

33. Bi M, Zhang Z, Jiang YZ, Xue P, Wang H, Lai Z, et al. Enhancer reprogramming driven by high-order assemblies of transcription factors promotes phenotypic plasticity and breast cancer endocrine resistance. *Nat Cell Biol* (2020) 22(6):701–15. doi: 10.1038/s41556-020-0514-z

34. Szklarczyk D, Gable AL, Nastou KC, Lyon D, Kirsch R, Pyysalo S, et al. The STRING database in 2021: customizable protein-protein networks, and functional characterization of user-uploaded gene/measurement sets. *Nucleic Acids Res* (2021) 49 (D1):D605–12. doi: 10.1093/nar/gkaa1074

35. de la Iglesia HO, Schwartz WJ. Minireview: timely ovulation: circadian regulation of the female hypothalamo-pituitary-gonadal axis. *Endocrinology* (2006) 147(3):1148–53. doi: 10.1210/en.2005-1311

36. de Paula DG, Bohlen TM, Zampieri TT, Mansano NS, Vieira HR, Gusmao DO, et al. Distinct effects of growth hormone deficiency and disruption of hypothalamic kisspeptin system on reproduction of male mice. *Life Sci* (2021) 285:119970. doi: 10.1016/j.lfs.2021.119970

37. Mohr MA, Esparza LA, Steffen P, Micevych PE, Kauffman AS. Progesterone receptors in AVPV kisspeptin neurons are sufficient for positive feedback induction of the LH surge. *Endocrinology* (2021) 162(11). doi: 10.1210/endocr/bqab161

38. Samson WK, Alexander BD, Skala KD, Huang FL, Fulton RJ. Central peptidergic mechanisms controlling reproductive hormone secretion: novel methodology reveals a role for the natriuretic peptides. *Can J Physiol Pharmacol* (1992) 70(5):773–8. doi: 10.1139/y92-102

39. Moenter SM, DeFazio RA. Endogenous gamma-aminobutyric acid can excite gonadotropin-releasing hormone neurons. *Endocrinology* (2005) 146 (12):5374–9. doi: 10.1210/en.2005-0788

40. Takacs S, Bardoczi Z, Skrapits K, Gocz B, Vaczi V, Magloczky Z, et al. Post mortem single-cell labeling with DiI and immunoelectron microscopy unveil the fine structure of kisspeptin neurons in humans. *Brain Struct Funct* (2018) 223 (5):2143–56. doi: 10.1007/s00429-018-1610-8

41. Ciofi P, Leroy D, Tramu G. Sexual dimorphism in the organization of the rat hypothalamic infundibular area. *Neuroscience* (2006) 141(4):1731–45. doi: 10.1016/j.neuroscience.2006.05.041

42. Moore AM, Lohr DB, Coolen LM, Lehman MN. Prenatal androgen exposure alters KNDy neurons and their afferent network in a model of polycystic ovarian syndrome. *Endocrinology* (2021) 162(11). doi: 10.1210/endocr/bqab158

43. Qiu J, Nestor CC, Zhang C, Padilla SL, Palmiter RD, Kelly MJ, et al. High-frequency stimulation-induced peptide release synchronizes arcuate kisspeptin neurons and excites GnRH neurons. *Elife* (2016) 5. doi: 10.7554/eLife.16246

44. Qiu J, Rivera HM, Bosch MA, Padilla SL, Stincic TL, Palmiter RD, et al. Estrogenic-dependent glutamatergic neurotransmission from kisspeptin neurons governs feeding circuits in females. *Elife* (2018) 7. doi: 10.7554/eLife.35656

45. Boughton CK, Patel SA, Thompson EL, Patterson M, Curtis AE, Amin A, et al. Neuromedin b stimulates the hypothalamic-pituitary-gonadal axis in male rats. *Regul Pept* (2013) 187:6–11. doi: 10.1016/j.regpep.2013.10.002

46. Todman MG, Han SK, Herbison AE. Profiling neurotransmitter receptor expression in mouse gonadotropin-releasing hormone neurons using green fluorescent protein-promoter transgenics and microarrays. *Neuroscience* (2005) 132(3):703–12. doi: 10.1016/j.neuroscience.2005.01.035

47. Dungan Lemko HM, Naderi R, Adjan V, Jennes LH, Navarro VM, Clifton DK, et al. Interactions between neurotensin and GnRH neurons in the positive feedback control of GnRH/LH secretion in the mouse. *Am J Physiol Endocrinol Metab* (2010) 298(1):E80–8. doi: 10.1152/ajpendo.00380.2009

48. Kim T, Gondre-Lewis MC, Arnaoutova I, Loh YP. Dense-core secretory granule biogenesis. *Physiol (Bethesda)* (2006) 21:124–33. doi: 10.1152/physiol.00043.2005

49. Harashima S, Clark A, Christie MR, Notkins AL. The dense core transmembrane vesicle protein IA-2 is a regulator of vesicle number and insulin secretion. *Proc Natl Acad Sci USA*. (2005) 102(24):8704–9. doi: 10.1073/pnas.0408887102

50. Stephens SBZ, Kauffman AS. Estrogen regulation of the molecular phenotype and active translatome of AVPV kisspeptin neurons. *Endocrinology* (2021) 162(9). doi: 10.1210/endocr/bqab080

51. Smith JT, Cunningham MJ, Rissman EF, Clifton DK, Steiner RA. Regulation of Kiss1 gene expression in the brain of the female mouse. *Endocrinology* (2005) 146(9):3686–92. doi: 10.1210/en.2005-0488

52. Gronemeyer H, Gustafsson JA, Laudet V. Principles for modulation of the nuclear receptor superfamily. *Nat Rev Drug Discovery* (2004) 3(11):950–64. doi: 10.1038/nrd1551

53. Farcas AM, Nagarajan S, Cosulich S, Carroll JS. Genome-wide estrogen receptor activity in breast cancer. *Endocrinology* (2021) 162(2). doi: 10.1210/endocr/bqaa224

54. Vaquerizas JM, Kummerfeld SK, Teichmann SA, Luscombe NM. A census of human transcription factors: function, expression and evolution. *Nat Rev Genet* (2009) 10(4):252–63. doi: 10.1038/nrg2538

frontiers | Frontiers in Endocrinology

TYPE Mini Review
PUBLISHED 15 September 2022
DOI 10.3389/fendo.2022.999236

OPEN ACCESS

EDITED BY
Andrea Kwakowsky,
National University of Ireland Galway, Ireland

REVIEWED BY
Kelli A. Duncan,
Vassar College, United States
Éva M. Szegő,
Technical University of Dresden, Germany

*CORRESPONDENCE
Rachel Y. Cheong
ry.cheong@gmail.com

SPECIALTY SECTION
This article was submitted to Reproduction, a section of the journal Frontiers in Endocrinology

RECEIVED 20 July 2022
ACCEPTED 15 August 2022
PUBLISHED 15 September 2022

CITATION
Koszegi Z and Cheong RY (2022) Targeting the non-classical estrogen pathway in neurodegenerative diseases and brain injury disorders. *Front. Endocrinol.* 13:999236. doi: 10.3389/fendo.2022.999236

Targeting the non-classical estrogen pathway in neurodegenerative diseases and brain injury disorders

Zsombor Koszegi[1] and Rachel Y. Cheong[2*]

[1]Institute of Metabolism and Systems Research, University of Birmingham, Birmingham, United Kingdom, [2]Timeline Bioresearch AB, Medicon Village, Lund, Sweden

Estrogens can alter the biology of various tissues and organs, including the brain, and thus play an essential role in modulating homeostasis. Despite its traditional role in reproduction, it is now accepted that estrogen and its analogues can exert neuroprotective effects. Several studies have shown the beneficial effects of estrogen in ameliorating and delaying the progression of neurodegenerative diseases, including Alzheimer's and Parkinson's disease and various forms of brain injury disorders. While the classical effects of estrogen through intracellular receptors are more established, the impact of the non-classical pathway through receptors located at the plasma membrane as well as the rapid stimulation of intracellular signaling cascades are still under active research. Moreover, it has been suggested that the non-classical estrogen pathway plays a crucial role in neuroprotection in various brain areas. In this mini-review, we will discuss the use of compounds targeting the non-classical estrogen pathway in their potential use as treatment in neurodegenerative diseases and brain injury disorders.

KEYWORDS

estrogen, non-classical, non-genomic, neurodegeneration, neuroprotection

Introduction

Estrogens are a group of gonadal sex hormones that exist naturally in three different forms in humans. 17β-estradiol (E2) is the most dominant biological form, followed by estrone (E1) the intermediate form, and estriol (E3), which has very low levels in the body that are only increased during pregnancy. In this mini-review, we will use the abbreviation E2 to refer to 17β-estradiol and will focus predominantly on this form as this is the most abundant and most of the research has been largely focused on studying this molecule. In addition to its role in reproductive functions, E2 has a profound influence on the central nervous system (1, 2). This has contributed to the interest generated around the impact of E2 on neuronal function in health and disease.

Investigations over the past few decades have shown that E2 has the potential to prevent or counterbalance the symptoms of neurodegenerative diseases. The gender differences observed in two of the most common neurodegenerative diseases, Alzheimer's disease (AD) and Parkinson's disease (PD), clearly suggest this role (3–5). Although there is no conclusive evidence for E2 treatment in neurodegenerative diseases in human clinical trials, there have been several *in vivo* rodent and *in vitro* cell line models that indicate the therapeutic effects of E2. This mini-review will discuss the neuroprotective, non-classical effects of E2 in the context of some of the most typical neurodegenerative cases (that is AD and PD) as well as brain injuries that possibly lead to neurodegeneration (traumatic brain injury and stroke) and highlight the use of some of the non-classical E2 analogues to potentially prevent or treat these disorders.

Classical versus non-classical estrogen pathways

E2 regulates cellular processes by binding to specific estrogen receptors (ERs) with two distinct modes of action, broadly classified as the classical and non-classical estrogen pathway. Stimulation of the classical pathway results in direct transcriptional effects through the binding of E2 to its intracellular receptors (ERα and ERβ) and activation of the estrogen response element (ERE) (6). In contrast, the non-classical pathway involves the rapid activation of ion channels and intracellular second messenger signaling pathways. The latter is followed by the stimulation of an array of gene transcription factors, but activation *via* the non-classical pathway is ERE-independent. The non-classical pathway is often described as rapid, as the activation of intracellular signaling pathways can be detected in a matter of seconds, as first demonstrated by Szego and Davis, whereby E2 induced an increase in cyclic adenosine monophosphate (cAMP) levels in the uterus few seconds following administration (7). However, this rapid signaling pathway activation will also often lead to gene transcription, which can be detected at a slower rate. One of the most important transcription factors of the non-classical pathway is the cAMP response element-binding protein (CREB), which has been implicated in multiple studies (8–10).

Apart from the classical ERα and ERβ, experiments looking at the rapid signaling pathway activation by E2 highlighted that these classical intracellular receptors – mediating ERE-dependent gene transcription – might not be sufficient to account for the variety of responses observed. This led to the discovery of membrane linked receptors, which can be membrane-localized classical ERα and ERβ or other types, for example, the ER-X and the G protein coupled GPR30 (GPER1) (11–13), which are all different from the classical receptors in their structure, localization, as well as modes of action. A schematic illustration of the classical and non-classical modes of E2 action is depicted in Figure 1.

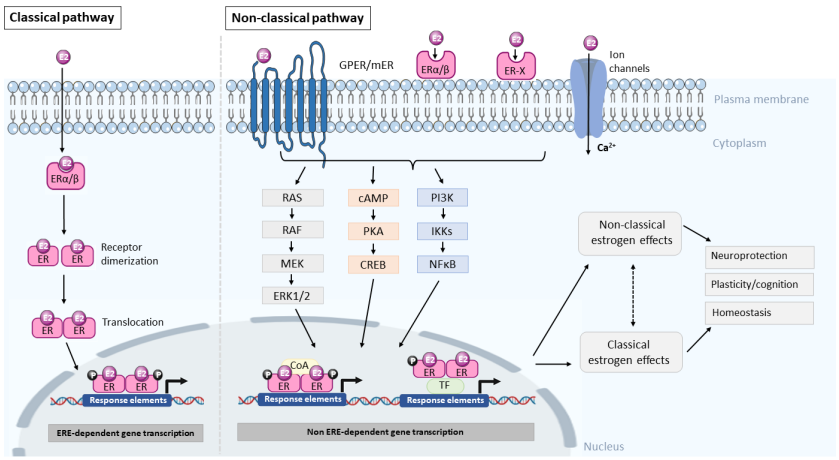

FIGURE 1
Summary diagram of the classical and non-classical modes of estrogen action. In the classical pathway, E2 crosses the plasma membrane by diffusion and binds to the estrogen receptor (ER) and forms an E2-receptor complex, which dimerizes and translocates to the nucleus to regulate gene transcription through an estrogen response element (ERE) dependent manner. In the non-classical pathway, E2 interacts with membrane bound estrogen receptors (mER), G-protein coupled estrogen receptors (GPER), ER-X, or classic ER (ERα/β) and activates kinases and second messenger signaling pathways to phosphorylate transcription factors (TF) or coactivators to influence gene transcription in the nucleus via a non-ERE-dependent manner. The resultant effect of activating these pathways is neuroprotection, modulating plasticity and cognition as well as maintenance of homeostasis. However, the extent to which the non-classical and classical pathways crosstalk or interact with each other is not known. It is likely that both pathways contribute to neuroprotection and homeostasis. RAS, Ras small GTPase, RAF, Raf kinase, MEK, mitogen-activated protein kinase, ERK1/2, extracellular signal-regulated kinase 1/2, cAMP, cyclic adenosine monophosphate, PKA, protein kinase A, CREB, cAMP-responsive element-binding protein, PI3K, phosphatidylinositol-3 kinase, IKKs, IκB kinases, NFκB, nuclear factor kappa-light-chain-enhancer of activated B cells, coA, coactivator.

Mechanism for non-classical E2 neuroprotection

There are several possible molecular mechanisms contributing to non-classical E2 neuroprotection, such as control of neuroinflammation, myelin protection, mitochondrial protection and control of oxidative stress, regulating autophagy as well as maintenance of synaptic transmission and plasticity. One of the important protective actions of E2 is in the control of neuroinflammation whereby E2 reduces the secretion of proinflammatory cytokines and interleukins and thereby reducing microglia activation *via* the inhibition of the nuclear factor kappa-light-chain-enhancer of activated B cells (NFκB) signaling pathway (14, 15). In addition, the neuroprotective effects of E2 are in part due to its protective actions on myelin and remyelination, which can be mediated by activation of the phosphoinositide 3-kinases (PI3K)/protein kinase B (Akt)/mammalian target of rapamycin (mTOR) signaling pathway (16–18). Dysfunction in the myelin sheaths is often a common feature in neurodegenerative diseases such as AD and PD as well as in other central nervous system pathologies, such as traumatic brain injury (TBI), stroke and multiple sclerosis. In these neuropathological conditions, E2 has been shown to upregulate genes involved in synaptogenesis, axonal repair and synaptic plasticity, such as Bcl2, TrkB and cadherin-2 (19–21). Another way in which E2 exerts its neuroprotective effects is against oxidative stress through the protection of mitochondrial function and by reducing the production of reactive oxygen species (22, 23). Under pathological conditions, E2 may also elicit various of the above-mentioned responses, but may also promote the release of different neurotrophic factors such as the glial cell line-derived neurotrophic factor (GDNF), insulin-like growth factor 1 (IGF-1) and brain-derived neurotrophic factor (BDNF) to protect neurons and promote reparation of injured neuronal circuits (24, 25).

Compounds targeting the non-classical estrogen pathway

Importantly, previous findings indicate that apart from the classical estrogen pathway, the non-classical pathway also plays a role in ameliorating neurodegeneration in disease models. The latter is of particular interest as E2 replacement therapy, which affects both the classical and non-classical pathways, has been shown to not only increase the risk of myocardial infarction or coronary heart disease but could potentially lead to an array of side effects, including increased risk of breast cancer and stroke (26–28). Therefore, there has been a renewed interest in developing new compounds that are able to trigger protective or restorative effects without the risk of unwanted side effects. One of these groups of such compounds is the 'selective estrogen-receptor modulators' (SERMs), which are non-steroidal molecules with specific mechanism of action in target tissues. They primarily act as partial ER agonists in the target tissue while being antagonists in non-target tissues. Some SERMs, for example, tamoxifen and raloxifene are already in clinical use for pre- and post-menopausal women (29), while others, such as the GPER1 agonist G-1 or the STX (a Gq-coupled membrane ER agonist) are used in preclinical animal studies (30, 31). The challenge with SERMs lies in the balance between the efficacy of the agonistic profile and, at the same time, the reduction of unwanted side effects on non-target tissues. While newer third generation SERMs, such as bazedoxifene, ospemifene and lasofoxifene, have improved efficacy, their use as SERMs in the brain is not known (32). Other important compounds are the 'activators of non-genomic estrogen-like signaling' (ANGELS), which is a novel group in E2 therapy that is aimed at targeting the non-classical E2 pathway. Three of these molecules are known, estren (4-estren-3alpha, 17beta-diol), compound A, and compound B, which are all capable of triggering the non-classical E2 pathway (33, 34). However, these compounds are yet to be used in clinical practice, although estren has been found to have protective effects on basal forebrain cholinergic neurons (35, 36), indicating that there is prospect for the use of these non-classical activators as treatment for neurodegenerative diseases.

Alzheimer's disease

Pathophysiology

Alzheimer's disease (AD) is a chronic progressive neurodegenerative disorder, characterized by distinct hallmark pathologies, such as the presence of amyloid plaques, which comprises primarily of aggregated amyloid β (Aβ) peptide, and formation of neurofibrillary tangles with hyperphosphorylated tau protein. These pathologies lead to progressive and selective neuronal loss in the hippocampus and temporal cortex, cognitive decline and eventual death. There is no curative treatment available for AD at present and current treatments only target the management of symptoms with no influence on disease progression. The pathogenesis of AD has been postulated to be due to the accumulation of Aβ as a result of altered amyloid precursor protein (APP), accumulation of tau, oxidative stress caused by mitochondrial dysfunction and persistent neuroinflammation.

Neuroprotective effects of E2 in AD

Neuroprotective effects of E2 have been proposed in experimental models of AD. Estrogen deficiency in the brain

accelerates Aβ plaque formation (37–39), while E2 treatment has been shown to reduce the expression of Aβ peptide and abnormal accumulation of amyloid proteins (40–42). The reduction of Aβ following E2 administration might be linked to the alteration of the APP gene, as APP protein levels are reduced following E2 treatment (43) as well as the cleavage of APP into toxic Aβ. E2 stimulation increases the secreted APPα, which can lead to a decrease in toxic Aβ species (44, 45). This neuroprotection against β-amyloid toxicity have been shown to occur *via* ERα and ERβ (46). In addition, to protection against Aβ accumulation, E2 is known to also decrease tau hyperphosphorylation in experimental models of AD (47, 48).

A loss of cholinergic neurons is recognized as one of the hallmarks of AD. There is considerable evidence showing the effects of E2 on plasticity and protection of cholinergic neurons through an ERα dependent pathway (49, 50). Accordingly, E2 has been reported to upregulate fiber density of the remaining cholinergic neurons after an excitotoxic insult *via* the mitogen-activated protein kinase (MAPK) signaling pathway, leading to the stimulation of CREB phosphorylation (8, 35, 51). E2 has also been known to alter the dynamics of neural circuits, such as modulating the plasticity of dendritic spines and stimulating neurogenesis and synaptic contacts in numerous brain regions like the hippocampus, hypothalamus and amygdala (52–54). In experimental models of AD, such as the transgenic APP/PS1 and 3xTg AD mice, ovariectomy increased the accumulation of the Aβ peptide and decreased hippocampal-dependent behavioral performance. Treatment with E2 not only prevented the worsening of pathologies, but also reduced the accumulation of Aβ in the hippocampus, subiculum and amygdala (55, 56), suggesting a protective role of E2 in AD progression. With the potential impact of E2 on systemic tissues, there is a need to develop brain-specific therapies. Treatment with a brain-selective prodrug, DHED (10β,17β-dihydroxyestra-1,4-dien-3-one), in APP/PS1 double transgenic mice showed no systemic off-target effects in the uterine tissue, but similar improvements in APP levels, suggesting that the brain-selective treatment with DHED can be used as an early-stage intervention for AD (57).

Taken together, E2 has the potential to regenerate, restore and strengthen the formation of new synaptic networks from the remaining neurons and/or rewire neural circuits under pathological conditions.

Targeting non-classical E2 pathway as potential treatment in AD

Given the neuroprotective potential of E2 in AD, targeting the non-classical E2 pathway selectively may provide an alternative treatment strategy. Studies have shown that ANGELS compounds, such as estren, can activate the non-classical E2 pathway and rescue the survival of basal forebrain cholinergic neurons after injection of Aβ (1–42) in mice (36) and is neuroprotective against Aβ-induced injury *in vitro* (58). A key important feature of estren treatment is that, unlike E2, it does not increase the size of the uterus, indicating that it might not have unwanted, genomic side effects (59). Regarding cognition, E2 has consistently been reported to have the ability to enhance cognitive function *via* the non-classical E2 pathway involving the ERK1/2 and Akt signaling pathways (60–64). A number of clinical trials in AD have been conducted with the second generation SERM, raloxifene, with varying results, in hope of alleviating cognitive deficits. While some showed that raloxifene improved verbal memory and reduced the risk of AD and mild cognitive impairment, others showed no significant changes in cognition (65–67).

More recent studies show that targeting non-nuclear ERs, such as GPER1, or using non-classical ligands, such as STX, could ameliorate memory impairments or protect against Aβ-toxicity in experimental models of AD *via* activation of the ERK and PI3K/Akt signaling pathways (68–70). These studies provide evidence that activation of the membrane-bound, non-nuclear ERs can provide an alternative therapeutic target in AD. Another novel compound that is of emerging interest is the Pathway Preferential Estrogen-1 (PaPE-1), which is a selective non-nuclear ER pathway activator, which can protect neurons against Aβ-induced toxicity through a mechanism that involves inhibition of oxidative stress and apoptosis (71). This compound strongly activates the MAPK and mTOR pathways without interaction with the nuclear receptors and has a broad spectrum of utility in other neurological disorders, where it also decreases the severity of stroke (72). However, there is a clear lack of clinical trials for these newly developed compounds and more studies are warranted to determine the viability of using non-classical E2 activators as a preventive treatment alternative for AD.

Parkinson's disease

Pathophysiology

Parkinson's disease (PD) is one of the most common age-related neurodegenerative movement disorders. The main pathological hallmark of PD is motor symptoms consisting of resting tremor, rigidity, bradykinesia and postural imbalance, attributed primarily to the substantial loss of midbrain dopamine (DA) neurons in the substantia nigra pars compacta and the accumulation of α-synuclein cytoplasmic protein deposits, termed Lewy Bodies, in the surviving neurons. The dopaminergic system is not the only affected network in PD. Degeneration of serotonergic neurons in the raphe nucleus, noradrenergic neurons of the locus coeruleus and cholinergic neurons of the nucleus basalis of Meynert have also been reported in PD. Numerous different treatment methods have been investigated to alleviate motor deficits, but no effective

clinical therapy has been found to be able to prevent or reverse the degeneration of DA neurons (73). There is currently no cure for PD and available treatments are only symptomatic. DA itself is not a suitable drug as it does not cross the blood-brain-barrier, has a short half-life and has peripheral hemodynamic side effects. Oral administration of L-DOPA remains the gold standard treatment today (74, 75). However, the challenge with L-DOPA is that it cannot be utilized as a long-term treatment for PD. As such, the development of new therapeutics and strategies with several mechanisms of action, such as neurosteroids, could provide an alternative treatment for PD.

Neuroprotective effects of E2 in PD

While E2 effects on the dopaminergic system have not been well characterized, there is some evidence of a modulatory effect of E2 in PD patients. Postmenopausal women who received hormone replacement therapy have a reduced risk of developing PD and lower disease severity in early stages of the disease (76, 77). E2 has been reported to be protective against 6-OHDA (6-hydroxy dopamine) toxicity in DA neurons (78). Similarly, in the neurotoxin MPTP (1-methyl-4-phenyl-1,2,3,6-tetrahydropyridine) model of PD, E2 treatment improved DA release in the striatum and nucleus accumbens and could protect DA neurons (79–82). In fact, E2 treatment has been shown to increase fiber density of tyrosine hydroxylase-positive DA neurons in both 6-OHDA and MPTP-induced models (83–85). In order to determine the ER subtype regulating neuroprotection in PD, studies have used selective ER agonists and found that the activation of ERα but not ERβ rescued the depletion of DA and prevented the loss of DA transporter in the striatum and cell death in the substantia nigra in MPTP-treated mice (86–88). These studies suggest that neuroprotection of DA neurons occurs through an ERα-specific manner in experimental models of PD.

Targeting non-classical E2 pathway as potential treatment in PD

There is a lack of research on SERMs in human studies of PD. The majority of the studies have been performed in rodent models with contradictory results. In the MPTP model, raloxifene treatment prevented the MPTP-induced DA depletion, restored DA levels and prevented DA cell death (89, 90) while in other studies was proven ineffective (91). The varying results could be due to differences in the models used, dosing paradigm or pharmacological properties of the different compounds. The other new estrogen analogue, the brain-selective estrogen prodrug, DHED, was found to protect DA neurons in the MPTP-toxicity model and in 3K α-synuclein transgenic mice (mouse model that exhibits many features of PD neuropathology) (92, 93). DHED was also found to selectively increase E2 in the brain while the periphery was spared, which in turn, reduced the secondary effects of E2 on the body (94). In addition, DHED treatment significantly alleviated the neuronal pathology of PD *via* decreasing α-synuclein monomer accumulation and aggregation, restoring vesicle and dopaminergic fiber densities as well as improving PD-associated motor deficits (92–94). Taken together, this evidence highlights the potential for modulating E2 signaling with pharmaceutical analogues for neuroprotection in PD. More investigations into the use of these non-classical activator compounds in PD models are warranted to determine their therapeutic potential.

Brain injury disorders

Pathophysiology

Brain injuries can be classified into two main categories, traumatic and non-traumatic. Traumatic brain injury (TBI) occurs when the original function of the brain or the underlying anatomy changes due to an external force (e.g., injury). Non-traumatic brain injury, also referred to as acquired brain injury, is caused by internal factors such as lack of oxygen, exposure to toxins or infection. Examples of non-traumatic brain injury include stroke and cerebral ischemia. Although brain injury is not a neurodegenerative disease per se, it is now clear that brain injuries can trigger progressive neurodegeneration and dementia (e.g., AD) (95). As TBI and stroke are recognized as one of the leading causes of disability and death in most societies (96, 97), it is important to discuss the potential of using alternative non-surgical therapies.

Neuroprotective effects of E2 in brain injury disorders

The evidence is not clear, especially when it comes to human studies, but there is a strong indication that there is a trend for sex differences, potentially due to differing circulating E2 levels, in the incidence and mortality rate of TBI (98–100). Another indication that E2 might play a role in ameliorating neuronal damage following injury is that the activity of aromatase (a key enzyme in E2 synthesis) increases, particularly in brain astroglia cells (101). This increased aromatase activity has been reported to be neuroprotective in various animal models (102). Besides locally produced E2 in the brain, exogenous E2 application before or immediately after injury has also been shown to rescue damage following a controlled impact in ovariectomized mice (103, 104),

indicating that E2 does have treatment potential following trauma in both the TBI and stroke experimental models.

Targeting non-classical E2 pathway as potential treatment in brain injury disorders

As in the case of other forms of neuronal brain damage, the non-classical estrogen pathway has been reported to have treatment potential in TBI and also in stroke. A known characteristic of TBI is that the primary injury due to the external force is often followed by a slower secondary injury. One of the most common secondary injuries is excessive glutamate release, which is followed by overactivation of NMDA (N-methyl-D-aspartate) and AMPA (α-amino-3-hydroxy-5-methyl-4-isoxazolepropionic acid) receptors and consequentially intracellular ion imbalance, leading to excitatory cell death (105). In an experimental model of NMDA-induced toxicity, E2 treatment following injury ameliorated the damage in basal forebrain cholinergic fibers in mice (35). Importantly, this study highlighted the involvement of the non-classical E2 pathway *via* the MAPK/PKA signaling system. The non-classical pathway activator, estren (a member of the ANGELS compounds), has also been able to trigger E2-like restorative actions. And, as for the receptor dependence of the protective actions of E2 in TBI, the above-mentioned study highlighted that ERα is required for the ameliorative effects after damage (35). However, another study has shown that both ERα and ERβ helped to reduce brain edema following TBI in rats (106). It has also been shown that E2 treatment following TBI can increase ERα and restore ERβ expression in the brain (107). In addition to these classical E2 receptors, it appears that GPER1 is also involved in neuroprotection following TBI. Both E2 and treatment with the GPER1 agonist, G-1, increased neuronal survival as well as decreased neuronal degeneration and apoptotic cell death in a rodent model of TBI (108). These results were corroborated in other rat TBI studies, where G-1 was found to promote neuronal survival and improve cognitive impairment (109) as well as reduced neuronal apoptosis and increased microglia polarization (110), through the PI3K/Akt signaling pathway. Likewise, the non-classical pathway has also been implicated as an alternative treatment in other brain injury disorders. Treatment with G-1 improved neuronal survival after brain ischemia, reduced infarct size, neuronal injury and improved neuroinflammation and immunosuppression after experimentally induced stroke and cerebral ischemia (104, 111, 112). Furthermore, treatment with other non-classical pathway activators, such as PaPE-1 and the SERM bazedoxifene, protected neurons against ischemic brain damage in rodents and in neuronal culture, potentially through the MAPK/ERK1/2 signaling pathway (113, 114).

Neuroinflammation can play a key role in the secondary injury observed in TBI as well as after stroke with the activation of microglia cells, among others, and the release of inflammatory factors (115–117). Following TBI, G-1 exerts anti-inflammatory effects, but it appears that there are sex specific differences as these results were observed in males and ovariectomized females, but not in intact females. Therefore, the circulating levels of E2 in patients will likely influence any potential medical treatment following brain injury. In addition to G-1, STX has also been found to be capable of attenuating ischemia-induced neuronal loss in middle-aged rats (30). Importantly, this study showed that animals which have not been exposed to E2 for some time still maintained their responsiveness to E2 and E2-like compounds as treatment, highlighting the use of non-feminizing estrogens, that can be candidates in both males and females and at different age groups. Taken together, these results strongly suggest that the non-classical pathway can be targeted as potential treatment in traumatic and non-traumatic brain injury disorders.

Conclusions

In this mini-review, we discussed the neuroprotective role of E2 and the potential involvement of the non-classical estrogen pathway in ameliorating or alleviating disease phenotype in experimental models of AD, PD and brain injury disorders. The results from *in vivo* and *in vitro* studies with selective non-classical pathway activators, such as raloxifene, estren, STX, G-1, PaPE-1 and DHED, are very promising targets and present hopeful beneficial effects on their potential use as treatment in neurodegenerative diseases. However, as both the classical and non-classical pathways are intact in most, if not all, of these studies, it is difficult to ascertain whether the observed neuroprotective effects of E2 are solely attributed to the non-classical pathway. Some of the ongoing challenges with these selective non-classical pathway activators include how to modulate selectivity and sensitivity to ensure that the non-classical pathway is stimulated without triggering the classical pathway. Extra caution also needs to be taken in their interpretation as, at present, there is a lack of conclusive evidence for their use in the human brain. More studies are warranted to translate these neuroprotective effects in human clinical trials before they can be utilized as a novel therapeutic strategy to ameliorate, prevent the onset and/or slow down disease progression in neurodegenerative diseases.

Author contributions

Both ZK and RC developed the concept and wrote the manuscript. Both authors have made a substantial, direct and

intellectual contribution to the work and approved the manuscript prior to its submission.

Conflict of interest

RC was employed by Timeline Bioresearch AB.

The remaining author declares that the research was conducted in the absence of any commercial or financial relationships that could be construed as a potential conflict of interest.

Publisher's note

References

1. McEwen B. Estrogen actions throughout the brain. *Recent Prog Horm Res* (2002) 57:357–84. doi: 10.1210/rp.57.1.357

2. McEwen BS, Alves SE. Estrogen actions in the central nervous system. *Endocr Rev* (1999) 20(3):279–307. doi: 10.1210/edrv.20.3.0365

3. Dluzen DE, McDermott JL. Gender differences in neurotoxicity of the nigrostriatal dopaminergic system: Implications for Parkinson's disease. *J Gend Specif Med* (2000) 3(6):36–42.

4. Baum LW. Sex, hormones, and Alzheimer's disease. *J Gerontol A Biol Sci Med Sci* (2005) 60(6):736–43. doi: 10.1093/gerona/60.6.736

5. Zhu D, Montagne A, Zhao Z. Alzheimer's pathogenic mechanisms and underlying sex difference. *Cell Mol Life Sci* (2021) 78(11):4907–20. doi: 10.1007/s00018-021-03830-w

6. Yaşar P, Ayaz G, User SD, Güpür G, Muyan M. Molecular mechanism of estrogen-estrogen receptor signaling. *Reprod Med Biol* (2017) 16(1):4–20. doi: 10.1002/rmb2.12006

7. Szego CM, Davis JS. Adenosine 3',5'-monophosphate in rat uterus: Acute elevation by estrogen. *Proc Natl Acad Sci U S A* (1967) 58(4):1711–8. doi: 10.1073/pnas.58.4.1711

8. Szego EM, Barabás K, Balog J, Szilágyi N, Korach KS, Juhász G, et al. Estrogen induces estrogen receptor α-dependent camp response element-binding protein phosphorylation *via* mitogen activated protein kinase pathway in basal forebrain cholinergic neurons *in vivo*. *J Neurosci* (2006) 26(15):4104–10. doi: 10.1523/jneurosci.0222-06.2006

9. Wade CB, Dorsa DM. Estrogen activation of cyclic adenosine 5'-monophosphate response element-mediated transcription requires the extracellularly regulated kinase/mitogen-activated protein kinase pathway. *Endocrinology* (2003) 144(3):832–8. doi: 10.1210/en.2002-220899

10. Cheong RY, Kwakowsky A, Barad Z, Porteous R, Herbison AE, Ábrahám IM. Estradiol acts directly and indirectly on multiple signaling pathways to phosphorylate cAMP-response element binding protein in GnRH neurons. *Endocrinology* (2012) 153(8):3792–803. doi: 10.1210/en.2012-1232

11. Prossnitz ER, Barton M. The G-protein-coupled estrogen receptor GPER in health and disease. *Nat Rev Endocrinol* (2011) 7(12):715–26. doi: 10.1038/nrendo.2011.122

12. Toran-Allerand CD, Guan X, MacLusky NJ, Horvath TL, Diano S, Singh M, et al. ER-X: A novel, plasma membrane-associated, putative estrogen receptor that is regulated during development and after ischemic brain injury. *J Neurosci* (2002) 22(19):8391–401. doi: 10.1523/jneurosci.22-19-08391.2002

13. Qiu J, Bosch MA, Tobias SC, Grandy DK, Scanlan TS, Ronnekleiv OK, et al. Rapid signaling of estrogen in hypothalamic neurons involves a novel G-protein-coupled estrogen receptor that activates protein kinase c. *J Neurosci* (2003) 23(29):9529–40. doi: 10.1523/jneurosci.23-29-09529.2003

14. Khaksari M, Abbasloo E, Dehghan F, Soltani Z, Asadikaram G. The brain cytokine levels are modulated by estrogen following traumatic brain injury: Which estrogen receptor serves as modulator? *Int Immunopharmacol* (2015) 28(1):279–87. doi: 10.1016/j.intimp.2015.05.046

15. Cerciat M, Unkila M, Garcia-Segura LM, Arevalo MA. Selective estrogen receptor modulators decrease the production of interleukin-6 and interferon-gamma-inducible protein-10 by astrocytes exposed to inflammatory challenge *in vitro*. *Glia* (2010) 58(1):93–102. doi: 10.1002/glia.20904

16. Xiao Q, Luo Y, Lv F, He Q, Wu H, Chao F, et al. Protective effects of 17β-estradiol on hippocampal myelinated fibers in ovariectomized middle-aged rats. *Neuroscience* (2018) 385:143–53. doi: 10.1016/j.neuroscience.2018.06.006

17. He Q, Luo Y, Lv F, Xiao Q, Chao F, Qiu X, et al. Effects of estrogen replacement therapy on the myelin sheath ultrastructure of myelinated fibers in the white matter of middle-aged ovariectomized rats. *J Comp Neurol* (2018) 526(5):790–802. doi: 10.1002/cne.24366

18. Kumar S, Patel R, Moore S, Crawford DK, Suwanna N, Mangiardi M, et al. Estrogen receptor β ligand therapy activates PI3k/Akt/mTOR signaling in oligodendrocytes and promotes remyelination in a mouse model of multiple sclerosis. *Neurobiol Dis* (2013) 56:131–44. doi: 10.1016/j.nbd.2013.04.005

19. Feng J, Zhang G, Hu X, Si Chen C, Qin X. Estrogen inhibits estrogen receptor α-mediated Rho-kinase expression in experimental autoimmune encephalomyelitis rats. *Synapse* (2013) 67(7):399–406. doi: 10.1002/syn.21650

20. Khan MM, Wakade C, de Sevilla L, Brann DW. Selective estrogen receptor modulators (SERMS) enhance neurogenesis and spine density following focal cerebral ischemia. *J Steroid Biochem Mol Biol* (2015) 146:38–47. doi: 10.1016/j.jsbmb.2014.05.001

21. Saraceno GE, Bellini MJ, Garcia-Segura LM, Capani F. Estradiol activates PI3k/Akt/GSK3 pathway under chronic neurodegenerative conditions triggered by perinatal asphyxia. *Front Pharmacol* (2018) 9:335. doi: 10.3389/fphar.2018.00335

22. Rettberg JR, Yao J, Brinton RD. Estrogen: A master regulator of bioenergetic systems in the brain and body. *Front Neuroendocrinol* (2014) 35(1):8–30. doi: 10.1016/j.yfrne.2013.08.001

23. Simpkins JW, Yi KD, Yang S-H, Dykens JA. Mitochondrial mechanisms of estrogen neuroprotection. *BBA-GEN Subj* (2010) 1800(10):1113–20. doi: 10.1016/j.bbagen.2009.11.013

24. Yuan LJ, Wang XW, Wang HT, Zhang M, Sun JW, Chen WF. G protein-coupled estrogen receptor is involved in the neuroprotective effect of IGF-1 against MPTP/MPP(+)-induced dopaminergic neuronal injury. *J Steroid Biochem Mol Biol* (2019) 192:105384. doi: 10.1016/j.jsbmb.2019.105384

25. Arevalo MA, Azcoitia I, Garcia-Segura LM. The neuroprotective actions of oestradiol and oestrogen receptors. *Nat Rev Neurosci* (2015) 16(1):17–29. doi: 10.1038/nrn3856

26. Anderson GL, Limacher M, Assaf AR, Bassford T, Beresford SA, Black H, et al. Effects of conjugated equine estrogen in postmenopausal women with hysterectomy: The women's health initiative randomized controlled trial. *Jama* (2004) 291(14):1701–12. doi: 10.1001/jama.291.14.1701

27. Chlebowski RT, Anderson GL, Aragaki AK, Manson JE, Stefanick ML, Pan K, et al. Association of menopausal hormone therapy with breast cancer incidence and mortality during long-term follow-up of the women's health initiative randomized clinical trials. *Jama* (2020) 324(4):369–80. doi: 10.1001/jama.2020.9482

28. Rossouw JE. Prescribing postmenopausal hormone therapy to women in their 50s in the post-women's health initiative era. *Maturitas* (2010) 65(3):179–80. doi: 10.1016/j.maturitas.2009.11.012

29. Maximov PY, Lee TM, Jordan VC. The discovery and development of selective estrogen receptor modulators (SERMS) for clinical practice. *Curr Clin Pharmacol* (2013) 8(2):135–55. doi: 10.2174/1574884711308020006

30. Lebesgue D, Traub M, De Butte-Smith M, Chen C, Zukin RS, Kelly MJ, et al. Acute administration of non-classical estrogen receptor agonists attenuates ischemia-induced hippocampal neuron loss in middle-aged female rats. *PloS One* (2010) 5(1):e8642. doi: 10.1371/journal.pone.0008642

31. Amirkhosravi L, Khaksari M, Soltani Z, Esmaeili-Mahani S, Asadi Karam G, Hoseini M. E2-BSA and G1 exert neuroprotective effects and improve behavioral abnormalities following traumatic brain injury: The role of classic and non-classic estrogen receptors. *Brain Res* (2021) 1750:147168. doi: 10.1016/j.brainres.2020.147168

32. Liu JH. Selective estrogen receptor modulators (SERMS): Keys to understanding their function. *Menopause* (2020) 27(10):1171–6. doi: 10.1097/gme.0000000000001585

33. Wessler S, Otto C, Wilck N, Stangl V, Fritzemeier KH. Identification of estrogen receptor ligands leading to activation of non-genomic signaling pathways while exhibiting only weak transcriptional activity. *J Steroid Biochem Mol Biol* (2006) 98(1):25–35. doi: 10.1016/j.jsbmb.2005.08.003

34. Kousteni S, Bellido T, Plotkin LI, O'Brien CA, Bodenner DL, Han L, et al. Nongenotropic, sex-nonspecific signaling through the estrogen or androgen receptors: Dissociation from transcriptional activity. *Cell* (2001) 104(5):719–30. doi: 10.1016/S0092-8674(01)00268-9

35. Koszegi Z, Szego EM, Cheong RY, Tolod-Kemp E, Abraham IM. Postlesion estradiol treatment increases cortical cholinergic innervations *via* estrogen receptor-α dependent nonclassical estrogen signaling *in vivo*. *Endocrinology* (2011) 152(9):3471–82. doi: 10.1210/en.2011-1017

36. Kwakowsky A, Potapov K, Kim S, Peppercorn K, Tate WP, Ábrahám IM. Treatment of β amyloid 1-42 (Aβ(1-42))-induced basal forebrain cholinergic damage by a non-classical estrogen signaling activator *in vivo*. *Sci Rep* (2016) 6:21101. doi: 10.1038/srep21101

37. Li R, He P, Cui J, Staufenbiel M, Harada N, Shen Y. Brain endogenous estrogen levels determine responses to estrogen replacement therapy *via* regulation of BACE1 and NEP in female Alzheimer's transgenic mice. *Mol Neurobiol* (2013) 47(3):857–67. doi: 10.1007/s12035-012-8377-3

38. Xu H, Wang R, Zhang YW, Zhang X. Estrogen, β-amyloid Metabolism/Trafficking, and Alzheimer's disease. *Ann N Y Acad Sci* (2006) 1089:324–42. doi: 10.1196/annals.1386.036

39. Yue X, Lu M, Lancaster T, Cao P, Honda S, Staufenbiel M, et al. Brain estrogen deficiency accelerates Aβ plaque formation in an Alzheimer's disease animal model. *Proc Natl Acad Sci U S A* (2005) 102(52):19198–203. doi: 10.1073/pnas.0505203102

40. Jayaraman A, Carroll JC, Morgan TE, Lin S, Zhao L, Arimoto JM, et al. 17β-estradiol and progesterone regulate expression of β-amyloid clearance factors in primary neuron cultures and female rat brain. *Endocrinology* (2012) 153(11):5467–79. doi: 10.1210/en.2012-1464

41. Xu H, Gouras GK, Greenfield JP, Vincent B, Naslund J, Mazzarelli L, et al. Estrogen reduces neuronal generation of Alzheimer β-amyloid peptides. *Nat Med* (1998) 4(4):447–51. doi: 10.1038/nm0498-447

42. Petanceska SS, Nagy V, Frail D, Gandy S. Ovariectomy and 17β-estradiol modulate the levels of Alzheimer's amyloid β peptides in brain. *Exp Gerontol* (2000) 35(9-10):1317–25. doi: 10.1016/s0531-5565(00)00157-1

43. Kim JY, Mo H, Kim J, Kim JW, Nam Y, Rim YA, et al. Mitigating effect of estrogen in Alzheimer's disease-mimicking cerebral organoid. *Front Neurosci* (2022) 16:816174. doi: 10.3389/fnins.2022.816174

44. Zhang S, Huang Y, Zhu YC, Yao T. Estrogen stimulates release of secreted amyloid precursor protein from primary rat cortical neurons *via* protein kinase C pathway. *Acta Pharmacol Sin* (2005) 26(2):171–6. doi: 10.1111/j.1745-7254.2005.00538.x

45. Manthey D, Heck S, Engert S, Behl C. Estrogen induces a rapid secretion of amyloid β precursor protein *via* the mitogen-activated protein kinase pathway. *Eur J Biochem* (2001) 268(15):4285–91. doi: 10.1046/j.1432-1327.2001.02346.x

46. Fitzpatrick JL, Mize AL, Wade CB, Harris JA, Shapiro RA, Dorsa DM. Estrogen-mediated neuroprotection against β-amyloid toxicity requires expression of estrogen receptor α or β and activation of the MAPK pathway. *J Neurochem* (2002) 82(3):674–82. doi: 10.1046/j.1471-4159.2002.01000.x

47. Liu XA, Zhu LQ, Zhang Q, Shi HR, Wang SH, Wang Q, et al. Estradiol attenuates tau hyperphosphorylation induced by upregulation of protein kinase-A. *Neurochem Res* (2008) 33(9):1811–20. doi: 10.1007/s11064-008-9638-4

48. Zhang QG, Wang R, Khan M, Mahesh V, Brann DW. Role of dickkopf-1, an antagonist of the WNT/β-catenin signaling pathway, in estrogen-induced neuroprotection and attenuation of tau phosphorylation. *J Neurosci* (2008) 28 (34):8430–41. doi: 10.1523/JNEUROSCI.2752-08.2008

49. Shughrue PJ, Scrimo PJ, Merchenthaler I. Estrogen binding and estrogen receptor characterization (ER α and ER β) in the cholinergic neurons of the rat basal forebrain. *Neuroscience* (2000) 96:41–9. doi: 10.1016/S0306-4522(99)00520-5

50. Miettinen RA, Kalesnykas G, Koivisto EH. Estimation of the total number of cholinergic neurons containing estrogen receptor-α in the rat basal forebrain. *J Histochem Cytochem* (2002) 50(7):891–902. doi: 10.1177/002215540205000703

51. Pongrac JL, Gibbs RB, Defranco DB. Estrogen-mediated regulation of cholinergic expression in basal forebrain neurons requires extracellular-signal-regulated kinase activity. *Neuroscience* (2004) 124(4):809–16. doi: 10.1016/j.neuroscience.2004.01.013

52. Brinton RD. Estrogen-induced plasticity from cells to circuits: Predictions for cognitive function. *Trends Pharmacol Sci* (2009) 30(4):212–22. doi: 10.1016/j.tips.2008.12.006

53. Hojo Y, Munetomo A, Mukai H, Ikeda M, Sato R, Hatanaka Y, et al. Estradiol rapidly modulates spinogenesis in hippocampal dentate gyrus: Involvement of kinase networks. *Hormones Behav* (2015) 74:149–56. doi: 10.1016/j.yhbeh.2015.06.008

54. Sheppard PAS, Choleris E, Galea LAM. Structural plasticity of the hippocampus in response to estrogens in female rodents. *Mol Brain* (2019) 12 (1):22. doi: 10.1186/s13041-019-0442-7

55. Carroll JC, Pike CJ. Selective estrogen receptor modulators differentially regulate Alzheimer-like changes in female 3xTg-AD mice. *Endocrinology* (2008) 149(5):2607–11. doi: 10.1210/en.2007-1346

56. Lai YJ, Zhu BL, Sun F, Luo D, Ma YL, Luo B, et al. Estrogen receptor α promotes Cav1.2 ubiquitination and degradation in neuronal cells and in APP/PS1 mice. *Aging Cell* (2019) 18(4):e12961. doi: 10.1111/acel.12961

57. Tschiffely AE, Schuh RA, Prokai-Tatrai K, Prokai L, Ottinger MA. A comparative evaluation of treatments with 17β-estradiol and its brain-selective prodrug in a double-transgenic mouse model of Alzheimer's disease. *Hormones Behav* (2016) 83:39–44. doi: 10.1016/j.yhbeh.2016.05.009

58. Cordey M, Gundimeda U, Gopalakrishna R, Pike CJ. The synthetic estrogen 4-Estren-3 α,17 β-diol (Estren) induces estrogen-like neuroprotection. *Neurobiol Dis* (2005) 19(1-2):331–9. doi: 10.1016/j.nbd.2005.01.011

59. Kwakowsky A, Koszegi Z, Cheong RY, Abraham IM. Neuroprotective effects of non-classical estrogen-like signaling activators: From mechanism to potential implications. *CNS Neurol Disord Drug Targets* (2013) 12(8):1219–25. doi: 10.2174/18715273113120012 3

60. Fernandez SM, Lewis MC, Pechenino AS, Harburger LL, Orr PT, Gresack JE, et al. Estradiol-induced enhancement of object memory consolidation involves hippocampal extracellular signal-regulated kinase activation and membrane-bound estrogen receptors. *J Neurosci* (2008) 28(35):8660–7. doi: 10.1523/jneurosci.1968-08.2008

61. Zhao Z, Fan L, Frick KM. Epigenetic alterations regulate estradiol-induced enhancement of memory consolidation. *Proc Natl Acad Sci U.S.A.* (2010) 107 (12):5605–10. doi: 10.1073/pnas.0910578107

62. Fortress AM, Fan L, Orr PT, Zhao Z, Frick KM. Estradiol-induced object recognition memory consolidation is dependent on activation of mTOR signaling in the dorsal hippocampus. *Learn Mem* (2013) 20(3):147–55. doi: 10.1101/lm.026732.112

63. Srivastava DP, Woolfrey KM, Penzes P. Insights into rapid modulation of neuroplasticity by brain estrogens. *Pharmacolo Rev* (2013) 65(4):1318–50. doi: 10.1124/pr.111.005272

64. Fan L, Zhao Z, Orr PT, Chambers CH, Lewis MC, Frick KM. Estradiol-induced object memory consolidation in middle-aged female mice requires dorsal hippocampal extracellular signal-regulated kinase and phosphatidylinositol 3-kinase activation. *J Neurosci* (2010) 30(12):4390–400. doi: 10.1523/jneurosci.4333-09.2010

65. Jacobsen DE, Samson MM, Emmelot-Vonk MH, Verhaar HJ. Raloxifene improves verbal memory in late postmenopausal women: A randomized, double-blind, placebo-controlled trial. *Menopause* (2010) 17(2):309–14. doi: 10.1097/gme.0b013e3181bd54df

66. Yaffe K, Krueger K, Cummings SR, Blackwell T, Henderson VW, Sarkar S, et al. Effect of raloxifene on prevention of dementia and cognitive impairment in older women: The multiple outcomes of raloxifene evaluation (MORE) randomized trial. *Am J Psychiatry* (2005) 162(4):683–90. doi: 10.1176/appi.ajp.162.4.683

67. Nickelsen T, Lufkin EG, Riggs BL, Cox DA, Crook TH. Raloxifene hydrochloride, a selective estrogen receptor modulator: Safety assessment of effects on cognitive function and mood in postmenopausal women. *Psychoneuroendocrinology* (1999) 24(1):115–28. doi: 10.1016/s0306-4530(98)00041-9

68. Kubota T, Matsumoto H, Kirino Y. Ameliorative effect of membrane-associated estrogen receptor G protein coupled receptor 30 activation on object recognition memory in mouse models of Alzheimer's disease. *J Pharmacol Sci* (2016) 131(3):219–22. doi: 10.1016/j.jphs.2016.06.005

69. Gray NE, Zweig JA, Kawamoto C, Quinn JF, Copenhaver PF. STX, a novel membrane estrogen receptor ligand, protects against amyloid-β toxicity. *J Alzheimers Dis* (2016) 51(2):391–403. doi: 10.3233/JAD-150756

70. Deng LJ, Cheng C, Wu J, Wang CH, Zhou HB, Huang J. Oxabicycloheptene sulfonate protects against β-Amyloid-Induced toxicity by activation of PI3k/Akt and ERK signaling pathways *via* GPER1 in C6 cells. *Neurochem Res* (2017) 42 (8):2246–56. doi: 10.1007/s11064-017-2237-5

71. Wnuk A, Przepiorska K, Rzemieniec J, Pietrzak B, Kajta M. Selective targeting of non-nuclear estrogen receptors with PaPE-1 as a new treatment strategy for Alzheimer's disease. *Neurotox Res* (2020) 38(4):957–66. doi: 10.1007/s12640-020-00289-8

72. Selvaraj UM, Zuurbier KR, Whoolery CW, Plautz EJ, Chambliss KL, Kong X, et al. Selective nonnuclear estrogen receptor activation decreases stroke severity and promotes functional recovery in female mice. *Endocrinology* (2018) 159 (11):3848–59. doi: 10.1210/en.2018-00600

73. Stocchi F, Olanow CW. Obstacles to the development of a neuroprotective therapy for Parkinson's disease. *Mov Disord* (2013) 28(1):3–7. doi: 10.1002/mds.25337

74. Cotzias GC, Papavasiliou PS, Gellene R. L-DOPA in Parkinson's syndrome. *N Engl J Med* (1969) 281(5):272. doi: 10.1056/NEJM196907312810518

75. Olanow CW, Stocchi F. Levodopa: A new look at an old friend. *Mov Disord* (2018) 33(6):859–66. doi: 10.1002/mds.27216

76. Saunders-Pullman R, Gordon-Elliott J, Parides M, Fahn S, Saunders HR, Bressman S. The effect of estrogen replacement on early Parkinson's disease. *Neurology* (1999) 52(7):1417–21. doi: 10.1212/wnl.52.7.1417

77. Song YJ, Li SR, Li XW, Chen X, Wei ZX, Liu QS, et al. The effect of estrogen replacement therapy on Alzheimer's disease and Parkinson's disease in postmenopausal women: A meta-analysis. *Front Neurosci* (2020) 14:157. doi: 10.3389/fnins.2020.00157

78. Callier S, Le Saux M, Lhiaubet AM, Di Paolo T, Rostene W, Pelaprat D. Evaluation of the protective effect of oestradiol against toxicity induced by 6-hydroxydopamine and 1-Methyl-4-Phenylpyridinium ion (MPP+) towards dopaminergic mesencephalic neurones in primary culture. *J Neurochem* (2002) 80(2):307–16. doi: 10.1046/j.0022-3042.2001.00693.x

79. Becker JB, Rudick CN. Rapid effects of estrogen or progesterone on the amphetamine-induced increase in striatal dopamine are enhanced by estrogen priming: A microdialysis study. *Pharmacol Biochem Behav* (1999) 64(1):53–7. doi: 10.1016/s0091-3057(99)00091-x

80. Sawada H, Ibi M, Kihara T, Honda K, Nakamizo T, Kanki R, et al. Estradiol protects dopaminergic neurons in a MPP+Parkinson's disease model. *Neuropharmacology* (2002) 42(8):1056–64. doi: 10.1016/s0028-3908(02)00049-7

81. Hwang CJ, Choi DY, Jung YY, Lee YJ, Yun JS, Oh KW, et al. Inhibition of P38 pathway-dependent MPTP-induced dopaminergic neurodegeneration in estrogen receptor α knockout mice. *Horm Behav* (2016) 80:19–29. doi: 10.1016/j.yhbeh.2016.01.011

82. Yoest KE, Cummings JA, Becker JB. Oestradiol influences on dopamine release from the nucleus accumbens shell: Sex differences and the role of selective oestradiol receptor subtypes. *Br J Pharmacol* (2019) 176(21):4136–48. doi: 10.1111/bph.14531

83. Liu B, Dluzen DE. Oestrogen and nigrostriatal dopaminergic neurodegeneration: Animal models and clinical reports of Parkinson's disease. *Clin Exp Pharmacol Physiol* (2007) 34(7):555–65. doi: 10.1111/j.1440-1681.2007.04616.x

84. Gillies GE, McArthur S. Estrogen actions in the brain and the basis for differential action in men and women: A case for sex-specific medicines. *Pharmacol Rev* (2010) 62(2):155–98. doi: 10.1124/pr.109.002071

85. Gillies GE, McArthur S. Independent influences of sex steroids of systemic and central origin in a rat model of Parkinson's disease: A contribution to sex-specific neuroprotection by estrogens. *Horm Behav* (2010) 57(1):23–34. doi: 10.1016/j.yhbeh.2009.06.002

86. D'Astous M, Morissette M, Di Paolo T. Effect of estrogen receptor agonists treatment in MPTP mice: Evidence of neuroprotection by an ER α agonist. *Neuropharmacology* (2004) 47(8):1180–8. doi: 10.1016/j.neuropharm.2004.08.020

87. Baraka AM, Korish AA, Soliman GA, Kamal H. The possible role of estrogen and selective estrogen receptor modulators in a rat model of Parkinson's disease. *Life Sci* (2011) 88(19-20):879–85. doi: 10.1016/j.lfs.2011.03.010

88. Yadav SK, Pandey S, Singh B. Role of estrogen and levodopa in 1-Methyl-4-Pheny-L-1, 2, 3, 6-tetrahydropyridine (MPTP)-induced cognitive deficit in parkinsonian ovariectomized mice model: A comparative study. *J Chem Neuroanat* (2017) 85:50–9. doi: 10.1016/j.jchemneu.2017.07.002

89. Callier S, Morissette M, Grandbois M, Pélaprat D, Di Paolo T. Neuroprotective properties of 17β-estradiol, progesterone, and raloxifene in MPTP C57BL/6 mice. *Synapse* (2001) 41(2):131–8. doi: 10.1002/syn.1067

90. Bourque M, Morissette M, Di Paolo T. Raloxifene activates G protein-coupled estrogen receptor 1/Akt signaling to protect dopamine neurons in 1-Methyl-4-Phenyl-1,2,3,6-Tetrahydropyridine mice. *Neurobiol Aging* (2014) 35 (10):2347–56. doi: 10.1016/j.neurobiolaging.2014.03.017

91. Ramirez AD, Liu X, Menniti FS. Repeated estradiol treatment prevents MPTP-induced dopamine depletion in male mice. *Neuroendocrinology* (2003) 77 (4):223–31. doi: 10.1159/000070277

92. Rajsombath MM, Nam AY, Ericsson M, Nuber S. Female sex and brain-selective estrogen benefit α-synuclein tetramerization and the PD-like motor syndrome in 3K transgenic mice. *J Neurosci* (2019) 39(38):7628–40. doi: 10.1523/JNEUROSCI.0313-19.2019

93. Thadathil N, Xiao J, Hori R, Alway SE, Khan MM. Brain selective estrogen treatment protects dopaminergic neurons and preserves behavioral function in MPTP-induced mouse model of Parkinson's disease. *J Neuroimmune Pharmacol* (2021) 16(3):667–78. doi: 10.1007/s11481-020-09972-1

94. Prokai L, Nguyen V, Szarka S, Garg P, Sabnis G, Bimonte-Nelson HA, et al. The prodrug DHED selectively delivers 17beta-estradiol to the brain for treating estrogen-responsive disorders. *Sci Transl Med* (2015) 7(297):297ra113. doi: 10.1126/scitranslmed.aab1290

95. Graham NS, Sharp DJ. Understanding neurodegeneration after traumatic brain injury: From mechanisms to clinical trials in dementia. *J Neurol Neurosurg Psychiatry* (2019) 90(11):1221–33. doi: 10.1136/jnnp-2017-317557

96. Maas AIR, Stocchetti N, Bullock R. Moderate and severe traumatic brain injury in adults. *Lancet Neurol* (2008) 7(8):728–41. doi: 10.1016/S1474-4422(08)70164-9

97. Feigin VL, Stark BA, Johnson CO, Roth GA, Bisignano C, Abady GG, et al. Global, regional, and national burden of stroke and its risk factors, 1990–2019: A systematic analysis for the global burden of disease study 2019. *Lancet Neurol* (2021) 20(10):795–820. doi: 10.1016/S1474-4422(21)00252-0

98. Armstead WM, Kiessling JW, Kofke WA, Vavilala MS. Impaired cerebral blood flow autoregulation during posttraumatic arterial hypotension after fluid percussion brain injury is prevented by phenylephrine in female but exacerbated in male piglets by extracellular signal-related kinase mitogen-activated protein kinase upregulation. *Crit Care Med* (2010) 38(9):1868–74. doi: 10.1097/CCM.0b013e3181e8ac1a

99. Groswasser Z, Cohen M, Keren O. Female TBI patients recover better than males. *Brain Inj* (1998) 12(9):805–8. doi: 10.1080/026990598122197

100. Khaksari M, Soltani Z, Shahrokhi N. Effects of female sex steroids administration on pathophysiologic mechanisms in traumatic brain injury. *Transl Stroke Res* (2018) 9(4):393–416. doi: 10.1007/s12975-017-0588-5

101. Saldanha CJ, Duncan KA, Walters BJ. Neuroprotective actions of brain aromatase. *Front Neuroendocrinol* (2009) 30(2):106–18. doi: 10.1016/j.yfrne.2009.04.016

102. Garcia-Segura LM, Veiga S, Sierra A, Melcangi RC, Azcoitia I. Aromatase: A neuroprotective enzyme. *Prog Neurobiol* (2003) 71(1):31–41. doi: 10.1016/j.pneurobio.2003.09.005

103. Lu H, Ma K, Jin L, Zhu H, Cao R. 17β-estradiol rescues damages following traumatic brain injury from molecule to behavior in mice. *J Cell Physiol* (2018) 233 (2):1712–22. doi: 10.1002/jcp.26083

104. Zhang B, Subramanian S, Dziennis S, Jia J, Uchida M, Akiyoshi K, et al. Estradiol and G1 reduce infarct size and improve immunosuppression after experimental stroke. *J Immunol* (2010) 184(8):4087–94. doi: 10.4049/jimmunol.0902339

105. Khatri N, Thakur M, Pareek V, Kumar S, Sharma S, Datusalia AK. Oxidative stress: Major threat in traumatic brain injury. *CNS Neurol Disord Drug Targets* (2018) 17(9):689–95. doi: 10.2174/1871527317666180627120501

106. Naderi V, Khaksari M, Abbasi R, Maghool F. Estrogen provides neuroprotection against brain edema and blood brain barrier disruption through both estrogen receptors α and β following traumatic brain injury. *Iran J Basic Med Sci* (2015) 18(2):138–44. doi: 10.22038/IJBMS.2015.4015

107. Khaksari M, Hajializadeh Z, Shahrokhi N, Esmaeili-Mahani S. Changes in the gene expression of estrogen receptors involved in the protective effect of estrogen in rat'S trumatic brain injury. *Brain Res* (2015) 1618:1–8. doi: 10.1016/j.brainres.2015.05.017

108. Day NL, Floyd CL, D'Alessandro TL, Hubbard WJ, Chaudry IH. 17β-estradiol confers protection after traumatic brain injury in the rat and involves activation of G protein-coupled estrogen receptor 1. *J Neurotrauma* (2013) 30 (17):1531–41. doi: 10.1089/neu.2013.2854

109. Wang ZF, Pan ZY, Xu CS, Li ZQ. Activation of G-protein coupled estrogen receptor 1 improves early-onset cognitive impairment *via* PI3k/Akt pathway in rats with traumatic brain injury. *Biochem Biophys Res Commun* (2017) 482(4):948–53. doi: 10.1016/j.bbrc.2016.11.138

110. Pan MX, Tang JC, Liu R, Feng YG, Wan Q. Effects of estrogen receptor GPR30 agonist G1 on neuronal apoptosis and microglia polarization in traumatic brain injury rats. *Chin J Traumatol* (2018) 21(4):224–8. doi: 10.1016/j.cjtee.2018.04.003

111. Kosaka Y, Quillinan N, Bond C, Traystman R, Hurn P, Herson P. GPER1/GPR30 activation improves neuronal survival following global cerebral ischemia induced by cardiac arrest in mice. *Transl Stroke Res* (2012) 3(4):500–7. doi: 10.1007/s12975-012-0211-8

112. Wang XS, Yue J, Hu LN, Tian Z, Zhang K, Yang L, et al. Activation of G protein-coupled receptor 30 protects neurons by regulating autophagy in astrocytes. *Glia* (2020) 68(1):27–43. doi: 10.1002/glia.23697

113. Wnuk A, Przepiórska K, Pietrzak BA, Kajta M. Posttreatment strategy against hypoxia and ischemia based on selective targeting of nonnuclear estrogen receptors with PaPE-1. *Neurotox Res* (2021) 39(6):2029–41. doi: 10.1007/s12640-021-00441-y

114. Jover-Mengual T, Castelló-Ruiz M, Burguete MC, Jorques M, López-Morales MA, Aliena-Valero A, et al. Molecular mechanisms mediating the neuroprotective role of the selective estrogen receptor modulator, bazedoxifene, in acute ischemic stroke: A comparative study with 17β-estradiol. *J Steroid Biochem Mol Biol* (2017) 171:296–304. doi: 10.1016/j.jsbmb.2017.05.001

115. Lozano D, Gonzales-Portillo GS, Acosta S, de la Pena I, Tajiri N, Kaneko Y, et al. Neuroinflammatory responses to traumatic brain injury: Etiology, clinical consequences, and therapeutic opportunities. *Neuropsychiatr Dis Treat* (2015) 11:97–106. doi: 10.2147/ndt.S65815

116. Witcher KG, Bray CE, Chunchai T, Zhao F, O'Neil SM, Gordillo AJ, et al. Traumatic brain injury causes chronic cortical inflammation and neuronal dysfunction mediated by microglia. *J Neurosci* (2021) 41(7):1597–616. doi: 10.1523/jneurosci.2469-20.2020

117. Maida CD, Norrito RL, Daidone M, Tuttolomondo A, Pinto A. Neuroinflammatory mechanisms in ischemic stroke: Focus on cardioembolic stroke, background, and therapeutic approaches. *Int J Mol Sci* (2020) 21 (18):6454. doi: 10.3390/ijms21186454

frontiers | Frontiers in Endocrinology

TYPE Review
PUBLISHED 20 September 2022
DOI 10.3389/fendo.2022.982551

OPEN ACCESS

EDITED BY
Bianca Bianco,
Faculdade de Medicina do ABC,
Brazil

REVIEWED BY
Antonio Simone Laganà,
University of Palermo, Italy
Marieke R. Gilmartin,
Marquette University, United States

*CORRESPONDENCE
Dora Reglodi
dora.reglodi@aok.pte.hu

SPECIALTY SECTION
This article was submitted to Reproduction, a section of the journal Frontiers in Endocrinology

RECEIVED 30 June 2022
ACCEPTED 31 August 2022
PUBLISHED 20 September 2022

CITATION
Koppan M, Nagy Z, Bosnyak I and Reglodi D (2022) Female reproductive functions of the neuropeptide PACAP. *Front. Endocrinol.* 13:982551. doi: 10.3389/fendo.2022.982551

Female reproductive functions of the neuropeptide PACAP

Miklos Koppan[1], Zsuzsanna Nagy[2], Inez Bosnyak[3] and Dora Reglodi[3]*

[1]Maternity Clinic, Budapest, Hungary, [2]Department of Physiology, University of Pecs Medical School, Pécs, Hungary, [3]Department of Anatomy, ELKH-PTE PACAP Research Group and Szentagothai Research Center, University of Pecs Medical School, Pécs, Hungary

Pituitary adenylate cyclase activating polypeptide (PACAP) is a neuropeptide originally isolated as a hypothalamic peptide. It has a widespread distribution in the body and has a diverse spectrum of actions. Among other processes, PACAP has been shown to be involved in reproduction. In this review we summarize findings related to the entire spectrum of female reproduction. PACAP is a regulatory factor in gonadal hormone production, influences follicular development and plays a role in fertilization and embryonic/placental development. Furthermore, PACAP is involved in hormonal changes during and after birth and affects maternal behavior. Although most data come from cell cultures and animal experiments, increasing number of evidence suggests that similar effects of PACAP can be found in humans. Among other instances, PACAP levels show changes in the serum during pregnancy and birth. PACAP is also present in the human follicular and amniotic fluids and in the milk. Levels of PACAP in follicular fluid correlate with the number of retrieved oocytes in hyperstimulated women. Human milk contains very high levels of PACAP compared to plasma levels, with colostrum showing the highest concentration, remaining steady thereafter for the first 7 months of lactation. All these data imply that PACAP has important functions in reproduction both under physiological and pathological conditions.

KEYWORDS
PACAP, GnRH, LH, FSH, ovary, placenta

Introduction

PACAP was discovered in the laboratory of professor Arimura in 1989 (1). The discovery was based on finding a novel hypothalamic peptide that stimulated anterior pituitary cells in addition to the already known releasing hormones. This led to the isolation of a peptide composed of 38 amino acid residues, named PACAP38, from ovine hypothalamic extracts. This was followed by the isolation of a shorter form with 27 amino acids, named PACAP27 (2).The name PACAP comes from the abbreviation of pituitary

adenylate cyclase activating polypeptide, referring to the first described action, in which it stimulates adenylate cyclase activity, and thus, cAMP in the pituitary gland. Both peptides show structural homology to the vasoactive intestinal peptide (VIP) and they belong to the VIP/secretin/glucagon peptide family.

PACAP acts through G protein-coupled receptors, namely the specific PAC1 and VPAC1 and VPAC2, which also bind VIP with equal affinity (2). PACAP activates mainly the adenylate cyclase/cAMP pathways, and through this, the activation of its receptors lead to activation of protein kinase A (PKA) and downstream pathways (3). It also activates several other pathways (4) and transactivates tyrosine kinase receptors (5). Moreover, PACAP38 (but not PACAP27) can enter through the cell membrane without receptorial mechanism, but the intracellular signaling activated this way has not been elucidated yet (6). The specific PAC1 receptor has several splice variants, inducing different signaling pathways, and thus, leading to different, sometimes opposing effects (2, 7).

PACAP and its receptors have widespread occurrence and thus, PACAP can exert variable biological actions. In the nervous system, it acts as a neurohormone and neuromodulator, and several different effects have been described. Among others, it plays a role in neuronal development like patterning of the neural tube, proliferation and migration of cortical and cerebellar neurons, axonal growth and glial cell maturation (8). These effects can also be observed in the mature nervous system in case of injuries, when PACAP can exert neuroprotective effects (9–12). Several other neuronal processes are influenced by PACAP: it has been shown to play a role in stress and anxiety responses (13), in diminishing the negative consequences of aversive events (14), it influences central energy homeostasis (15, 16), thermoregulation (17) and memory (18). In the periphery (19, 20), several actions have been described regarding the cardiovascular system, where the peptide influences cardiac neuronal excitability and heart muscle contractility (21). In the gastrointestinal and respiratory tract PACAP plays a role in neuroendocrine secretion, smooth muscle contractility and blood supply (22, 23). Endocrine glands show high levels of expression of PACAP and the peptide is involved in secretion of several hormones (19–23).

Regarding reproductive functions, several lines of evidence show that the peptide centrally regulates gonadal hormones as well as acts in the periphery, the ovary, the placenta, the mammary gland and the uterus. Male reproductive functions are also known to be influenced by PACAP at both central and peripheral levels. At central level, PACAP influences hypothalamic and hypophyseal gonadal hormone secretion, while in the periphery, PACAP regulates spermatogenesis at various stages (24–26), influences sperm cell motility (27), and modulates Leydig and Sertoli cell functions (28–30). The reproductive functions of PACAP seem to be evolutionarily conserved, as it has also been revealed in several non-mammalian species (31). In seasonal animals, PACAP expression and effects are season-dependent (32), while in non-seasonal breeding species, the PACAP system shows alterations throughout the life-span, before and after puberty, during the hormonal cycle and during pregnancy (33). The aim of the present mini-review is to summarize findings regarding the effects of PACAP in the female reproductive system.

PACAP in the central regulation of female reproductive functions

Soon after the discovery of PACAP it became evident that the neuropeptide plays a role in modulating the secretion of releasing hormones, such as the main hypothalamic hormone playing a role in gonadal regulation, gonadotropin-releasing hormone (GnRH) and pituitary hormones, including follicle-stimulating hormone (FSH) and luteinizing hormone (LH) influencing peripheral reproductive functions. Early studies revealed that PACAP occurs at highest concentrations in the hypothalamus, although several other brain areas express significant amount of the peptide as well (2). Hypothalamic neuronal endings release PACAP in the median eminence where the primary capillary plexus of the hypophyseal portal system is found. The concentration of PACAP in the hypophyseal portal venous blood has been shown to be higher than in the periphery, proving the release and transport of the peptide to the adenohypophysis (34). PACAP is thus carried *via* the portal vessels to the anterior pituitary where it acts, among others, on the gonadotroph cells. Strong PACAP immunoreactivity was found in several hypothalamic nuclei, such as arcuate, dorsomedial, ventromedial, paraventricular nuclei, lateral and preoptic hypothalamic areas. mRNA has also been shown in the perikarya of some of these nuclei. Regarding PACAP binding sites, receptors PAC1 and VPAC1/2 are present in many brain areas. In the hypothalamus, receptors have been identified in the arcuate, dorsomedial, ventromedial, paraventricular, supraoptic, preoptic and suprachiasmatic nuclei, in the lateral hypothalamic area and in the mamillary bodies. These data mostly come from rat experiments, but subsequent studies have also mapped PACAP and its receptors in several other species, including the human brain (35–37). Distribution of PACAP in the human hypothalamic nuclei closely resembles that described in rodents (35), underlining the translational value of the rodent studies. Various hypothalamic functions are influenced by PACAP. For example, PACAP is involved in the hypothalamic regulation of body temperature (38, 39), food and water intake (40–43), energy homeostasis (16, 44) and in the circadian rhythmic activity of the suprachiasmatic nucleus (45). All these hypothalamic actions are in a complex interplay with the regulatory mechanisms of reproductive functions.

The hypothalamic nuclei playing a role in the hypothalamo-hypophyseal hormonal system can be divided into

magnocellular and parvocellular nuclei. Magnocellular nuclei are the supraoptic and paraventricular nuclei that produce vasopressin and oxytocin, both of which are transported by axonal transport *via* the hypothalamohypophyseal tract to the posterior lobe of the pituitary gland, where they are released into the bloodstream. High expression of both PACAP and its receptors are found in these nuclei. Intracerebral injection of PACAP increases activity of these neurons and plasma vasopressin levels (46–48). PACAP increases oxytocin and vasopressin release in the posterior lobe of the hypophysis (49). Parvocellular nuclei of the hypothalamus are mainly involved in the production of releasing hormones that influence the production of anterior pituitary trophic hormones, such as FSH, LH, thyroid-stimulating hormone (TSH), adrenocorticotropic hormone (ACTH), growth hormone (GH) and prolactin (PRL). The main parvocellular nuclei are the ventromedial, dorsomedial, preoptic, arcuate nuclei and the parvocellular part of the paraventricular nucleus. PACAP has been proven to act as a modulator and transmitter in the regulation of hypophysiotropic hormones in the parvocellular system (2). Several lines of evidence prove that PACAP is involved in the GnRH-gonadotropin axis (50, 51). PACAP leads to an increase in the gene expression of GnRH, somatostatin and corticotrope-releasing hormone (CRH), while the injection of the PACAP antagonist PACAP6-38 inhibits this increase.

In the adenohypophysis, PACAP receptors are found in all endocrine cells and also in folliculostellate cells (2). Moore et al. (52) investigated the expression of PACAP mRNA during the estrus cycle. They found that PACAP mRNA expression in the paraventricular nucleus and pituitary shows significant changes during the estrous cycle, with the greatest alterations on the day of proestrus. PACAP mRNA in the paraventricular nucleus decreases on the morning of diestrus, while increases 3 h prior to the gonadotropin surge and then declines in proestrus. A moderate decline at the time of the gonadotropin surge on the afternoon of proestrus and an increase later in the evening was observed in the pituitary. Expression of the follistatin mRNA increased following the rise in pituitary PACAP mRNA, after the secondary surge in FSH beta (Fshb) gene expression. They concluded that PACAP is involved in events before and after the gonadotropin surge, possibly through increased sensitivity to GnRH and suppression of Fshb subunit expression, similarly to *in vitro* observations (52). Others have also confirmed the rise of PACAP in the anterior pituitary during proestrus (53–55).

Early studies have shown that PACAP stimulates release of GH, ACTH, LH, FSH and PRL (2). PACAP can alone stimulate LH and FSH but also acts synergistically with GnRH (2). PACAP also stimulates GnRH receptor gene promoter activity, while GnRH stimulates PACAP gene expression, highlighting the complex relationship between PACAP and GnRH systems (2). This complexity is further deepened by the somewhat contradictory results regarding the relationship between PACAP, GnRH and the gonadotrophs. Although some studies found no effect of intravenous PACAP administration on LH levels (56, 57), the same authors described inhibition of the LH surge when PACAP was administered intracerebroventricularly. Interestingly, PACAP27 and 38 had opposing effects: while PACAP38 inhibited LH surge, PACAP27 elevated LH plasma levels. Also, PACAP38 inhibited ovulation when given intracerebroventricularly or intranasally, while PACAP27 had no effect on it (57, 58). Others also found inhibitory action of PACAP on LH release (59). Similarly, injection into another area, the medial basal hypothalamus, led to decreases in LH secretion, LH pulse frequency and ovulation (59). Contradictory results show that the relationship between PACAP and the gonadotropin axis is very complex, as other studies have found stimulatory action on LH release (60–62). Most probably the opposite findings can be explained by the different experimental setups, as it was shown that the action of PACAP depends on the age of the animal, time of day, gender, the day of the estrous cycle, GnRH pulse frequency, using PACAP27 versus 38, and there are differences also between *in vitro* and *in vivo* findings (63). This complex system and the effects of PACAP were thoroughly and critically analyzed in the review by Koves et al. (51).

The first studies on PACAP and the onset of puberty showed that neonatally administered subcutaneous PACAP delayed puberty and a lower number of eggs were released at ovulation, accompanied by lower pituitary LH content (64). Another study revealed that disruption of PAC1 receptor synthesis delayed puberty and decreased GnRH receptor and LH in the pituitary (65). A further insight into the complexity of the interaction between PACAP and gonadotropin system comes from studies investigating other influencing factors, such as other releasing hormones, interleukins, estradiol and progesterone, and several neuropeptides (51). Recent results indicate that PACAP acts also *via* kisspeptin neurons on GnRH secretion. While PACAP can affect GnRH neurons in the hypothalamus directly or indirectly through CRH, it can also influence kisspeptin neurons which create the pulse generator (51). The relationship between kisspeptin and PACAP was suggested in studies by Mijjiddorj et al. (66). These investigations have shown that PACAP and kisspeptin synergistically increase gonadotropin subunit expression, Cre promoter expression, prolactin-promoter activity and kisspeptin increases the expression of PAC1 receptor (66, 67). Tumurbaatar and colleagues have confirmed the relationship between kisspeptin neurons and PACAP, as they showed a stimulation of the gene encoding kisspeptin by PACAP in hypothalamic cells derived from the kisspeptin-expressing periventricular and arcuate nuclei (68).

PACAP or PAC1 receptor knockout animals have high mortality and lower reproduction rate (69–71). PACAP KO mice have numerous abnormalities and pathological symptoms with several biochemical and developmental alterations (71–76).

No exact explanation for the lower fertility is known, but several factors seem to play a role, including hormonal differences. Although most authors working with knockout animals have described decreased fertility, differences can be found in the background. While some investigators found no difference in the onset of puberty and estrous cycle, others have found disturbed estrous cycle (70, 77). Isaac and Sherwood (78) described lower implantation rate associated with reduced prolactin and progesterone levels. Shintani et al. (70) reported reduced mating and maternal behaviour. Immune-checkpoint molecules were investigated in decidual and peripheral immune cells in the periphery and in the decidua of pregnant KO mice. The only noteworthy finding was the recruitment of galectin-9 Th cells to the decidua promoting local immune homeostasis in PACAP KO mice, but this difference alone is not significant enough to explain the background of the reduced fertility, but point to a role of PACAP in the immune regulation of pregnancy (79). A pioneer study by Ross et al. (80) provided more insight into the relationship between neurons expressing PACAP, kisspeptin or leptin, and thus, providing a possible explanation for the altered estrous cycle seen in some studies. They showed that the main site of leptin receptor and PACAP co-expression is the ventral premamillary nucleus of the hypothalamus. A targeted deletion of PACAP from this nucleus led to delayed onset of puberty, measured by delayed vaginal opening and first estrous cycle. These mice had also dysregulated estrous cycle later and had impaired reproductive functions, as pregnant mice had fewer pups per litter. These were accompanied by blunted LH surge and a smaller number of follicles maturing per cycle. As the PACAP/leptin neurons project to kisspeptin neurons, a new role for PACAP-expressing neurons has been suggested based on these observations: PACAP expressing neurons in the ventral premamillary nucleus play a role in the relay of nutritional status to regulate GnRH release by modulating kisspeptin neurons (80). Our preliminary results also confirm this relationship between PACAP and kisspeptin expression and disturbed estrous cycle in PACAP deficient animals (77). Altogether, studies on PACAP and the hypothalamo-hypophyseal system clearly show that PACAP plays a role in the central reproductive functions, but more studies are needed to resolve the controversies in the hormonal regulation. Furthermore, the lack of human data in this regard makes the translational value of these studies questionable, as the reproductive functions are well-known to be highly species-specific.

PACAP in the gonads

It is well known that interactions between peptide and steroid hormone-signaling cascades influence the growth of follicles, ovulation, and luteinization in the ovary. Following the gonadotropin-independent follicular development, a cohort of hormone sensitive follicles are selected that rapidly grow into immature and mature tertiary follicles. LH surge induces ovulation and the formation of the corpus luteum from the remaining granulosa and theca cells of the follicles. Follicles produce estrogen, while corpus luteum is responsible for both estrogen and progesterone production. Although FSH and LH play a fundamental regulatory role in follicular maturation, synthesis of steroids, and ovulation, several peptidergic and non-peptidergic signaling pathways may alter their actions (81–85). Influence of PACAP in gonadal functions is further supported by research data showing that PACAP reduces follicular apoptosis in the ovary (86). Follicular development might also correlate with concentrations of PACAP in granulosa cells. In the rat, PACAP expression in the granulosa cells of large mature follicles prior to ovulation is stage-specific, whereas weaker expression could be detected in immature antral and pre-antral follicles (87–89). Both PACAP and PAC1 receptors are found in the rat corpus luteum (90). Moreover, PACAP might also be involved in the regulation of primordial germ cell proliferation (91), as well as cyclic recruitment of immature follicles (89), follicular apoptosis (86, 92), and ovarian hormone and enzyme production in humans, rats, and cows (93–96). These effects have been reviewed by our research group (97) and by Canipari and colleagues (98). A recent study has suggested a novel link between kisspeptin and PACAP at the ovarian level: suppressed PACAP expression after ablation of kisspeptin signaling in oocytes may be an additional factor in the ovulatory failure in mice (99). These studies clearly indicate that PACAP plays a role in follicular development, both through hormonal interactions and locally, influencing oogenesis.

PACAP in the uterus and placenta

Isaac and Sherwood reported a lower rate of reproduction in PACAP deficient mice, mainly due to insufficient implantation (78). Although the uterine and placental functions of the neuropeptide are somewhat neglected in the literature, findings of the above study might indicate a placental role of endogenous PACAP. Expression of PACAP27 and PACAP38 in human placentas and uterus was first confirmed by radioimmunoassay and immunocytochemistry (100). The uterus consists of a body and cervix, with an isthmus at the border of the two parts. The uterine wall has three layers: endometrium (a columnar epithelial layer), myometrium (a thick smooth muscle layer) and perimetrium (a part of the peritoneum with a thin squamous cell layer) from inside to outside. After implantation, the placenta is formed, consisting of a maternal and a fetal part. Maternal part is the decidua basalis, made up of the pregnant endometrium facing the embryo, while the fetal part consists of the chorion frondosum, which has cyto- and syncytiotrophoblast cells and extraembryonic mesoderm. In

the human placenta, PACAP38 concentrations were higher than PACAP27 levels, uterus and placenta had similar levels of immunoreactivity, but the umbilical cord showed weaker intensity (100). Uterine isthmus and myometrium showed stronger immunoreactivity than pregnant uterus, but no immunoreactive nerve fibers could be detected in the placenta or umbilical cord. Radioimmunoassay studies have revealed similar levels of PACAPs in different parts of the human placenta (central/peripheral maternal, central/peripheral fetal). PACAP38-like immunoreactivity was stronger in both maternal and fetal sides in full-term placenta compared to younger samples, while PACAP27-like immunoreactivity increased only on the maternal side (101). Similar to the above data, Scaldaferri and colleagues observed PACAP and PAC1 receptor in both rat and full-term human placentas using Northern blot analysis, polymerase chain reaction (PCR) and immunohistochemistry (102). In human placentas, a marked difference was observed in the immunohistochemical staining characteristics of different parts of the placenta, showing strong staining in stromal cells around blood vessels and weaker signal in vessel walls in stem villi. In terminal villi, stromal cell PACAP38 immunoreactivity was obvious. In stem villi, the stromal immunoreactivity showed a spatial distribution pattern with immunoreactivity only in the periphery, while terminal villi had dispersed positivity in the entire stroma. RT-PCR studies have revealed expression of different isoforms of the PAC1 receptor in rat and human placentas. In the rat placenta, 3 isoforms were described: the short, hip or hop variant and the hip-hop variant. In contrast, in the human placenta only expression of the SV2 form was detected, that is homologous to the rat hop form. PACAP27, PACAP38 had almost equipotent binding to these receptors, while VIP had weaker binding affinity (102).

PAC1 receptor mRNA has been recently demonstrated in the uterus of healthy pigs, and the abundance of PAC1 receptor protein was reduced in inflammatory conditions (103). Endometrial inflammation also leads to changes in PACAP expression of the dorsal root ganglia supplying the porcine uterus (104). PACAP is expressed in the cervix, lumbosacral dorsal root ganglion and spinal cord supplying the uterus, showing time-dependent changes during pregnancy: initial elevation is later followed by decrease during the end of pregnancy in rats (105). Rat placenta is comprised of decidua basalis, junctional and labyrinth zones, where PACAP and PAC1 receptor mRNAs were detected in decidual cells, as well as in chorionic vessels and stromal cells of the labyrinth zone (106). In the decidua, strongest signals were detected on day 13.5, with decreasing strength in more advanced stages. The junctional zone showed no signal, while the labyrinth zone branching villi, stem villi and chorionic vessels showed a gradually increasing signal parallel with advancing pregnancy age (106). Expression of PACAP and PAC1 receptor mRNA from human legal abortions of 6–7 weeks, from induced abortions of 14–24 weeks (second trimester) and term placentas was proven by *in situ* hybridization in stem villi and terminal villi (107). In first and second trimester samples, moderate PACAP mRNA expression was detected in stroma cells surrounding blood vessels within stem villi, while strong expression was found in full term placentas (107). Only weak expression was found in cyto- and syncytiotrophoblasts. PAC1 receptor expression showed a similar distribution pattern: stronger expression was described in the villus stroma, while weaker expression in the trophoblast cells. This increasing expression pattern of mRNA for both PACAP and its receptor suggests a potential role of the peptide in placental growth and development. Radioimmunoassay also confirmed an increase in the levels of PACAP and its specific receptor in late placentas compared to early placentas (101). Oride and colleagues reported on the presence of PACAP mRNA and PACAP immunoreactive cells in mouse primary placental cell cultures (108). PACAP expression was increased upon treatment with estradiol, progesterone, GnRH or kisspeptin. Conversely, PACAP induced kisspeptin expression in the placenta, showing that PACAP, kisspeptin, and GnRH are interrelated also at the placental level (108).

There are only a few studies dealing with the actions of PACAP in the uterus and placenta. According to a recent study, PACAP treatment leads to decrease of amplitude and an increase in frequency of myometrium contraction in pigs (103). Effects of PACAP on blood vessels and smooth muscle contractility in the uteroplacental unit was also thoroughly investigated. Preincubation with PACAP or VIP significantly inhibited the norepinephrine-induced contraction of arteries of the myometrium and stem villus in a concentration-dependent manner (100). The high concentration needed for significant relaxation indicates the necessity of local peptide release to achieve for the *in vivo* effect. Most results show that PACAP leads to placental vessel relaxation, but no effect could be observed on amplitude, tone, or frequency of strips of spontaneously contracted myometrium of pregnant women (100). Data altogether support the view that PACAP may be involved in the regulation of the uteroplacental blood flow, and results from Spencer and colleagues suggest that PACAP could facilitate endometrial blood flow, thus increasing availability of metabolic substrates to the developing decidua or the embryo (109). Involvement of PACAP placental hormone secretion has also been suggested, probably due to an induction of cAMP secretion. As PACAP and VIP acted similarly, these effects are most probably mediated by VPAC receptors (110). A recent study has detected a robust elevation of PACAP mRNA in female mice uteri with blastocyst embryos compared with non-blastocysts. Also, correlation was found between PACAP and HB-EGF (coding region of heparin-binding EGF-like growth factor) mRNA expression, which is an early embryo implantation marker. This result also supports the role of PACAP during the peri-implantation period of early mouse development (111).

Actions of PACAP have also been investigated in normal and tumorous trophoblast cells. PACAP is well-known for its general cytoprotective and survival-promoting effects in numerous cell

types (19, 20). This could be confirmed in non-tumorous trophoblast cells (HTR-8/SV cells). PACAP pretreatment led to increased survival rate, increased proliferation, while it had no effect on invasion (112). However, PACAP decreased the invasion in another trophoblast cell line, HIPEC, which are invasive, proliferative extravillous trophoblast cells (112). Regulating angiogenesis may also be a function of PACAP during placental growth, as several angiogenic factors were found to be altered upon PACAP treatment of trophoblast cells (112). The disturbed intracellular signaling cascades in tumorous cells can alter the antiapoptotic, thus survival-promoting, effects of PACAP, as it has been shown in various tumour cell lines. In some tumours, PACAP has no effect on survival, while in others, PACAP is antiapoptotic, similarly to its general effects. And yet in others, PACAP is proapoptotic, thus enhances cell death, in contrast to its general protective effects. This was the case in choriocarcinoma cells, where PACAP treatment led to further decrease in survival in cells exposed to hydrogen peroxide-induced oxidative stress or chemically induced *in vitro* hypoxia (113). However, no effect was observed in lipopolysaccharide-, ethanol or methotrexate-treated cells (113, 114). Furthermore, in JAR choriocarcinoma cells, PACAP influenced the expression of several signaling molecules, such as ERK1/2, JNK, Akt, GSK, Bax, p38 MAPK (113). Altogether, these data show that PACAP and its receptors are present in the uterus and placenta, and propose some functions on blood supply, contractions, and growth both under physiological and pathological conditions, but more studies are needed to elucidate the exact function of PACAP at this level.

Human findings

The role of PACAP in a multitude of physiological processes has drawn the attention to elucidating the physiological roles of PACAP in the human body. As the possibility of exogenous PACAP administration in humans is limited, only a few such examples are known from the literature. Regarding hormonal regulations, for example, intravenous PACAP was shown to stimulate vasopressin and PRL levels but not those of oxytocin, gonadotrophs or GH in normal men (115, 116). However, no data are available in women. Based mainly on the cytoprotective functions of PACAP, there are several promising data for its potential future therapeutic use, such as in diabetes (117), multiple sclerosis (118), the intranasal administration in neurodegenerative diseases, cognitive impairment and stroke (119–121), in form of eye drops in corneal and retinal lesions (122, 123) and dry eye disease (124). In contrast, the migraine-provoking effect of PACAP has drawn the interest towards antagonizing PACAP's effects in migraine therapy (125, 126).

More studies are available on the distribution of PACAP in the human body and several papers have described changes of PACAP levels in different body fluids and tissues in physiological and pathological conditions. PACAP has been previously investigated in body fluids with mass spectrometry (MS), radioimmunoassay (RIA) and enzyme-linked immunosorbent assay (127), and has been found in several human body fluids: blood plasma (128–130), cerebrospinal fluid (CSF) (131) and ovarian follicular fluid (132, 133), milk (134, 135) and synovial fluid (136). The source of PACAP in human biological fluids is mainly unknown, but these studies have highlighted the potential use of PACAP as a biomarker in certain diseases, where changes can reflect the presence and/or progression of a disease (127). Among others, PACAP has a potential biomarker value in dilatative cardiomyopathy, cardiac infarct, Parkinson's disease, migraine, polytrauma and chronic rhinosinusitis (127, 137–141). A most recent study has highlighted the potential use of PACAP, together with calcitonin gene related peptide (CGRP), in differentiating pediatric migraine from non-migraine headaches (142), while another recent study has shown the association between COVID-survival and VIP/PACAP plasma levels (143). Regarding reproductive functions, PACAP has been measured in the serum during pregnancy and delivery, and high levels of PACAP were detected in human ovarian follicular fluid, milk and amniotic fluid, as detailed below.

PACAP in the human follicular fluid

PACAP has been detected in the human ovarian follicular fluid after superovulation treatment, with mass spectrometry (132) and radioimmunoassay (133). The potential role of PACAP in the regulation of follicular growth and maturation is further demonstrated by results showing a correlation between human follicular fluid PACAP concentration and ovarian response to superovulation treatment in infertile women (133). In this study, PACAP could be detected in all follicular fluid samples, implying an important biological role for PACAP in this culture medium for the developing oocyte. These data are in line with those demonstrating receptors for PACAP in developing follicles (92, 144). Interestingly, it appeared that low-PACAP concentrations did not correlate with the oocyte numbers: both low and high values could be measured. However, high-PACAP levels correlated with low-oocyte numbers in all cases, allowing us to conclude that below a given threshold value of PACAP it may not have a significant impact on the number of developing oocytes, while above that value, PACAP may override other intraovarian regulatory mechanisms lowering the final number of retrievable oocytes. This finding might draw attention to a derailed regulatory mechanism behind a well-known iatrogenic and potentially life-threatening condition, known as ovarian hyperstimulation syndrome (OHSS). This condition results from excessive ovarian stimulation with an incidence between 1 and 10% of IVF cycles (145). Patients have a higher chance to develop OHSS after superovulation treatment if they have significantly more follicles

on the day of human chorionic gonadotropin (hCG) treatment compared with those without developing OHSS (146, 147). An earlier prospective study demonstrated that the cutoff number of developing follicles on the day of hCG administration for the occurrence of OHSS is 13 follicles (148), that is in harmony with our data (133), where a significant decrease in PACAP concentrations of the follicular fluid was found. From these a conclusion could be drawn that higher PACAP concentrations in the follicular fluid might indicate a well-regulated follicular development, while decreased concentrations could demonstrate a condition favoring the development of OHSS. The exact physiological role of PACAP in the intraovarian regulatory mechanisms influencing follicular maturation and growth is still unclear. However, based on the above data, the neuropeptide found in follicular fluid might play a role in oocyte recruitment and follicular development. Moreover, it appears that higher PACAP concentrations are associated with lower number of developing oocytes, while low PACAP concentrations might correlate with a significantly higher number of retrievable ova, thus predicting a higher chance for ovarian hyperstimulation.

PACAP during pregnancy and in human amniotic fluid

During pregnancy, plasma PACAP38-like immunoreactivity (PACAP38-LI) was found increased in the 2nd and 3rd trimesters, indicating that the neuropeptide might be synthesized by either the placenta or other maternal tissues (33). However, in the same study, a rapid decrease in maternal plasma PACAP level could be found during labour, which might indicate a role between PACAP synthesis/function and the uteroplacental circulation and/or uterine contractions. Three days after delivery the PACAP38-LI decreased to normal levels (33). These data are not surprising, because PACAP38 was earlier detected with RIA and immunocytochemistry in each part of the uteroplacental unit (100). Further supporting the view of PACAP having significant role in placental functions, full-term placentas showed stronger PACAP38-LI on both the maternal and fetal sides, while PACAP27-LI increased only on the maternal side (101).

The amniotic fluid is a complex biological fluid, initially deriving from maternal plasma and passing through fetal membranes according to hydrostatic and osmotic pressure (149). Composition of the fluid is similar to that of fetal plasma until fetal skin keratinization, which usually occurs between 19 and 20 weeks of gestation. In a recent study, amniotic fluid samples were collected between the 15–19th weeks of gestation from volunteering pregnant women undergoing amniocentesis as a prenatal diagnostic tool. Samples were processed to detect PACAP38-LI with radioimmunoassay (150), revealing PACAP38-LI in each amniotic fluid sample, with an average level of 401 ± 142 fmol/ml. Earlier data showed higher levels of PACAP in maternal serum in late pregnancy (33) and the increasing content of PACAP in the placenta during pregnancy (101), indicating its probable placental and/or maternal origin. The higher PACAP levels found in umbilical arteries compared to the umbilical veins suggest fetal PACAP synthesis (33). Based on above results and the fact that the composition of amniotic fluid is similar to fetal plasma in this period (151), we can suggest a fetal and/or placental origin of PACAP in the amniotic fluid, with a yet unknown physiological role.

PACAP in the human milk

Experimental data suggest that PACAP is involved in the regulation of lactation and milk ejection *via* influencing prolactin and oxytocin production and release. However, the central regulatory role of PACAP in these processes is not yet clear, as contradictory data are available on the effects of PACAP on prolactin secretion (152). While no effect was also described, stimulatory and even inhibitory effects on prolactin release have also been found depending on the route of administration, on the *in vitro* conditions and on the timing of the injections (153, 154). Prolactin mRNA was found to be stimulated by PACAP, but injection into the arcuate nucleus reduces concentration of prolactin in the plasma (51). Oxytocin has also been described to be stimulated by PACAP (155). Regarding human data, extremely high levels of PACAP-LI were measured in the human milk by RIA (134), exceeding those of plasma by about 10 times. Even higher levels were measured in the colostrum compared to transitional and mature human milk samples (135, 156). During the first 10 months of lactation, a stable high level can be observed (135). The presence of these high levels was also confirmed in domestic animals the milk of which is commonly consumed and in human milk formulas (157–159). Although the exact function of PACAP in the milk is not known at the moment, it can be suggested that it is either needed for the postnatal development or for the growth of the mammary gland itself, as several effects on the growth, differentiation and proliferation on mammary glandular epithelial cells have been described (156, 159, 160).

In summary, in the present review we summarized main findings on PACAP and reproduction (Figures 1, 2). As seen from the experimental and human data, PACAP and its receptors are present in the hypothalamo-hypophyseal system, in the gonads and in the uterus and placenta. Several roles of PACAP have been described in the central regulation of the reproductive functions, although there are still controversial issues that need to be resolved. In addition, the peptide influences reproductive functions in the periphery, at the ovarian and placental levels. Human data indicate that PACAP is present not only in the

10.3389/fendo.2022.982551

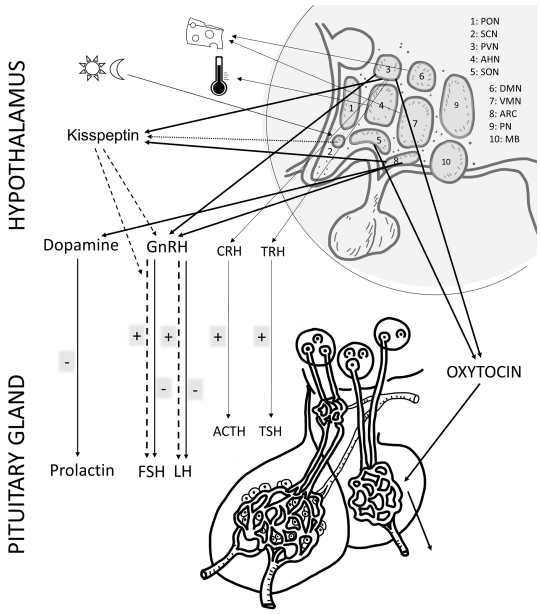

FIGURE 1
Schematic drawing of the main effects of PACAP in the female reproductive system at hypothalamic and pituitary. The main hormones/factors playing a role in reproduction and influenced by PACAP are highlighted. hypothalamic nuclei, PON (preoptic), SCH (suprachiasmatic), PVN (paraventricular), AHN (anterior hypothalamic), SON (supraoptic), DMN (dorsomedial), VMN (ventromedial), ARC (arcuate), PN (posterior), MB (mammillary body). GnRH: gonadotropin releasing hormone; TRH, thyreotropin releasing hormone; CRH, corticotropin releasing hormone; GHRH, growth hormone releasing hormone; FSH, follicule stimulating hormone; LH, luteinizing hormone; ACTH, adrenocorticotropic hormone; GH, growth hormone; ADH, antidiuretic hormone.

reproductive tissues and brain, but can also be detected in the follicular and amniotic fluid, and levels change during pregnancy. In addition, PACAP can be found in the mammary gland and milk, however, its exact function at this level still awaits future investigation. Recent data have provided evidence that PACAP might be a central regulator of puberty and female hormonal cycles, *via* interactions with the kisspeptin-GnRH system. The clinical importance of kisspeptin in several diseases has been highlighted in recent publications (161, 162). Studies summarized in the present review prove that PACAP is both a central and peripheral modulator of reproductive functions and call for further investigations to elucidate the exact role in some processes and to evaluate the potential diagnostic and/or therapeutic use of PACAP in biological fluids as a biomarker, as

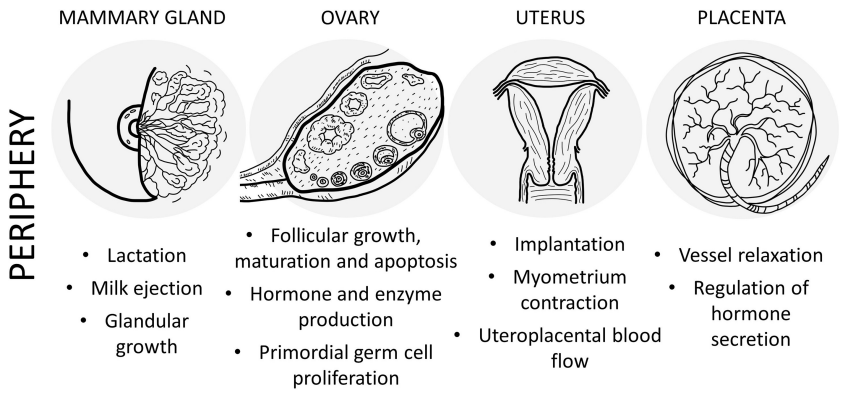

FIGURE 2
Schematic drawing of the main effects of PACAP in the female reproductive system at peripheral level.

it has been also shown for the other players in these complex regulatory mechanisms.

Author contributions

MK, ZN, IB, DR conceptualized, and wrote the manuscript, conceptualized and designed the figure. All authors contributed to the article and approved the submitted version.

Funding

Supported by the Thematic Excellence Program 2021 Health Subprogram of the Ministry for Innovation and Technology in Hungary, within the framework of the EGA-16 project of the Pecs of University. This study was supported by the National Research, Development, and Innovation Fund (FK129190, K119759, K135457); National Brain Research Program (NAP2017-1.2.1-NKP-2017-00002); ELKH-TKI-14016; FIKP III. Project No. TKP2020-IKA-08 was implemented with the support provided from the National Research, Development, and Innovation Fund of Hungary, financed under the 2020-4.1.1-TKP2020 funding scheme.

Acknowledgments

The authors thank Lili Schwieters for proofreading the manuscript.

Conflict of interest

The authors declare that the research was conducted in the absence of any commercial or financial relationships that could be construed as a potential conflict of interest.

Publisher's note

References

1. Miyata A, Arimura A, Dahl RR, Minamino N, Uehara A, Jiang L, et al. Isolation of a novel 38 residue-hypothalamic polypeptide which stimulates adenylate cyclase in pituitary cells. *Biochem Biophys Res Commun* (1989) 164:567–74. doi: 10.1016/0006-291x(89)91757-9

2. Vaudry D, Falluel-Morel A, Bourgault S, Basille M, Burel D, Wurtz O, et al. Pituitary adenylate cyclase-activating polypeptide and its receptors: 20 years after the discovery. *Pharmacol Rev* (2009) 61:283–357. doi: 10.1124/pr.109.001370

3. Langer I, Jeandriens J, Couvineau A, Sanmukh S, Latek D. Signal transduction by VIP and PACAP receptors. *Biomedicines* (2022) 10:406. doi: 10.3390/biomedicines10020406

4. May V, Johnson GC, Hammack SE, Braas KM, Parsons RL. PAC1 receptor internalization and endosomal MEK/ERK activation is essential for PACAP-mediated neuronal excitability. *J Mol Neurosci* (2021) 71:1536–42. doi: 10.1007/s12031-021-01821-x

5. Moody TW, Lee L, Jensen RT. The G protein-coupled receptor PAC1 regulates transactivation of the receptor tyrosine kinase HER3. *J Mol Neurosci* (2021) 71:1589–97. doi: 10.1007/s12031-020-01711-8

6. Doan ND, Chatenet D, Letourneau M, Vaudry H, Vaudry D, Fournier A. Receptor-independent cellular uptake of pituitary adenylate cyclase-activating polypeptide. *Biochim Biophys Acta* (2012) 1823:940–9. doi: 10.1016/j.bbamcr.2012.02.001

7. Li J, Remington JM, Liao C, Parsons RL, Schneebeli S, Braas KM, et al. GPCR intracellular loop regulation of beta-arrestin-mediated endosomal signaling dynamics. *J Mol Neurosci* (2022) 72:1358–73. doi: 10.1007/s12031-022-02016-8

8. Watanabe J, Nakamachi T, Matsuno R, Hayashi D, Nakamura M, Kikuyama S, et al. Localization, characterization and function of pituitary adenylate cyclase-activating polypeptide during brain development. *Peptides* (2007) 28:1713–9. doi: 10.1016/j.peptides.2007.06.029

9. Reglodi D, Tamas A, Jungling A, Vaczy A, Rivnyak A, Fulop BD, et al. Protective effects of pituitary adenylate cyclase activating polypeptide against neurotoxic agents. *Neurotoxicology* (2018) 66:185–94. doi: 10.1016/j.neuro.2018.03.010

10. D'Amico AG, Maugeri G, Vanella L, Pittala V, Reglodi D, D'Agata V. Multimodal role of PACAP in glioblastoma. *Brain Sci* (2021) 11:994. doi: 10.3390/brainsci11080994

11. Martinez-Rojas VA, Jimenez-Garduno AM, Michelatti D, Tosatto L, Marchioretto M, Arosio D, et al. ClC-2-like chloride current alterations in a cell model of spinal and bulbar muscular atrophy, a polyglutamine disease. *J Mol Neurosci* (2021) 71:662–74. doi: 10.1007/s12031-020-01687-5

12. Broome ST, Musumeci G, Castorina A. PACAP and VIP mitigate rotenone-induced inflammation in BV-2 microglial cells. *J Mol Neurosci* (2022). doi: 10.1007/s12031-022-01968-1

13. Boucher MN, Aktar M, Braas KM, May V, Hammack SE. Activation of lateral parabrachial nucleus (LPBn) PACAP-expressing projection neurons to the bed nucleus of the stria terminalis (BNST) enhances anxiety-like behavior. *J Mol Neurosci* (2022) 72:451–8. doi: 10.1007/s12031-021-01946-z

14. Levinstein MR, Bergkamp DJ, Lewis ZK, Tsobanoudis A, Hashikawa K, Stuber GD, et al. PACAP-expressing neurons in the lateral habenula diminish negative emotional valence. *Genes Brain Behav* (2022) 21(7):e12801. doi: 10.1111/gbb.12801

15. Gastelum C, Perez L, Hernandez J, Le N, Vahrson I, Sayers S, et al. Adaptive changes in the central control of energy homeostasis occur in response to variations in energy status. *Int J Mol Sci* (2021) 22:2728. doi: 10.3390/ijms22052728

16. Maunze B, Bruckner KW, Desai NN, Chen C, Chen F, Baker D, et al. Pituitary adenylate cyclase-activating polypeptide receptor activation in the hypothalamus recruits unique signaling pathways involved in energy homeostasis. *Am J Physiol Endocrinol Metab* (2022) 322:E199–210. doi: 10.1152/ajpendo.00320.2021

17. Banki E, Pakai E, Gaszner B, Zsiboras C, Czett A, Bhuddi PRP, et al. Characterization of the thermoregulatory response to pituitary adenylate cyclase-activating polypeptide in rodents. *J Mol Neurosci* (2014) 54:543–54. doi: 10.1007/s12031-014-0361-0

18. Ciranna L, Costa L. Pituitary adenylate cyclase-activating polypeptide modulates hippocampal synaptic transmission and plasticity: new therapeutic suggestions for fragile X syndrome. *Front Cell Neurosci* (2019) 13:524. doi: 10.3389/fncel.2019.00524

19. Toth D, Szabo E, Tamas A, Juhasz T, Horvath G, Fabian E, et al. Protective effects of PACAP in peripheral organs. *Front Endocrinol (Lausanne)* (2020) 11:377. doi: 10.3389/fendo.2020.00377

20. Horvath G, Reglodi D, Fabian E, Opper B. Effects of pituitary adenylate cyclase activating polypeptide on cell death. *Int J Mol Sci* (2022) 23:4953. doi: 10.3390/ijms23094953

21. Parsons RL, May V. PACAP-induced PAC1 receptor internalization and recruitment of endosomal signaling regulate cardiac neuron excitability. *J Mol Neurosci* (2019) 68:340–7. doi: 10.1007/s12031-018-1127-x

22. Chiba Y, Ueda C, Kohno N, Yamashita M, Miyakawa Y, Ando Y, et al. Attenuation of relaxing response induced by pituitary adenylate cyclase-activating polypeptide in bronchial smooth muscle of experimental asthma. *Am J Physiol Lung Cell Mol Physiol* (2020) 319:L786–93. doi: 10.1152/ajplung.00315.2020

23. Karpiesiuk A, Palus K. Pituitary adenylate cyclase-activating polypeptide (PACAP) in physiological and pathological processes within the gastrointestinal tract: a review. *Int J Mol Sci* (2021) 22:8682. doi: 10.3390/ijms22168682

24. Reglodi D, Cseh S, Somoskoi B, Fulop BD, Szentleleky E, Szegeczki V, et al. Disturbed spermatogenic signaling in pituitary adenylate cyclase activating polypeptide-deficient mice. *Reproduction* (2018) 155:129–39. doi: 10.1530/REP-17-0470

25. Meggyes M, Lajko A, Fulop BD, Reglodi D, Szereday L. Phenotypic characterization of testicular immune cells expressing immune checkpoint molecules in wild-type and pituitary adenylate cyclase-activating polypeptide-deficient mice. *Am J Reprod Immunol* (2020) 83:e13212. doi: 10.1111/aji.13212

26. Prisco M, Rosati L, Morgillo E, Mollica MP, Agnese M, Andreuccetti P, et al. Pituitary adenylate cyclase-activating peptide (PACAP) and its receptors in mus musculus testis. *Gen Comp Endocrinol* (2020) 286:113297. doi: 10.1016/j.ygcen.2019.113297

27. Brubel R, Kiss P, Vincze A, Varga A, Varnagy A, Bodis J, et al. Effects of pituitary adenylate cyclase activating polypeptide on human sperm motility. *J Mol Neurosci* (2012) 48:623–30. doi: 10.1007/s12031-012-9806-5

28. Heindel JJ, Powell CJ, Paschall CS, Arimura A, Culler MD. A novel hypothalamic peptide, pituitary adenylate cyclase activating peptide, modulates sertoli cell function *in vitro*. *Biol Reprod* (1992) 47:800–6. doi: 10.1095/biolreprod47.5.800

29. El-Gehani F, Tena-Sempere M, Huhtaniemi I. Evidence that pituitary adenylate cyclase-activating polypeptide is a potent regulator of fetal rat testicular steroidogenesis. *Biol Reprod* (2000) 63:1482–9. doi: 10.1095/biolreprod63.5.1482

30. Matsumoto S, Arakawa Y, Ohishi M, Yanaihara H, Iwanaga T, Kurokawa N. Suppressive action of pituitary adenylate cyclase activating polypeptide (PACAP) on proliferation of immature mouse leydig cell line TM3 cells. *BioMed Res* (2008) 29:321–30. doi: 10.2220/biomedres.29.321

31. Yamashita J, Nishiike Y, Fleming T, Kayo D, Okubo K. Estrogen mediates sex differences in preoptic neuropeptide and pituitary hormone production in medaka. *Commun Biol* (2021) 4:948. doi: 10.1038/s42003-021-02476-5

32. Tang Z, Yuan X, Bai Y, Guo Y, Zhang H, Han Y, et al. Seasonal changes in the expression of PACAP, VPAC1, VPAC2, PAC1 and testicular activity in the testis of the muskrat (Ondatra zibethicus). *Eur J Histochem* (2022) 66:3398. doi: 10.4081/ejh.2022.3398

33. Reglodi D, Gyarmati J, Ertl T, Borzsei R, Bodis J, Tamas A, et al. Alterations of pituitary adenylate cyclase-activating polypeptide-like immunoreactivity in the human plasma during pregnancy and after birth. *J Endocrinol Invest* (2010) 33:443–5. doi: 10.1007/BF03346621

34. Dow RC, Bennie J, Fink G. Pituitary adenylate cyclase-activating peptide-38 (PACAP)-38 is released into hypophysial portal blood in the normal male and female rat. *J Endocrinol* (1994) 142:R1–4. doi: 10.1677/joe.0.142R001

35. Palkovits M, Somogyvari-Vigh A, Arimura A. Concentrations of pituitary adenylate cyclase activating polypeptide (PACAP) in human brain nuclei. *Brain Res* (1995) 699:116–20. doi: 10.1016/0006-8993(95)00869-r

36. Yon L, Alexandre D, Montero M, Chartrel N, Jeandel L, Vallarino M, et al. Pituitary adenylate cyclase-activating polypeptide and its receptors in amphibians. *Microsc. Res Tech.* (2001) 54:137–57. doi: 10.1002/jemt.1129

37. Jolivel V, Basille M, Aubert N, de Jouffrey S, Ancian P, le Bigot J-F, et al. Distribution and functional characterization of pituitary adenylate cyclase–activating polypeptide receptors in the brain of non-human primates. *Neuroscience* (2009) 160:434–51. doi: 10.1016/j.neuroscience.2009.02.028

38. Garami A, Pakai E, Rumbus Z, Solymar M. The role of PACAP in the regulation of body temperature. In: D Reglodi and A Tamas, editors. *Pituitary adenylate cyclase activating polypeptide - PACAP*, vol. . p. Switzerland: Springer International Publishing (2016). p. 239–57. doi: 10.1007/978-3-319-35135-3_15

39. Machado NLS, Saper CB. Genetic identification of preoptic neurons that regulate body temperature in mice. *Temp. (Austin)* (2022) 9:14–22. doi: 10.1080/23328940.2021.1993734

40. Puig de Parada M, Parada MA, Hernandez L. Dipsogenic effect of pituitary adenylate cyclase activating polypeptide (PACAP38) injected into the lateral hypothalamus. *Brain Res* (1995) 696:254–7. doi: 10.1016/0006-8993(95)00824-a

41. Kiss P, Reglodi D, Tamas A, Lubics A, Lengvari I, Jozsa R, et al. Changes of PACAP levels in the brain show gender differences following short-term water and food deprivation. *Gen Comp Endocrinol* (2007) 152:225–30. doi: 10.1016/j.ygcen.2006.12.012

42. Sureshkumar K, Saenz A, Ahmad SM, Lutfy K. The PACAP/PAC1 receptor system and feeding. *Brain Sci* (2021) 12:13. doi: 10.3390/brainsci12010013

43. Martins AB, Brownlow ML, Araujo BB, Garnica-Siqueira MC, Zaia DAM, Leite CM, et al. Arcuate nucleus of the hypothalamus contributes to the hypophagic effect and plasma metabolic changes induced by vasoactive intestinal peptide and pituitary adenylate cyclase-activating polypeptide. *Neurochem Int* (2022) 155:105300. doi: 10.1016/j.neuint.2022.105300

44. Le N, Sayers S, Mata-Pacheco V, Wagner EJ. The PACAP paradox: dynamic and surprisingly pleiotropic actions in the central regulation of energy homeostasis. *Front Endocrinol (Lausanne)* (2022) 13:877647. doi: 10.3389/fendo.2022.877647

45. Lindberg PT, Mitchell JW, Burgoon PW, Beaule C, Weihe E, Schafer MKH, et al. Pituitary adenylate cyclase-activating peptide (PACAP)-glutamate co-transmission drives circadian phase-advancing responses to intrinsically photosensitive retinal ganglion cell projections by suprachiasmatic nucleus. *Front Neurosci* (2019) 13:1281. doi: 10.3389/fnins.2019.01281

46. Murase T, Kondo K, Otake K, Oiso Y. Pituitary adenylate cyclase-activating polypeptide stimulates arginine vasopressin release in conscious rats. *Neuroendocrinology* (1993) 57:1092–6. doi: 10.1159/000126475

47. Seki Y, Suzuki Y, Baskaya MK, Saito K, Takayasu M, Shibuya M, et al. Central cardiovascular effects induced by intracisternal PACAP in dogs. *Am J Physiol* (1995) 269:H135–9. doi: 10.1152/ajpheart.1995.269.1.H135

48. Nomura M, Ueta Y, Serino R, Yamamoto Y, Shibuya I, Yamashita H. Effects of centrally administered pituitary adenylate cyclase-activating polypeptide on c-fos gene expression and heteronuclear RNA for vasopressin in rat paraventricular and supraoptic nuclei. *Neuroendocrinology* (1999) 69:167–80. doi: 10.1159/000054416

49. Lutz-Bucher B, Monnier D, Koch B. Evidence for the presence of receptors for pituitary adenylate cyclase-activating polypeptide in the neurohypophysis that are positively coupled to cyclic AMP formation and neurohypophyseal hormone secretion. *Neuroendocrinology* (1996) 64:153–61. doi: 10.1159/000127113

50. Counis R, Laverriere JN, Garrel-Lazayres G, Cohen-Tannoudji J, Lariviere S, Bleux C, et al. What is the role of PACAP in gonadotrope function? *Peptides* (2007) 28:1797–804. doi: 10.1016/j.peptides.2007.05.011

51. Koves K, Szabo E, Kantor O, Heinzlmann A, Szabo F, Csaki A. Current state of understanding of the role of PACAP in the hypothalamo-hypophyseal gonadotropin functions of mammals. *Front Endocrinol (Lausanne)* (2020) 11:88. doi: 10.3389/fendo.2020.00088

52. Moore JP, Burger LL, Dalkin AC, Winters SJ. Pituitary adenylate cyclase activating polypeptide messenger RNA in the paraventricular nucleus and anterior pituitary during the rat estrous cycle. *Biol Reprod* (2005) 73:491–9. doi: 10.1095/biolreprod.105.041624

53. Wuttke W, Benter S, Jarry H. Evidence for a steroid modulated expression of pituitary adenylate cyclase activating polypeptide (PACAP) in the anterior pituitary of rats. *Neuroendocrinology* (1994) 60(suppl. 1):17.

54. Koves K, Kantor O, Scammell JG, Arimura A. PACAP colocalizes with luteinizing and follicle-stimulating hormone immunoreactivities in the anterior lobe of the pituitary gland. *Peptides* (1998) 19:1069–72. doi: 10.1016/s0196-9781(98)00049-7

55. Heinzlmann A, Kirilly E, Meltzer K, Szabo E, Baba A, Hashimoto H, et al. PACAP is transiently expressed in anterior pituitary gland of rats: *In situ* hybridization and cell immunoblot assay studies. *Peptides* (2008) 29:571–7. doi: 10.1016/j.peptides.2007.12.009

56. Koves K, Molnar J, Kantor O, Gorcs TJ, Lakatos A, Arimura A. New aspects of the neuroendocrine role of PACAP. *Ann N Y Acad Sci* (1996) 805:648–54. doi: 10.1111/j.1749-6632.1996.tb17535.x

57. Kantor O, Molnar J, Arimura A, Koves K. PACAP38 and PACAP27 administered intracerebroventricularly have an opposite effect on LH secretion. *Peptides* (2000) 21:817–20. doi: 10.1016/s0196-9781(00)00214-x

58. Heinzlmann A, Olah M, Koves K. Intranasal application of PACAP and β-cyclodextrin before the "critical period of proestrous stage" can block ovulation. *Biol Futur* (2019) 70:62–70. doi: 10.1556/019.70.2019.08

59. Anderson ST, Sawangjaroen K, Curlewis JD. Pituitary adenylate cyclase-activating polypeptide acts within the medial basal hypothalamus to inhibit prolactin and luteinizing hormone secretion. *Endocrinology* (1996) 137:3424–9. doi: 10.1210/endo.137.8.8754770

60. Hart GR, Gowing H, Burrin JM. Effects of a novel hypothalamic peptide, pituitary adenylate cyclase-activating polypeptide, on pituitary hormone release in rats. *J Endocrinol* (1992) 134:33–41. doi: 10.1677/joe.0.1340033

61. Szabo E, Nemeskeri A, Arimura A, Koves K. Effect of PACAP on LH release studied by cell immunoblot assay depends on the gender, on the time of day and in female rats on the day of the estrous cycle. *Regul Pept* (2004) 123:139–45. doi: 10.1016/j.regpep.2004.04.021

62. Kanasaki H, Purwana IN, Miyazaki K. Possible role of PACAP and its PAC1 receptor in the differential regulation of pituitary LHbeta- and FSHbeta-subunit gene expression by pulsatile GnRH stimulation. *Biol Reprod* (2013) 88:1–5. doi: 10.1095/biolreprod.112.105601

63. Kanasaki H, Oride A, Tselmeg M, Sukhbaatar U, Kyo S. Role of PACAP and its PACAP type I receptor in the central control of reproductive hormones. In: D Reglodi and A Tamas, editors. *Pituitary adenylate cyclase activating polypeptide - PACAP*. Switzerland: International Publishing, (2016). p. 375–87. doi: 10.1007/978-3-319-35135-3_22

64. Szabo F, Horvath J, Heinzlmann A, Arimura A, Koves K. Neonatal PACAP administration in rats delays puberty through the influence of the LHRH neuronal system. *Regul Pept* (2002) 109:49–55. doi: 10.1016/s0167-0115(02)00185-4

65. Choi EJ, Ha CM, Kim MS, Kang JH, Park SK, Choi WS, et al. Central administration of an antisense oligodeoxynucleotide against type I pituitary adenylate cyclase-activating polypeptide receptor suppresses synthetic activities of LHRH-LH axis during the pubertal process. *Brain Res Mol Brain Res* (2000) 80:35–45. doi: 10.1016/s0169-328x(00)00116-9

66. Mijiddorj T, Kanasaki H, Oride A, Hara T, Sukhbaatar U, Tumurbaatar T, et al. Interaction between kisspeptin and adenylate cyclase-activating polypeptide 1 on the expression of pituitary gonadotropin subunits: a study using mouse pituitary lbetaT2 cells. *Biol Reprod* (2017) 96:1043–51. doi: 10.1093/biolre/iox030

67. Hara T, Kanasaki H, Tumurbaatar T, Oride A, Okada H, Kyo S. Role of kisspeptin and Kiss1R in the regulation of prolactin gene expression in rat somatolactotroph GH3 cells. *Endocrine* (2019) 63:101–11. doi: 10.1007/s12020-018-1759-1

68. Tumurbaatar T, Kanasaki H, Oride A, Okada H, Hara T, Tumurgan Z, et al. Effect of pituitary adenylate cyclase-activating polypeptide (PACAP) in the regulation of hypothalamic kisspeptin expression. *Gen Comp Endocrinol* (2019) 270:60–6. doi: 10.1016/j.ygcen.2018.10.006

69. Jamen F, Rodriguez-Henche N, Pralong F, Jegou B, Gaillard R, Bockaert J, et al. PAC1 null females display decreased fertility. *Ann N Y Acad Sci* (2000) 921:400–4. doi: 10.1111/j.1749-6632.2000.tb07004.x

70. Shintani N, Mori W, Hashimoto H, Imai M, Tanaka K, Tomimoto S, et al. Defects in reproductive functions in PACAP-deficient female mice. *Regul Pept* (2002) 109:45–8. doi: 10.1016/s0167-0115(02)00169-6

71. Hashimoto H, Shintani N, Baba A. New insights into the central PACAPergic system from the phenotypes in PACAP- and PACAP receptor-knockout mice. *Ann N Y Acad Sci* (2006) 1070:75–89. doi: 10.1196/annals.1317.038

72. Yamada K, Matsuzaki S, Hattori T, Kuwahara R, Taniguchi M, Hashimoto H, et al. Increased stathmin1 expression in the dentate gyrus of mice causes abnormal axonal arborizations. *PloS One* (2010) 5:e8596. doi: 10.1371/journal.pone.0008596

73. Reglodi D, Kiss P, Szabadfi K, Atlasz T, Gabriel R, Horvath G, et al. PACAP is an endogenous protective factor - insights from PACAP-deficient mice. *J Mol Neurosci* (2012) 48:482–92. doi: 10.1007/s12031-012-9762-0

74. Maasz G, Pirger Z, Reglodi D, Petrovics D, Schmidt J, Kiss P, et al. Comparative protein composition of the brains of PACAP-deficient mice using mass spectrometry-based proteomic analysis. *J Mol Neurosci* (2014) 54:310–9. doi: 10.1007/s12031-014-0264-0

75. Reglodi D, Jungling A, Longuespee R, Kriegsmann J, Casadonte R, Kriegsmann M, et al. Accelerated pre-senile systemic amyloidosis in PACAP knockout mice - a protective role of PACAP in age-related degenerative processes. *J Pathol* (2018) 245:478–90. doi: 10.1002/path.5100

76. Ivic I, Balasko M, Fulop BD, Hashimoto H, Toth G, Tamas A, et al. VPAC1 receptors play a dominant role in PACAP-induced vasorelaxation in female mice. *PloS One* (2019) 14:e0211433. doi: 10.1371/journal.pone.0211433

77. Vertes V, Reglodi D, Fulop B, Abraham IM, Nagy Zs. (2019). Stereology of gonadotropin-releasing hormone (GnRH) and kisspeptin (KP) neurons in PACAP gene deficient female mice. Poster presented at the Akira Arimura Memorial VIP/PACAP and Related Peptides Symposium: 30 Years After PACAP Discovery.

78. Isaac ER, Sherwood NM. Pituitary adenylate cyclase-activating polypeptide (PACAP) is important for embryo implantation in mice. *Mol Cell Endocrinol* (2008) 280:13–9. doi: 10.1016/j.mce.2007.09.003

79. Lajko A, Meggyes M, Fulop BD, Gede N, Reglodi D, Szereday L. Comparative analysis of decidual and peripheral immune cells and immune-checkpoint molecules during pregnancy in wild-type and PACAP-deficient mice. *Am J Reprod Immunol* (2018) 80:e13035. doi: 10.1111/aji.13035

80. Ross RA, Leon S, Madara JC, Schafer D, Fergani C, Maguire CA, et al. PACAP neurons in the ventral premammillary nucleus regulate reproductive function in the female mouse. *Elife* (2018) 7:e35960. doi: 10.7554/eLife.35960

81. Bodis J, Koppan M, Kornya L, Tinneberg HR, Torok A. Influence of melatonin on basal and gonadotropin-stimulated progesterone and estradiol secretion of cultured human granulosa cells and in the superfused granulosa cell system. *Gynecol. Obstet. Invest* (2001) 52:198–202. doi: 10.1159/000052973

82. Kornya L, Bodis J, Koppan M, Tinneberg HR, Torok A. Modulatory effect of acetylcholine on gonadotropin-stimulated human granulosa cell steroid secretion. *Gynecol. Obstet. Invest* (2001) 52:104–7. doi: 10.1159/000052952

83. Bodis J, Koppan M, Kornya L, Tinneberg HR, Torok A. The effect of catecholamines, acetylcholine and histamine on progesterone release by human granulosa cells in a granulosa cell superfusion system. *Gynecol. Endocrinol* (2002) 16:259–64. doi: 10.1080/gye.16.4.259.264

84. Richards JS. Novel signaling pathways that control ovarian follicular development, ovulation, and luteinization. *Recent Prog Horm Res* (2002) 57:195–220. doi: 10.1210/rp.57.1.195

85. Koppan M, Bodis J, Verzar Z, Tinneberg H-R, Torok A. Serotonin may alter the pattern of gonadotropin-induced progesterone release of human granulosa cells in superfusion system. *Endocrine* (2004) 24:155–60. doi: 10.1385/ENDO:24:2:155

86. Lee J, Park HJ, Choi HS, Kwon HB, Arimura A, Lee BJ, et al. Gonadotropin stimulation of pituitary adenylate cyclase-activating polypeptide (PACAP) messenger ribonucleic acid in the rat ovary and the role of PACAP as a follicle survival factor. *Endocrinology* (1999) 140:818–26. doi: 10.1210/endo.140.2.6485

87. Gras S, Hannibal J, Georg B, Fahrenkrug J. Transient periovulatory expression of pituitary adenylate cyclase activating peptide in rat ovarian cells. *Endocrinology* (1996) 137:4779–85. doi: 10.1210/endo.137.11.8895347

88. Park JY, Park JH, Park HJ, Lee JY, Lee YI, Lee K, et al. Stage-dependent regulation of ovarian pituitary adenylate cyclase-activating polypeptide mRNA levels by GnRH in cultured rat granulosa cells. *Endocrinology* (2001) 142:3828–35. doi: 10.1210/endo.142.9.8384

89. Gras S, Høst E, Fahrenkrug J. Role of pituitary adenylate cyclase-activating peptide (PACAP) in the cyclic recruitment of immature follicles in the rat ovary. *Regul Pept* (2005) 128:69–74. doi: 10.1016/j.regpep.2004.12.021

90. Kotani E, Usuki S, Kubo T. Rat corpus luteum expresses both PACAP and PACAP type IA receptor mRNAs. *Peptides* (1997) 18:1453–5. doi: 10.1016/s0196-9781(97)00142-3

91. Pesce M, Canipari R, Ferri GL, Siracusa G, de Felici M. Pituitary adenylate cyclase-activating polypeptide (PACAP) stimulates adenylate cyclase and promotes proliferation of mouse primordial germ cells. *Development* (1996) 122:215–21. doi: 10.1242/dev.122.1.215

92. Vaccari S, Latini S, Barberi M, Teti A, Stefanini M, Canipari R. Characterization and expression of different pituitary adenylate cyclase-activating polypeptide/vasoactive intestinal polypeptide receptors in rat ovarian follicles. *J Endocrinol* (2006) 191:287–99. doi: 10.1677/joe.1.06470

93. Zhong Y, Kasson BG. Pituitary adenylate cyclase-activating polypeptide stimulates steroidogenesis and adenosine 3',5'-monophosphate accumulation in cultured rat granulosa cells. *Endocrinology* (1994) 135:207–13. doi: 10.1210/endo.135.1.8013355

94. Apa R, Lanzone A, Mastrandrea M, Miceli F, de Feo D, Caruso A, et al. Control of human luteal steroidogenesis: role of growth hormone-releasing hormone, vasoactive intestinal peptide, and pituitary adenylate cyclase-activating peptide. *Fertil. Steril.* (1997) 68:1097–102. doi: 10.1016/s0015-0282(97)00370-1

95. Apa R, Lanzone A, Miceli F, Vaccari S, Macchione E, Stefanini M, et al. Pituitary adenylate cyclase-activating polypeptide modulates plasminogen activator expression in rat granulosa cell. *Biol Reprod* (2002) 66:830–5. doi: 10.1095/biolreprod66.3.830

96. Sayasith K, Brown KA, Sirois J. Gonadotropin-dependent regulation of bovine pituitary adenylate cyclase-activating polypeptide in ovarian follicles prior to ovulation. *Reproduction* (2007) 133:441–53. doi: 10.1530/REP-06-0188

97. Reglodi D, Tamas A, Koppan M, Szogyi D, Welke L. Role of PACAP in female fertility and reproduction at gonadal level – recent advances. *Front Endocrinol (Lausanne)* (2012) 3:155. doi: 10.3389/fendo.2012.00155

98. Canipari R, di Paolo V, Barberi M, Cecconi S. PACAP in the reproductive system. In: D Reglodi and A Tamas, editors. *Pituitary adenylate cyclase activating polypeptide - PACAP*, vol. p . Switzerland: Springer International Publishing (2016). p. 405–20. doi: 10.1007/978-3-319-35135-3_24

99. Ruohonen ST, Gaytan F, Usseglio Gaudi A, Velasco I, Kukoricza K, Perdices-Lopez C, et al. Selective loss of kisspeptin signaling in oocytes causes progressive premature ovulatory failure. *Hum Reprod* (2022) 37:806–21. doi: 10.1093/humrep/deab287

100. Steenstrup BR, Jørgensen JC, Alm P, Hannibal J, Junge J, Fahrenkrug J, et al. Pituitary adenylate cyclase activating polypeptide (PACAP): occurrence and vasodilatory effect in the human uteroplacental unit. *Regul Pept* (1996) 61:197–204. doi: 10.1016/0167-0115(95)00156-5

101. Brubel R, Boronkai A, Reglodi D, Racz B, Nemeth J, Kiss P, et al. Changes in the expression of pituitary adenylate cyclase-activating polypeptide in the human placenta during pregnancy and its effects on the survival of JAR choriocarcinoma cells. *J Mol Neurosci* (2010) 42:450–8. doi: 10.1007/s12031-010-9374-5

102. Scaldaferri ML, Modesti A, Palumbo C, Ulisse S, Fabbri A, Piccione E, et al. Pituitary adenylate cyclase-activating polypeptide (PACAP) and PACAP-receptor type 1 expression in rat and human placenta. *Endocrinology* (2000) 141:1158–67. doi: 10.1210/endo.141.3.7346

103. Jana B, Całka J, Witek K. Investigation of the role of pituitary adenylate cyclase-activating peptide (PACAP) and its type 1 (PAC1) receptor in uterine contractility during endometritis in pigs. *Int J Mol Sci* (2022) 23:5467. doi: 10.3390/ijms23105467

104. Bulc M, Całka J, Meller K, Jana B. Endometritis affects chemical coding of the dorsal root ganglia neurons supplying uterus in the sexually mature gilts. *Res Vet Sci* (2019) 124:417–25. doi: 10.1016/j.rvsc.2019.05.003

105. Papka RE, Workley M, Usip S, Mowa CN, Fahrenkrug J. Expression of pituitary adenylate cyclase activating peptide in the uterine cervix, lumbosacral dorsal root ganglia and spinal cord of rats during pregnancy. *Peptides* (2006) 27:743–52. doi: 10.1016/j.peptides.2005.08.005

106. Koh PO, Kwak SD, Kim HJ, Roh G, Kim JH, Kang SS, et al. Expression patterns of pituitary adenylate cyclase activating polypeptide and its type I receptor mRNAs in the rat placenta. *Mol Reprod Dev* (2003) 64:27–31. doi: 10.1002/mrd.10221

107. Koh PO, Won CK, Noh HS, Cho GJ, Choi WS. Expression of pituitary adenylate cyclase activating polypeptide and its type I receptor mRNAs in human placenta. *J Vet Sci* (2005) 6:1–5. doi: 10.4142/jvs.2005.6.1.1

108. Oride A, Kanasaki H, Mijiddorj T, Sukhbaatar U, Yamada T, Kyo S. Expression and regulation of pituitary adenylate cyclase-activating polypeptide in rat placental cells. *Reprod Sci* (2016) 23:1080–6. doi: 10.1177/1933719116630421

109. Spencer F, Chi L, Zhu MX. Temporal relationships among uterine pituitary adenylate cyclase-activating polypeptide, decidual prolactin-related protein and progesterone receptor mRNAs expressions during decidualization and gestation in rats. *Comp Biochem Physiol C Toxicol Pharmacol* (2001) 129:25–34. doi: 10.1016/s1532-0456(01)00177-6

110. Desai BJ, Burrin JM. PACAP-38 positively regulates glycoprotein hormone α-gene expression in placental cells. *Mol Cell Endocrinol* (1994) 99:31–7. doi: 10.1016/0303-7207(94)90143-0

111. Somoskoi B, Torok D, Reglodi D, Tamas A, Fulop BD, Cseh S. Possible effects of pituitary adenylate cyclase activating polypeptide (PACAP) on early embryo implantation marker HB-EGF in mouse. *Reprod Biol* (2020) 20:9–13. doi: 10.1016/j.repbio.2020.01.005

112. Horvath G, Reglodi D, Brubel R, Halasz M, Barakonyi A, Tamas A, et al. Investigation of the possible functions of PACAP in human trophoblast cells. *J Mol Neurosci* (2014) 54:320–30. doi: 10.1007/s12031-014-0337-0

113. Boronkai A, Brubel R, Racz B, Tamas A, Kiss P, Horvath G, et al. Effects of pituitary adenylate cyclase activating polypeptide on the survival and signal transduction pathways in human choriocarcinoma cells. *Ann N Y Acad Sci* (2009) 1163:353–7. doi: 10.1111/j.1749-6632.2008.03630.x

114. Horvath G, Nemeth J, Brubel R, Opper B, Koppan M, Tamas A, et al. Occurrence and functions of PACAP in the placenta. In: D Reglodi and A Tamas, editors. *Pituitary adenylate cyclase activating polypeptide - PACAP*. Switzerland: Springer International Publishing (2016). p. 389–403. doi: 10.1007/978-3-319-35135-3_23

115. Chiodera P, Volpi R, Capretti L, Coiro V. Effects of intravenously infused pituitary adenylate cyclase-activating polypeptide on arginine vasopressin and oxytocin secretion in man. *Neuroreport* (1995) 6:1490–2. doi: 10.1097/00001756-199507310-00006

116. Chiodera P, Volpi R, Capretti L, Caffarri G, Magotti MG, Coiro V. Effects of intravenously infused pituitary adenylate cyclase-activating polypeptide on adenohypophyseal hormone secretion in normal men. *Neuroendocrinology* (1996) 64:242–6. doi: 10.1159/000127124

117. Sanlioglu AD, Karacay B, Balci MK, Griffith TS, Sanlioglu S. Therapeutic potential of VIP vs PACAP in diabetes. *J Mol Endocrinol* (2012) 49:R157–67. doi: 10.1530/JME-12-0156

118. Jansen MI, Thomas Broome S, Castorina A. Exploring the pro-phagocytic and anti-inflammatory functions of PACAP and VIP in microglia: implications for multiple sclerosis. *Int J Mol Sci* (2022) 23:4788. doi: 10.3390/ijms23094788

119. Soles-Tarres I, Cabezas-Llobet N, Vaudry D, Xifro X. Protective effects of pituitary adenylate cyclase-activating polypeptide and vasoactive intestinal peptide against cognitive decline in neurodegenerative diseases. *Front Cell Neurosci* (2020) 14:221. doi: 10.3389/fncel.2020.00221

120. Cherait A, Maucotel J, Lefranc B, Leprince J, Vaudry D. Intranasal administration of PACAP is an efficient delivery route to reduce infarct volume and promote functional recovery after transient and permanent middle cerebral artery occlusion. *Front Endocrinol (Lausanne)* (2021) 11:585082. doi: 10.3389/fendo.2020.585082

121. Guo X, Tian Y, Yang Y, Li S, Guo L, Shi J. Pituitary adenylate cyclase-activating polypeptide protects against cognitive impairment caused by chronic cerebral hypoperfusion. *Mol Neurobiol* (2021) 58:4309–22. doi: 10.1007/s12035-021-02381-2

122. Nakamachi T, Ohtaki H, Seki T, Yofu S, Kagami N, Hashimoto H, et al. PACAP suppresses dry eye signs by stimulating tear secretion. *Nat Commun* (2016) 7:12034. doi: 10.1038/ncomms12034

123. Szabo E, Patko E, Vaczy A, Molitor D, Csutak A, Toth G, et al. Retinoprotective effects of PACAP eye drops in microbead-induced glaucoma model in rats. *Int J Mol Sci* (2021) 22:8825. doi: 10.3390/ijms22168825

124. Hirabayashi T, Shibato J, Kimura A, Yamashita M, Takenoya F, Shioda S. Potential therapeutic role of pituitary adenylate cyclase-activating polypeptide for dry eye disease. *Int J Mol Sci* (2022) 23:664. doi: 10.3390/ijms23020664

125. Togha M, Ghorbani Z, Ramazi S, Zavvari F, Karimzadeh F. Evaluation of serum levels of transient receptor potential cation channel subfamily V member 1, vasoactive intestinal polypeptide, and pituitary adenylate cyclase-activating polypeptide in chronic and episodic migraine: the possible role in migraine transformation. *Front Neurol* (2021) 12:770980. doi: 10.3389/fneur.2021.770980

126. Dominguez-Moreno R, Do TP, Ashina M. Calcitonin gene-related peptide and pituitary adenylate cyclase-activating polypeptide in migraine treatment. *Curr Opin Endocrinol Diabetes Obes* (2022) 29:225–31. doi: 10.1097/MED.0000000000000717

127. Reglodi D, Helyes Z, Nemeth J, Vass RA, Tamas A. PACAP as a potential biomarker: Alterations of PACAP levels in human physiological and pathological conditions. In: D Reglodi and A Tamas, editors. *Pituitary adenylate cyclase activating polypeptide - PACAP*. Switzerland: Springer International Publishing (2016). p. 815–32. doi: 10.1007/978-3-319-35135-3_48

128. Birk S, Sitarz JT, Petersen KA, Oturai PS, Kruuse C, Fahrenkrug J, et al. The effect of intravenous PACAP38 on cerebral hemodynamics in healthy volunteers. *Regul Pept* (2007) 140:185–91. doi: 10.1016/j.regpep.2006.12.010

129. Li M, Maderdrut JL, Lertora JJL, Batuman V. Intravenous infusion of pituitary adenylate cyclase-activating polypeptide (PACAP) in a patient with multiple myeloma and myeloma kidney: A case study. *Peptides* (2007) 28:1891–5. doi: 10.1016/j.peptides.2007.05.002

130. Sarszegi Z, Szabo D, Gaszner B, Konyi A, Reglodi D, Nemeth J, et al. Examination of pituitary adenylate cyclase-activating polypeptide (PACAP) as a potential biomarker in heart failure patients. *J Mol Neurosci* (2019) 68:368–76. doi: 10.1007/s12031-017-1025-7

131. Bukovics P, Czeiter E, Amrein K, Kovacs N, Pal J, Tamas A, et al. Changes of PACAP level in cerebrospinal fluid and plasma of patients with severe traumatic brain injury. *Peptides* (2014) 60:18–22. doi: 10.1016/j.peptides.2014.07.001

132. Brubel R, Reglodi D, Jambor E, Koppan M, Varnagy A, Zs B, et al. Investigation of pituitary adenylate cyclase activating polypeptide in human gynecological and other biological fluids by using MALDI TOF mass spectrometry. *J Mass Spectrom.* (2011) 46:189–94. doi: 10.1002/jms.1884

133. Koppan M, Varnagy A, Reglodi D, Brubel R, Nemeth J, Tamas A, et al. Correlation between oocyte number and follicular fluid concentration of pituitary adenylate cyclase-activating polypeptide (PACAP) in women after superovulation treatment. *J Mol Neurosci* (2012) 48:617–22. doi: 10.1007/s12031-012-9743-3

134. Borzsei R, Mark L, Tamas A, Bagoly T, Bay C, Csanaky K, et al. Presence of pituitary adenylate cyclase activating polypeptide-38 in human plasma and milk. *Eur J Endocrinol* (2009) 160:561–5. doi: 10.1530/EJE-08-0911

135. Csanaky K, Banki E, Szabadfi K, Reglodi D, Tarcai I, Czegledi L, et al. Changes in PACAP immunoreactivity in human milk and presence of PAC1 receptor in mammary gland during lactation. *J Mol Neurosci* (2012) 48:631–7. doi: 10.1007/s12031-012-9779-4

136. Sun BY, Sun ZP, Pang ZC, Huang WT, Wu SP. Decreased synovial fluid pituitary adenylate cyclase-activating polypeptide (PACAP) levels may reflect disease severity in post-traumatic knee osteoarthritis after anterior cruciate ligament injury. *Peptides* (2019) 116:22–9. doi: 10.1016/j.peptides.2019.04.009

137. Hu S, Huang S, Ma J, Li D, Zhao Z, Zheng J, et al. Correlation of decreased serum pituitary adenylate cyclase-activating polypeptide and vasoactive intestinal peptide levels with non-motor symptoms in patients with parkinson's disease. *Front Aging Neurosci* (2021) 13:689939. doi: 10.3389/fnagi.2021.689939

138. Tamas A, Toth D, Pham D, Loibl C, Rendeki S, Csontos C, et al. Changes of pituitary adenylate cyclase activating polypeptide (PACAP) level in polytrauma patients in the early post-traumatic period. *Peptides* (2021) 146:170645. doi: 10.1016/j.peptides.2021.170645

139. Mihalj H, Butkovic J, Tokic S, Stefanic M, Kizivat T, Bujak M, et al. Expression of oxidative stress and inflammation-related genes in nasal mucosa and nasal polyps from patients with chronic rhinosinusitis. *Int J Mol Sci* (2022) 23:5521. doi: 10.3390/ijms23105521

140. Pham D, Polgar B, Toth T, Jungling A, Kovacs N, Balas I, et al. Examination of pituitary adenylate cyclase-activating polypeptide in parkinson's disease focusing on correlations with motor symptoms. *Geroscience* (2022) 44:785–803. doi: 10.1007/s11357-022-00530-6

141. Szabo D, Sarszegi Z, Polgar B, Saghy E, Reglodi D, Toth T, et al. PACAP-38 and PAC1 receptor alterations in plasma and cardiac tissue samples of heart failure patients. *Int J Mol Sci* (2022) 23:3715. doi: 10.3390/ijms23073715

142. Liu J, Wang G, Dan Y, Liu X. CGRP and PACAP-38 play an important role in diagnosing pediatric migraine. *J Headache Pain* (2022) 23:68. doi: 10.1186/s10194-022-01435-7

143. Temerozo JR, Sacramento CQ, Fintelman-Rodrigues N, Pao CRR, Freitas CS, Dias SSG, et al. VIP Plasma levels associate with survival in severe COVID-19 patients, correlating with protective effects in SARS-CoV-2-infected cells. *J Leukoc Biol* (2022) 111:1107–21. doi: 10.1002/JLB.5COVA1121-626R

144. Barberi M, Muciaccia B, Morelli MB, Stefanini M, Cecconi S, Canipari R. Expression localisation and functional activity of pituitary adenylate cyclase-activating polypeptide, vasoactive intestinal polypeptide and their receptors in mouse ovary. *Reproduction* (2007) 134:281–92. doi: 10.1530/REP-07-0051

145. D'Angelo A, Brown J, Amso NN. Coasting (withholding gonadotrophins) for preventing ovarian hyperstimulation syndrome. In: A D'Angelo, editor. *Cochrane database of systematic reviews*. Chichester, UK: John Wiley & Sons, Ltd (2011). p. CD002811. doi: 10.1002/14651858.CD002811.pub3

146. Navot D, Bergh PA, Laufer N. Ovarian hyperstimulation syndrome in novel reproductive technologies: prevention and treatment. *Fertil. Steril.* (1992) 58:249–61. doi: 10.1016/s0015-0282(16)55188-7

147. Jayaprakasan K, Herbert M, Moody E, Stewart JA, Murdoch AP. Estimating the risks of ovarian hyperstimulation syndrome (OHSS): implications for egg donation for research. *Hum Fertil. (Camb)* (2007) 10:183–7. doi: 10.1080/14647270601021743

148. Papanikolaou EG, Pozzobon C, Kolibianakis EM, Camus M, Tournaye H, Fatemi HM, et al. Incidence and prediction of ovarian hyperstimulation syndrome in women undergoing gonadotropin-releasing hormone antagonist *in vitro* fertilization cycles. *Fertil. Steril.* (2006) 85:112–20. doi: 10.1016/j.fertnstert.2005.07.1292

149. Underwood MA, Gilbert WM, Sherman MP. Amniotic fluid: Not just fetal urine anymore. *J Perinatol.* (2005) 25:341–8. doi: 10.1038/sj.jp.7211290

150. Toth D, Veszpremi B, Koppan M, Tamas A, Szogyi D, Brubel R, et al. Investigation of pituitary adenylate cyclase activating polypeptide (PACAP) in human amniotic fluid samples. *Reprod Biol* (2020) 20:491–5. doi: 10.1016/j.repbio.2020.07.013

151. Cho CK, Shan SJ, Winsor EJ, Diamandis EP. Proteomics analysis of human amniotic fluid. *Mol Cell Proteomics* (2007) 6:1406–15. doi: 10.1074/mcp.M700090-MCP200

152. Oride A, Kanasaki H, Kyo S. Role of pituitary adenylate cyclase-activating polypeptide in modulating hypothalamic-pituitary system. *Reprod Med Biol* (2018) 17:234–41. doi: 10.1002/rmb2.12094

153. Nagy GM, Vigh S, Arimura A. PACAP induces prolactin and growth hormone release in lactating rats separated from their pups. *Endocr. J* (1993) 40:169–73.

154. Tohei A, Ikeda M, Hokao R, Shinoda M. The different effects of i.c.v. injection of pituitary adenylate cyclase activating polypeptide (PACAP) on prolactin secretion in adult male and lactating rats. *Exp Anim* (2009) 58:489–95. doi: 10.1538/expanim.58.489

155. Jamen F, Alonso G, Shibuya I, Widmer H, Vacher CM, Calas A, et al. Impaired somatodendritic responses to pituitary adenylate cyclase-activating polypeptide (PACAP) of supraoptic neurones in PACAP type I -receptor deficient mice. *J Neuroendocrinol.* (2003) 15:871–81. doi: 10.1046/j.1365-2826.2003.01075.x

156. Tamas A, Vass RA, Helyes Z, Csanaky K, Szanto Z, Nemeth J, et al. Examination of PACAP during lactation. In: D Reglodi and A Tamas, editors. *Pituitary adenylate cyclase activating polypeptide - PACAP*. Switzerland: Springer International Publishing (2016). p. 833–40. doi: 10.1007/978-3-319-35135-3_49

157. Czegledi L, Tamas A, Borzsei R, Bagoly T, Kiss P, Horvath G, et al. Presence of pituitary adenylate cyclase-activating polypeptide (PACAP) in the plasma and milk of ruminant animals. *Gen Comp Endocrinol* (2011) 172:115–9. doi: 10.1016/j.ygcen.2010.12.012

158. Csanaky K, Reglodi D, Banki E, Tarcai I, Mark L, Helyes Z, et al. Examination of PACAP38-like immunoreactivity in different milk and infant formula samples. *Acta Physiol Hung* (2013) 100:28–36. doi: 10.1556/APhysiol.100.2013.1.2

159. Pohoczky K, Tamas A, Reglodi D, Kemeny A, Zs H, Czegledi L. Pituitary adenylate cyclase activating polypeptide concentrations in the sheep mammary gland, milk, and in the lamb blood plasma after suckling. *Physiol Int* (2020) 107:92–105. doi: 10.1556/2060.2020.00006

160. Csanaky K, Doppler W, Tamas A, Kovacs K, Toth G, Reglodi D. Influence of terminal differentiation and PACAP on the cytokine, chemokine, and growth factor secretion of mammary epithelial cells. *J Mol Neurosci* (2014) 52:28–36. doi: 10.1007/s12031-013-0193-3

161. de Assis Rodrigues NP, Laganà AS, Zaia V, Vitagliano A, Barbosa CP, de Oliveira R, et al. The role of kisspeptin levels in polycystic ovary syndrome: a systematic review and meta-analysis. *Arch Gynecol. Obstet.* (2019) 300:1423–34. doi: 10.1007/s00404-019-05307-5

162. Cintra RG, Wajnsztejn R, Trevisan CM, Zaia V, Laganà AS, Bianco B, et al. Kisspeptin levels in girls with precocious puberty: A systematic review and meta-analysis. *Horm Res Paediatr* (2020) 93:589–98. doi: 10.1159/000515660

frontiers | Frontiers in Endocrinology

TYPE Mini Review
PUBLISHED 29 September 2022
DOI 10.3389/fendo.2022.1009379

OPEN ACCESS

EDITED BY
Allan Herbison,
University of Cambridge,
United Kingdom

REVIEWED BY
Kyle Flippo,
The University of Iowa, United States

*CORRESPONDENCE
Caroline S. Johnson
joh20852@umn.edu

SPECIALTY SECTION
This article was submitted to Reproduction, a section of the journal Frontiers in Endocrinology

RECEIVED 01 August 2022
ACCEPTED 13 September 2022
PUBLISHED 29 September 2022

CITATION
Johnson CS, Micevych PE and Mermelstein PG (2022) Membrane estrogen signaling in female reproduction and motivation. *Front. Endocrinol.* 13:1009379. doi: 10.3389/fendo.2022.1009379

Membrane estrogen signaling in female reproduction and motivation

Caroline S. Johnson[1]*, Paul E Micevych[2] and Paul G. Mermelstein[1]

[1]Department of Neuroscience, University of Minnesota, Minneapolis, MN, United States, [2]Laboratory of Neuroendocrinology, Department of Neurobiology, David Geffen School of Medicine at University of California, Los Angeles, Los Angeles, CA, United States

Estrogen receptors were initially identified in the uterus, and later throughout the brain and body as intracellular, ligand-regulated transcription factors that affect genomic change upon ligand binding. However, rapid estrogen receptor signaling initiated outside of the nucleus was also known to occur *via* mechanisms that were less clear. Recent studies indicate that these traditional receptors, estrogen receptor-α and estrogen receptor-β, can also be trafficked to act at the surface membrane. Signaling cascades from these membrane-bound estrogen receptors (mERs) not only rapidly effect cellular excitability, but can and do ultimately affect gene expression, as seen through the phosphorylation of CREB. A principal mechanism of neuronal mER action is through glutamate-independent transactivation of metabotropic glutamate receptors (mGluRs), which elicits multiple signaling outcomes. The interaction of mERs with mGluRs has been shown to be important in many diverse functions in females, including, but not limited to, reproduction and motivation. Here we review membrane-initiated estrogen receptor signaling in females, with a focus on the interactions between these mERs and mGluRs.

KEYWORDS

estrogen, estrogen receptors, membrane estrogen receptors, metabotropic glutamate (mGlu) receptors, estrogen receptor signaling

Introduction

The estrogen receptors, estrogen receptor-α (ERα) and estrogen receptor-β (ERβ) were initially identified as intracellular, ligand-regulated transcription factors (1), members of the larger nuclear receptor superfamily (2, 3). Originally identified in the uterus (4, 5), these estrogen receptors are expressed throughout the body, including in a multitude of brain regions (6, 7). Estradiol binding to these receptors was initially demonstrated to induce transcriptional changes at estrogen response elements (EREs) (8). However, this classical signaling pathway is not the only mechanism through which

estrogen receptors directly elicit genomic change. Many estrogen-regulated genes lack ERE sequences (9, 10), which led to the discovery of additional genomic actions occurring *via* other response elements and transcription factors (11, 12). However, even with multiple pathways leading to direct genomic effects, this was still insufficient to fully explain the plethora of actions estradiol was observed to induce both inside and outside the nervous system.

Membrane-initiated signaling

The first clues that estrogen signaling could be initiated outside the nucleus came from Szego & Davis in the late 1960s. Following ovariectomy (ovx) in rats, acute exogenous estradiol treatment resulted in an increase in uterine cAMP accumulation within seconds, concentrations indistinguishable from intact animals (13). The speed at which these changes occurred eliminated the possibility of nuclear-initiated action and strongly suggested the recruitment of a surface-initiated second messenger signaling pathway. Rapid effects of estradiol were subsequently noted within the nervous system, first in female preoptic-septal neurons in the hypothalamus. Within seconds of application, estradiol modulated firing rates, returning to experimental baseline when the steroid was removed (14). The use of estradiol conjugated to bovine serum albumen (BSA) further implicated membrane-associated estrogen receptors (15). However, skepticism remained, as there was suspicion that estradiol might be cleaved from BSA (16). Thus, large dendrimer macromolecules conjugated to estrogens were produced. These conjugates avoided the potential for cleaving and were unable to cross the cellular membrane, precluding the activation of nuclear ERs, but still resulted in rapid estradiol signaling (17). While in 2000 a novel estrogen receptor potentially located at the membrane was identified, i.e. G protein-coupled estrogen receptor 1 (GPER1) (18), overexpression of both ERα and ERβ (19), along with immunohistochemical (20) and co-immunoprecipitation studies (21) also indicated that a subpopulation of these classical receptors are trafficked to the membrane (19). The development of transgenic mice allowed researchers to explore the effects of rapid signaling *in vivo*. In transgenic knockout mice devoid of ERα, and/or ERβ, rapid estradiol signaling was eliminated in a brain-region and signaling pathway-dependent manner, suggesting that these receptors are responsible for many of the membrane signaling effects (22).

Membrane-initiated estrogen receptor signaling does not preclude downstream influences on gene expression. Particularly prominent is estradiol activation of PKC-MAPK signaling, ultimately resulting in the phosphorylation of CREB (23–26). Serine-133 phosphorylation of CREB can initiate a diverse array of transcriptional and behavioral changes, including by estradiol-mediated CREB activation *via* membrane ER (mER) interactions with metabotropic glutamate receptors (mGluRs) (23). Initial findings in hippocampal neurons found estradiol acting through ERα-mGluR1a leads to MAPK-dependent CREB phosphorylation. This study elucidated a separate second pathway whereby activation of ERα or ERβ associated with mGluR2 (and Gi/o-mediated inhibition of cAMP) resulted in a decrease in L-type calcium-channel mediated CREB phosphorylation (23). Follow-up studies found mER signaling through mGluR activation throughout the brain, which appears to be a mechanism allowing for diverse signaling outcomes. Not only does mER activation of group I or group II mGluRs activate separate cell signaling pathways, but mER pairing with different group I or II mGluRs (i.e. mGluR1 vs. mGluR5 and mGluR2 vs. mGluR3) can differentially impact neuronal function as well (27).

The interaction of mERs with mGluRs requires caveolin (CAV) (28–30), a family of scaffolding proteins involved in trafficking receptors to the membrane (31). The particular ER-mGluR pairing is mediated through the CAV isoform associated with the ER (28) (Figure 1). A single point mutation in ERα that disrupts receptor localization with CAV1 inhibited estradiol-induced CREB phosphorylation. Reducing CAV1 expression through siRNA knockdown inhibited estradiol-induced CREB phosphorylation while leaving the estradiol-induced L-type calcium channel-dependent decrease in CREB phosphorylation intact. In reciprocal experiments, siRNA knockdown of CAV3 inhibited estradiol-dependent activation of group II mGluRs without affecting estradiol-mediated CREB phosphorylation. In both cases, siRNA knockdown did not grossly impact mGluR signaling, demonstrating the essential nature of caveolin proteins to mER signaling (28). These data contribute to the understanding that CAV1 mediates ERα interactions with group I mGluRs through clustering the receptor at the membrane (28, 29, 33), while CAV3 is involved in the interactions between mERs and group II mGluRs (28). Additionally, an alternatively spliced form of ERα, ERαΔ4, is highly expressed in membrane fractions derived from cultured cells. This receptor has been shown to associate with both mGluR2/3 and CAV3 in ARH membrane fractions (34).

Following these experiments, the precise mechanism of action linking ERs to mGluRs and to the membrane remained unclear, though palmitoylation was an attractive hypothesis. Palmitoylation is a reversible, post-transcriptional modification involved in the trafficking and function of proteins both within and outside the nervous system (35). Global pharmacological blockade of palmitoylation inhibited the downstream outcomes of membrane estradiol signaling, while introducing single point mutations at palmitoylation sites in both ERα and ERβ was sufficient to inhibit membrane signaling (36). Two palmitoyl acetyltransferases (DHHC-7 and DHHC-21) have been shown to be crucial in ER membrane localization (37). Disrupting expression of either was sufficient to inhibit estradiol-dependent CREB phosphorylation (36), and to prevent ERα

10.3389/fendo.2022.1009379

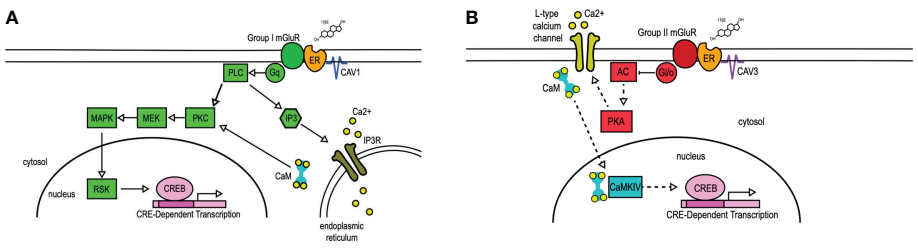

FIGURE 1
mER transactivation of group I and group II mGluRs. 17β-Estradiol (17βE) binds to membrane-bound estrogen receptors (ER) to activate distinct signaling pathways *via* Group I **(A)** or Group II **(B)** mGluRs. **(A)** Membrane-ER interactions with Group I mGluRs, dependent on CAV1, activates G_q-mediated signaling through protein lipase C (PLC) and protein kinase C (PKC), subsequent activation of MEK, MAPK, and RSK, and ultimately the phosphorylation of CREB. PLC also activates IP3, which binds to the IP3 receptor (IP3R) to result in the release of intracellular calcium (Ca^{2+}). **(B)** Membrane-ER activation of Group II mGluRs, dependent on CAV3, results in the $G_{i/o}$-mediated inhibition of adenylyl cyclase (AC), decreasing the activity (indicated by dashed lines) of protein kinase A (PKA). This results in reduced L-type calcium channel currents and L-type calcium channel-dependent CREB phosphorylation. CaM, Calmodulin; CaMKIV, calmodulin-dependent protein kinase IV; CAV, caveolin; IP3, inositol triphosphate; MEK, MAPK/ERK kinase; MAPK, mitogen-activated protein kinase; RSK, ribosomal S6 kinase. Figure adapted from (32).

from associating with CAV1 (38). siRNA knockdown of these enzymes together, but not separately, was sufficient to decrease the palmitoylation of CAV1 itself (38). These data suggest that palmitoylation is a crucial component in the interaction of mERs with CAV proteins, the coupling of mERs with mGluRs, and the subsequent signaling cascades.

While estrogen-mediated signaling plays a crucial role in the female brain, estrogen-mediated signaling is not absent in the male brain. Estrogen plays an important role in masculinizing the brain (39), and rapid estradiol signaling occurs in adult males, including through mGluRs. Estradiol activation of mGluR1a through ERβ modulates sexual behavior in male quails (40, 41), and rodent studies have confirmed rapid mER-mGluR signaling in both the male and female adult cerebellum (42). In females, though, rapid signaling of estradiol, including through mGluRs, has been shown to be incredibly important in driving reproduction, including in the development of the luteinizing hormone surge which stimulates ovulation, the central event in female reproduction. In rodents, and certain other species, rapid membrane signaling is also crucial in the physical display of the principal reproductive behavior, lordosis. Finally, rapid membrane signaling has been shown to play an important role in female motivation for reproduction.

Ovulation and the luteinizing hormone surge

Ovulation is the central event in female reproduction, controlled by a network of neurons and astrocytes in the hypothalamus that act as a pattern generator, releasing gonadotropin-releasing hormone (GnRH) onto luteinizing hormone (LH) neurons in the anterior pituitary in small, rhythmic pulses (43, 44). Rising estradiol concentrations *via* ovarian release, trigger a switch from an estrogen-negative to an estrogen-positive feedback loop. This estrogen-positive feedback loop, which is unique to females, is crucial in the surge release of LH that ultimately triggers ovulation (45). The preovulatory rise in circulating estradiol sharply increases GnRH neuronal activity and the release of LH from the pituitary to elicit ovulation (46, 47). Blocking either progesterone receptors or progesterone synthesis prevents the surge release of both GnRH and LH and halts the estrous cycle (48, 49). While GnRH neurons do not express ERα or nuclear progesterone receptors (45, 50, 51), kisspeptin neurons that are upstream regulators of GnRH signaling do express the necessary steroid receptors (52–54).

Classically it has been understood that both estradiol and progesterone released from the ovaries orchestrate the LH surge, but it has become apparent that progesterone is also synthesized *de novo* in the brain (55–57), and that it is this neuroprogesterone (neuroP) that is vital in the LH surge that ultimately leads to ovulation (58). Neuroprogesterone is synthesized in hypothalamic astrocytes that express mERα and mGluRs, and it has been shown that the LH surge relies upon the mER-mGluR signaling in these astrocytes (55, 59). Estradiol activation of mERα directly leads to the activation of mGluR1 and its downstream signaling cascades. mGluR1 activity increases inositol triphosphate and allows for the release of intracellular calcium ($[Ca^{2+}]_i$) stores (59, 60). The release of $[Ca^{2+}]_i$ activates a Ca^{2+}-sensitive adenylyl cyclase (AC-1), which increases the production of cAMP. This cAMP activates protein kinase A (60), leading to the synthesis of neuroP (56, 57, 59). Blocking neuroP synthesis in rats that had both ovaries and adrenals removed is sufficient to prevent the LH surge (61). Cell culture experiments in astrocytes isolated this signaling pathway. Blocking mGluR1a activity, or any part of the cell signaling cascade initiated by the ERα activation of mGluR1, in astrocytes inhibits neuroP synthesis (49, 55, 59, 60). Further, in the absence of estradiol, activating mGluR1a directly is sufficient to release $[Ca^{2+}]_i$ and induce neuroP synthesis (59, 62).

Lordosis

Another important aspect of reproduction controlled by ER interactions with mGluRs is lordosis. Lordosis is a reflexive behavior that is acutely triggered by mounting from a conspecific male. This behavior consists of an arching of the spine, the raising of both the head and the hindquarters, and the lifting of the tail (63). While integration of the tactile cues with other externosensory cues is crucial for the display of lordosis, this behavior depends heavily on the appropriate timing of the release of ovarian hormones and the subsequent priming of neural circuits by these hormones. The role of intracellular and membrane-bound ERs, as well as the interaction between mERs and mGluRs, have all been shown to be important components in driving lordosis (64, 65).

A core circuit controlling lordosis is within the hypothalamus. Here, signaling between the arcuate nucleus (ARH), the medial preoptic nucleus (MPN), and the ventromedial nucleus of the hypothalamus (VMH) have been shown to be fundamental in the expression of lordosis (64, 66–70) (Figure 2). Within this circuit, estradiol first acts on ERα-containing neuropeptide Y (NPY) neurons in the ARH (21, 68, 71), allowing for the release of NPY onto NPY-Y1 receptors in ARH proopiomelanocortin (POMC) neurons. The subset of POMC neurons that are involved in reproduction project further to the MPN where they release β-End onto neurons that express μ-opioid receptors (MORs). The estradiol-induced activation, and subsequent internalization, of MOR depends upon ERα activity (65). Throughout the estrous cycle the activation/internalization of this receptor is out of phase with the ability to express lordosis (69). That is, when MOR is internalized, a measure of activation, the display of lordosis is prohibited. As the cycle progresses, increasing progesterone levels ultimately result in the restoration of MOR to the membrane, a measure indicating that the receptors are not stimulated (72), and the behavior can be expressed. While counterintuitive, this estradiol inhibition of lordosis is necessary for its later full expression. While many neural changes must occur to result in the production of lordosis, recent work has shown that much of the machinery involved in this behavior utilizes fast-acting mER signaling cascades, and particularly those signaling through mGluRs.

Within the ARH, a subset of the NPY neurons express both ERα and mGluR1a, which have been shown to interact at the membrane to initiate signaling (21). The mER-mGluR signaling in the ARH has been shown to be crucial in both the internalization of MOR and the subsequent display of lordosis. The level of estradiol determines the expression of the mERα-mGluR1 complex in the ARH. When estradiol is low, the mERα-mGluR1 complex is present, but as estradiol levels rise the

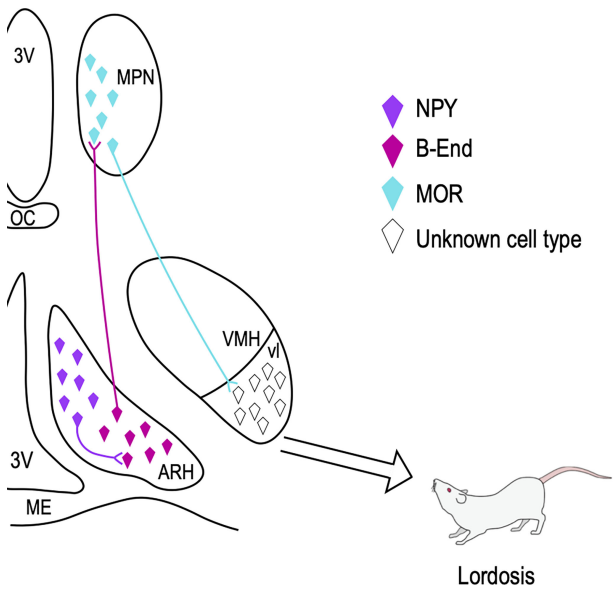

FIGURE 2
Hypothalamic lordosis circuit. Estradiol acts on estrogen receptor-containing NPY neurons in the ARH, which further project to and activate ARH POMC/B-End neurons. These POMC neurons project to the MPN where the release of B-End activates and internalizes MORs. When these receptors are internalized, lordosis is attenuated. In the ARH, the interaction of mERα & mGluR1a is important for both the internalization of MOR and ultimately the display of lordosis. These MOR-containing neurons in the MPN project further to the ventrolateral (vl) part of the VMH, where signals from other circuits are integrated. Projections from the VMHvl reach lower brain regions which ultimately innervate the spinal motor neurons responsible for the production of the behavior. 3V, 3rd ventricle; OC, optic chiasm; ME, median eminence. Figure adapted from (66).

expression of mERα-mGluR1 is reduced (73). In the ARH, antagonizing mGluR1a activity before estradiol treatment is sufficient to attenuate the internalization of MOR in the MPN as well as the ensuing expression of lordosis (20, 21). Activating mGluR1a in the ARH to circumvent the necessity of estradiol is sufficient to result in the internalization of MOR and lordosis (20). Both *in vitro* and *in vivo* activating mGluR1a through estradiol-induced mERα activity increases many important phosphoproteins, including PKC and CREB (20, 21, 23), and the internalization of MOR appears to depend at least in part upon PKC signaling. Downstream from mGluR1a activity, activating PKC signaling in the ARH in the absence of estradiol was sufficient to result in the internalization of MOR, and the amount of this internalization was comparable to that seen following estradiol treatment alone (21).

Another key component in the production of lordosis regulated by fast mER-mGluR activity is morphological changes to neuronal structure. Estradiol affects both the generation and pruning of dendritic spines, though this is not unique to the hypothalamic lordosis circuit but occurs throughout the brain (64, 74, 75) and appears due to retrograde signaling by endogenous opioids (76–78). Within this circuit, important morphological changes can be induced rapidly through mERα-mGluR1a signaling in the ARH. Within 4 hours, estradiol activation of mGluR1a results in an increase in the total number of dendritic spines, which remains for at least 48 hours. By 20 hours these spines display mushroom-shaped morphology, suggesting that these synapses are functional. Blocking mGluR1a activity prevented this spinogenesis, as well as attenuated the display of lordosis (64). Importantly, this time course of changes in morphology lines up with that of the display of lordosis.

Motivation

Estrogen membrane-receptor signaling has also been found to play a role in motivation. Though the long-term consequence of reproduction is the survival of the species through the production of offspring, the short-term motivation of reproduction is often the immediate drive for the rewarding aspects of the behavior, in females as much as in males (79). While work has focused on the physiology of ovulation and the rodent's reflexive response to mounting by a male, female sexual behavior is indicative of a motivational drive. Female rats placed in a modified operant chamber, in which the female can choose if and when she wants to copulate, will seek the male for copulation timed to maximize reward (80, 81). Additionally, other pre-copulatory behaviors from female rodents, such as hopping or darting (82, 83), further indicate a level of control over the mating process. This pre-copulatory activity, which is called "pacing," contributes to a robust dopamine response in the female nucleus accumbens (NAc) in response to mating (84–87). This dopamine response, as well as further structural changes, in the NAc is regulated at least in part by estradiol signaling at the membrane.

The NAc is a key region in reward and incentive salience, and the limbic control of behavioral motivation, and inputs here affect structural morphology and subsequently behavioral output. The limbic system is important in the motivation to engage in reproductive behaviors in both males and females (67, 79), and projections from the hypothalamic nuclei robustly innervate this circuit. The reproductive limbic circuit consists of the MPN, the ventral tegmental area (VTA), and the NAc. A key node connecting the hypothalamus to the limbic component includes the MPN (88). Projections from here reciprocally innervate the mesolimbic dopamine system, including the VTA (89). The VTA projections to the NAc arise from cells that contain ERs (90) and are sensitive to fluctuations in estradiol levels (91), as well as estradiol-mediated signals arising from the MPN (90). These estradiol-mediated changes in VTA signaling have been shown to further affect the subsequent release of DA in the NAc (90).

The predominant output neuron in the NAc is the medium spiny neuron (MSN) - named due to the density of spines it possesses (92). The MSNs in the NAc receive both DAergic and glutamatergic inputs (93), and it has been shown that estradiol plays an important role in modulating both inputs (94–97). MSNs contain few nuclear ERs, suggesting that estradiol acts primarily through membrane-bound receptors ERs (98–103). As in the hypothalamus, estradiol modulates spine density in the NAc and the estradiol-induced morphological changes in the MSNs of the NAc are dramatic in terms of functional circuitry and neuronal morphology (104, 105). In female rodents, sexual experience modulates future sexual behavior through estradiol-mediated morphological changes within the limbic circuit (79). While the complete mechanisms of estradiol modulation on motivational circuity have yet to be fully elucidated, it is likely that mER-mGluR signaling plays a role.

The role of membrane estradiol signaling, and particularly the interaction between mERs and mGluRs, in reproductive motivational drive can be further extrapolated from studies investigating when motivational drive becomes maladaptive, such as in drug addiction. In comparison with men, women tend to show heightened vulnerability to developing a drug addiction (106, 107). Additionally, subjective effects of a drug can vary across the menstrual cycle, as has been reported in response to cocaine. When estrogen levels are high, women report the greatest effects of the drug (108). Interest in the interaction between membrane ERs and group I mGluRs has been taken in understanding the influence of estradiol on drug addiction. In ovx rats, estradiol activation of mGluR5 has been shown to facilitate self-administration of cocaine, while inhibiting this signaling through an mGluR5 antagonist before estradiol administration is sufficient to attenuate this intake of the drug (109). Estradiol activation of mGluR5 in MSNs also

results in an increase in the phosphorylation of CREB (100), and a decrease in dendritic spine density in both the core region of the NAc (27, 104, 105). Conversely, estradiol activation of mGluR1 can result in an increase in spine density in the shell region of NAc (27). Taken together, the data suggest that mER-mGluR signaling are important in the drive to seek reward generally, as is apparent in drug taking behaviors, and in the reinforcement of reproductive behaviors.

Discussion

A great deal of progress has been made in understanding the physiology of rapid estradiol signaling, including the relationship between mERs and mGluRs. Rapid estradiol signaling has been found throughout the brain and the body. In the central nervous system, the signaling cascades initiated by the mER/mGluR complex has been shown to be involved in many physiological functions in both sexes, but particularly in females. In females, the diverse signaling cascades initiated by the interaction of mERs with mGluRs have been shown to play important roles in mediating key aspects of reproduction and motivation, among other crucial functions. While uncovering the roles of CAV and palmitoylation has led to further understanding of this complex signaling cascade, current and future research will inevitably expand our knowledge of mER/mGluR signaling and its physiological and behavioral outcomes.

Author contributions

CJ wrote the first draft of the manuscript, and revised subsequent drafts. PMe, PMi contributed to and revised the manuscript. All authors read and approved the submitted version.

Funding

This work was supported by DA041808 and HD10007 to PGM and HD098284 to PEM. CSJ was supported by DA007234.

Conflict of interest

The authors declare that the research was conducted in the absence of any commercial or financial relationships that could be construed as a potential conflict of interest.

Publisher's note

References

1. McKenna NJ, Lanz RB, O'Malley BW. Nuclear receptor coregulators: Cellular and molecular biology. *Endocr Rev* (1999) 20(3):321–44. doi: 10.1210/edrv.20.3.0366

2. Evans RM. The steroid and thyroid hormone receptor superfamily. *Science* (1988) 240(4854):889–95. doi: 10.1126/science.3283939

3. Giguère V, Yang N, Segui P, Evans RM. Identification of a new class of steroid hormone receptors. *Nature* (1988) 331(6151):91–4. doi: 10.1038/331091a0

4. Jensen EV, Jacobsonk HI. Basic guides to the mechanism of estrogen action. *Recent Progr Hormone Res* (1962) 18:387–414.

5. Toft D, Gorski J. A receptor molecule for estrogens: Isolation from the rat uterus and preliminary characterization. *Proc Natl Acad Sci* (1966) 55(6):1574–81. doi: 10.1073/pnas.55.6.1574

6. Shughrue PJ, Lane MV, Merchenthaler I. Comparative distribution of estrogen receptor-α and -β mRNA in the rat central nervous system. *J Comp Neurol* (1997) 388(4):507–25. doi: 10.1002/(SICI)1096-9861(19971201)388:4<507::AID-CNE1>3.0.CO;2-6

7. Simerly RB, Swanson LW, Chang C, Muramatsu M. Distribution of androgen and estrogen receptor mRNA-containing cells in the rat brain: An *in situ* hybridization study. *J Comp Neurol* (1990) 294(1):76–95. doi: 10.1002/cne.902940107

8. O'Malley BW, Tsai MJ. Molecular pathways of steroid receptor action. *Biol Reprod* (1992) 46(2):163–7. doi: 10.1095/biolreprod46.2.163

9. Marino M, Galluzzo P, Ascenzi P. Estrogen signaling multiple pathways to impact gene transcription. *Curr Genomics* (2006) 7(8):497–508. doi: 10.2174/138920206779315737

10. Vrtačnik P, Ostanek B, Mencej-Bedrač S, Marc J. The many faces of estrogen signaling. *Biochem Medica* (2014) 24(3):329–42. doi: 10.11613/BM.2014.035

11. Aranda A, Pascual A. Nuclear hormone receptors and gene expression. *Physiol Rev* (2001) 81(3):1269–304. doi: 10.1152/physrev.2001.81.3.1269

12. Göttlicher M, Heck S, Herrlich P. Transcriptional cross-talk, the second mode of steroid hormone receptor action. *J Mol Med* (1998) 76(7):480–9. doi: 10.1007/s001090050242

13. Szego CM, Davis JS. Adenosine 3',5'-monophosphate in rat uterus: Acute elevation by estrogen. *Proc Natl Acad Sci* (1967) 58(4):1711–8. doi: 10.1073/pnas.58.4.1711

14. Kelly MJ, Moss RL, Dudley CA. Differential sensitivity of preoptic-septal neurons to microelectrophoressed estrogen during the estrous cycle. *Brain Res* (1976) 114(1):152–7. doi: 10.1016/0006-8993(76)91017-9

15. Zheng J, Ramirez VD. Demonstration of membrane estrogen binding proteins in rat brain by ligand blotting using a 17β-estradiol-[125I]bovine serum albumin conjugate. *J Steroid Biochem Mol Biol* (1997) 62(4):327–36. doi: 10.1016/S0960-0760(97)00037-X

16. Stevis PE, Deecher DC, Suhadolnik L, Mallis LM, Frail DE. Differential effects of estradiol and estradiol-BSA conjugates. *Endocrinology* (1999) 140 (11):5455–8. doi: 10.1210/endo.140.11.7247

17. Harrington WR, Kim SH, Funk CC, Madak-Erdogan Z, Schiff R, Katzenellenbogen JA, et al. Estrogen dendrimer conjugates that preferentially activate extranuclear, nongenomic versus genomic pathways of estrogen action. *Mol Endocrinol* (2006) 20(3):491–502. doi: 10.1210/me.2005-0186

18. Filardo EJ, Quinn JA, Bland KI, Frackelton AR. Estrogen-induced activation of erk-1 and erk-2 requires the G protein-coupled receptor homolog, GPR30, and occurs *via* trans-activation of the epidermal growth factor receptor through release of HB-EGF. *Mol Endocrinol* (2000) 14(10):1649–60. doi: 10.1210/mend.14.10.0532

19. Razandi M, Pedram A, Greene G, Levin E. Cell membrane and nuclear estrogen receptors (ERs) originate from a single transcript: Studies of ERα and ERβ

expressed in Chinese hamster ovary cells. *Mol Endocrinol* (1999) 13(2):307–19. doi: 10.1210/me.13.2.307

20. Dewing P, Boulware MI, Sinchak K, Christensen A, Mermelstein PG, Micevych P. Membrane estrogen receptor-α interactions with metabotropic glutamate receptor 1a modulate female sexual receptivity in rats. *J Neurosci* (2007) 27(35):9294–300. doi: 10.1523/JNEUROSCI.0592-07.2007

21. Dewing P, Christensen A, Bondar G, Micevych P. Protein kinase c signaling in the hypothalamic arcuate nucleus regulates sexual receptivity in female rats. *Endocrinology* (2008) 149(12):5934–42. doi: 10.1210/en.2008-0847

22. Aíbrahaím IM, Todman MG, Korach KS, Herbison AE. Critical *in vivo* roles for classical estrogen receptors in rapid estrogen actions on intracellular signaling in mouse brain. *Endocrinology* (2004) 145(7):3055–61. doi: 10.1210/en.2003-1676

23. Boulware MI, Weick JP, Becklund BR, Kuo SP, Groth RD, Mermelstein PG. Estradiol activates group I and II metabotropic glutamate receptor signaling, leading to opposing influences on cAMP response element-binding protein. *J Neurosci* (2005) 25(20):5066–78. doi: 10.1523/JNEUROSCI.1427-05.2005

24. Gu G, Rojo AA, Zee MC, Yu J, Simerly RB. Hormonal regulation of CREB phosphorylation in the anteroventral periventricular nucleus. *J Neurosci* (1996) 16 (9):3035–44. doi: 10.1523/JNEUROSCI.16-09-03035.1996

25. Szego EM, Barabás K, Balog J, Szilágyi N, Korach KS, Juhász G, et al. Estrogen induces estrogen receptor α-dependent cAMP response element-binding protein phosphorylation *via* mitogen activated protein kinase pathway in basal forebrain cholinergic neurons *in vivo*. *J Neurosci* (2006) 26(15):4104–10. doi: 10.1523/JNEUROSCI.0222-06.2006

26. Wade CB, Dorsa DM. Estrogen activation of cyclic adenosine 5′-monophosphate response element-mediated transcription requires the extracellularly regulated kinase/mitogen-activated protein kinase pathway. *Endocrinology* (2003) 144(3):832–8. doi: 10.1210/en.2002-220899

27. Gross KS, Brandner DD, Martinez LA, Olive MF, Meisel RL, Mermelstein PG. Opposite effects of mGluR1a and mGluR5 activation on nucleus accumbens medium spiny neuron dendritic spine density. *PloS One* (2016) 11(9):e0162755. doi: 10.1371/journal.pone.0162755

28. Boulware MI, Kordasiewicz H, Mermelstein PG. Caveolin proteins are essential for distinct effects of membrane estrogen receptors in neurons. *J Neurosci* (2007) 27(37):9941–50. doi: 10.1523/JNEUROSCI.1647-07.2007

29. Christensen A, Micevych P. CAV1 siRNA reduces membrane estrogen receptor-α levels and attenuates sexual receptivity. *Endocrinology* (2012) 153 (8):3872–7. doi: 10.1210/en.2012-1312

30. Razandi M, Oh P, Pedram A, Schnitzer J, Levin ER. Ers associate with and regulate the production of caveolin: Implications for signaling and cellular actions. *Mol Endocrinol* (2002) 16(1):100–15. doi: 10.1210/mend.16.1.0757

31. Anderson RGW. The caveolae membrane system. *Annu Rev Biochem* (1998) 67(1):199–225. doi: 10.1146/annurev.biochem.67.1.199

32. Eisinger KRT, Gross KS, Head BP, Mermelstein PG. Interactions between estrogen receptors and metabotropic glutamate receptors and their impact on drug addiction in females. *Horm Behav* (2018) 104:130–7. doi: 10.1016/j.yhbeh.2018.03.001

33. Bondar G, Kuo J, Hamid N, Micevych P. Estradiol-induced estrogen receptor-α trafficking. *J Neurosci* (2009) 29(48):15323–30. doi: 10.1523/JNEUROSCI.2107-09.2009

34. Wong AM, Scott AK, Johnson CS, Mohr MA, Mittelman-Smith M, Micevych PE. ERαΔ4, an ERα splice variant missing exon4, interacts with caveolin-3 and mGluR2/3. *J Neuroendocrinol* (2019) 31(6):e12725. doi: 10.1111/jne.12725

35. Fukata Y, Fukata M. Protein palmitoylation in neuronal development and synaptic plasticity. *Nat Rev Neurosci* (2010) 11(3):161–75. doi: 10.1038/nrn2788

36. Meitzen J, Luoma JI, Boulware MI, Hedges VL, Peterson BM, Tuomela K, et al. Palmitoylation of estrogen receptors is essential for neuronal membrane signaling. *Endocrinology* (2013) 154(11):4293–304. doi: 10.1210/en.2013-1172

37. Pedram A, Razandi M, Deschenes RJ, Levin ER. DHHC-7 and -21 are palmitoylacyltransferases for sex steroid receptors. *Mol Biol Cell* (2012) 23(1):188–99. doi: 10.1091/mbc.e11-07-0638

38. Eisinger KRT, Woolfrey KM, Swanson SP, Schnell SA, Meitzen J, Dell'Acqua M, et al. Palmitoylation of caveolin-1 is regulated by the same DHHC acyltransferases that modify steroid hormone receptors. *J Biol Chem* (2018) 293(41):15901–11. doi: 10.1074/jbc.RA118.004167

39. Schwarz JM, McCarthy MM. Cellular mechanisms of estradiol-mediated masculinization of the brain. *J Steroid Biochem Mol Biol* (2008) 109(3–5):300–6. doi: 10.1016/j.jsbmb.2008.03.012

40. Cornil CA, Ball GF, Balthazart J. Rapid control of male typical behaviors by brain-derived estrogens. *Front Neuroendocrin* (2012) 33(4):425–46. doi: 10.1016/j.yfrne.2012.08.003

41. Seredynski AL, Balthazart J, Ball GF, Cornil CA. Estrogen receptor β activation rapidly modulates male sexual motivation through the transactivation of metabotropic glutamate receptor 1a. *J Neurosci* (2015) 35(38):13110–23. doi: 10.1523/JNEUROSCI.2056-15.2015

42. Hedges VL, Chen G, Yu L, Krentzel AA, Starrett JR, Zhu JN, et al. Local estrogen synthesis regulates parallel fiber–purkinje cell neurotransmission within the cerebellar cortex. *Endocrinology* (2018) 159(3):1328–38. doi: 10.1210/en.2018-00039

43. Herbison AE. The gonadotropin-releasing hormone pulse generator. *Endocrinology* (2018) 159(11):3723–36. doi: 10.1210/en.2018-00653

44. Kauffman AS, Smith JT eds. *Kisspeptin signaling in reproductive biology* Vol. Vol. 342). New York: Springer (2013).

45. Wintermantel TM, Campbell RE, Porteous R, Bock D, Gröne HJ, Todman MG, et al. Definition of estrogen receptor pathway critical for estrogen positive feedback to gonadotropin-releasing hormone neurons and fertility. *Neuron* (2006) 52(2):271–80. doi: 10.1016/j.neuron.2006.07.023

46. Ferin M, Tempone A, Zimmering PE, Wiele RLV. Effect of antibodies to 17 β-estradiol and progesterone on the estrous cycle of the rat. *Endocrinology* (1969) 85(6):1070–8. doi: 10.1210/endo-85-6-1070

47. Labhsetwar AP. Role of estrogens in ovulation: A study using the estrogen-antagonist, I.C.I. 46,474. *Endocrinology* (1970) 87(3):542–51. doi: 10.1210/endo-87-3-542

48. Chappell PE. Stimulation of gonadotropin-releasing hormone surges by estrogen. i. role of hypothalamic progesterone receptors. *Endocrinology* (2000) 141 (4):1477–85.

49. Micevych P, Sinchak K. Estradiol regulation of progesterone synthesis in the brain. *Mol Cell Endocrinol* (2008) 290(1–2):44–50. doi: 10.1016/j.mce.2008.04.016

50. Herbison AE, Theodosis DT. Localization of oestrogen receptors in preoptic neurons containing neurotensin but not tyrosine hydroxylase, cholecystokinin or luteinizing hormone-releasing hormone in the male and female rat. *Neuroscience* (1992) 50(2):283–98. doi: 10.1016/0306-4522(92)90423-Y

51. Shivers BD, Harlan RE, Morrell JI, Pfaff DW. Absence of oestradiol concentration in cell nuclei of LHRH-immunoreactive neurones. *Nature* (1983) 304(5924):345–7. doi: 10.1038/304345a0

52. Clarkson J, de Tassigny Xd'Anglemont, Moreno AS, Colledge WH, Herbison AE. Kisspeptin-GPR54 signaling is essential for preovulatory gonadotropin-releasing hormone neuron activation and the luteinizing hormone surge. *J Neurosci* (2008) 28(35):8691–7. doi: 10.1523/JNEUROSCI.1775-08.2008

53. Navarro VM, Gottsch ML, Chavkin C, Okamura H, Clifton DK, Steiner RA. Regulation of gonadotropin-releasing hormone secretion by kisspeptin/dynorphin/neurokinin b neurons in the arcuate nucleus of the mouse. *J Neurosci* (2009) 29 (38):11859–66. doi: 10.1523/JNEUROSCI.1569-09.2009

54. Wakabayashi Y, Nakada T, Murata K, Ohkura S, Mogi K, Navarro VM, et al. Neurokinin b and dynorphin a in kisspeptin neurons of the arcuate nucleus participate in generation of periodic oscillation of neural activity driving pulsatile gonadotropin-releasing hormone secretion in the goat. *J Neurosci* (2010) 30 (8):3124–32. doi: 10.1523/JNEUROSCI.5848-09.2010

55. Kuo J, Hamid N, Bondar G, Prossnitz ER, Micevych P. Membrane estrogen receptors stimulate intracellular calcium release and progesterone synthesis in hypothalamic astrocytes. *J Neurosci* (2010) 30(39):12950–7. doi: 10.1523/JNEUROSCI.1158-10.2010

56. Micevych PE, Chaban V, Ogi J, Dewing P, Lu JKH, Sinchak K. Estradiol stimulates progesterone synthesis in hypothalamic astrocyte cultures. *Endocrinology* (2007) 148(2):782–9. doi: 10.1210/en.2006-0774

57. Sinchak K, Mills RH, Tao L, LaPolt P, Lu JKH, Micevych P. Estrogen induces *de novo* progesterone synthesis in astrocytes. *Dev Neurosci-basel* (2003) 25 (5):343–8. doi: 10.1159/000073511

58. Micevych P, Sinchak K. The neurosteroid progesterone underlies estrogen positive feedback of the LH surge. *Front Endocrinol* (2011) 2:90. doi: 10.3389/fendo.2011.00090

59. Kuo J, Hariri OR, Bondar G, Ogi J, Micevych P. Membrane estrogen receptor-α interacts with metabotropic glutamate receptor type 1a to mobilize intracellular calcium in hypothalamic astrocytes. *Endocrinology* (2009) 150 (3):1369–76. doi: 10.1210/en.2008-0994

60. Chen C, Kuo J, Wong A, Micevych P. Estradiol modulates translocator protein (TSPO) and steroid acute regulatory protein (StAR) *via* protein kinase a (PKA) signaling in hypothalamic astrocytes. *Endocrinology* (2014) 155(8):2976–85. doi: 10.1210/en.2013-1844

61. Micevych P, Sinchak K, Mills RH, Tao L, LaPolt P, Lu JKH. The luteinizing hormone surge is preceded by an estrogen-induced increase of hypothalamic progesterone in ovariectomized and adrenalectomized rats. *Neuroendocrinology* (2003) 78(1):29–35. doi: 10.1159/000071703

62. Mittelman-Smith MA, Wong AM, Kathiresan ASQ, Micevych PE. Classical and membrane-initiated estrogen signaling in an *in vitro* model of anterior hypothalamic kisspeptin neurons. *Endocrinology* (2015) 156(6):2162–73. doi: 10.1210/en.2014-1803

63. Beach FA. Sexual attractivity, proceptivity, and receptivity in female mammals. *Horm Behav* (1976) 7(1):105–38. doi: 10.1016/0018-506X(76)90008-8

64. Christensen A, Dewing P, Micevych P. Membrane-initiated estradiol signaling induces spinogenesis required for female sexual receptivity. *J Neurosci* (2011) 31(48):17583–9. doi: 10.1523/JNEUROSCI.3030-11.2011

65. Micevych PE, Rissman EF, Gustafsson J, Sinchak K. Estrogen receptor-α is required for estrogen-induced μ-opioid receptor internalization. *J Neurosci Res* (2003) 71(6):802–10. doi: 10.1002/jnr.10526

66. Johnson C, Hong W, Micevych P. Optogenetic activation of β-endorphin terminals in the medial preoptic nucleus regulates sexual receptivity. *Eneuro* (2020) 7(1):ENEURO.0315–19.2019. doi: 10.1523/ENEURO.0315-19.2019

67. Micevych PE, Meisel RL. Integrating neural circuits controlling female sexual behavior. *Front Syst Neurosci* (2017) 11:42. doi: 10.3389/fnsys.2017.00042

68. Mills RH, Sohn RK, Micevych PE. Estrogen-induced μ-opioid receptor internalization in the medial preoptic nucleus is mediated *via* neuropeptide y-Y1 receptor activation in the arcuate nucleus of female rats. *J Neurosci* (2004) 24 (4):947–55. doi: 10.1523/JNEUROSCI.1366-03.2004

69. Sinchak K, Micevych P. Visualizing activation of opioid circuits by internalization of G protein-coupled receptors. *Mol Neurobiol* (2003) 27(2):197–222. doi: 10.1385/MN:27:2:197

70. Sinchak K, Dewing P, Ponce L, Gomez L, Christensen A, Berger M, et al. Modulation of the arcuate nucleus–medial preoptic nucleus lordosis regulating circuit: A role for GABAB receptors. *Horm Behav* (2013) 64(1):136–43. doi: 10.1016/j.yhbeh.2013.06.001

71. Sar M, Sahu A, Wr C. Kalra sp. localization of neuropeptide-y immunoreactivity in estradiol-concentrating cells in the hypothalamus. *Endocrinology* (1990) 127(6):2752–6. doi: 10.1210/endo-127-6-2752

72. Sinchak K, Micevych PE. Progesterone blockade of estrogen activation of μ-opioid receptors regulates reproductive behavior. *J Neurosci* (2001) 21(15):5723–9. doi: 10.1523/JNEUROSCI.21-15-05723.2001

73. Mahavongtrakul M, Kanjiya MP, Maciel M, Kanjiya S, Sinchak K. Estradiol dose-dependent regulation of membrane estrogen receptor-α, metabotropic glutamate receptor-1a, and their complexes in the arcuate nucleus of the hypothalamus in female rats. *Endocrinology* (2013) 154(9):3251–60. doi: 10.1210/en.2013-1235

74. Gross KS, Mermelstein PG. Estrogen receptor signaling through metabotropic glutamate receptors. *Vitam Horm* (2020) 114:211–32. doi: 10.1016/bs.vh.2020.06.003

75. Woolley C, McEwen B. Estradiol mediates fluctuation in hippocampal synapse density during the estrous cycle in the adult rat [published erratum appears in J neurosci 1992 Oct;12(10):following table of contents]. *J Neurosci* (1992) 12(7):2549–54. doi: 10.1523/JNEUROSCI.12-07-02549.1992

76. Torres-Reveron A, Khalid S, Williams TJ, Waters EM, Jacome L, Luine VN, et al. Hippocampal dynorphin immunoreactivity increases in response to gonadal steroids and is positioned for direct modulation by ovarian steroid receptors. *Neuroscience* (2009) 159(1):204–16. doi: 10.1016/j.neuroscience.2008.12.023

77. Cholanian M, Krajewski-Hall SJ, McMullen NT, Rance NE. Chronic oestradiol reduces the dendritic spine density of KNDy (kisspeptin/neurokinin b/dynorphin) neurones in the arcuate nucleus of ovariectomised Tac2-enhanced green fluorescent protein transgenic mice. *J Neuroendocrinol* (2015) 27(4):253–63. doi: 10.1111/jne.12263

78. Moore AM, Coolen LM, Porter DT, Goodman RL, Lehman MN. KNDy cells revisited. *Endocrinology* (2018) 159(9):3219–34. doi: 10.1210/en.2018-00389

79. Meisel RL, Mullins AJ. Sexual experience in female rodents: Cellular mechanisms and functional consequences. *Brain Res* (2006) 1126(1):56–65. doi: 10.1016/j.brainres.2006.08.050

80. Mermelstein PG, Becker JB. Increased extracellular dopamine in the nucleus accumbens and striatum of the female rat during paced copulatory behavior. *Behav Neurosci* (1995) 109(2):354–65. doi: 10.1037/0735-7044.109.2.354

81. Xiao L, Becker JB. Hormonal activation of the striatum and the nucleus accumbens modulates paced mating behavior in the female rat. *Horm Behav* (1997) 32(2):114–24. doi: 10.1006/hbeh.1997.1412

82. Erskine MS. Solicitation behavior in the estrous female rat: A review. *Horm Behav* (1989) 23(4):473–502. doi: 10.1016/0018-506X(89)90037-8

83. McClintock MK, Adler NT. The role of the female during copulation in wild and domestic norway rats (Rattus norvegicus). *Behaviour* (1978) 67(1–2):67–95. doi: 10.1163/156853978X00260

84. Becker JB, Rudick CN, Jenkins WJ. The role of dopamine in the nucleus accumbens and striatum during sexual behavior in the female rat. *J Neurosci* (2001) 21(9):3236–41. doi: 10.1523/JNEUROSCI.21-09-03236.2001

85. Guarraci FA, Megroz AB, Clark AS. Paced mating behavior in the female rat following lesions of three regions responsive to vaginocervical stimulation. *Brain Res* (2004) 999(1):40–52. doi: 10.1016/j.brainres.2003.10.056

86. Jenkins WJ, Becker JB. Role of the striatum and nucleus accumbens in paced copulatory behavior in the female rat. *Behav Brain Res* (2001) 121(1–2):119–28. doi: 10.1016/S0166-4328(00)00394-6

87. Jenkins WJ, Becker JB. Dynamic increases in dopamine during paced copulation in the female rat. *Eur J Neurosci* (2003) 18(7):1997–2001. doi: 10.1046/j.1460-9568.2003.02923.x

88. Simerly RB, Swanson LW. Projections of the medial preoptic nucleus: A phaseolus vulgaris leucoagglutinin anterograde tract-tracing study in the rat. *J Comp Neurol* (1988) 270(2):209–42. doi: 10.1002/cne.902700205

89. Kokane SS, Perrotti LI. Sex differences and the role of estradiol in mesolimbic reward circuits and vulnerability to cocaine and opiate addiction. *Front Behav Neurosci* (2020) 14:74. doi: 10.3389/fnbeh.2020.00074

90. Tobiansky DJ, Will RG, Lominac KD, Turner JM, Hattori T, Krishnan K, et al. Estradiol in the preoptic area regulates the dopaminergic response to cocaine in the nucleus accumbens. *Neuropsychopharmacol* (2016) 41(7):1897–906. doi: 10.1038/npp.2015.360

91. Zhang D, Yang S, Yang C, Jin G, Zhen X. Estrogen regulates responses of dopamine neurons in the ventral tegmental area to cocaine. *Psychopharmacology* (2008) 199(4):625–35. doi: 10.1007/s00213-008-1188-6

92. Yager LM, Garcia AF, Wunsch AM, Ferguson SM. The ins and outs of the striatum: Role in drug addiction. *Neuroscience* (2015) 301:529–41. doi: 10.1016/j.neuroscience.2015.06.033

93. Russo SJ, Nestler EJ. The brain reward circuitry in mood disorders. *Nat Rev Neurosci* (2013) 14(9):609–25. doi: 10.1038/nrn3381

94. Becker JB. Direct effect of 17β-estradiol on striatum: Sex differences in dopamine release. *Synapse [Internet]* (1990) 5(2):157–64. doi: 10.1002/syn.890050211

95. Mermelstein PG, Becker JB, Surmeier DJ. Estradiol reduces calcium currents in rat neostriatal neurons *via* a membrane receptor. *J Neurosci Off J Soc Neurosci* (1996) 16(2):595–604. doi: 10.1523/JNEUROSCI.16-02-00595.1996

96. Surmeier DJ, Ding J, Day M, Wang Z, Shen W. D1 and D2 dopamine-receptor modulation of striatal glutamatergic signaling in striatal medium spiny neurons. *Trends Neurosci* (2007) 30(5):228–35. doi: 10.1016/j.tins.2007.03.008

97. Thompson TL, Moss RL. Estrogen regulation of dopamine release in the nucleus accumbens: Genomic-and nongenomic-mediated effects. *J Neurochem* (1994) 62(5):1750–6. doi: 10.1046/j.1471-4159.1994.62051750.x

98. Almey A, Filardo EJ, Milner TA, Brake WG. Estrogen receptors are found in glia and at extranuclear neuronal sites in the dorsal striatum of female rats: Evidence for cholinergic but not dopaminergic colocalization. *Endocrinology* (2012) 153(11):5373–83. doi: 10.1210/en.2012-1458

99. Almey A, Milner TA, Brake WG. Estrogen receptor α and G-protein coupled estrogen receptor 1 are localized to GABAergic neurons in the dorsal striatum. *Neurosci Lett* (2016) 622:118–23. doi: 10.1016/j.neulet.2016.04.023

100. Grove-Strawser D, Boulware MI, Mermelstein PG. Membrane estrogen receptors activate the metabotropic glutamate receptors mGluR5 and mGluR3 to bidirectionally regulate CREB phosphorylation in female rat striatal neurons. *Neuroscience* (2010) 170(4):1045–55. doi: 10.1016/j.neuroscience.2010.08.012

101. Küppers E, Beyer C. Expression of estrogen receptor-α and β mRNA in the developing and adult mouse striatum. *Neurosci Lett* (1999) 276(2):95–8. doi: 10.1016/S0304-3940(99)00815-0

102. Schultz KN, von Esenwein SA, Hu M, Bennett AL, Kennedy RT, Musatov S, et al. Viral vector-mediated overexpression of estrogen receptor-α in striatum enhances the estradiol-induced motor activity in female rats and estradiol-modulated GABA release. *J Neurosci* (2009) 29(6):1897–903. doi: 10.1523/JNEUROSCI.4647-08.2009

103. Stanić D, Dubois S, Chua HK, Tonge B, Rinehart N, Horne MK, et al. Characterization of aromatase expression in the adult male and female mouse brain. i. coexistence with oestrogen receptors α and β, and androgen receptors. *PloS One* (2014) 9(3):e90451. doi: 10.1371/journal.pone.0090451

104. Peterson BM, Mermelstein PG, Meisel RL. Estradiol mediates dendritic spine plasticity in the nucleus accumbens core through activation of mGluR5. *Brain Struct Funct* (2015) 220(4):2415–22. doi: 10.1007/s00429-014-0794-9

105. Staffend NA, Loftus CM, Meisel RL. Estradiol reduces dendritic spine density in the ventral striatum of female Syrian hamsters. *Brain Struct Funct* (2011) 215(3–4):187–94. doi: 10.1007/s00429-010-0284-7

106. Brady KT, Randall CL. Gender differences in substance use disorders. *Psychiat Clin N Am* (1999) 22(2):241–52. doi: 10.1016/S0193-953X(05)70074-5

107. Hernandez-Avila CA, Rounsaville BJ, Kranzler HR. Opioid-, cannabis- and alcohol-dependent women show more rapid progression to substance abuse treatment. *Drug Alcohol Depen* (2004) 74(3):265–72. doi: 10.1016/j.drugalcdep.2004.02.001

108. Evans SM, Haney M, Foltin RW. The effects of smoked cocaine during the follicular and luteal phases of the menstrual cycle in women. *Psychopharmacology* (2002) 159(4):397–406. doi: 10.1007/s00213-001-0944-7

109. Martinez LA, Gross KS, Himmler BT, Emmitt NL, Peterson BM, Zlebnik NE, et al. Estradiol facilitation of cocaine self-administration in female rats requires activation of mGluR5. *Eneuro* (2016) 3(5):ENEURO.0140–16.2016. doi: 10.1523/ENEURO.0140-16.2016

frontiers | Frontiers in Endocrinology

TYPE Original Research
PUBLISHED 11 October 2022
DOI 10.3389/fendo.2022.985424

OPEN ACCESS

EDITED BY
Allan Herbison,
University of Cambridge,
United Kingdom

REVIEWED BY
Lucia Karailievova,
Slovak Academy of Sciences, Slovakia
Firat Kara,
Mayo Clinic, United States
Ingrid Y Liu,
Tzu Chi University, Taiwan

*CORRESPONDENCE
Dóra Zelena
zelena.dora@pte.hu

SPECIALTY SECTION
This article was submitted to Reproduction, a section of the journal Frontiers in Endocrinology

RECEIVED 03 July 2022
ACCEPTED 20 September 2022
PUBLISHED 11 October 2022

CITATION
Farkas S, Szabó A, Török B, Sólyomvári C, Fazekas CL, Bánrévi K, Correia P, Chaves T and Zelena D (2022) Ovariectomy-induced hormone deprivation aggravates $A\beta_{1-42}$ deposition in the basolateral amygdala and cholinergic fiber loss in the cortex but not cognitive behavioral symptoms in a triple transgenic mouse model of Alzheimer's disease. *Front. Endocrinol.* 13:985424. doi: 10.3389/fendo.2022.985424

Ovariectomy-induced hormone deprivation aggravates $A\beta_{1-42}$ deposition in the basolateral amygdala and cholinergic fiber loss in the cortex but not cognitive behavioral symptoms in a triple transgenic mouse model of Alzheimer's disease

Szidónia Farkas[1,2], Adrienn Szabó[1,2,3], Bibiána Török[1,2], Csenge Sólyomvári[1], Csilla Lea Fazekas[1,2,3], Krisztina Bánrévi[2], Pedro Correia[1,2,3], Tiago Chaves[1,2,3] and Dóra Zelena[1,2]*

[1]Institute of Physiology, Medical School, University of Pécs, Centre for Neuroscience, Szentágothai Research Centre, Pécs, Hungary, [2]Laboratory of Behavioral and Stress Studies, Institute of Experimental Medicine, Budapest, Hungary, [3]János Szentágothai School of Neurosciences, Semmelweis University, Budapest, Hungary

Alzheimer's disease is the most common type of dementia, being highly prevalent in elderly women. The advanced progression may be due to decreased hormone synthesis during post-menopause as estradiol and progesterone both have neuroprotective potentials. We aimed to confirm that female hormone depletion aggravates the progression of dementia in a triple transgenic mouse model of Alzheimer's disease (3xTg-AD). As pathological hallmarks are known to appear in 6-month-old animals, we expected to see disease-like changes in the 4-month-old 3xTg-AD mice only after hormone depletion. Three-month-old female 3xTg-AD mice were compared with their age-matched controls. As a menopause model, ovaries were removed (OVX or Sham surgery). After 1-month recovery, the body composition of the animals was measured by an MRI scan. The cognitive and anxiety parameters were evaluated by different behavioral tests, modeling different aspects (Y-maze, Morris water maze, open-field, social discrimination, elevated plus maze, light–dark box, fox odor, operant conditioning, and conditioned fear test). At the end of the experiment, uterus was collected, amyloid-β accumulation, and the cholinergic system in the brain was examined by immunohistochemistry. The uterus weight decreased, and the body weight increased significantly in the OVX animals. The MRI data showed that the body weight change can be due to fat accumulation. Moreover, OVX increased anxiety in control, but decreased in 3xTg-AD animals, the later genotype being more anxious by default based on the

10.3389/fendo.2022.985424

anxiety z-score. In general, 3xTg-AD mice moved less. In relation to cognition, neither the 3xTg-AD genotype nor OVX surgery impaired learning and memory in general. Despite no progression of dementia-like behavior after OVX, at the histological level, OVX aggravated the amyloid-β plaque deposition in the basolateral amygdala and induced early cholinergic neuronal fiber loss in the somatosensory cortex of the transgenic animals. We confirmed that OVX induced menopausal symptoms. Removal of the sexual steroids aggravated the appearance of AD-related alterations in the brain without significantly affecting the behavior. Thus, the OVX in young, 3-month-old 3xTg-AD mice might be a suitable model for testing the effect of new treatment options on structural changes; however, to reveal any beneficial effect on behavior, a later time point might be needed.

KEYWORDS

Alzheimer's disease, hormone deprivation, ovariectomy, cognitive function, anxiety, estrogen, cholinergic neurons

1 Introduction

Alzheimer's disorder (AD) is the most common type of dementia, which is among the top 10 leading causes of death in the world (1, 2). It is characterized by disturbances of memory, attention, and sleep (1, 3). The patients often have difficulties in their daily life due to their impaired behavioral abilities (4). Morphologically, amyloid plaques [formed by amyloid-β 1-42 ($A\beta_{1\text{-}42}$)] and hyperphosphorylated tau aggregates appear in the hippocampus, cortex, and amygdala, brain areas that are critical in cognitive and emotional function (5, 6).

Plenty of risk factors have been identified regarding AD. These can be lifestyle related, like diet, physical activity, and environmental conditions, or medical factors, like obesity and cardiovascular conditions (1). However, the three major risk factors are age, gender, and genetical mutations (7–9). It is well known that the incidence of AD is increasing with age, but it is also important to note that women represent 70% of the patients (10). The increasing female prevalence among elderly can be due to hormonal change during menopause (11, 12). Namely, the low levels of sex steroids, like 17β-estradiol (E2) and progesterone (PG), may have an important role in the pathomechanism (13). Indeed, both E2 and PG play a pivotal role in neuroprotection, thereby improving cognitive function, memory, attention, synaptic plasticity, spine density, and dendrite formation (14–17). The loss of the ovarian hormones can affect these functions, and also increase the appearance of amyloidogenic markers, aggravating the progression of AD (18–20). Beside the natural decrease in ovarian steroids during menopause, the surgical removal of the gland in younger generation may also have detrimental effect on their cognitive capabilities (21, 22). It is estimated that, in USA, 100,000 cases of dementia may be attributable annually to bilateral oophorectomy (23). This later state can be modeled by ovariectomy (OVX) in animals (24, 25).

AD can also be characterized by genetical mutations, leading to family accumulations. Research has identified five main "AD genes": apolipoprotein E (ApoE) ϵ4 allele, amyloid precursor protein (APP), presenilin-1 (PSEN1), presenilin-2 (PSEN2), and microtubule-associated protein tau (MAPT). These genes may contribute to the formation of amyloid plaques, leading to memory loss and behavioral changes (8, 26–33), as well as to different tauopathies such as AD (34, 35). Genetic animal models were generated based on these human mutations. The triple transgenic mouse (3xTg-AD), bearing the humanoid mutation of APP, PSEN1, and tau, is widely used and well characterized (36–38). This mouse strain develops AD-like structural (amyloid plaques and hyperphosphorylated tau) and behavioral (progressive cognitive decline) symptoms.

The most relevant and affected neurocircuit in AD patients is the cholinergic system (39, 40), most of all the basal forebrain cholinergic (BFC) neurons (41, 42), being the main therapeutic target (43). The cholinergic neurons from the medial septum (MS), nucleus basalis magnocellularis (NBM), and substantia innominata complex are highly affected in AD, and also express E2 receptors (44–48), proving the importance of sexual steroids in the pathophysiology of the disease. OVX may decrease, while E2 treatment normalizes the number of cholinergic neurons in the BFC, as well as the length and branching of these neurons (49–51). In the 3xTg-AD mouse model, a cholinergic decline was also discovered, showing the loss of ChAT immunoreactive neurons in the MS and in the vertical limb of the diagonal band of Broca (52, 53).

Based on the important role of sexual steroids in neuronal health and their role in mental diseases, we aimed to investigate the aggravating effect of hormone deprivation induced by bilateral OVX on AD-related somatic, behavioral, and histological changes in the 3xTg-AD mice. The lack of E2 and PG may anticipate difficulties in cognitive function and anxiety-related behavior, perturbs somatic characteristics (like body weight or body fat ratio), and assumes morphological changes on amyloid deposition and in the cholinergic system. To test this hypothesis, the following concepts were used: (I) As OVX is often accompanied by body weight increase (54), and uterus weight decrease (55, 56), we were concentrating on these somatic parameters mainly to confirm the effectiveness of the OVX surgery. (II) The major symptom of dementia is cognitive disability; therefore, we used behavioral tests measuring (57) (i) short-term memory [Y-maze, often used in AD testing (58); based on spontaneous exploration of the mice]; (ii) social discrimination (SD); (iii) spatial memory [Morris water maze (MWM) as the gold standard in AD research (59, 60); also known as avoidance-based complex association]; (iv) reward-based simple association [operant conditioning (OC)]; and (v) punishment-based simple association [conditioned fear test (CFT)]. (III) As anxiety is often comorbid with AD (61, 62), and is a core symptom during menopause, or after OVX (63), we tested these symptoms by (i) elevated plus maze (EPM), as a gold standard in anxiety research (64), showing changes during the menstrual cycle (65); (ii) light–dark box (LD) test, which utilizes the fear from open, light spaces, similarly to EPM; and (iii) fox odor test (FOT), measuring the innate fear from a predator odor. (IV) At the structural level, we were concentrating on Aβ accumulation as well as cholinergic cell and fiber loss.

2 Materials and methods

2.1 Mouse strains

Three-month-old 3xTg-AD [B6;129-Tg(APPSwe,tauP301L) 1Lfa Psen1tm1Mpm/Mmjax] mice and their control strains (C57BL6/J) were used (66). This age corresponds to young adult humans without hormonal disturbances. The 3xTg-AD animals were homozygotes for three AD-related human-based genetic mutations: PSEN1, APPSwe, and tauP30IL (36–38). We maintained the colony by breeding homozygous mice to each other. Only females were used in this experiment. All animals were bred and housed at the Institute of Experimental Medicine, Budapest, Hungary. The mice were maintained under reversed light–dark cycle (lights off at 8:00 a.m., lights on at 8:00 p.m.) and provided with standard mice chow [without estrogen-free dietary restrictions (67)] and water *ad libitum*. The animal rooms have a temperature of 22 ± 2°C and a relative humidity of 55 ± 10%. All tests were approved by the local committee of animal health and care (PE/EA/918-7/2019) and performed according to the European Communities Council Directive recommendations for the care and use of laboratory animals (2010/63/EU).

2.2 Experimental design

Mice were ovariectomized (OVX) or Sham operated without removing the ovaries (Sham), under ketamine–xylazine anesthesia (dose: 125 mg/kg ketamine and 25 mg/kg xylazine dissolved in 0.9% saline, administered in 10 ml/kg concentration intraperitoneally). During surgery, the animals were divided into the following four groups: (1) Control-Sham (n = 8), (2) Control-OVX (n = 9), (3) 3xTg-AD-Sham (n = 7), and (4) 3xTg-AD-OVX (n = 12) (Figure 1A; the unequal animal numbers are due to surgical-related loss). Two series were conducted; each contained all four groups. After 1 month, a magnetic resonance imaging (MRI) measurement was performed. During this period, the ovarian hormones were supposed to disappear [maximal luteinizing hormone levels can be detected at this point (68)] and enough time has passed for the development of supposed behavioral changes. Then, the following behavioral test battery was used: Y-maze, SD, EPM, LD, FOT, MWM, OC, and CFT, with at least 24-h rest between the different tests (Figure 1B). The order of the tests was chosen from the milder stressors (5–10 min single test) to more burdensome ones (through restricted diet in OC till foot shock in CFT). All behavioral tests were performed during the first half of the active (dark) cycle (between 9:00 a.m. and 2:00 p.m.). At the end of the experiments, animals were sacrificed, and brains were dissected and post-fixed in 4% PFA for 24 h, dehydrated in 30% sucrose solution for 24 h, and then 30-μm-thick slices were made with a freezing microtome (Leica SM2010 R). Uterus dissection and weighting were also performed to validate the success of the OVX. Due to technical reasons (e.g., missing video recording and loss of brain slide during staining) in some experiments, data from one to two animals are missing.

2.3 Magnetic resonance imaging measurements

Body composition (body weight, fat, lean, free water, and total water) measurements were performed with a body composition analyzer for live small animals (EchoMRI™-700, EchoMRI LLC, Houston, TX), as described by the manufacturer. The animals were put in a restrainer and placed in the MRI machine for approximately 1 min (Figure 2A). The measurement was done in duplicate consecutively, without a time gap, and averaged. The body fat and lean weight were expressed as percentage of the body weight, and hydration ratio was calculated as the following:

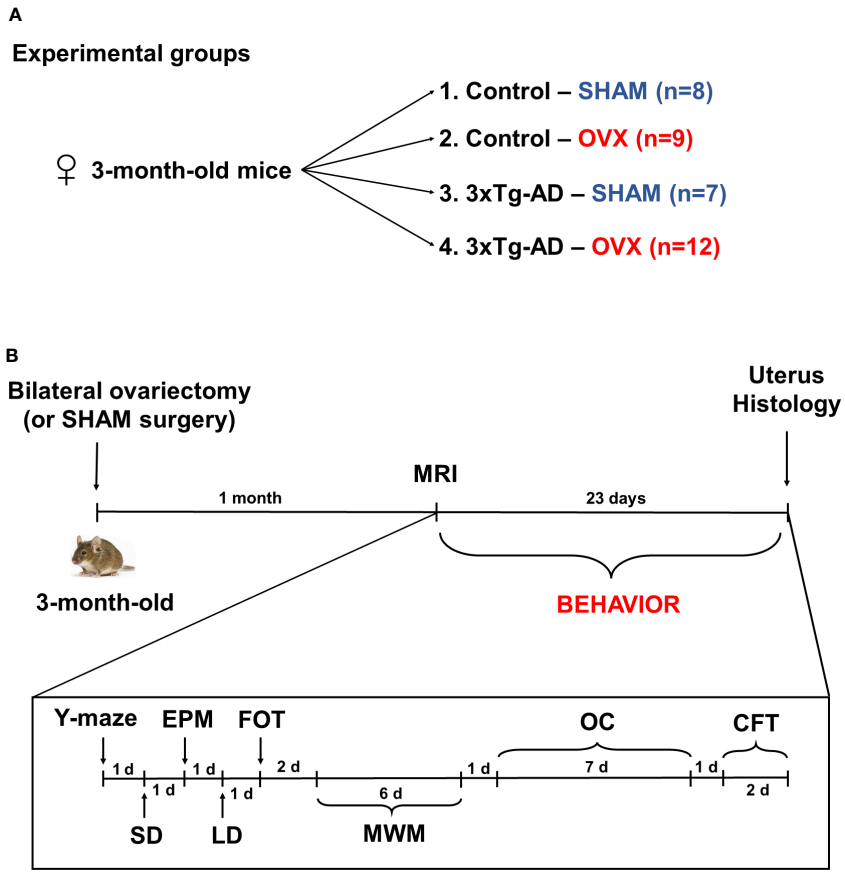

FIGURE 1
Experimental design. **(A)** Three-month-old female 3xTg-AD and C57BL6/J mice were used and divided into the following groups: (1) Control-Sham (n = 8), (2) Control-OVX (n = 9), (3) 3xTg-AD-Sham (n = 7), and (4) 3xTg-AD-OVX (n = 12). **(B)** Chronological order of experimental procedures. On 3-month-old mice, a bilateral ovariectomy (OVX) or Sham surgery was performed, then after 1 month, magnetic resonance imaging (MRI) measurements were conducted followed by behavioral experiments in this order: Y-maze, social discrimination (SD), elevated plus maze (EPM), light–dark box (LD), fox odor test (FOT), Morris water maze (MWM), operant conditioning (OC), and conditioned fear test (CFT). The duration and time between different tests are marked in the chronological axis as days (d). At the end of the experiment, uterus and brain were dissected for histological staining. OVX, ovariectomy; 3xTg-AD, triple transgenic mouse model of Alzheimer's disorder.

$$HR = \frac{total\ \ water - free\ \ water}{lean} \times 100$$

2.4 Behavioral tests

2.4.1 Cognitive behavioral tests

2.4.1.1 Y-maze test

The test was performed in a Y-shaped apparatus, with 3 arms (A, B, and C), with 30 × 7 × 20 cm dimensions, and in a 15–20 lux environment (Figure 3A) (57). Mice were placed in arm A and were allowed to explore the maze freely for 10 min. Before the entry of each animal, the maze was cleaned with 70% ethanol. Locomotion was calculated based on the total number of entries, while the spontaneous alternation reflects short-term memory and was calculated as the percentage (%) of "correct" alternation/total alterations. "Correct" alternation means entry into all three arms on consecutive choices (i.e., ABC, BCA, or CAB). Parameters were measured manually by an experimenter blind to the treatment groups.

2.4.1.2 Social discrimination test

The test was performed in a 40 × 40 × 15 cm apparatus under red light (69). The experiment consisted of four phases, each lasting 5 min (Figure 3D). Firstly, the mice were placed in the box for acclimatization [open-field phase (OF)]. Secondly, two metal cages were placed into the box and fear from objects as well as side preference was evaluated. The goal was to habituate the animals to the container (object habituation). Then, a stimulus mouse [C57BL6, 25- to 30-day-old male, test naïve, sexually immature (70)] was placed under one of the metal cages (sociability phase). In the last 5 min, another stimulus mouse

was placed under the other metal cage, and the position of the two cages was swapped [social discrimination (SD)]. The mice were left to explore freely the two animals. In the OF, the distance moved, and the time spent in the central or peripheral zone was analyzed automatically by EthoVision XT (Noldus IT, Wageningen, The Netherlands, version 15). Other parts of the test were analyzed using Solomon Coder (Solomon Coder, Hungary; https://solomoncoder.com/) by an experimenter blind to the treatment groups. The time and frequency sniffing the left or right container were evaluated. The sociability index (third phase) was calculated as:

$$SI = \frac{time\ \ spent\ \ sniffing\ \ the\ \ mice\ \ container}{time\ \ spent\ \ sniffing\ \ the\ \ mice\ \ container + empty\ \ container} * 100$$

The discrimination index (DI, fourth phase) was calculated as:

$$DI = \frac{time\ \ spent\ \ sniffing\ \ new - old\ \ mice}{time\ \ spent\ \ sniffing\ \ new + old\ \ mice}$$

2.4.1.3 Morris water maze test

A plastic circular pool (90 cm in diameter and 40 cm in height) was filled with tap water (24 ± 2°C), made opaque by white wall paint (Figure 4A) (38). A platform (6 cm in diameter) was placed 1 cm above the water for learning day 1, then moved 1 cm lower than the level of the water for days 2–5. The apparatus was divided into four quadrants and the platform was installed in the middle of one quadrant. Mice were released into the water from different points across trials (Figure 4A, marks 1–4) and were allowed to swim freely for 60 s to find the platform. If the mice could not find the platform during the 1 min, then it was guided there and left on the platform for 10 s. The learning phase (days 1–5) consisted of four trials with 30-min intertrial interval (ITI) when the animals were dried by a towel and returned to their home cages. On day 6 (probe day), the platform was removed from the water and the mice had 60 s to search for it. Latency to reach the platform during the learning phase was recorded manually, while during the probe test, time spent in different zones was calculated by EthoVision XT 15.

2.4.1.4 Operant conditioning test

The test was performed in an automated operant chamber (Med Associates, St. Albans, VT, USA) with two nose holes (Figure 5A) (57). As a reward, 45 mg of food pellets (Bio-Serv Dustless Precision Rodent Pellet, Bilaney Consultants GmbH, Germany) was used (71). Animals were placed inside a test chamber for 30 min to freely explore the environment. A nose poke into one of the nose holes was immediately associated with a reward followed by a 25-s-long time out with the chamber light switched on (time-out period), while the other nose hole was not baited (incorrect). During the time-out period, responses were not rewarded, but were registered. The test was divided into two phases: habituation (days 1–2) and learning (days 3–7), and data only from the learning phase is shown (Figures 5B, C, days 1–5). Reward preference (RP) (ratio of responses on the rewarded nose hole) was calculated. Number of rewarded responses and time-out reward hole nose pokes were also recorded.

$$RP = \frac{correct\ \ nose\ \ poke}{incorrect + correct\ \ nose\ \ poke} \times 100$$

2.4.1.5 Conditioned fear test

The mouse was placed into a Plexiglas chamber (25 × 25 × 30 cm) with an electrical grid floor (Coulbourn Instruments) that delivered the foot shocks (SuperTech Instruments). For 2.5 min, the animals were left in the boxes for habituation [baseline (BL)]. Then, at pseudorandom intervals (60–90 s), a 30-s-long conditioned stimulus (CS: 80 dB pure tone at 7 kHz) was played and co-terminated with an unconditioned stimulus (foot shock: 0.7 mA, 1 s long, seven times in total), for a total of 11 min (Figure 5D). The following day, the experiment was repeated, except that the animals did not receive foot shocks at the end of the CSs (72). The chambers were cleaned with soap water and water after every trial. The experiment was conducted in bright light (700 lux). Time spent in immobility was measured automatically by Ethovision XT 15 on the second day. Time spent in immobility was calculated for the BL (mean for 10 s) as well as for CSs (mean for 7 CS per 10 s).

2.4.2 Anxiety-related behavioral tests

2.4.2.1 Elevated plus maze test

A plus-shaped device was used, which comprised two opposite open arms and two enclosed arms (30 × 7 × 30 cm) (Figure 6A) (73). The mice were placed in the center of the apparatus facing the open arm and were allowed to explore the maze for 5 min. Before the entry of each animal, the maze was cleaned with 70% ethanol. The time spent and number of entries into the different arms as well as the distance moved (cm) were quantified with EthoVision XT 15. The open arm preference (OP) (74) was calculated as:

$$OP = \frac{open\ \ arm\ \ entries}{open\ \ arm\ \ entries + closed\ \ arm\ \ entries}$$

2.4.2.2 Light–dark box test

LD was performed in a 40 × 20 × 25 cm box, which had two compartments: a light (white colored) compartment that is open from above and a dark (black colored) compartment that is closed from every side (Figure 6B). A small gate (5 × 5 cm) between the two compartments, where the animal can freely pass, was present. The mice were placed in the light part of the box and were allowed to explore the environment for 10 min. The duration of time spent in each compartment, the total number of entries, and latency to dark compartments were measured by Solomon Coder.

2.4.2.3 Fox odor avoidance test

Exposure to fox-derived synthetic predator odor, 2-methyl-2-thriazoline (2MT, #M83406, Sigma Aldrich), was performed in a separate experimental room under a fume hood. A transparent Plexiglas arena (43 × 27 × 19 cm) was used (Figure 7A). During the test, a 2MT solution-soaked filter paper (40 µl in 1 ml of distilled water, 50 µl/animal) was placed in a plastic 50-ml conical tube cap in one corner of the box (75). A 7 × 11 cm "odor zone" around the odor source was defined. The opposite part (25%) of the box was appointed as "avoidance zone". During the test, the animal was placed in the avoidance zone and left to freely explore the arena for 10 min. Time spent in the odor zone and the distance moved (cm) was measured with EthoVision XT 15. Different anxiety-related behaviors, like the time spent freezing, grooming, and sniffing as well as the exploratory behaviors like time spent rearing and exploring was analyzed manually by Solomon Coder by an experimenter blind to the treatment groups.

2.5 Histological evaluations

2.5.1 Hematoxylin–eosin staining for uterus morphology

After weighing, uteruses were fixed in 4% PFA for 24 h, then dehydrated with 30% sucrose solution. Thirty-micrometer slices were made with a freezing microtome (Leica SM2010 R). Hematoxylin–eosin (HE) staining was performed on the slices to see morphological changes in the epithelium layer thickness, lumen size, and the integrity of the endometrial glands (Figure 8A). Samples were imaged with a Nikon Eclipse E1 R (Nikon, Tokyo, Japan) microscope at 4× magnification.

2.5.2 Amyloid-$\beta_{1\text{-}42}$ and choline acetyltransferase immunohistochemistry

For $A\beta_{1\text{-}42}$ and ChAT staining, peroxidase-based immunohistochemistry with nickel-diaminobenzidine tetrahydrochloride (Ni-DAB) visualization was undertaken (17). Firstly, only for the Aβ staining, a 10-min concentrated formic acid (Sigma-Aldrich, #F0507) exploration was implemented. Secondly, endogen peroxidase was blocked by a 3% peroxide (H_2O_2) solution. After blocking, slices were incubated 72 h with the primary antibody recognizing Aβ (Rabbit, 1:500, Invitrogen, #71-5800) or ChAT (Goat, 1:1,000, Millipore, #AB144P). After 72 h, brain slices were incubated with a biotinylated secondary antibody (biotinylated anti-rabbit, 1:200, Jackson ImmunoResearch, #111-065-003 or biotinylated anti-goat 1:200, Jackson ImmunoResearch, #705-065-147) at room temperature (RT), for 2 h. An avidin–biotin kit (VECTASTAIN Elite ABC-Peroxidase Kits, PK-6100, Vector Laboratories) was used for 2 h, RT, to detect biotinylated molecules. Then, the visualization was performed with a Ni-DAB and glucose oxidase mixture. Samples were imaged with a Nikon Eclipse E1 R (Nikon, Tokyo, Japan) microscope at 4× magnification.

In case of Aβ plaques, the integrated optical density (IOD) was measured by ImageJ/Fiji in the basolateral amygdala (BLA), the somatosensory and motor cortex (CTX) between Bregma 0.50 mm and −1.20 mm, and the CA1 region of the hippocampus (CA1-HC) between Bregma −1.19 mm and −2.69 mm (Figure 9A). In other brain areas of 5-month-old 3xTg-AD mice, no amyloid deposition was found. After ChAT staining, the number of ChAT-positive cells was counted in the NBM, a brain region containing cholinergic cell bodies, and highly affected in AD (Figure 10A) (76, 77).

2.5.3 Acetylcholinesterase histochemistry

To label cholinergic fibers in the somatosensory cortex (SSC), the target area of the NBM neurons (78), an AChE histochemistry was performed (17). Slices were selected from the coordinates: Bregma +0.50 mm to −1.06 mm (Figure 10A). Free-floating brain slices were incubated in a mixture of sodium acetate buffer (0.1 M; pH 6) acetylthiocholine iodide (0.05%), sodium citrate (0.1 M), copper sulfate (0.03 M), and potassium ferricyanide (5 mM). This was followed by ammonium sulfide (1%) and then silver nitrate (1%) incubation (17, 79). Analysis was performed with ImageJ/Fiji software. Samples were imaged with a Nikon Eclipse E1 R (Nikon, Tokyo, Japan) microscope at 10× magnification. IOD was measured between layer IV and V of the SSC (Figure 10A).

2.6 Z-score calculations

Integrated z-score was calculated for four major parameters: somatic, cognitive, anxiety, and locomotion, as proposed by Guilloux et al. (80), and previously presented in (73, 81). For each parameter, a normalized value (studentization) was calculated according to the following equation:

$$z - score = \frac{individual\ \ value - mean_{control}}{standard\ \ deviation_{control}}$$

and the included parameters were adjusted to have the same directionality. Somatic z-score was calculated from the averages of body weight change, fat/BW percentage, and uterus weight (×−1) z-scores. Cognitive z-score was calculated from alteration in the Y-maze; the area under the curve (AUC) of the latencies to platform during learning days 1–5 in MWM (×−1), and latency to platform on the probe day (×−1) in MWM; average freezing during baseline and conditioned stimuli in CFT; and the AUC of the reward preference learning days 3–7 in operant conditioning. Anxiety z-score was averaged from the z-scores of open arm duration (×0.5) and open arm preference (×0.5) in EPM; time spent in light compartment in LD; time spent freezing (×−1) and percentage of time spent in the odor zone in FOT; and percentage of time spent with freezing in CFT day 2 (×−1). Locomotion z-score was calculated from the parameters that reflected mobility in the given experiment [distance moved in EPM (×0.5), OF and fox odor tests; total number of entries in

the Y-maze, EPM (×0.5), and LD], then averaged for each animal. Somatic, cognitive, anxiety, and locomotor z-scores were averaged for every group and statistically tested. If multiple parameters indicating the same meaning within an experiment were included in averaged z-score calculations (e.g., distance moved and closed arm entries on EPM in the locomotion z-score), then they were multiplied by ×0.5 in order to avoid unwanted weighting of the specific test.

2.7 Statistical analysis

GraphPad Prism (version 6.0) was used for statistical analyses. Two-way ANOVA (MRI, Y-maze, OF, Sociability, SD, EPM, LD box, FOT, and histology; on factors genotype and OVX) or repeated-measures ANOVA (MWM, body weight change, OC, and CFT; additional factor: time) was used to compare the groups, followed by Tukey HSD or Sidak *post-hoc* test. For comparison of two groups, Student's *t*-test was used (Aβ staining). All data are presented as mean ± SEM and $p< 0.05$ was considered as a statistically significant difference.

3 Results

3.1 Changes in body composition measured with MRI

Regarding body weight changes, a difference was found between the two genotypes [$F_{(3,59)} = 12.59$, $p< 0.0001$], the 3xTg-AD mice being heavier than the controls. However, OVX surgery itself increased the body weight during a 40-day period [$F_{(1,19)} = 16.35$, $p = 0.0007$] without any influence of the genotype (Figure 2B). This increased body weight can be explained by the increased body fat ratio, where a genotype effect was also detectable with more fat in 3xTg-AD animals [$F_{(1,32)} = 10.01$, $p = 0.0034$] (Figure 2C). OVX was able to increase the fat accumulation in both genotypes [$F_{(1,32)} = 38.38$, $p< 0.0001$] (Figure 2C). Simultaneously, lean body weight ratio decreased [genotype: $F_{(1,32)} = 11.97$, $p = 0.0016$, OVX: $F_{(1,32)} = 47.45$, $p< 0.0001$] (Figure 2D). A significant negative correlation between body fat and lean ratio was also detected ($r = -0.9870$, $p< 0.0001$) (Figure 2E). The hydration ratio (((total water – free water)/lean)*100) of all animals was in the normal range (80 ± 5%), without any effect of genotype or OVX (Figure 2F).

3.2 Behavioral tests

3.2.1 Cognitive behavioral tests

3.2.1.1 Y-maze test

There was no difference between the groups in the main parameter of short-term memory, the alternation (Figure 3B). The 3xTg-AD mice moved significantly less compared to control animals [$F_{(1,31)} = 19.52$, $p = 0.0001$] without any effect or influence of OVX (Figure 3C).

3.2.1.2 Social discrimination (SD) test

We confirmed the reduced locomotion of 3xTg-AD mice during the first 5 min OF phase [$F_{(1,32)} = 13.80$, $p = 0.0008$], without OVX effect (Figure 3E). Neither the genotype, nor the OVX influenced the number of entries or time spent in the centrum, not even if we corrected it with locomotion (Table 1).

During the object habituation phase, none of the mice preferred any side; thus, the next phases did not require any correction (Figure 3F). OVX did not significantly affect the number of object approaches as well [$F_{(1,32)} = 3.05$, $p = 0.1298$; Table 1].

In the sociability phase, every mouse showed more interest to the stimulus mouse-containing cage [repeated-measures ANOVA: $F_{(1,32)} = 33.81$, $p< 0.0001$; single-sample *t*-test against 50%; Control-Sham: $t_{(7)} = 4.27$, $p = 0.0037$; Control-OVX: $t_{(9)} = 5.49$, $p = 0.0004$; 3xTg-AD-Sham: $t_{(6)} = 3.50$, $p = 0.0128$; 3xTg-AD-OVX: $t_{(9)} = 3.90$, $p = 0.0036$] without significant difference between groups (Figure 3G). There was a tendency for OVX animals to approach the social container a fewer number of times [$F_{(1,32)} = 3.89$, $p = 0.0881$; Table 1].

In the social discrimination phase, an increased interest towards the new mouse was detected in all groups [$F_{(1,62)} = 7.75$, $p = 0.0071$], suggesting that—in general—the test animals preferred the new stimulus mice, as expected (Figure 3H). However, when we checked the groups one by one, only the Control-OVX group seemed to have intact memory with a tendency in the 3xTg-AD-OVX group [single-sample *t*-test against 0; Control-Sham: $t_{(7)} = 1.17$, $p = 0.2806$; Control-OVX: $t_{(9)} = 2.48$, $p = 0.0348$; 3xTg-AD-Sham: $t_{(6)} = 0.53$, $p = 0.6179$; 3xTg-AD-OVX: $t_{(9)} = 2.03$, $p = 0.0732$]. A larger number of animals are probably needed for this test to work properly. Nevertheless, there was no overall difference between groups.

3.2.1.3 Morris water maze test

The latencies to reach the platform showed a significant improvement in time during the learning phase, independently from genotypes or surgery [$F_{(4,132)} = 43.42$, $p< 0.0001$] (Figure 4B). At the end of the 5th day, the animals were able to find the platform within 20 s (o average: 17.01 ± 1.21 s), suggesting that all groups learned the task. A significant interaction between OVX and time was detected [$F_{(4,128)} = 4.31$, $p = 0.0026$]; the OVX groups started to learn the task a bit later, as day 2 was not significantly different from day 1 in contrast to Sham-operated groups. Moreover, during days 4 and 5, the OVX groups differed significantly from the Sham-operated ones [$F_{(1,32)} = 6.09$, $p = 0.0191$], suggesting a flatter learning curve. Additionally, the fluctuation observable in the 3xTg-AD-OVX group suggests random choice, thus, not

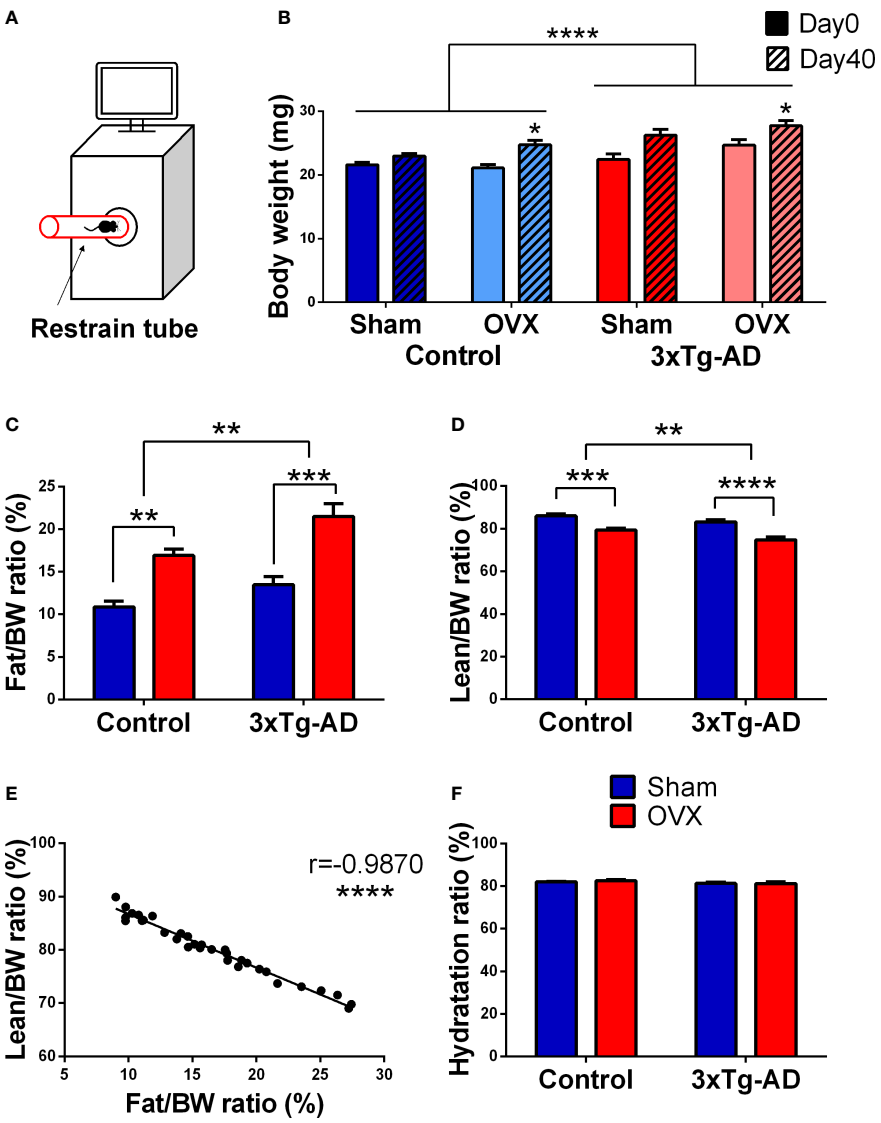

FIGURE 2
Magnetic resonance imaging (MRI) measurements. **(A)** Representative figure of the procedure. Animals were placed in a restrained tube, then inserted into an EchoMRI^{TM}-700 machine for approximately 1 min. **(B)** Body weight change of the animals from day 0 to day 40. 3xTg-AD animals were heavier than their controls ($p < 0.0001$). OVX induced body weight increase, irrespective of the genotype ($p = 0.007$). **(C)** Body fat percentage at 1-month post-surgery. 3xTg-AD animals had higher body fat percentage [Fat/Body weight (BW)*100] ($p = 0.0034$), which was aggravated by OVX in both genotypes ($p < 0.0001$). **(D)** Body lean percentage 1-month after surgery. A decrease in the body lean ratio [Lean/Body weight (BW)*100] was detected after OVX ($p < 0.0001$), and between the two genotypes ($p = 0.0016$). **(E)** Correlation between body fat and lean ratio. A negative and significant correlation was seen between the body fat and lean ratio ($p < 0.0001$). **(F)** Hydration ratio of the different animal groups. The hydration ratio (HR = ((total water – free water)/lean)*100) was normal in all animals (80% ± 5). OVX, ovariectomy; 3xTg-AD, triple transgenic mouse model of Alzheimer's disorder. Data are shown as mean ± SEM, *$p < 0.05$, **$p < 0.01$, ***$p < 0.001$, ****$p < 0.0001$.

appropriate learning of this group. The genotype also showed a tendency for time dependence [$F_{(4,128)} = 2.18$, $p = 0.0744$], with a subtle learning impairment of the 3xTg-AD mice. All the animals remembered the place of the platform as during the probe test they spent more than 25% of the time in the platform quadrant [single-sample t-test against 25; Control-Sham: $t_{(7)} = 2.14$, $p = 0.0701$; Control-OVX: $t_{(9)} = 5.50$, $p = 0.0004$; 3xTg-AD-Sham: $t_{(6)} = 6.12$, $p = 0.0009$; 3xTg-AD-OVX: $t_{(9)} = 3.02$, $p = 0.0130$]. No difference was found between groups in the probe day in the latency to reach the platform or time spent in the quadrant, where the platform was during the probe day (Figure 4C).

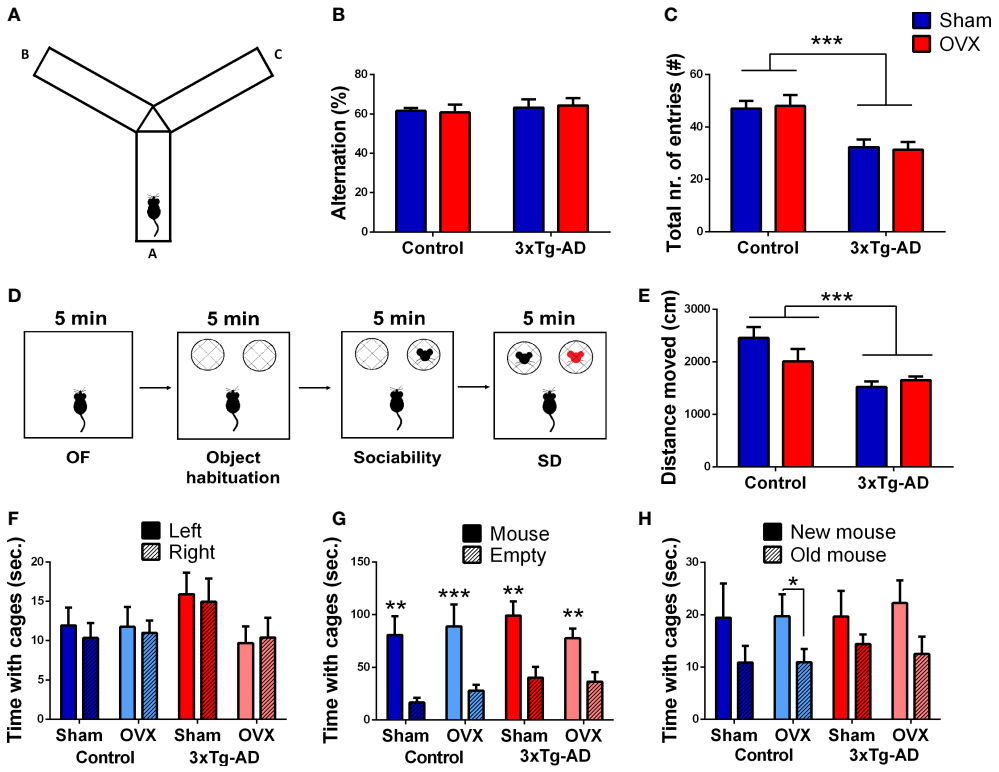

FIGURE 3
Y-maze and social discrimination (SD) tests. **(A)** Representative image of the Y-maze apparatus with three arms (A, B, and C). **(B)** Percentage of the good alternation in the Y-maze test. There was no significant difference between the groups. **(C)** Locomotor activity of the animals represented by the total number of entries. 3xTg-AD animals moved less than controls (p = 0.0001), without any OVX effect. **(D)** Representative figure of the different phases of the SD test. **(E)** Open-field (OF) test was the first 5-min phase of the SD test. A decreased locomotor activity, expressed in the distance moved (cm), was seen in the 3xTg-AD groups (p = 0.0008). **(F)** Object habituation phase of the SD test. No side preference was detected; thus, the next phases did not require any correction. **(G)** Sociability phase of the SD test. Every test mouse showed more interest towards the stimulus mouse containing cage ($p < 0.0001$); asterisks (*) show the result from the single-sample t-test against 50%. **(H)** SD phase. An increased interest towards the new mouse was detected in all groups (p = 0.0071). OVX, ovariectomy; 3xTg-AD, triple transgenic mouse model of Alzheimer's disorder. Data are shown as mean ± SEM, $^{**}p < 0.01$, $^{***}p < 0.001$, *p < 0,05.

3.2.1.4 Operant conditioning test

In reward preference, an improvement during time was detected [$F_{(4,128)}$ = 9.73, $p< 0.0001$] without any influence of the genotype or surgical removal of the ovaries (Figure 5B). In the number of rewarded responses, a similar time effect was seen [$F_{(4,128)}$ = 16.10, $p< 0.001$] (Figure 5C), with a tendency for genotype × OVX interaction [$F_{(1,32)}$ = 53.49, p = 0.0707]. There was a tendency for 3xTg-AD-Sham-operated animals to respond fewer times than Control-Sham-operated ones (p = 0.0794), while 3xTg-AD animals after OXV responded significantly more than the Sham-operated ones (p = 0.0407).

3.2.1.5 Conditioned fear test

We expressed the time spent in immobile posture during different phases as the percentage of the time period to get comparable values [i.e., the 150-s BL period is hardly comparable to the 30-s CS periods or random breaks (Br)] (Figure 5E). When we were concentrating on CS-induced changes, there was a significant interaction between the genotype and OVX [repeated-measures ANOVA on the seven CS: $F_{(1,31)}$ = 4.72, p = 0.0375]; the OXV increased freezing in control, but decreased in 3xTg-AD mice. The same effect was also seen in the cumulative time spent in freezing (in 1-min bins) (Figure 5F); not surprisingly this time, the interaction was significant between all three (genotype, OVX, and time) factors [$F_{(10,320)}$ = 53.26, p = 0.0005]. The time spent with inactivity during the initial context-dependent phase (BL, 150 s) (Figure 5G) and during the seven CS (conditioned phase, Figure 5H) was also calculated. Using repeated-measures ANOVA on context and cue-induced freezing, the CS, as a cue, significantly elevated the immobility time [$F_{(1,32)}$ = 8.16, p = 0.0075]. There was a tendency again for genotype and OVX interaction [$F_{(1,32)}$ = 4.03, p = 0.0531]. This was due to the significant interaction during tone-dependent freezing [$F_{(1,32)}$ =

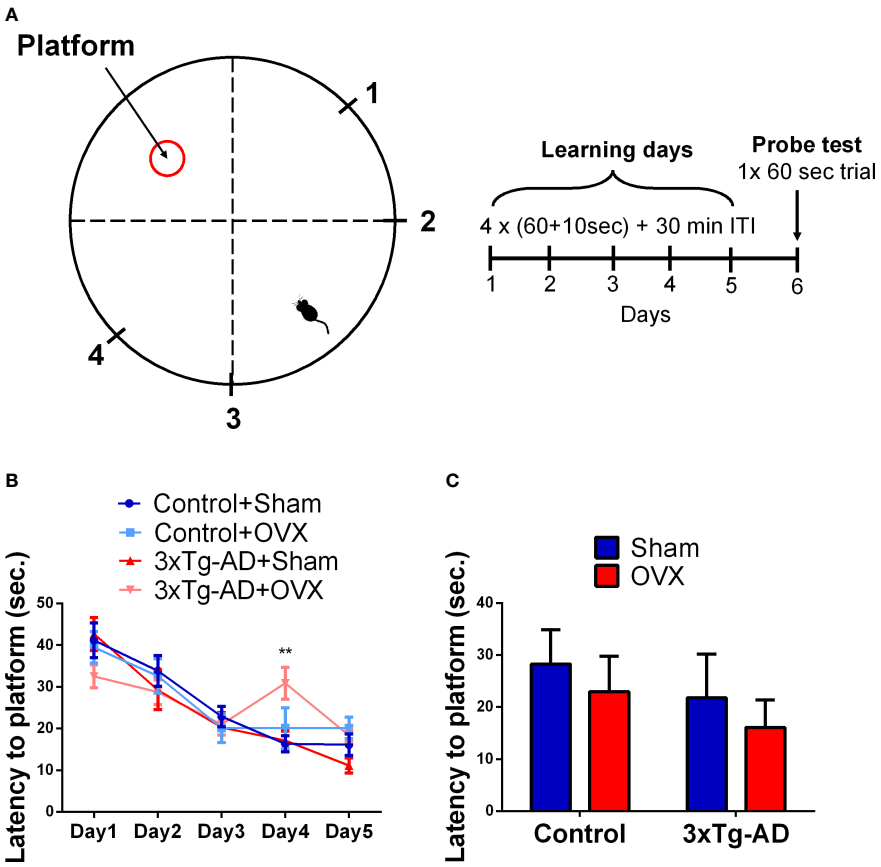

FIGURE 4
Morris water maze (MWM) test. **(A)** Representative figure of the MWM circular pool, with the location of the hidden platform, and the four starting points marked with 1–4. The learning phase consisted of 5 days; on each day, 4 × (60 + 10)-s trials were performed, with 30-min intertrial intervals (ITI). In the probe day (6th) one 60-s trial was done without the platform. **(B)** Latency to platform in seconds during the 5-day learning period. An improvement during the learning phase was seen in all groups ($p < 0.0001$). An interaction between OVX and time was detected, with a flatter learning curve of the OVX groups ($p = 0.0004$). **(C)** Latency to reach the platform on the probe day. No significant difference was found between the groups in the spatial memory. OVX, ovariectomy; 3xTg-AD, triple transgenic mouse model of Alzheimer's disorder. Data are shown as mean ± SEM. **p<0,01.

5.53, $p = 0.0251$] (Figure 5H) as no difference was detectable in the context-dependent phase [$F_{(1,32)} = 3.12$, $p = 0.0871$] (Figure 5G).

3.2.2 Anxiety-related behavioral tests

3.2.2.1 Elevated plus maze test

There was a significant interaction between genotype and OVX in the time spent in open arms [$F_{(1,32)} = 7.774$, $p = 0.0088$], and in open arm preference [$F_{(1,32)} = 4.484$, $p = 0.0421$] (Figures 6C, D), but no difference was detected in the time spent in the closed arm [time %; Control-Sham: 239.52 ± 9.99, Control-OVX: 250.09 ± 10.68, 3xTg-AD-Sham: 237.62 ± 14.09, 3xTg-AD-OVX: 260.13 ± 7.06; genotype: $F_{(1,32)} = 0.1554$, $p = 0.6961$; OVX: $F_{(1,32)} = 2.569$, $p = 0.1188$]. More specifically, Control-OVX animals spent less time in the open arm compared to the Control-Sham group ($p = 0.0192$), whose effect was not detectable in 3xTg-AD mice. In the locomotion parameters, similar to distance moved and the number of entries into the closed arms, no significant differences were detected between the groups (Figures 6E, F).

3.2.2.2 Light–dark box test

No differences were seen in the anxiety-related parameters like time spent in the light compartment (Figure 6G). However, in the locomotor activity represented by the number of entries to the dark compartment, a genotype effect was detected [$F_{(1,30)} = 9.80$, $p = 0.0039$] (Figure 6H). 3xTg-AD animals moved significantly less than the controls.

3.2.2.3 Fox odor test

A tendency for decreased time spent in the odor zone was seen in the 3xTg-AD animals compared to the control groups

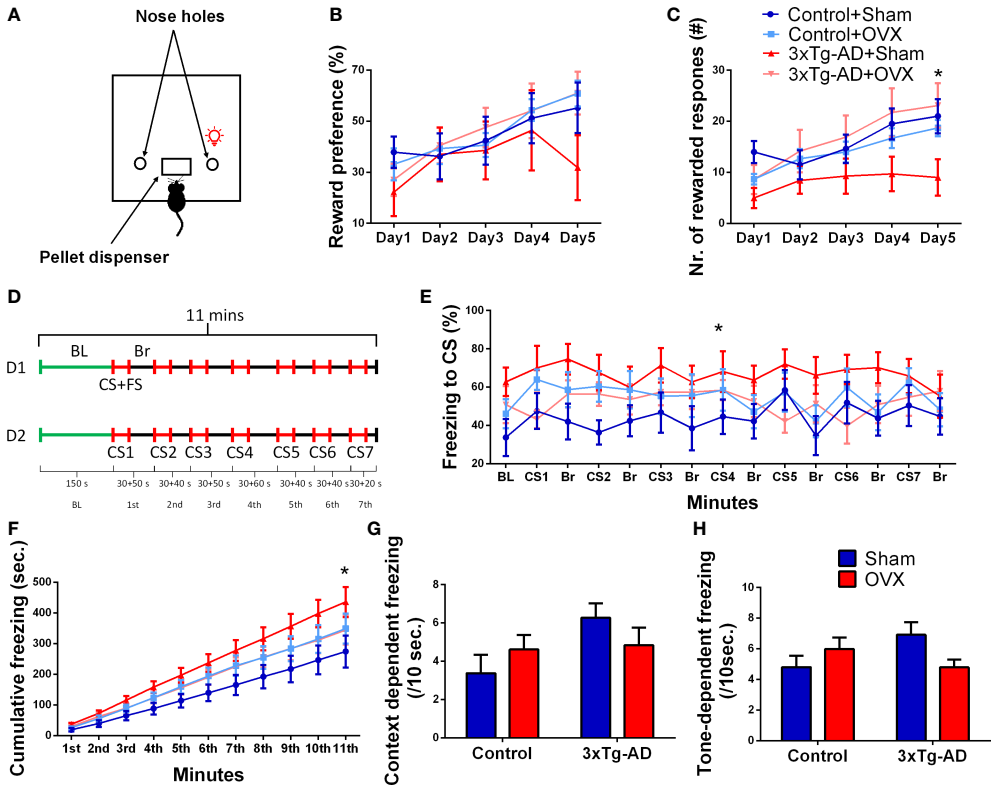

FIGURE 5
Operant conditioning (OC) and conditioned fear (CFT) tests. **(A)** Representative figure of the OC apparatus, with the light on above the reward associated nose hole. **(B)** Reward preference (ratio of responses on the rewarded vs. all nose pokes) during the OC test. An improvement during time was seen in all groups ($p < 0.0001$). **(C)** Number of rewarded responses during the OC test. Besides the time effect ($p < 0.0001$), a tendency for genotype × OVX interaction was also detected ($p = 0.0707$). 3xTg-AD animals after OXV responded significantly more than the Sham-operated ones ($p = 0.0407$). **(D)** Representative timeline of the 2 days (D1 and D2) lasting CFT test. D1 started with a 2.5-s baseline (BL) measurement, followed by a 30-s-long conditioned stimulus (CS: 80 dB pure tone at 7 kHz), which was co-terminated with an unconditioned stimulus [foot shock (FS): 0.7 mA, 1 s long, seven times in total], for a total of 11 min with random intertrial intervals (ITI, or break, Br). On D2, the experiment was repeated except that the animals did not receive an FS at the end of the CS. **(E)** Time spent freezing during CS and Br periods. For comparability, the values were calculated to 10-s bins. The AD × OVX interaction on CS meant that in the Control-Sham group, OVX aggravated, while in the 3xTg-AD group, the immobility was diminished ($p = 0.0375$). **(F)** The cumulative time spent in freezing (in 1-min bins) showed interaction between genotype, OVX, and time ($p = 0.0005$) with similar differences as seen on subgraph **(E)**. **(G)** Context and **(H)** tone or CS-dependent freezing (/10 s) during CFT. Repeated-measures ANOVA on time showed a significant elevation in freezing after CS ($p = 0.0075$). Again, a tendency for genotype and OVX interaction was detected ($p = 0.0531$), mainly due to the differences during tone dependency ($p = 0.0251$). OVX, ovariectomy; 3xTg-AD, triple transgenic mouse model of Alzheimer's disorder. Data are shown as mean ± SEM, *$p < 0.05$.

[$F_{(1,27)} = 3.51$, $p = 0.0719$] (Figure 7B). Accordingly, the 3xTg-AD animals spent more time freezing [$F_{(1,31)} = 25.33$, $p < 0.0001$] (Figure 7C) and reared [$F_{(1,31)} = 7.15$, $p = 0.0118$] (Figure 7E) and vertically explored the environment [$F_{(1,31)} = 22.48$; $p < 0.0001$] (Figure 7D) less than controls. These may suggest that 3xTg-AD animals were more anxious in the presence of a predator odor. A tendency of genotype difference was also seen in the locomotor activity, expressed by the distance moved [$F_{(1,31)} = 3.46$, $p = 0.0723$] (Figure 7F). Other parameters (like grooming and sniffing) were not different between groups and thereby not shown. The OVX surgery had no significant effect on the parameters examined during FOT.

3.3 Z-scores

The somatic z-score showed a significant interaction between genotype and surgery groups [$F_{(1,32)} = 41.35$, $p < 0.0001$] (Table 2). Animals who underwent OVX surgery had a higher somatic z-score [$F_{(1,32)} = 12.92$, $p = 0.0010$], whose effect was more pronounced in Control than in 3xTg-AD mice. In cognitive z-score, no significant differences were detected between the groups. Anxiety z-score showed an interaction between genotype and surgery groups [$F_{(1,32)} = 23.26$, $p < 0.0001$]. Namely, OVX increased anxiety in Control, but decreased in 3xTg-AD animals. Indeed, in general, 3xTg-AD animals had a lower anxiety z-score, meaning more anxious behavior [$F_{(1,32)} = 17.61$, $p = 0.0002$]. The

10.3389/fendo.2022.985424

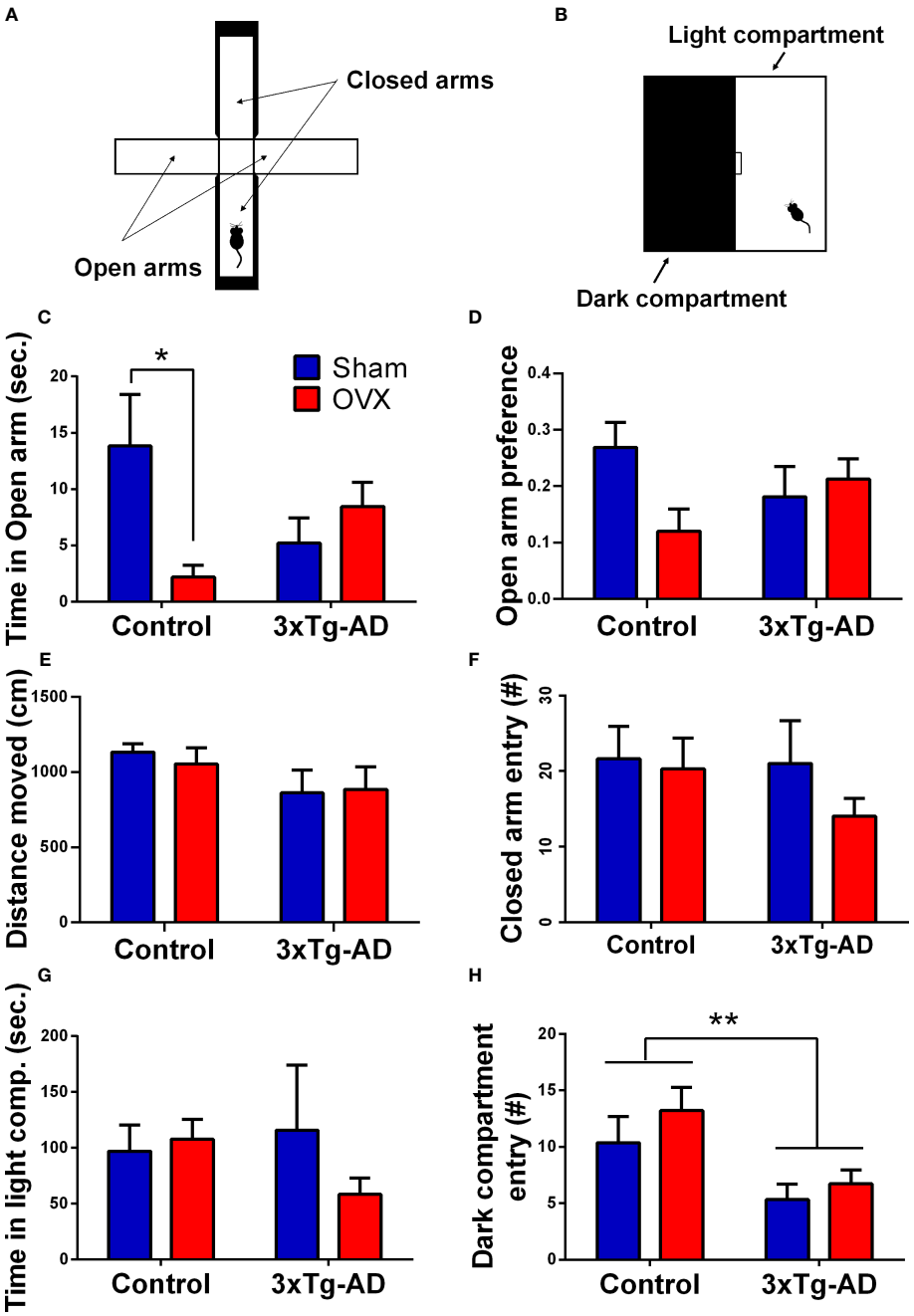

FIGURE 6
Elevated plus maze (EPM) and light–dark box (LD) tests. **(A)** Representative figure of the EPM apparatus, with two open and two closed arms. **(B)** Representative image of the LD equipment, with a light and a dark compartment, separated with a small gateway. **(C)** Time spent in the open arm of the EPM. A significant interaction between genotype and surgery groups was detected (p = 0.0088). Control-OVX animals spent less time in the open arm compared to Control-Sham ones (p = 0.0192). **(D)** Open arm preference in the EPM test. A significant interaction between genotype and surgery groups was seen (p = 0.0421). **(E)** Distance moved (cm) during the 5-min EPM test. No difference between the groups was detected. **(F)** Total number of entries into the closed arms in the EPM test. Differences between the groups were not significant. **(G)** Time spent in the light compartment during the LD test. No difference regarding genotype or OVX surgery was detected. **(H)** Number of entries in the dark compartment during LD test. 3xTg-AD mice moved significantly less, than controls (p = 0.0044), without any OVX effect. OVX, ovariectomy; 3xTg-AD, triple transgenic mouse model of Alzheimer's disorder. Data are shown as mean ± SEM, *p < 0.05, **p < 0.01.

10.3389/fendo.2022.985424

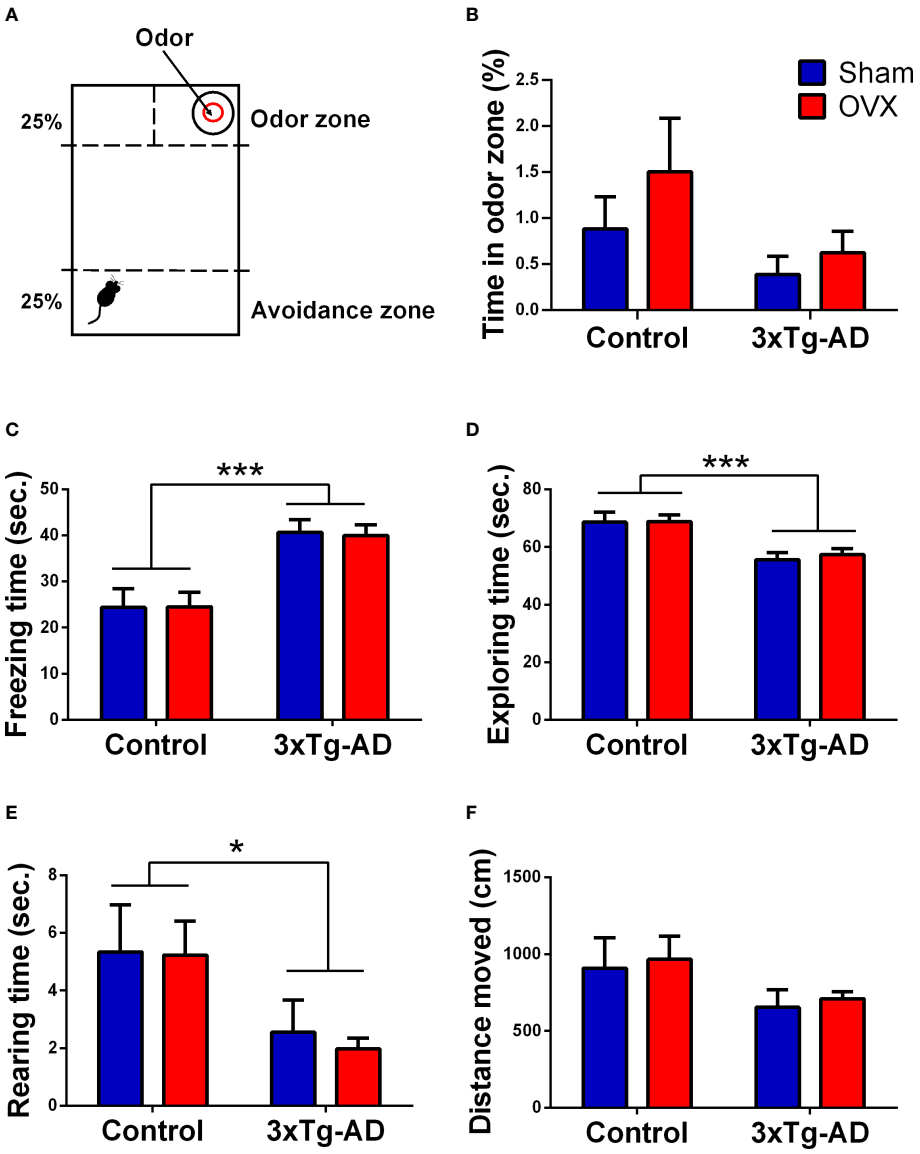

FIGURE 7
Fox odor test (FOT). **(A)** Representative figure of the FOT apparatus, presented with the odor zone [where the 2-methyl-2-thriazoline (2MT, fox odor) was placed] and the avoidance zone (distant part from the odor). **(B)** Time (in seconds) spent in the odor zone. No significant difference between genotypes or between surgery groups was detected. **(C)** Time (in seconds) spent freezing. 3xTg-AD mice spent more time freezing compared to control groups ($p < 0.0001$). **(D)** Time (in seconds) spent exploring the FOT box. The 3xTg-AD group showed reduced exploration time compared to controls ($p < 0.0001$). **(E)** Time (in seconds) spent rearing. A genotype effect was visible with less vertical movement in 3xTg-AD animals ($p = 0.0118$). **(F)** Distance moved (cm). A tendency for genotype difference was seen, with the 3xTg-AD mice moving less than controls ($p = 0.0723$). OVX, ovariectomy; 3xTg-AD, triple transgenic mouse model of Alzheimer's disorder. Data are shown as mean ± SEM, $*p < 0.05$, $***p < 0.001$.

locomotor differences were also supported by its z-score. Namely, the 3xTg-AD animals had a lower z-score number, meaning, in general, they moved less [$F_{(1,32)} = 19.64$, $p = 0.0001$]. A significant interaction between genotype and surgery groups was also detected [$F_{(1,32)} = 27.45$, $p < 0.0001$]. More specifically, OVX reduced locomotion in Control, but not that much in 3xTg-AD mice, which was moving less even before that.

3.4 Histological evaluations

3.4.1 Uterus

The representative pictures with HE staining showed increased epithelium thickness, deteriorated endometrial glands, and a substantial difference between the size of the uterus and lumen (Figure 8A). Both in the control and 3xTg-

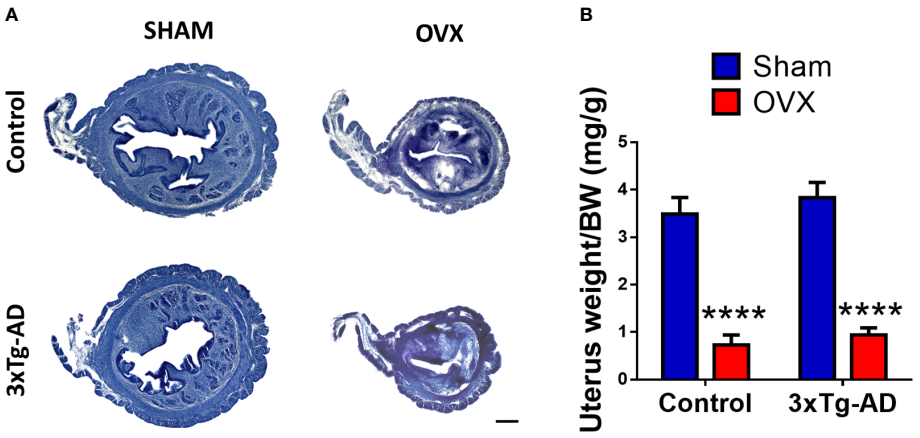

FIGURE 8
Changes in the uterus 2 months after Sham or OVX surgery. **(A)** Representative figure of the uterus stained with hematoxylin–eosin (HE). A decrease in size and epithelial layer thickness, and damaged integrity of the endometrial glands is visible. **(B)** Uterus weight normalized to the body weight (BW) of the animals. A significant decrease was seen after OVX surgery ($p < 0.0001$). OVX, ovariectomy; 3xTg-AD, triple transgenic mouse model of Alzheimer's disorder. Data are shown as mean ± SEM, ****$p < 0.0001$. Scale bar, 200 µm.

AD groups, the normalized weight of the uterus was significantly lower after OVX compared to the Sham group [$F_{(1,31)} = 121.80$, $p< 0.0001$] (Figure 8B).

3.4.2 Amyloid-β accumulation in different brain areas

Amyloid-β plaques were only quantified in 3xTg-AD mice, because no deposition was detected in the Control-Sham or Control-OVX groups (see Supplementary Figure 1). In the BLA, the 3xTg-AD-OVX mice had significantly more plaques than their Sham-operated mates [$t_{(9)} = 2.72$, $p = 0.0236$] (Figures 9B, C). In the CTX and CA1-HC, no significant effect of OVX was found (Figures 9D–G).

3.4.3 Morphological changes in the cholinergic system

ChAT-positive cells were counted in the NBM region. We found no difference in the number of the cells between 3xTg-AD and control animal, neither in Sham-operated nor in OVX groups (Figure 10C). However, the AChE fiber density was significantly decreased in 3xTg-AD animals [$F_{(1,22)} =29.49$, $p< 0.0001$], with a significant interaction between genotype and OVX [$F_{(1,22)} = 11.61$, $p = 0.0025$]. In 3xTg-AD mice, OVX surgery exacerbated the fiber loss compared to the Sham group ($p = 0.0147$) (Figures 10B, D).

4 Discussion

In contrast to our hypothesis, OVX did not aggravate the appearance of AD-related symptoms in the cognitive behavioral tests, but in morphological examinations, signs of neurodegeneration were visible (see amyloid deposition in the BLA, and cholinergic fiber density in the SSC). Table 3 contains the summary of the changes.

We confirmed that our model worked, as OVX induced the expected increase in body weight with fat accumulation as well as decrease in uterus weight and lean body percentage. The lack of sexual steroids can cause an increased risk for obesity, since E2 and PG also mediate glucose and lipid metabolism, and also affects adipocyte physiology (54, 82, 83). Indeed, in human studies, an increased visceral fat mass can be seen on women after menopause (84, 85). This is supported in mice by our MRI findings, where the body fat ratio of the OVX groups increased. Importantly, obesity is a prominent risk factor for AD: increasing Aβ plaques, adipokines, and cytokines, and effecting insulin homeostasis [reviewed in (86–88)]. Thus, this might be associated with how OVX might aggravate the development of AD-like symptoms. In support, 3xTg-AD animals per se were fatter and greasier, suggesting—together with the OC data—some metabolic disturbances, which require further studies. In contrast, after OVX, the weight of the uterus decreased, which can be explained by the estrogen deficit. Indeed, E2 has a proliferative effect on the uterus; hence, its lack causes hypotrophy (55, 89, 90). In future studies, luteinizing hormone measurements can help better understand the effect of OVX on the hypothalamic–hypophyseal–gonadal axis and their role in the development of AD (91–93). The MRI data also showed a decreased body lean ratio in the OVX groups, which may be the prodrome of a most common problem in menopausal patients, osteoporosis. Indeed, female sex hormone depletion was linked closely to low bone mineral density (94). Estrogen receptors can be also found in the bone, mediating protection of the bone structure, by inhibiting osteoclast activity and stimulating

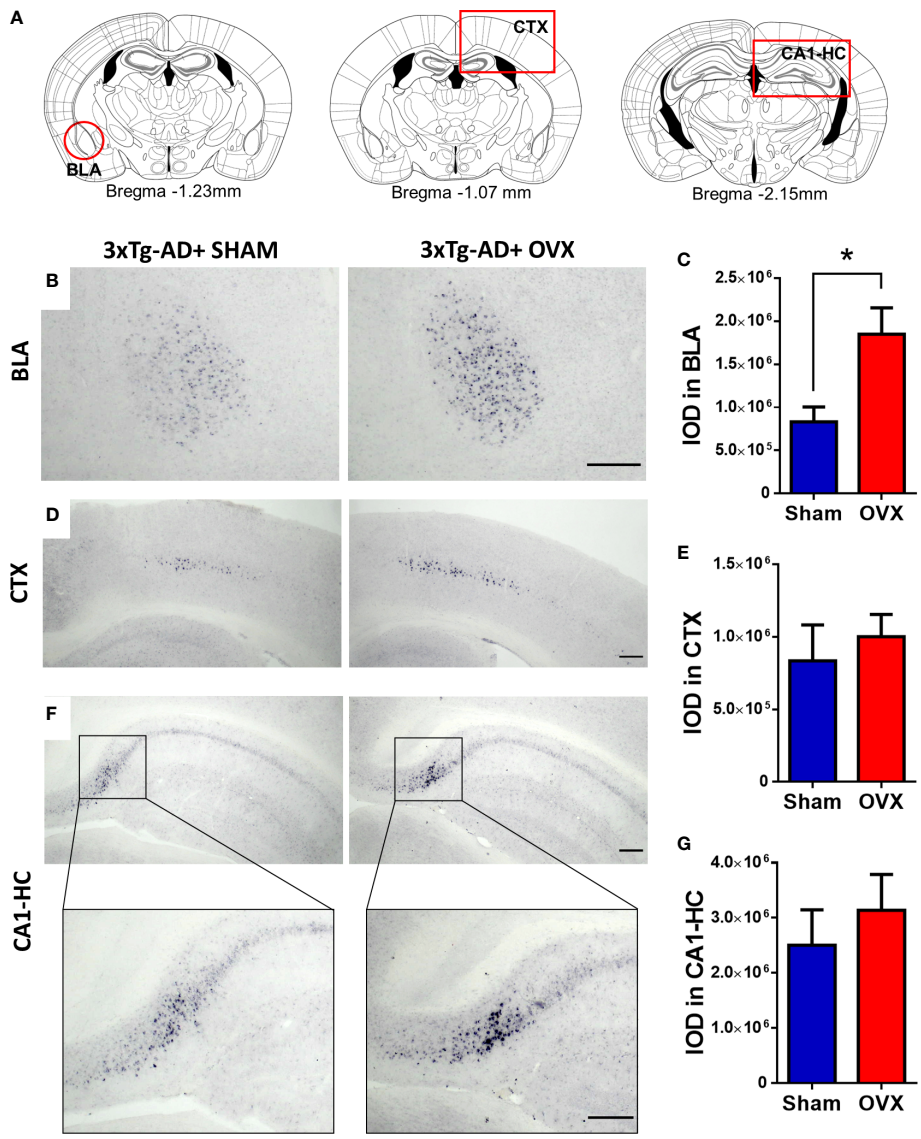

FIGURE 9
Immunohistochemical staining (NiDAB) of amyloid-$\beta_{1\text{-}42}$ (Aβ) plaques in different brain regions. There was no Aβ signal detectable in the brain of control animals; therefore, we compared 3xTg-AD with and without ovariectomy (OVX). **(A)** Representative figures based on the Paxinos Mouse Brain atlas (4th Edition) about the brain regions of interest, framed with red: Basolateral amygdala (BLA), at Bregma –1.23 mm, Motor and somatosensory cortex (CTX) at Bregma –1.07 mm, and CA1 hippocampal region (CA1-HC) presented at Bregma –2.15 mm. **(B)** Representative pictures of Aβ plaques in the BLA of the 3xTg-AD animals after Sham or OVX surgery. **(C)** The integrated optical density (IOD) of Aβ plaques measured in the BLA. A significant increase was detected after OVX surgery (p = 0.0236). **(D)** Representative pictures of Aβ plaques in the CTX in 3xTg-AD animals after Sham or OVX surgery. **(E)** The IOD of Aβ plaques measured in the CTX. No significant difference was detected. **(F)** Representative pictures of Aβ plaques in the CA1-HC of 3xTg-AD animals after Sham or OVX surgery, with a close-up to a small part of the CA1 region. **(G)** The IOD of Aβ plaques measured in the HC. The difference between the two surgery groups was not significant. 3xTg-AD, triple transgenic mouse model of Alzheimer's disorder. Data are shown as mean ± SEM, *p < 0.05. Scale bar: 200 μm.

development of long bones and pubic epiphyses (94–96). The OVX-induced somatic changes presented in the literature were also supported by the somatic z-score, calculated from the body weight change, body fat ratio, and uterus weight. Interestingly, the OVX-induced changes were smaller in 3xTg-AD mice (see genotype × OVX interaction in somatic z-score).

As the major symptom of dementia is the cognitive decline, we evaluated five different memory tests to have a comprehensive picture. They measure different modalities [spontaneous exploration (Y-maze), social stimulus, simple association-based reward (OC) or punishment (CFT), or even complex association based on spatial memory (MWM)]. The

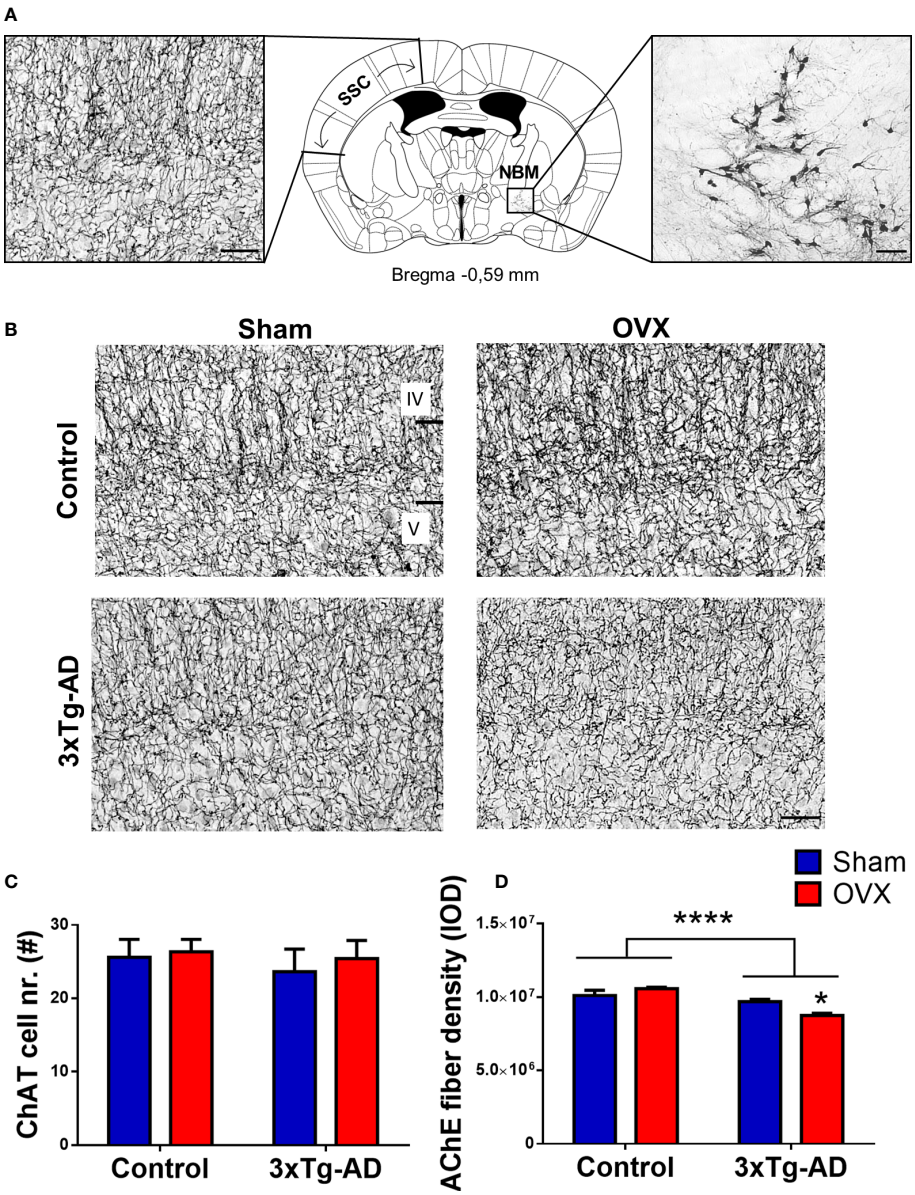

FIGURE 10
Immunohistochemical and histochemical staining of the cholinergic cell bodies and fibers. **(A)** Neuroanatomical location of the cholinergic choline-acetyltransferase (ChAT)-positive neurons in the nucleus basalis magnocellularis (NBM) and their acetylcholinesterase (AChE)-positive fibers in the somatosensory cortex (SSC). Schematic coronal brain section was adapted from Franklin and Paxinos (4th Edition) Mouse Brain atlas. **(B)** Representative pictures of the AChE-positive fibers in layers IV and V of SSC. Black bars indicate layers IV and V of the SSC. **(C)** Number of ChAT-positive cell bodies in the NBM region, stained with NiDAB immunohistochemistry. No significant difference was detected between groups. **(D)** AChE-positive fiber density measured in the SSC, expressed in integrated optical density (IOD). 3xTg-AD mice have a lower AChE fiber density compared to controls ($p < 0.0001$), with a significant interaction between groups ($p = 0.0025$). The decrease in density was exacerbated by OVX surgery in the 3xTg-AD group ($p = 0.0147$). OVX, ovariectomy; 3xTg-AD, triple transgenic mouse model of Alzheimer's disorder. Data are shown as mean ± SEM, $*p < 0.05$, $***p < 0.001$. Scale bar: **(A)** AChE staining in the SSC, 50 µm, and ChAT staining in the NBM, 100 µm. **(B)** 50 µm.

cumulative effect (z-score) was very similar to the single tests, with overall ineffectiveness of the genetic deletion in the 3xTg-AD animals as well as the OVX. According to the literature, 3xTg-AD animals develop memory loss after 6 months (36, 38). Hence, for our animals that were between 4 and 5 months old, the results are not unexpected. However, we could not support our hypothesis, as the OVX did not aggravate the cognitive decline (no OVX effect was detected whatsoever). Even the

TABLE 1 Detailed results of the social discrimination tests.

Test Phase	Behavior		Experimental groups								Statistics		
			Control		Control		3xTg-AD		3xTg-AD				
			Sham		OVX		Sham		OVX		*p*-value		
			Average	SEM	Average	SEM	Average	SEM	Average	SEM	Genotype	OVX	Interaction
Open-field phase	% time spent in centrum		17.01	2.98	16.60	3.33	16.55	4.71	20.22	4.31	0.6955	0.6865	0.6135
	Centrum frequency		32.00	3.59	28.40	3.65	25.29	5.12	24.91	3.06	0.1901	0.6055	0.6752
Habituation phase	Sniffing frequency	Cage inside	20.38	2.57	19.30	3.59	25.86	4.54	13.45	2.79	0.9099	0.0817	0.1474
		Cage outside	16.13	2.36	16.30	2.65	21.14	5.18	13.27	2.86	0.6118	0.3327	0.3072
	Σ	36.50	3.75	35.60	5.67	47.00	9.14	26.73	5.26	0.7353	0.1298	0.1696	
	% time spent with sniffing cages		22.29	3.18	22.74	3.34	30.86	5.16	20.12	4.28	0.3331	0.3076	0.2595
	Bout length		0.58	0.06	0.69	0.08	0.66	0.11	0.67	0.08	0.5417	0.3646	0.7367
Sociability	Sniffing frequency	Cage with mouse	18.38	4.16	13.90	2.05	22.14	2.09	15.64	2.40	0.1960	0.0881	0.9309
		Empty cage	7.25	1.91	13.80	2.19	14.29	1.80	11.18	1.93	0.1979	0.2901	0.0391
	SI		76.40	6.18	72.97	4.18	71.52	6.14	70.16	5.17	0.4810	0.6602	0.8499
	Bout length mouse		3.73	0.52	4.85	0.88	6.57	1.88	5.20	0.73	0.5915	0.5915	0.4337
Social discrimination	Sniffing frequency	Known mouse	16.38	3.19	16.30	2.88	14.86	1.52	14.00	2.73	0.5045	0.8701	0.8909
		Unknown mouse	16.25	1.41	18.00	1.80	14.57	2.95	14.82	2.74	0.3173	0.6792	0.7554
	DI		0.20	0.17	0.25	0.10	0.06	0.11	0.30	0.15	0.7194	0.2943	0.4958
	Bout length two mice		2.82	0.63	2.86	0.56	3.43	0.53	3.24	0.45	0.3772	0.8899	0.8411

Data are expressed as mean ± SEM. The results of the statistical analysis (two-way ANOVA) are presented. Significant differences are marked with red, bold numbers. OVX, ovariectomy; 3xTg-AD, triple transgenic mouse model of Alzheimer's disorder, SI, Sociability index, DI, Discrimination index.

TABLE 2 Z-scores calculated from somatic, cognitive, anxiety, and locomotor parameters.

Type	Experimental groups	Z-score ± SEM	Genotype	Surgery	Interaction
Somatic	Control-Sham	(−0.0070) ± 0.1387	$p = 0.2902$	$\mathbf{p = 0.0010}$	$\mathbf{p = 0.0000}$
	Control-OVX	3.8905 ± 0.5631			
	3xTg-AD-Sham	0.6443 ± 0.4267			
	3xTg-AD-OVX	3.7049 ± 0.4227			
Cognitiv	Control-Sham	(−0.000) ± 0.1197	$p = 0.6754$	$p = 0.3038$	$p = 0.2349$
	Control-OVX	0.1442 ± 0.1645			
	3xTg-AD-Sham	0.0302 ± 0.2340			
	3xTg-AD-OVX	0.2686 ± 0.1861			
Anxiety	Control-Sham	0.0000 ± 0.3964	$\mathbf{p = 0.0002}$	$p = 0.8743$	$\mathbf{p = 0.0000}$
	Control-OVX	(−0.2518) ± 0.4862			
	3xTg-AD-Sham	(−2.0022) ± 0.2444			
	3xTg-AD-OVX	(−1.6222) ± 0.3366			
Locomotor	Control-Sham	0.000 ± 0.4750	$\mathbf{p = 0.0001}$	$p = 0.6097$	$\mathbf{p = 0.0000}$
	Control-OVX	(−0.4145) ± 0.6432			
	3xTg-AD-Sham	(−2.4225) ± 0.4375			
	3xTg-AD-OVX	(−2.5365) ± 0.3748			

Data are expressed as z-score (mean) ± SEM. Statistical data (two-way ANOVA) is presented. Significant differences are marked with red, bold numbers. OVX, ovariectomy; 3xTg-AD, triple transgenic mouse model of Alzheimer's disorder.

TABLE 3 Summary table of the main effect of genotype, OVX surgery, and interaction between the two parameters in the different procedures.

Category	Parameters	3xTg-AD	OVX	Interaction
Somatic	Body weight	↑	↑	Ø
	Fat	↑	↑	Ø
	Lean	↓	↓	Ø
	Uterus	Ø	↓	Ø
	Z-score	Ø	↑	+
Cognitiv	Short term in Y-maze	Ø	Ø	Ø
	SD	Ø	Ø	Ø
	MWM	Ø	Ø	Ø
	OC	↓	Ø	Ø
	CFT: freezing	↑	Ø	+
	Z-score	Ø	Ø	Ø
Anxiety	EPM: open arm time	Ø	↓	+
	EPM: open arm preference	Ø	Ø	+
	LD	Ø	Ø	Ø
	Fox odor	↑	Ø	Ø
	Z-score	↑	Ø	+
Locomotor	Y-maze	↓	Ø	Ø
	OF	↓	Ø	Ø
	EPM	(↓)	Ø	Ø
	LD box	↓	Ø	Ø
	Fox odor	(↓)	Ø	Ø
	Z-score	↓	Ø	+
Social interaction	Sociability	Ø	Ø	Ø
Morphology	Amyloid-β	N.M.	↑	N.M.
	ChAT cell number	Ø	Ø	Ø
	AChE fiber density	Ø	↓	+

Up arrow ↑—increased, Down arrow ↓—decreased, Ø—no effect, +—positive interaction, ()—tendency, N.M. not measured.

tendencies for learning impairment in MWM were detected separately for OVX and AD without any interaction. The only genotype × OVX interaction in cognition was seen during the CS-induced freezing in CFT, when OVX aggravated the symptoms in Control, but decreased in 3xTg-AD animals. Although we used CFT as an associative learning and memory test (97), its result strongly depends on the animal's anxiety state (98). Indeed, these CFT results were very similar to the anxiety z-score data. The intact memory can also be explained by the lack of Aβ deposition in the hippocampus and cortical areas (99, 100). We might assume that more time is needed for the development of the symptoms; therefore, investigating memory deficit would be informative with older animals only even after OVX (101).

Anxiety is a core symptom of postmenopausal women (102), as well as might be comorbid with AD (103). However, anxiety symptoms remain largely unexplored, despite the significant impact on quality of life, if not diagnosed and treated (102). As anxiety is associated with both AD and OVX (23), we assumed that both interventions will increase its level in mice, with a possible synergistic effect. However, we found a significant anxiogenic effect of OVX in EPM only, the most frequently used anxiety test (64, 104). On the contrary, an AD effect was visible in the FOT test measuring innate fear and anxiety-related behavior (75). We found that 3xTg-AD animals spend more time freezing, which suggests that these animals were more frightened (75, 105). Also, 3xTg-AD animals spend less time exploring and rearing, which might reflect anxiety, too (see immobility in CFT) (106). Nevertheless, these findings may be related to the increased Aβ deposition in the BLA (Figure 9), as this region is responsible for formation of fear-related responses and can be linked to anxious behavior (105, 107–109). The increased overall anxiety z-score of 3xTg-AD animals coincides with the increased anxiety in human AD patients (110, 111).

Moreover, the locomotor activity shown by the different behavioral tests (distance moved in EPM, OF, and FOT; total number of entries in the Y-maze; and number of entries to closed arms or dark compartment in EPM and LD) and the locomotion z-score calculated from these parameters showed a difference between the two genotypes with lower levels in 3xTg-AD animals. In line with previous results, this decreased locomotor activity may reflect anxious behavior. However, we

cannot close out a moderate motoric disabilities as well (112, 113). The decrease in movement can be related to the presence of Aβ in the motoric and somatosensory cortex (Figure 9) (114). Nevertheless, in line with an anxious phenotype, OVX also decreased locomotion, which was mainly detectable in controls. In support, volcano mice presented a scalloped pattern of daily activity during the estrous cycle and OVX reduced the total movement (115). Moreover, in estrogen receptor knockout mice (on C57BL6 background), E2 injection to OVX animals increased total activity and amplitude (116). The smaller effects in the AD model might be due to the already low levels, which cannot be easily decreased further.

Despite subtle behavioral changes, morphological changes were more equivocal. Namely, Aβ plaques, one of the most characteristic morphological changes of AD (99, 117), appeared only in 3xTg-AD animals; however, we could detect their presence already around 5 months. Although we expected that OXV alone will lead to the appearance of pathological hallmarks in control animals, in humans, OVX induced behavioral and morphological changes only in the elderly or those having genetic mutations [e.g., ApoE-4 genotype (118–120)]. In line with this, OVX was able to increase the number of amyloid plaques in the 3xTg-AD animals, further increasing the translational values of our model. However, we detected changes in the BLA, but not in the HC and CTX. We have to note that in much older animals, OVX-induced Aβ formation was found also in the CTX and HC (121–123). Thus, BLA might be a sensitive area, where changes occur earlier than in other parts of the brain. It is known that stress, i.e., glucocorticoids, increases excitability of BLA, while E2 decreases it (124). Thus, in our hands, repeated testing, as a stressor, as well as E2 decline due to OVX, might have promoted the stress sensitivity of BLA (125, 126). In support of the E2 effect, the replacement of the hormone after OVX can decrease the number and density of Aβ plaques in rodents (25, 100, 121). This is also in line with human studies, where OXV patients were treated with hormone replacement therapy, resulting in no difference in Aβ deposition (120). These differences (namely, age, genetic predisposition, and hormone replacement) might be the cause of the controversy in the literature on OVX-induced amyloidosis in the brain reported to be missing by some (120, 127) or increased by others (13, 128–130). However, Palm et al., also using 3xTg-AD mice, showed no difference after E2 treatment in Aβ deposition (123), while Carroll et al. (121) used PG to reduce the p-Tau accumulation in the CA1 region of the hippocampus, subiculum, and frontal cortex.

The novelty of our study is that we included more behavioral tests and examined the cholinergic system as well. The importance of the cholinergic system in AD is outstanding, being the target of almost all the drugs in the market (131, 132). Thus, we decided to examine the cell numbers in the NBM (133), and their projections to the SSC (79). In the ChAT-positive cell numbers, no difference was found in 5-month-old mice, probably because of their young age. However, AChE-positive fiber degeneration was detected in 3xTg-AD mice and even aggravated after OVX, suggesting that axonal and dendritic degenerations start earlier than behavioral decline (114, 134).

Our study has certain limitations. First, we used standard diet, and phytoestrogens might have influenced the outcome. Next, we did not monitor the cycle, and the cyclic changes might increase variability in Sham-operated groups. Furthermore, to keep the number of used animals as low as possible, we used repeated testing, which might influence each other's results. For some tests, more animals/group might have been required to see statistically significant differences.

All in all, we confirmed that OVX induced menopausal symptoms and removal of the sexual steroids aggravated the appearance of AD-related alterations in the brain without significantly influencing behavior. Thus, the OVX in young, 3-month-old 3xTg-AD mice might be a suitable model for testing the effect of new treatment options at the structural level, which can speed up testing (it is not necessary to wait 6–12 months for the animals to age). However, to reveal any beneficial effect on behavior, a later time point might be needed.

Data availability statement

The raw data supporting the conclusions of this article will be made available by the authors, without undue reservation.

Ethics statement

The animal study was reviewed and approved by Local committee of animal health and care and Baranya Country Office for Animal Welfare (PE/EA/918-7/2019).

Author contributions

Conceptualization, DZ; methodology, SF, AS, BT, CS, CF, KB, PC, and TC; investigation, SF, AS, BT, CS, CF, KB, PC, and TC; validation, DZ; formal analysis, SF, AS, BT, CS, and CF; writing—original draft preparation, SF, AS, BT, CF, and DZ; writing—review and editing, CS, KB, PC, and TC; visualization, SF, AS, BT, CS, CF, and DZ; supervision, DZ; project administration, DZ; funding acquisition, DZ. All authors have read and agreed to the published version of the manuscript.

Funding

This study was supported by the National Research Development and Innovation Office of Hungary (grant

numbers K141934, K138763, and K120311) as well as by the Thematic Excellence Program 2021 Health Sub-programme of the Ministry for Innovation and Technology in Hungary, within the framework of the TKP2021-EGA-16 project of the Pécs of University. The agencies had no further role in study design, and in the collection, analysis, or interpretation of the data.

Acknowledgments

We thank all the core facilities of our institute for their supportive help: the Behavioral Studies Unit for help with behavioral testing (Dr. Kornél Demeter), the Nikon Microscopy Center for help with microscopy (Dr. László Barna and Dr. Pál Vági), the Virus Technology Unit and the Medical Gene Technology Unit for help with mouse lines, and the Metabolic Phenotyping Unit (Dr Csaba Fekete) for the help by the MRI measurement.

Conflict of interest

The authors declare that the research was conducted in the absence of any commercial or financial relationships that could be construed as a potential conflict of interest.

Publisher's note

Supplementary material

The Supplementary Material for this article can be found online at: https://www.frontiersin.org/articles/10.3389/fendo.2022.985424/full#supplementary-material

SUPPLEMENTARY FIGURE 1
Immunohistochemical staining (NiDAB) of Amyloid-β_{1-42} (Aβ) plaques in different brain regions of the control animals. There was no Aβ signal detectable in the brain of control animals, therefore no quantitative measurement was possible. **(A)** Representative figures based on the Paxinos Mouse Brain atlas (4th Edition) about the brain regions of interest, framed with red: Basolateral amygdala (BLA), at Bregma -1.23 mm, Motor and somatosensory cortex (CTX) at Bregma -1.07 mm and CA1 hippocampal region (CA1-HC) presented at Bregma -2.15 mm. **(B)** Representative pictures of the BLA of the control animals after Sham or OVX surgery. **(C)** Representative pictures of the CTX of control animals after Sham or OVX surgery. **(D)** Representative pictures of the HC of control animals after Sham or OVX surgery, with a close-up to a small part of the CA1 region. Scale bar: 200μm.

References

1. Alzheimer's Association. 2020 alzheimer's disease facts and figures. *Alzheimer's Dement* (2020) 16:391–460. doi: 10.1002/alz.12068

2. WHO. *The top 10 causes of death* (2020). Available at: https://www.who.int/news-room/fact-sheets/detail/the-top-10-causes-of-death.

3. Lyketsos CG, Carrillo MC, Ryan JM, Khachaturian AS, Trzepacz P, Amatniek J, et al. Neuropsychiatric symptoms in alzheimer's disease. *Alzheimers Dement* (2011) 7:532–9. doi: 10.1016/j.jalz.2011.05.2410

4. Scheltens P, Blennow K, Breteler MMB, de Strooper B, Frisoni GB, Salloway S, et al. Alzheimer's disease. *Lancet (London England)* (2016) 388:505–17. doi: 10.1016/S0140-6736(15)01124-1

5. LaFerla FM, Oddo S. Alzheimer's disease: Abeta, tau and synaptic dysfunction. *Trends Mol Med* (2005) 11:170–6. doi: 10.1016/j.molmed.2005.02.009

6. Querfurth HW, LaFerla FM. Alzheimer's disease. *N Engl J Med* (2010) 362:329–44. doi: 10.1056/NEJMra0909142

7. Nebel RA, Aggarwal NT, Barnes LL, Gallagher A, Goldstein JM, Kantarci K, et al. Understanding the impact of sex and gender in alzheimer's disease: A call to action. *Alzheimers Dement* (2018) 14:1171–83. doi: 10.1016/j.jalz.2018.04.008

8. Cacace R, Sleegers K, Van Broeckhoven C. Molecular genetics of early-onset alzheimer's disease revisited. *Alzheimers Dement* (2016) 12:733–48. doi: 10.1016/j.jalz.2016.01.012

9. Rettberg JR, Dang H, Hodis HN, Henderson VW, St. John JA, Mack WJ, et al. Identifying postmenopausal women at risk for cognitive decline within a healthy cohort using a panel of clinical metabolic indicators: potential for detecting an at-alzheimer's risk metabolic phenotype. *Neurobiol Aging* (2016) 40:155–63. doi: 10.1016/j.neurobiolaging.2016.01.011

10. Fisher DW, Bennett DA, Dong H. Sexual dimorphism in predisposition to alzheimer's disease. *Neurobiol Aging* (2018) 70:308–24. doi: 10.1016/j.neurobiolaging.2018.04.004

11. Pike CJ. Sex and the development of alzheimer's disease. *J Neurosci Res* (2017) 95:671–80. doi: 10.1002/jnr.23827

12. Roof RL, Hall ED. Gender differences in acute CNS trauma and stroke: neuroprotective effects of estrogen and progesterone. *J Neurotrauma* (2000) 17:367–88. doi: 10.1089/neu.2000.17.367

13. Yao J, Irwin R, Chen S, Hamilton R, Cadenas E, Brinton RD. Ovarian hormone loss induces bioenergetic deficits and mitochondrial β-amyloid. *Neurobiol Aging* (2012) 33:1507–21. doi: 10.1016/j.neurobiolaging.2011.03.001

14. Cersosimo MG, Benarroch EE. Estrogen actions in the nervous system: Complexity and clinical implications. *Neurology* (2015) 85:263–73. doi: 10.1212/WNL.0000000000001776

15. Kramár EA, Babayan AH, Gall CM, Lynch G. Estrogen promotes learning-related plasticity by modifying the synaptic cytoskeleton. *Neuroscience* (2013) 239:3–16. doi: 10.1016/j.neuroscience.2012.10.038

16. Sellers KJ, Erli F, Raval P, Watson IA, Chen D, Srivastava DP. Rapid modulation of synaptogenesis and spinogenesis by 17β-estradiol in primary cortical neurons. *Front Cell Neurosci* (2015) 9:137. doi: 10.3389/fncel.2015.00137

17. Kwakowsky A, Potapov K, Kim S, Peppercorn K, Tate WP, Abraham IM. Treatment of beta amyloid 1-42 (Abeta(1-42))-induced basal forebrain cholinergic damage by a non-classical estrogen signaling activator *in vivo*. *Sci Rep* (2016) 6:21101. doi: 10.1038/srep21101

18. Hayward GC, Baranowski BJ, Marko DM, MacPherson REK. Examining the effects of ovarian hormone loss and diet-induced obesity on alzheimer's disease markers of amyloid-β production and degradation. *J Neurophysiol* (2021) 125:1068–78. doi: 10.1152/jn.00489.2020

19. Qin Y, An D, Xu W, Qi X, Wang X, Chen L, et al. Estradiol replacement at the critical period protects hippocampal neural stem cells to improve cognition in APP/PS1 mice. *Front Aging Neurosci* (2020) 12:240. doi: 10.3389/fnagi.2020.00240

20. Mosconi L, Berti V, Quinn C, McHugh P, Petrongolo G, Varsavsky I, et al. Sex differences in Alzheimer risk: Brain imaging of endocrine vs chronologic aging. *Neurology* (2017) 89:1382–90. doi: 10.1212/WNL.0000000000004425

21. Georgakis MK, Beskou-Kontou T, Theodoridis I, Skalkidou A, Petridou ET. Surgical menopause in association with cognitive function and risk of dementia: A systematic review and meta-analysis. *Psychoneuroendocrinology* (2019) 106:9–19. doi: 10.1016/J.PSYNEUEN.2019.03.013

22. Rocca WA, Bower JH, Maraganore DM, Ahlskog JE, Grossardt BR, De Andrade M, et al. Increased risk of cognitive impairment or dementia in women who underwent oophorectomy before menopause. *Neurology* (2007) 69:1074–83. doi: 10.1212/01.WNL.0000276984.19542.E6

23. Parker WH, Jacoby V, Shoupe D, Rocca W. Effect of bilateral oophorectomy on women's long-term health. *Womens Health (Lond Engl)* (2009) 5:565–76. doi: 10.2217/WHE.09.42

24. Brinton RD. Minireview: Translational animal models of human menopause: Challenges and emerging opportunities. *Endocrinology* (2012) 153:3571–8. doi: 10.1210/EN.2012-1340

25. Kara F, Belloy ME, Voncken R, Sarwari Z, Garima Y, Anckaerts C, et al. Long-term ovarian hormone deprivation alters functional connectivity, brain neurochemical profile and white matter integrity in the Tg2576 amyloid mouse model of alzheimer's disease. *Neurobiol Aging* (2021) 102:139–50. doi: 10.1016/J.NEUROBIOLAGING.2021.02.011

26. Corder EH, Saunders AM, Strittmatter WJ, Schmechel DE, Gaskell PC, Small GW, et al. Gene dose of apolipoprotein e type 4 allele and the risk of alzheimer's disease in late onset families. *Science* (1993) 261:921–3. doi: 10.1126/science.8346443

27. Hori Y, Hashimoto T, Nomoto H, Hyman BT, Iwatsubo T. Role of apolipoprotein e in β-amyloidogenesis: Isoform-specific effects on protofibril to fibril conversion of aβ in vitro and brain aβ deposition in vivo. *J Biol Chem* (2015) 290:15163–74. doi: 10.1074/jbc.M114.622209

28. Hashimoto T, Serrano-Pozo A, Hori Y, Adams KW, Takeda S, Banerji AO, et al. Especially apolipoprotein E4, increases the oligomerization of amyloid β peptide. *J Neurosci* (2012) 32:15181–92. doi: 10.1523/JNEUROSCI.1542-12.2012

29. Liu C-C, Zhao N, Fu Y, Wang N, Linares C, Tsai C-W, et al. ApoE4 accelerates early seeding of amyloid pathology. *Neuron* (2017) 96:1024–1032.e3. doi: 10.1016/j.neuron.2017.11.013

30. Castellano JM, Kim J, Stewart FR, Jiang H, DeMattos RB, Patterson BW, et al. Human apoE isoforms differentially regulate brain amyloid-β peptide clearance. *Sci Transl Med* (2011) 3:89ra57. doi: 10.1126/scitranslmed.3002156

31. Duan Y, Ye T, Qu Z, Chen Y, Miranda A, Zhou X, et al. Brain-wide Cas9-mediated cleavage of a gene causing familial alzheimer's disease alleviates amyloid-related pathologies in mice. *Nat BioMed Eng* (2021) 6 (2):168–180. doi: 10.1038/s41551-021-00759-0

32. Lanoiselée H-M, Nicolas G, Wallon D, Rovelet-Lecrux A, Lacour M, Rousseau S, et al. APP, PSEN1, and PSEN2 mutations in early-onset Alzheimer disease: A genetic screening study of familial and sporadic cases. *PloS Med* (2017) 14:e1002270. doi: 10.1371/journal.pmed.1002270

33. Jonsson T, Atwal JK, Steinberg S, Snaedal J, Jonsson PV, Bjornsson S, et al. A mutation in APP protects against alzheimer's disease and age-related cognitive decline. *Nature* (2012) 488:96–9. doi: 10.1038/nature11283

34. Sergeant N, David JP, Goedert M, Jakes R, Vermersch P, Buée L, et al. Two-dimensional characterization of paired helical filament-tau from alzheimer's disease: demonstration of an additional 74-kDa component and age-related biochemical modifications. *J Neurochem* (1997) 69:834–44. doi: 10.1046/j.1471-4159.1997.69020834.x

35. Goedert M, Spillantini MG, Cairns NJ, Crowther RA. Tau proteins of alzheimer paired helical filaments: Abnormal phosphorylation of all six brain isoforms. *Neuron* (1992) 8:159–68. doi: 10.1016/0896-6273(92)90117-V

36. Oddo S, Caccamo A, Shepherd JD, Murphy MP, Golde TE, Kayed R, et al. Triple-transgenic model of alzheimer's disease with plaques and tangles: intracellular abeta and synaptic dysfunction. *Neuron* (2003) 39:409–21. doi: 10.1016/s0896-6273(03)00434-3

37. Oddo S, Caccamo A, Kitazawa M, Tseng BP, LaFerla FM. Amyloid deposition precedes tangle formation in a triple transgenic model of alzheimer's disease. *Neurobiol Aging* (2003) 24:1063–70. doi: 10.1016/j.neurobiolaging.2003.08.012

38. Belfiore R, Rodin A, Ferreira E, Velazquez R, Branca C, Caccamo A, et al. Temporal and regional progression of alzheimer's disease-like pathology in 3xTg-AD mice. *Aging Cell* (2019) 18:e12873. doi: 10.1111/acel.12873

39. Ballinger EC, Ananth M, Talmage DA, Role LW. Basal forebrain cholinergic circuits and signaling in cognition and cognitive decline. *Neuron* (2016) 91:1199–218. doi: 10.1016/j.neuron.2016.09.006

40. Záborszky L, Gombkoto P, Varsanyi P, Gielow MR, Poe G, Role LW, et al. Specific basal forebrain-cortical cholinergic circuits coordinate cognitive operations. *J Neurosci* (2018) 38:9446–58. doi: 10.1523/JNEUROSCI.1676-18.2018

41. Whitehouse PJ, Price DL, Struble RG, Clark AW, Coyle JT, DeLong MR. Alzheimer's disease and senile dementia: loss of neurons in the basal forebrain. *Science* (1982) 215:1237–9. doi: 10.1126/SCIENCE.7058341

42. Schmitz TW, Nathan Spreng R. Basal forebrain degeneration precedes and predicts the cortical spread of alzheimer's pathology. *Nat Commun 2016 71* (2016) 7:1–13. doi: 10.1038/ncomms13249

43. Desmarais JE, Gauthier S. Clinical use of cholinergic drugs in Alzheimer disease. *Nat Rev Neurol 2010 68* (2010) 6:418–20. doi: 10.1038/nrneurol.2010.105

44. Kalesnykas G, Roschier U, Puoliväli J, Wang J, Miettinen R. The effect of aging on the subcellular distribution of estrogen receptor-alpha in the cholinergic neurons of transgenic and wild-type mice. *Eur J Neurosci* (2005) 21:1437–42. doi: 10.1111/J.1460-9568.2005.03953.X

45. Kim SH, Barad Z, Cheong RY, Ábrahám IM. Sex differences in rapid nonclassical action of 17β-oestradiol on intracellular signalling and oestrogen receptor α expression in basal forebrain cholinergic neurones in mouse. *J Neuroendocrinol* (2020) 32:e12830. doi: 10.1111/JNE.12830

46. Sarchielli E, Guarnieri G, Idrizaj E, Squecco R, Mello T, Comeglio P, et al. The G protein-coupled oestrogen receptor, GPER1, mediates direct anti-inflammatory effects of oestrogens in human cholinergic neurones from the nucleus basalis of meynert. *J Neuroendocrinol* (2020) 32:e12837. doi: 10.1111/jne.12837

47. Mitra SW, Hoskin E, Yudkovitz J, Pear L, Wilkinson HA, Hayashi S, et al. Immunolocalization of estrogen receptor β in the mouse brain: Comparison with estrogen receptor α. *Endocrinology* (2003) 144:2055–67. doi: 10.1210/EN.2002-221069

48. Merchenthaler I, Lane MV, Numan S, Dellovade TL. Distribution of estrogen receptor alpha and beta in the mouse central nervous system: *in vivo* autoradiographic and immunocytochemical analyses. *J Comp Neurol* (2004) 473:270–91. doi: 10.1002/CNE.20128

49. Ping SE, Trieu J, Wlodek ME, Barrett GL. Effects of estrogen on basal forebrain cholinergic neurons and spatial learning. *J Neurosci Res* (2008) 86:1588–98. doi: 10.1002/JNR.21609

50. Saenz C, Dominguez R, De Lacalle S. Estrogen contributes to structural recovery after a lesion. *Neurosci Lett* (2006) 392:198–201. doi: 10.1016/J.NEULET.2005.09.023

51. Ábrahám IM, Koszegi Z, Tolod-Kemp E, Szego ÉM. Action of estrogen on survival of basal forebrain cholinergic neurons: Promoting amelioration. *Psychoneuroendocrinology* (2009) 34 (Suppl 1):S104–12. doi: 10.1016/j.psyneuen.2009.05.024

52. Perez SE, He B, Muhammad N, Oh KJ, Fahnestock M, Ikonomovic MD, et al. Cholinotrophic basal forebrain system alterations in 3xTg-AD transgenic mice. *Neurobiol Dis* (2011) 41:338–52. doi: 10.1016/J.NBD.2010.10.002

53. Zhu D, Montagne A, Zhao Z. Alzheimer's pathogenic mechanisms and underlying sex difference. *Cell Mol Life Sci* (2021) 78:4907–20. doi: 10.1007/s00018-021-03830-w

54. Mauvais-Jarvis F. Estrogen and androgen receptors: regulators of fuel homeostasis and emerging targets for diabetes and obesity. *Trends Endocrinol Metab* (2011) 22:24–33. doi: 10.1016/J.TEM.2010.10.002

55. Cooke PS, Buchanan DL, Young P, Setiawan T, Brody J, Korach KS, et al. Stromal estrogen receptors mediate mitogenic effects of estradiol on uterine epithelium. *Proc Natl Acad Sci U.S.A.* (1997) 94:6535–40. doi: 10.1073/PNAS.94.12.6535

56. Quispe Calla NE, Vicetti Miguel RD, Aceves KM, Huang H, Howitt B, Cherpes TL. Ovariectomized mice and postmenopausal women exhibit analogous loss of genital epithelial integrity. *Tissue Barriers* (2021) 9(2):1865760. doi: 10.1080/21688370.2020.1865760

57. Fazekas CL, Balázsfi D, Horváth HR, Balogh Z, Aliczki M, Puhova A, et al. Consequences of VGluT3 deficiency on learning and memory in mice. *Physiol Behav* (2019) 212:112688. doi: 10.1016/j.physbeh.2019.112688

58. Prieur E, Jadavji N. Assessing spatial working memory using the spontaneous alternation y-maze test in aged Male mice. *Bio-protocol* (2019) 9(3):e3162. doi: 10.21769/BIOPROTOC.3162

59. Brandeis R, Brandys Y, Yehuda S. The use of the morris water maze in the study of memory and learning. *Int J Neurosci* (1989) 48:29–69. doi: 10.3109/00207458909002151

60. Vorhees CV, Williams MT. Morris water maze: procedures for assessing spatial and related forms of learning and memory. *Nat Protoc* (2006) 1:848–58. doi: 10.1038/NPROT.2006.116

61. Roberto N, Portella MJ, Marquié M, Alegret M, Hernández I, Mauleón A, et al. Neuropsychiatric profile as a predictor of cognitive decline in mild cognitive impairment. *Front Aging Neurosci* (2021) 13:718949. doi: 10.3389/FNAGI.2021.718949

62. Johansson M, Stomrud E, Lindberg O, Westman E, Johansson PM, van Westen D, et al. Apathy and anxiety are early markers of alzheimer's disease. *Neurobiol Aging* (2020) 85:74–82. doi: 10.1016/J.NEUROBIOLAGING.2019.10.008

63. Rocca WA, Grossardt BR, Geda YE, Gostout BS, Bower JH, Maraganore DM, et al. Long-term risk of depressive and anxiety symptoms after early bilateral oophorectomy. *Menopause* (2018) 25:1275–85. doi: 10.1097/GME.0000000000001229

64. Rodgers RJ, Dalvi A. Anxiety, defence and the elevated plus-maze. *Neurosci Biobehav Rev* (1997) 21:801–10. doi: 10.1016/S0149-7634(96)00058-9

65. Byrnes EM, Bridges RS. Reproductive experience alters anxiety-like behavior in the female rat. *Horm Behav* (2006) 50:70–6. doi: 10.1016/J.YHBEH.2006.01.006

66. Pairojana T, Phasuk S, Suresh P, Huang SP, Pakaprot N, Chompoopong S, et al. Age and gender differences for the behavioral phenotypes of 3xTg alzheimer's disease mice. *Brain Res* (2021) 1762:147437. doi: 10.1016/J.BRAINRES.2021.147437

67. Thigpen JE, Setchell KDR, Saunders HE, Haseman JK, Grant MG, Forsythe DB. Selecting the appropriate rodent diet for endocrine disruptor research and testing studies. *ILAR J* (2004) 45:401–16. doi: 10.1093/ILAR.45.4.401/2/ILAR-45-4-401IGF7.GIF

68. Gee DM, Flurkey K, Finch CE. Aging and the regulation of luteinizing hormone in C57BL/6J mice: impaired elevations after ovariectomy and spontaneous elevations at advanced ages. *Biol Reprod* (1983) 28:598–607. doi: 10.1095/BIOLREPROD28.3.598

69. Chaves T, Török B, Fazekas CL, Correia P, Sipos E, Várkonyi D, et al. Median raphe region GABAergic neurons contribute to social interest in mouse. *Life Sci* (2022) 289:120223. doi: 10.1016/J.LFS.2021.120223

70. Engelmann M, Hädicke J, Noack J. Testing declarative memory in laboratory rats and mice using the nonconditioned social discrimination procedure. *Nat Protoc* (2011) 6:1152–62. doi: 10.1038/NPROT.2011.353

71. Aliczki M, Fodor A, Balogh Z, Haller J. *Behavior DZ-h and, 2014 undefined. the effects of lactation on impulsive behavior in vasopressin-deficient brattleboro rats*. Available at: https://www.sciencedirect.com/science/article/pii/S0018506X14001597 (Accessed June 16, 2022).

72. Bruzsik B, Biro L, Zelena D, Sipos E, Szebik H, Sarosdi KR, et al. Somatostatin neurons of the bed nucleus of stria terminalis enhance associative fear memory consolidation in mice. *J Neurosci* (2021) 41:1982. doi: 10.1523/JNEUROSCI.1944-20.2020

73. Balázsfi D, Fodor A, Török B, Ferenczi S, Kovács KJ, Haller J, et al. Enhanced innate fear and altered stress axis regulation in VGluT3 knockout mice. *Stress* (2018) 21:151–61. doi: 10.1080/10253890.2017.1423053

74. Gáll Z, Farkas S, Albert Á, Ferencz E, Vancea S, Urkon M, et al. Effects of chronic cannabidiol treatment in the rat chronic unpredictable mild stress model of depression. *Biomolecules* (2020) 10(5):801. doi: 10.3390/biom10050801

75. Bruzsik B, Biro L, Sarosdi KR, Zelena D, Sipos E, Szebik H, et al. Neurochemically distinct populations of the bed nucleus of stria terminalis modulate innate fear response to weak threat evoked by predator odor stimuli. *Neurobiol Stress* (2021) 15:100415. doi: 10.1016/J.YNSTR.2021.100415

76. Hanna Al-Shaikh FS, Duara R, Crook JE, Lesser ER, Schaeverbeke J, Hinkle KM, et al. Selective vulnerability of the nucleus basalis of meynert among neuropathologic subtypes of Alzheimer disease. *JAMA Neurol* (2020) 77:225–33. doi: 10.1001/JAMANEUROL.2019.3606

77. George AA, Vieira JM, Xavier-Jackson C, Gee MT, Cirrito JR, Bimonte-Nelson HA, et al. Implications of oligomeric amyloid-beta (oAβ 42) signaling through α7β2-nicotinic acetylcholine receptors (nAChRs) on basal forebrain cholinergic neuronal intrinsic excitability and cognitive decline. *J Neurosci* (2021) 41:555–75. doi: 10.1523/JNEUROSCI.0876-20.2020

78. Lehmann J, Nagy JI, Atmadja S, Fibiger HC. The nucleus basalis magnocellularis: the origin of a cholinergic projection to the neocortex of the rat. *Neuroscience* (1980) 5:1161–74. doi: 10.1016/0306-4522(80)90195-5

79. Koszegi Z, Szego ÉM, Cheong RY, Tolod-Kemp E, Ábrahám IM. Postlesion estradiol treatment increases cortical cholinergic innervations *via* estrogen receptor-α dependent nonclassical estrogen signaling *in vivo*. *Endocrinology* (2011) 152:3471–82. doi: 10.1210/en.2011-1017

80. Guilloux JP, Seney M, Edgar N, Sibille E. Integrated behavioral z-scoring increases the sensitivity and reliability of behavioral phenotyping in mice: relevance to emotionality and sex. *J Neurosci Methods* (2011) 197:21–31. doi: 10.1016/J.JNEUMETH.2011.01.019

81. Fazekas CL, Sipos E, Klaric T, Török B, Bellardie M, Erjave GN, et al. Searching for glycomic biomarkers for predicting resilience and vulnerability in a rat model of posttraumatic stress disorder. *Stress* (2020) 23:715–31. doi: 10.1080/10253890.2020.1795121

82. Heine PA, Taylor JA, Iwamoto GA, Lubahn DB, Cooke PS. Increased adipose tissue in male and female estrogen receptor-alpha knockout mice. *Proc Natl Acad Sci U.S.A.* (2000) 97:12729–34. doi: 10.1073/PNAS.97.23.12729

83. Beck P. Effect of progestins on glucose and lipid metabolism. *Ann N Y Acad Sci* (1977) 286:434–45. doi: 10.1111/J.1749-6632.1977.TB29435.X

84. Abildgaard J, Ploug T, Al-Saoudi E, Wagner T, Thomsen C, Ewertsen C, et al. Changes in abdominal subcutaneous adipose tissue phenotype following menopause is associated with increased visceral fat mass. *Sci Rep* (2021) 11(1):14750. doi: 10.1038/S41598-021-94189-2

85. Ambikairajah A, Walsh E, Tabatabaei-Jafari H, Cherbuin N. Fat mass changes during menopause: a metaanalysis. *Am J Obstet Gynecol* (2019) 221:393–409.e50. doi: 10.1016/J.AJOG.2019.04.023

86. Picone P, Di Carlo M, Nuzzo D. Obesity and alzheimer's disease: Molecular bases. *Eur J Neurosci* (2020) 52:3944–50. doi: 10.1111/EJN.14758

87. Kang S, Lee YH, Lee JE. Metabolism-centric overview of the pathogenesis of alzheimer's disease. *Yonsei Med J* (2017) 58:479–88. doi: 10.3349/YMJ.2017.58.3.479

88. Medina-Contreras J, Villalobos-Molina R, Zarain-Herzberg A, Balderas-Villalobos J. Ovariectomized rodents as a menopausal metabolic syndrome model. a minireview. *Mol Cell Biochem* (2020) 475:261–76. doi: 10.1007/S11010-020-03879-4

89. Alderman MH, Taylor HS. Molecular mechanisms of estrogen action in female genital tract development. *Differentiation* (2021) 118:34–40. doi: 10.1016/J.DIFF.2021.01.002

90. Levin ER. Membrane estrogen receptors signal to determine transcription factor function. *Steroids* (2018) 132:1–4. doi: 10.1016/j.steroids.2017.10.014

91. Kwakowsky A, Herbison AE, Ábrahám IM. The role of cAMP response element-binding protein in estrogen negative feedback control of gonadotropin-releasing hormone neurons. *J Neurosci* (2012) 32:11309–17. doi: 10.1523/JNEUROSCI.1333-12.2012

92. Cheong RY, Czieselsky K, Porteous R, Herbison AE. Expression of ESR1 in glutamatergic and GABAergic neurons is essential for normal puberty onset, estrogen feedback, and fertility in female mice. *J Neurosci* (2015) 35:14533. doi: 10.1523/JNEUROSCI.1776-15.2015

93. Yip SH, Liu X, Hessler S, Cheong I, Porteous R, Herbison AE. Indirect suppression of pulsatile LH secretion by CRH neurons in the female mouse. *Endocrinology* (2021) 162(3):bqaa237. doi: 10.1210/ENDOCR/BQAA237

94. Farkas S, Szabó A, Hegyi AE, Török B, Fazekas CL, Ernszt D, et al. Estradiol and estrogen-like alternative therapies in use: The importance of the selective and non-classical actions. *Biomedicines* (2022) 10(4):861. doi: 10.3390/BIOMEDICINES10040861

95. Liedert A, Nemitz C, Haffner-Luntzer M, Schick F, Jakob F, Ignatius A. Effects of estrogen receptor and wnt signaling activation on mechanically induced bone formation in a mouse model of postmenopausal bone loss. *Int J Mol Sci* (2020) 21:1–12. doi: 10.3390/IJMS21218301

96. Wei Z, Ge F, Che Y, Wu S, Dong X, Song D. Metabolomics coupled with pathway analysis provides insights into sarco-osteoporosis metabolic alterations and estrogen therapeutic effects in mice. *Biomolecules* (2021) 12(1):41. doi: 10.3390/BIOM12010041

97. Webster SJ, Bachstetter AD, Nelson PT, Schmitt FA, Van Eldik LJ. Using mice to model alzheimer's dementia: an overview of the clinical disease and the preclinical behavioral changes in 10 mouse models. *Front Genet* (2014) 5:88. doi: 10.3389/FGENE.2014.00088

98. Campos AC, Fogaça MV, Aguiar DC, Guimarães FS. Animal models of anxiety disorders and stress. *Rev Bras Psiquiatr* (2013) 35(Suppl 2):S101–11. doi: 10.1590/1516-4446-2013-1139

99. Furcila D, Defelipe J, Alonso-Nanclares L. A study of amyloid-β and phosphotau in plaques and neurons in the hippocampus of alzheimer's disease patients. *J Alzheimers Dis* (2018) 64:417–35. doi: 10.3233/JAD-180173

100. Behnamedin Jameie S, Pirasteh A, Naseri A, Sadat Jameie M, Farhadi M, Fahanik Babaee J, et al. β-amyloid formation, memory, and learning decline following long-term ovariectomy and its inhibition by systemic administration of apigenin and β-estradiol. *Basic Clin Neurosci* (2021) 12(3):383–94. doi: 10.32598/BCN.2021.2634.1

101. Stover KR, Campbell MA, Van Winssen CM, Brown RE. Early detection of cognitive deficits in the 3xTg-AD mouse model of alzheimer's disease. *Behav Brain Res* (2015) 289:29–38. doi: 10.1016/J.BBR.2015.04.012

102. Siegel AM, Mathews SB. Diagnosis and treatment of anxiety in the aging woman. *Curr Psychiatry Rep* (2015) 17(12):93. doi: 10.1007/S11920-015-0636-3

103. Botto R, Callai N, Cermelli A, Causarano L, Rainero I. Anxiety and depression in alzheimer's disease: a systematic review of pathogenetic mechanisms and relation to cognitive decline. *Neurol Sci* (2022) 43(7):4107–24. doi: 10.1007/S10072-022-06068-X

104. Arrant AE, Schramm-Sapyta NL, Kuhn CM. Use of the light/dark test for anxiety in adult and adolescent male rats. *Behav Brain Res* (2013) 256:119–27. doi: 10.1016/J.BBR.2013.05.035

105. Adhikari A, Lerner TN, Finkelstein J, Pak S, Jennings JH, Davidson TJ, et al. Basomedial amygdala mediates top-down control of anxiety and fear. *Nature* (2015) 527:179–85. doi: 10.1038/NATURE15698

106. Sturman O, Germain PL, Bohacek J. Exploratory rearing: a context- and stress-sensitive behavior recorded in the open-field test. *Stress* (2018) 21:443–52. doi: 10.1080/10253890.2018.1438405

107. Janak PH, Tye KM. From circuits to behaviour in the amygdala. *Nature* (2015) 517:284–92. doi: 10.1038/NATURE14188

108. Sah P. Fear, anxiety, and the amygdala. *Neuron* (2017) 96:1–2. doi: 10.1016/J.NEURON.2017.09.013

109. Etkin A, Prater KE, Schatzberg AF, Menon V, Greicius MD. Disrupted amygdalar subregion functional connectivity and evidence of a compensatory network in generalized anxiety disorder. *Arch Gen Psychiatry* (2009) 66:1361–72. doi: 10.1001/ARCHGENPSYCHIATRY.2009.104

110. Patel P, Masurkar AV. The relationship of anxiety with alzheimer's disease: A narrative review. *Curr Alzheimer Res* (2021) 18:359–71. doi: 10.2174/1567205018666210823095603

111. Zhao QF, Tan L, Wang HF, Jiang T, Tan MS, Tan L, et al. The prevalence of neuropsychiatric symptoms in alzheimer's disease: Systematic review and meta-analysis. *J Affect Disord* (2016) 190:264–71. doi: 10.1016/J.JAD.2015.09.069

112. Lee G. Impaired cognitive function is associated with motor function and activities of daily living in mild to moderate alzheimer's dementia. *Curr Alzheimer Res* (2020) 17:680–6. doi: 10.2174/1567205017666200818193916

113. Albers MW, Gilmore GC, Kaye J, Murphy C, Wingfield A, Bennett DA, et al. At The interface of sensory and motor dysfunctions and alzheimer's disease. *Alzheimers Dement* (2015) 11:70–98. doi: 10.1016/J.JALZ.2014.04.514

114. Jawhar S, Trawicka A, Jenneckens C, Bayer TA, Wirths O. Motor deficits, neuron loss, and reduced anxiety coinciding with axonal degeneration and intraneuronal aβ aggregation in the 5XFAD mouse model of alzheimer's disease. *Neurobiol Aging* (2012) 33:196.e29–196.e40. doi: 10.1016/J.NEUROBIOLAGING.2010.05.027

115. Juárez-Tapia C, Miranda-Anaya M. Ovariectomy influences the circadian rhythm of locomotor activity and the photic phase shifts in the volcano mouse. *Physiol Behav* (2017) 182:77–85. doi: 10.1016/J.PHYSBEH.2017.10.002

116. Royston SE, Yasui N, Kondilis AG, Lord SV, Katzenellenbogen JA, Mahoney MM. ESR1 and ESR2 differentially regulate daily and circadian activity rhythms in female mice. *Endocrinology* (2014) 155:2613–23. doi: 10.1210/EN.2014-1101

117. Kazim SF, Seo JH, Bianchi R, Larson CS, Sharma A, Wong RKS, et al. Neuronal network excitability in alzheimer's disease: The puzzle of similar versus divergent roles of amyloid β and tau. *eNeuro* (2021) 8(2):ENEURO.0418-20. doi: 10.1523/ENEURO.0418-20.2020

118. Bove R, Secor E, Chibnik LB, Barnes LL, Schneider JA, Bennett DA, et al. Age at surgical menopause influences cognitive decline and Alzheimer pathology in older women. *Neurology* (2014) 82:222–9. doi: 10.1212/WNL.0000000000000033

119. Mosconi L, Berti V, Dyke J, Schelbaum E, Jett S, Loughlin L, et al. Menopause impacts human brain structure, connectivity, energy metabolism, and amyloid-beta deposition. *Sci Rep 2021 111* (2021) 11:1–16. doi: 10.1038/s41598-021-90084-y

120. Zeydan B, Tosakulwong N, Schwarz CG, Senjem ML, Gunter JL, Reid RI, et al. Association of bilateral salpingo-oophorectomy before menopause onset with medial temporal lobe neurodegeneration. *JAMA Neurol* (2019) 76:95–100. doi: 10.1001/JAMANEUROL.2018.3057

121. Carroll JC, Rosario ER, Chang L, Stanczyk FZ, Oddo S, LaFerla FM, et al. Progesterone and estrogen regulate Alzheimer-like neuropathology in female 3xTg-AD mice. *J Neurosci* (2007) 27:13357. doi: 10.1523/JNEUROSCI.2718-07.2007

122. Zhao L, Yao J, Mao Z, Chen S, Wang Y, Brinton RD. 17β-estradiol regulates insulin-degrading enzyme expression *via* an ERβ/PI3-K pathway in hippocampus: relevance to alzheimer's prevention. *Neurobiol Aging* (2011) 32:1949–63. doi: 10.1016/J.NEUROBIOLAGING.2009.12.010

123. Palm R, Chang J, Blair J, Garcia-Mesa Y, Lee HG, Castellani RJ, et al. Down-regulation of serum gonadotropins but not estrogen replacement improves cognition in aged-ovariectomized 3xTg AD female mice. *J Neurochem* (2014) 130:115. doi: 10.1111/JNC.12706

124. Rodrigues SM, Sapolsky RM. Disruption of fear memory through dual-hormone gene therapy. *Biol Psychiatry* (2009) 65:441–4. doi: 10.1016/J.BIOPSYCH.2008.09.003

125. Shansky RM, Hamo C, Hof PR, Lou W, McEwen BS, Morrison JH. Estrogen promotes stress sensitivity in a prefrontal cortex-amygdala pathway. *Cereb Cortex* (2010) 20:2560–7. doi: 10.1093/CERCOR/BHQ003

126. Tian Z, Wang Y, Zhang N, yan GY, Feng B, bing LS, et al. Estrogen receptor GPR30 exerts anxiolytic effects by maintaining the balance between GABAergic and glutamatergic transmission in the basolateral amygdala of ovariectomized mice after stress. *Psychoneuroendocrinology* (2013) 38:2218–33. doi: 10.1016/J.PSYNEUEN.2013.04.011

127. Green PS, Bales K, Paul S, Bu G. Estrogen therapy fails to alter amyloid deposition in the PDAPP model of alzheimer's disease. *Endocrinology* (2005) 146:2774–81. doi: 10.1210/EN.2004-1433

128. Ding F, Yao J, Zhao L, Mao Z, Chen S, Brinton RD. Ovariectomy induces a shift in fuel availability and metabolism in the hippocampus of the female transgenic model of familial alzheimer's. *PloS One* (2013) 8(3):e59825. doi: 10.1371/JOURNAL.PONE.0059825

129. Levin-Allerhand JA, Lominska CE, Wang J, Smith JD. 17Alpha-estradiol and 17beta-estradiol treatments are effective in lowering cerebral amyloid-beta levels in AbetaPPSWE transgenic mice. *J Alzheimers Dis* (2002) 4:449–57. doi: 10.3233/JAD-2002-4601

130. Yao Q, Feng M, Yang B, Long Z, Luo S, Luo M, et al. Effects of ovarian hormone loss on neuritic plaques and autophagic flux in the brains of adult female APP/PS1 double-transgenic mice. *Acta Biochim Biophys Sin (Shanghai)* (2018) 50:447–55. doi: 10.1093/ABBS/GMY032

131. Hampel H, Mesulam M-M, Cuello AC, Farlow MR, Giacobini E, Grossberg GT, et al. The cholinergic system in the pathophysiology and treatment of alzheimer's disease. *Brain* (2018) 141:1917–33. doi: 10.1093/brain/awy132

132. Chen ZR, Huang JB, Yang SL, Hong FF. Role of cholinergic signaling in alzheimer's disease. *Molecules* (2022) 27(6):1816. doi: 10.3390/MOLECULES27061816

133. Gibbs RB. Effects of ageing and long-term hormone replacement on cholinergic neurones in the medial septum and nucleus basalis magnocellularis of ovariectomized rats. *J Neuroendocrinol* (2003) 15:477–85. doi: 10.1046/J.1365-2826.2003.01012.X

134. Oakley H, Cole SL, Logan S, Maus E, Shao P, Craft J, et al. Intraneuronal beta-amyloid aggregates, neurodegeneration, and neuron loss in transgenic mice with five familial alzheimer's disease mutations: potential factors in amyloid plaque formation. *J Neurosci* (2006) 26:10129–40. doi: 10.1523/JNEUROSCI.1202-06.2006

frontiers | Frontiers in Endocrinology

TYPE Original Research
PUBLISHED 25 October 2022
DOI 10.3389/fendo.2022.993228

OPEN ACCESS

EDITED BY
Katja Teerds,
Wageningen University and Research, Netherlands

REVIEWED BY
Richard Piet,
Kent State University, United States
Chunheng Mo,
Sichuan University, China

*CORRESPONDENCE
Klaudia Barabás
klaudia.barabas@aok.pte.hu
Gergely Kovács
gergely.kovacs@aok.pte.hu

†These authors have contributed equally to this work and share first authorship

SPECIALTY SECTION
This article was submitted to Reproduction, a section of the journal Frontiers in Endocrinology

RECEIVED 13 July 2022
ACCEPTED 05 October 2022
PUBLISHED 25 October 2022

CITATION
Barabás K, Kovács G, Vértes V, Kövesdi E, Faludi P, Udvarácz I, Pham D, Reglődi D, Abraham IM and Nagy Z (2022) Stereology of gonadotropin-releasing hormone and kisspeptin neurons in PACAP gene-deficient female mice. *Front. Endocrinol.* 13:993228. doi: 10.3389/fendo.2022.993228

Stereology of gonadotropin-releasing hormone and kisspeptin neurons in PACAP gene-deficient female mice

Klaudia Barabás[1,2*†], Gergely Kovács[1,2*†], Viola Vértes[1], Erzsébet Kövesdi[1,2], Péter Faludi[1,2], Ildikó Udvarácz[1,2], Dániel Pham[2,3], Dóra Reglődi[2,3], Istvan M. Abraham[1,2] and Zsuzsanna Nagy[1]

[1]Institute of Physiology, Medical School, University of Pécs, Pécs, Hungary, [2]Centre for Neuroscience, Szentágothai Research Centre, Pécs, Hungary, [3]Department of Anatomy, Medical School, University of Pécs, Pécs, Hungary

The hypothalamic gonadotropin-releasing hormone (GnRH)–kisspeptin neuronal network regulates fertility in all mammals. Pituitary adenylate cyclase-activating polypeptide (PACAP) is a neuropeptide isolated from the hypothalamus that is involved in the regulation of several releasing hormones and trop hormones. It is well-known that PACAP influences fertility at central and peripheral levels. However, the effects of PACAP on GnRH and kisspeptin neurons are not well understood. The present study investigated the integrity of the estrous cycle in PACAP-knockout (KO) mice. The number and immunoreactivity of GnRH (GnRH-ir) neurons in wild-type (WT) and PACAP KO female mice were determined using immunohistochemistry. In addition, the number of kisspeptin neurons was measured by counting kisspeptin mRNA-positive cells in the rostral periventricular region of the third ventricle (RP3V) and arcuate nucleus (ARC) using the RNAscope technique. Finally, the mRNA and protein expression of estrogen receptor alpha (ERα) was also examined. Our data showed that the number of complete cycles decreased, and the length of each cycle was longer in PACAP KO mice. Furthermore, the PACAP KO mice experienced longer periods of diestrus and spent significantly less time in estrus. There was no difference in GnRH-ir or number of GnRH neurons. In contrast, the number of kisspeptin neurons was decreased in the ARC, but not in the R3PV, in PACAP KO mice compared to WT littermates. Furthermore, ERα mRNA and protein expression was decreased in the ARC, whereas in the R3PV region, ERα mRNA levels were elevated. Our results demonstrate that embryonic deletion of PACAP significantly changes the structure and presumably the function of the GnRH–kisspeptin neuronal network, influencing fertility.

KEYWORDS

PACAP, GnRH, kisspeptin, estrogen receptor α, estrous cycle

1 Introduction

Fertility is regulated by complex neuronal networks. At the hypothalamic level, gonadotropin-releasing hormone (GnRH) neurons form the final output, which controls reproduction in all mammalian species. GnRH is secreted in a pulsatile and surge-like manner in females. Pulsatile secretion of GnRH induces a periodic release of pituitary gonadotrophs that govern gonadal functions and is controlled by the negative feedback actions of gonadal steroids (1). Prior to ovulation, circulating gonadal steroid estradiol levels are elevated, which switches its negative feedback to positive, triggering GnRH and luteinizing hormone (LH) surge to initiate ovulation (2–4).

GnRH release is regulated by a plethora of upstream neuronal signals in the brain (5, 6). Kisspeptin is a neuropeptide synthesized in two major populations of hypothalamic neurons. Kisspeptin neurons integrate and transmit most of the signals, including the aforementioned effects of estradiol, to GnRH neurons (1). The negative feedback of estradiol on GnRH neurons occurs through kisspeptin neurons located in the arcuate nucleus (ARC), which project to the distal dendrons and axon terminals of GnRH neurons (1, 7). These kisspeptin neurons act as gonadotropin-releasing hormone (GnRH) pulse generators. The positive feedback of estradiol evoking the LH surge is conveyed to GnRH neurons *via* kisspeptin neurons located in the rostral periventricular area of the third ventricle (RP3V) axons, which target the cell bodies and proximal dendrites of GnRH neurons (1, 7).

It has been established that both negative and positive estradiol feedback are mediated by estrogen receptor alpha (ERα) expressed in kisspeptin neurons (2, 8). The finding that estradiol regulates kisspeptin neurons *via* ERα in the female brain has been supported by data demonstrating that estradiol upregulates kisspeptin expression in the RP3V, while downregulating it in the ARC through ERα (8).

Although kisspeptin and gonadal steroids play an essential role in the regulation of fertility *via* GnRH neurons, other factors, such as the pituitary adenylate cyclase-activating polypeptide (PACAP), are also markedly involved in controlling fertility. PACAP and its receptors are abundantly expressed at all three levels of the hypothalamic–pituitary–gonadal (HPG) axis (9–11). In addition, there is a reciprocal interaction between ovarian hormones and PACAP; that is, the synthesis of PACAP and the expression of its receptors are modulated by sex steroids (12, 13), while PACAP triggers the synthesis of sexual hormones (10, 14). Furthermore, it is clearly demonstrated that whole-body deletion of the PACAP gene reduces fertility (15). These data implicate the involvement of PACAP in the regulation of reproductive function and fertility. On the other hand, the observed effects of exogenously administered PACAP are dependent on many factors, such as the dose and route of PACAP administration, sex of the animal, and species, indicating the complexity of the effects of PACAP on fertility (11).

To date, only one recently published study demonstrated the regulation of reproductive function by PACAP neurons in the ventral premammillary nucleus by modulating the activity of kisspeptin neurons in female mice (16). However, the mechanisms underlying fertility regulation by PACAP, particularly at the hypothalamic level, have not been fully explored.

In the present study, we investigated the estrous cycle in PACAP-knockout (KO) mice and attempted to shed light on the underlying mechanisms of the chronic effect of PACAP deletion on the organization of GnRH neurons in the basal forebrain, the number of kisspeptin neurons, and ERα expression in the RP3V and ARC.

2 Materials and methods

2.1 Animals

All experiments were performed using adult (12 weeks old) female homozygous PACAP KO and wild-type (WT) (CD1) mice (n = 6, WT; n = 6–8, KO). Mice were bred and housed in the Animal House of the Department of Pharmacology and Pharmacotherapy at the University of Pécs, according to the regulations of the European Community Council Directive and the Animal Welfare Committee of the University of Pécs. Mice were kept under a 12:12-h light/dark cycle, with food and water available *ad libitum*. PACAP KO mice were generated according to Hashimoto et al. (17). This animal study was approved by the Local Animal Care Committee of the University of Pécs (BA02/2000-24/2011 University of Pécs, Hungary).

2.2 Evaluation of the estrous cycle

To evaluate the effect of PACAP deletion on the estrous cycle, PACAP KO mice and WT littermates were assessed by daily (10 a.m.) vaginal smear for a period of 4 weeks (n = 6–6). For immunohistochemical staining and RNAscope *in situ* hybridization, PACAP KO and WT female mice in the estrus stage were selected for perfusion (n = 6–6). Dried smears were stained with methylene blue solution, and cell types were determined with an Olympus CX22 brightfield microscope using a 10× objective (N.A. 0.2) for the evaluation of the estrus stage (18).

2.3 Perfusion and sectioning

Mice were deeply anesthetized by an overdose of 2.5% 2,2,2-tribromoethanol (Avertin, i.p.; Sigma, St. Louis, MO, USA) (0.3 ml/20 g b.w.) and transcardially perfused with ice-cold PBS (4–5

ml) to wash the blood out, followed by ice-cold 4% paraformaldehyde in phosphate-buffered saline buffer (20 ml, pH 7.6). Brains were post-fixed for 2 h at 4°C and cryoprotected in 30% sucrose in Tris-buffered saline (TBS) solution overnight at 4°C. The next day, serial 30-µm-thick coronal sections were cut on an SM 2000R freezing microtome (Leica Microsystems, Nussloch GmbH, Germany) and stored in antifreeze solution (30% ethylene glycol; 25% glycerol; 0.05 M phosphate buffer; pH 7.4) at −20°C until use.

2.4 Immunohistochemistry

All steps were performed at room temperature, except for incubation with primary antibodies. Free-floating brain sections were washed three times in 1× TBS for 10 min, and the endogenous peroxidase activity was blocked with 30% H_2O_2 for 15 min. After the permeabilization and the blocking step with 0.2% Triton X-100 in 10% horse serum for 2 h, the sections were incubated with rat anti-GnRH primary antibody (1:10,000; gift of Erik Hrabovszky) or rabbit anti-ERα (Santa Cruz Biotechnology) diluted in TBS containing 5% horse serum and 0.02% Triton X-100 for 2 days at 4°C. After three consecutive 10-min washes with 1× TBS, slices were incubated in biotinylated donkey anti-rat IgG or donkey anti-rabbit for 2 h (1:300; Jackson ImmunoResearch Laboratories). The washed samples were then incubated with the avidin–biotin–HRP complex (1:200; Vector Elite ABC kit, Vector Laboratories) according to the manufacturer's protocol for 2 h. Labeling was visualized with nickel-diaminobenzidine tetrahydrochloride (DAB) using glucose oxidase, which resulted in a black precipitate within the labeled cells. The chemical reaction was terminated using a brightfield microscope to optimize the signal/background ratio. Finally, the preparations were mounted onto gelatin-coated slides. After drying, slides were transferred into distilled water and ascending ethanol solutions (70%, 95%, and absolute for 10 min, respectively), then into xylene for 10 min and coverslipped using DEPEX (VWR, West Chester, PA, USA) mounting medium.

2.5 Brightfield microscopy and image analysis

Images were captured with a Hamamatsu Orca Flash 4.0 camera attached to a Nikon Ti-E inverted microscope equipped with a motorized x-y-z stage using NIS-Elements imaging software. Images were collected under "Koehler" conditions. To identify the plane of the coronal brain slices, whole sections were imaged using a 10× Plan Apo objective lens (N.A. 0.64). The final large 2D mosaic image was obtained by aligning and stitching the overlapping images during the acquisition. Next, the z-stack of brightfield images (11 slices, 4-µm steps) of the region of interest was acquired along the axial axis using the same 10× objective. Images of the same layer were automatically stitched together using the NIS-Elements software, resulting in a large composite image per layer. Focus stacking of each z-stack of large composite images was achieved using the Stack Focuser plug-in of Fiji software. The number of GnRH neurons in the region of interest was counted manually, while GnRH immunoreactivity (GnRH-ir) was calculated using the Analyze Particles function of Software Fiji after application of the Adaptive Threshold plug-in. The number of ERα-immunoreactive cells was counted automatically using a custom-made macro containing Otsu automatic thresholding and watershed segmentation in Fiji software. Imaging and image analyses were performed in a blinded manner.

Based on the Franklin and Paxinos mouse brain atlas (19), the following planes were selected for analysis in case of the examination of GnRH neurons: medial septum (MS), Plates 24–26; medial preoptic area (MPOA), Plates 28–30; and lateral hypothalamus (LH), Plates 34–36. GnRH-ir was observed in the following brain areas: MS, MPOA, LH, organum vasculosum of lamina terminalis (OVLT), and eminentia mediana (EM). To count ERα-immunoreactive cells in the RP3V and ARC brain regions, sections with plate numbers 29–30 and 51–53 were analyzed, respectively (19). To investigate GnRH-ir and the number of GnRH neurons or ERα-immunoreactive cells, two sections were selected at the appropriate level from each animal in each brain region, and the analysis was performed bilaterally.

2.6 RNAscope *in situ* hybridization

mRNA transcripts of kisspeptin (*Kiss1)* and ERα (*Esr1*) were detected using a multiplex fluorescence RNAscope *in situ* hybridization assay (Advanced Cell Diagnostics, Newark, CA) in 30-µm-thick, paraformaldehyde-fixed coronal brain sections. First, free-floating brain slices were mounted on Superfrost Plus Gold adhesion slides, following three washes in TBS (Thermo Scientific, 630-1324, VWR). The selected transcripts were labeled according to the manufacturer's instructions, followed by sequential amplification and detection steps. To ensure specific staining of *Kiss1* transcripts, labeling of these mRNAs was first performed. *Kiss1* mRNA was labeled with Cy3 fluorophore, whereas Cy5 was used to detect *Esr1* transcripts. Nuclei were counterstained with Hoechst 33342, and the finished samples were covered with ProLong Diamond Antifade Mountant. After 24 h of curing, the mounting medium slices were sealed using a nail polisher. 3-plex negative control probes for mouse tissue were used each time the RNAscope labeling was performed. RP3V and ARC brain regions were analyzed in sections with plate numbers 29–30 and 48–50, respectively (19). For both regions, two sections from each animal were selected and analyzed.

2.7 Confocal imaging

Fluorescent samples were imaged using a Nikon C2+ confocal laser scanning imaging system less than 1 week after the samples were ready. First, a large, composite image of the entire coronal slice was created by stitching individual image tiles taken with a 10× objective (N.A. 0.64). This image was used to determine the plane of the image slice. Next, using a Plan Apo 20× magnification objective (N.A. 0.75), z-stacks of 12-bit fluorescent images (512 × 512 pixels) were taken over the region of interest (RP3V or ARC) in a range of 5 to 15 µm below the surface of the slice with a 1-µm interslice distance, and a pinhole size less than one Airy unit. The laser power and gain of the photomultiplier tube for each channel were set during imaging slices labeled with 3-plex negative probes. All images from the same animal were captured using the same imaging parameters.

Image analysis of the obtained z-stacks was performed using Fiji software. Kisspeptin neurons were manually counted. To assess *Esr1* mRNA expression, images were converted from 12- to 8-bit, followed by Phansalkar local image thresholding. Finally, the *Esr1* mRNA-positive fraction area of the region of interest in all z-layers was calculated in percentage and averaged.

RP3V and ARC brain regions were analyzed in sections with plate numbers 29–30 and 51–53, respectively (19). In both regions, two sections were selected from each animal and *Kiss1* mRNA-positive cells were counted bilaterally.

2.8 Statistical analysis

Data are presented as mean ± SD or median ± range, depending on whether the data showed a normal distribution. To test for normal distribution, the Shapiro–Wilk test was applied. In case data were not normally distributed, the Mann–Whitney *U* test was performed. Data with a normal distribution were analyzed using an unpaired *t*-test. Statistical significance was set at $p < 0.05$.

3 Results

3.1 Estrous cyclicity is altered in PACAP KO mice

Genetic deletion of PACAP induced significant changes in female estrous cycle as it is illustrated in Figure 1A. Vaginal smear assessment of PACAP KO mice and WT littermates demonstrated that the number of cycles decreased in a 28-day period (WT: 4.5 ± 1, KO: 2.5± 1; $p = 0.0022$, Figure 1B), while the length of cycle increased (WT: 4.95 days ± 0.45, KO: 9.75 days ± 1.72; $p < 0.0001$, Figure 1C) in PACAP KO mice compared to WT littermates. Furthermore, the length of the estrus phase significantly decreased in PACAP-deficient female mice (WT: 28.88% ± 5.89, KO: 19.58% ± 5.31; $p = 0.0166$, Figure 1D), while they spent more time in the diestrus stage compared to WT littermates (WT: 30.65% ± 28.48, KO: 66.60% ± 4342; $p = 0.0303$, Figure 1E).

3.2 Effect of PACAP deletion on the number of GnRH neurons and GnRH-ir

To test the effect of PACAP on the central hub of the HPG axis, we examined the number of GnRH neurons in three different regions (MS, MPOA, and LH) (Figures 2A–C). Quantitative immunohistochemical analysis revealed that the number of GnRH neurons was not altered in PACAP KO female mice compared to that in WT littermates in any of the examined brain areas (Figures 3A–C). In addition, we examined GnRH-ir in different brain areas (MS, MPOA, LH, OVLT, and EM) (Figures 2A–D) to assess the effect of PACAP deletion on the arborization of GnRH neurons. Our data showed no change in GnRH-ir levels in the PACAP KO mice (Figures 4A–E).

3.3 Effect of PACAP deletion on the number of kisspeptin neurons

Because of the lack of specific antibodies against kisspeptin protein, the number of kisspeptin neurons was evaluated in RP3V (Figure 5) and ARC regions (Figure 6) of PACAP KO female and WT mice using RNAscope *in situ* hybridization. Figure 7A shows that PACAP deletion had no effect on the number of *Kiss1* mRNA-positive cells in the RP3V region, which is mainly responsible for the initiation of the preovulatory LH surge in female mice (WT: 53.21 ± 10.59, KO: 52.75 ± 13.47; $p = 0.949$). On the other hand, the number of *Kiss1* mRNA-positive cells in the ARC, which plays a pivotal role in GnRH pulse generation, was significantly decreased in (WT 45.04 ± 9.75, KO: 28.92 ± 8.22, $p < 0.0113$, Figure 7B).

3.4 Effect of PACAP deletion on ERα expression

Esr1 expression in the RP3V and ARC regions was examined at the mRNA level using RNAscope *in situ* hybridization (Figures 5, 6). ERα protein expression was detected by immunohistochemistry (Figure 8). Using the RNAscope *in situ* hybridization assay, we calculated the percentage of *Esr1* mRNA-positive areas in RP3V and ARC. The analysis revealed

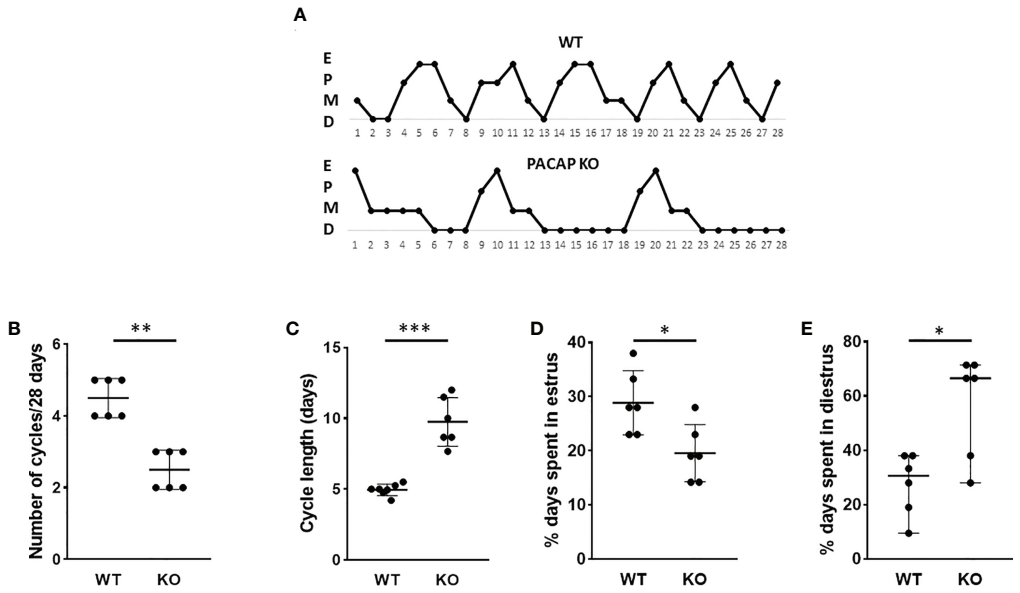

FIGURE 1
Disrupted estrous cyclicity in PACAP KO mice. Representative estrous cycle diagrams illustrate the alterations in estrous cycle in WT and PACAP KO mice **(A)**. Dot plots depict the number of estrous cycles in 4 weeks **(B)**, the cycle length **(C)**, and the percentage of time spent in estrus **(D)** and diestrus **(E)**. Graphs show the mean ± SD for panels **(C, D)** and the median ± range for panels **(B, E)** n = 6–6, *p < 0.05, **p < 0.01, ***p < 0.001.

that *Esr1* mRNA expression in the RP3V was elevated in PACAP KO female mice when compared with WT mice (WT: 4.06% ± 1.51, KO: 6.97% ± 2.60; p= 0.0391, Figure 9A). However, we found no change in the number of ERα-immunoreactive cells in WT and KO females in the RP3V (WT: 107.90 ± 40.17, KO: 119.60 ± 46.25; p = 0.2403, Figure 9B). In contrast to RP3V, *Esr1* mRNA expression showed no significant decrease in the ARC of PACAP-deficient mice (WT: 4.205% ± 1.98, KO: 3.07% ± 1.65, p = 0.3068, Figure 9C). However, the number of ERα-immunoreactive cells significantly decreased in the ARC of mutant female mice compared to their WT littermates (WT: 69.28 ± 5.89, KO: 37.29 ± 14.63; p = 0.053, Figure 9D). In addition, all kisspeptin neurons were *Esr1* mRNA-positive in RP3V and ARC in both groups. This finding is in accordance with previously published data (2).

4 Discussion

Although impaired reproductive functions are well documented in PACAP KO female mice (20–22), the underlying mechanisms and site(s) of action of PACAP remain unclear. Several features of reproduction have been reported to be altered in PACAP-null female mice, including decreased fertility, delayed puberty onset, reduced mating frequency, and impaired embryo implantation (20, 22–24). The regularity of the estrous cycle has also been examined in PACAP KO mice; however, the results have been contradictory. One study using PACAP KO mice found that female mice exhibited a normal estrous cycle (22), while Ross et al. demonstrated that targeted deletion of PACAP from the ventral premammillary nucleus (PMV) of the hypothalamus caused estrous cycle irregularity: increased cycle length and a resulting reduction in the number of cycles (24). Our findings confirmed the results of the latter study. In our study, we showed that estrous cyclicity was altered in whole-body PACAP KO female mice. Deletion of PACAP results in increased cycle length, decreased number of cycles, shorter estrus, and a longer diestrus phase. Our findings indicate that disturbance of the estrous cycle may contribute to reproductive defects observed in PACAP KO female mice.

The role of PACAP in the regulation of the estrous cycle is indicated by the discovery that PACAP mRNA expression in the hypothalamic paraventricular nucleus (PVN) exhibits cyclic fluctuations, with a peak 3 h before the time of GnRH and the subsequent LH surge (25). In addition, intracerebroventricular (i.c.v.) administration of PACAP-38 has been demonstrated to induce GnRH gene expression (16) and inhibit ovulation when applied just before the critical period of the proestrus phase (26, 27). These studies also suggest that PACAP plays a critical role in

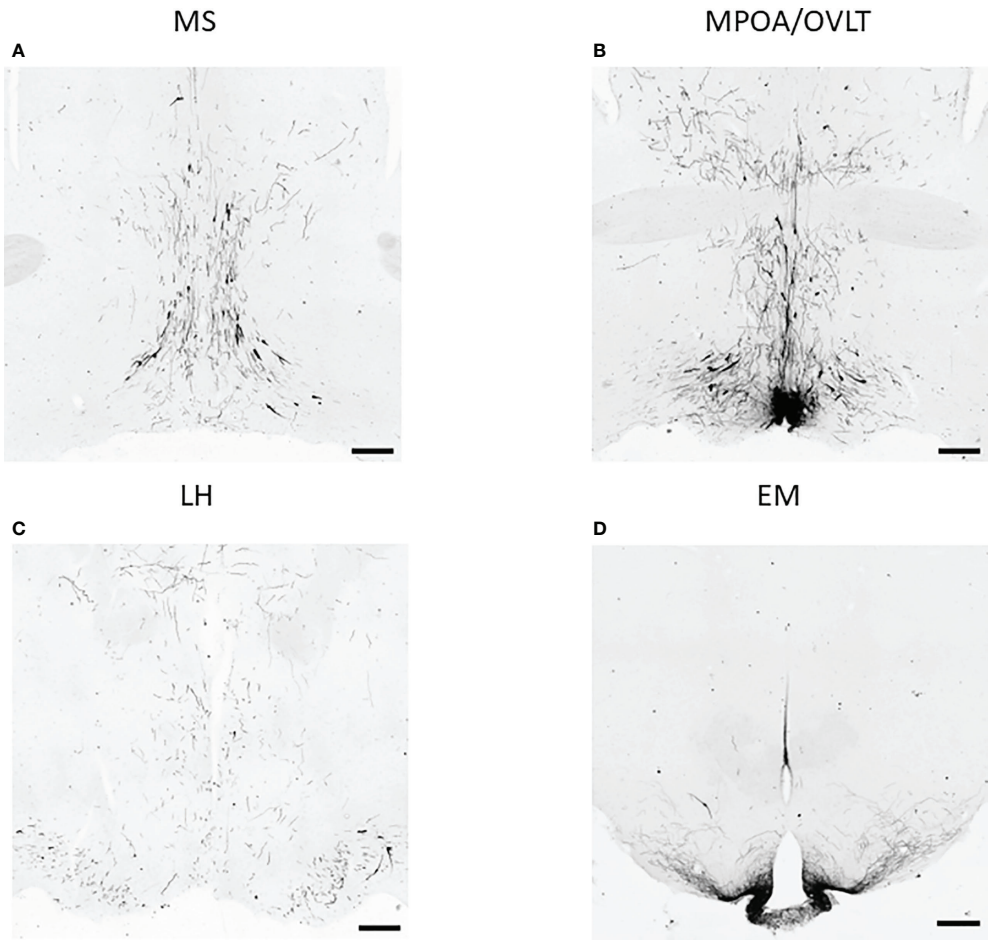

FIGURE 2
GnRH neurons and their arborization in different brain regions. Representative images of immunohistochemical labeling of GnRH neurons and their fibers located in the medial septum (MS), medial preoptic area (MPOA) together with organum vasculosum of lamina terminalis (OVLT), lateral hypothalamus (LH), and eminentia mediana (EM) are shown in panels **(A–D)** respectively (scale bar: 200 μm).

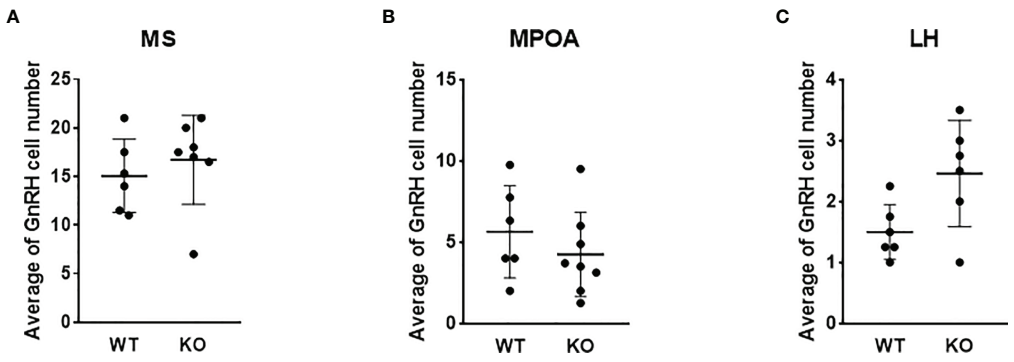

FIGURE 3
Number of GnRH neurons in wild-type and PACAP KO female mice. Summarized data of the number of GnRH neurons in regions of medial septum (MS), medial preoptic area (MPOA), and lateral hypothalamus (LH) from WT and PACAP KO mice are presented in panels **(A–C)** respectively. Experiments were performed in female mice in estrus phase. Data are presented as mean ± SD, n = 6–8.

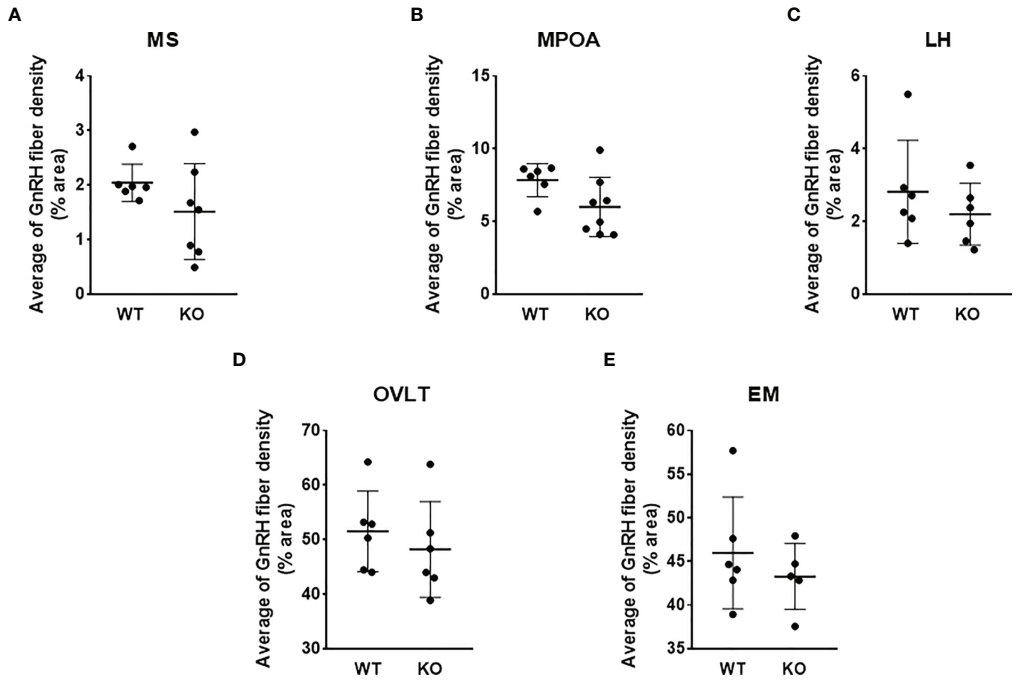

FIGURE 4
GnRH-ir in wild-type and PACAP KO female mice. GnRH-ir data in regions of medial septum (MS), medial preoptic area (MPOA), lateral hypothalamus (LH), organum vasculosum of lamina terminalis (OVLT), and eminentia mediana (EM) obtained from WT and PACAP KO mice are presented in panels **A–E**, respectively. Experiments were performed in female mice in estrus phase. Data are presented as mean ± SD, *n* = 6–8.

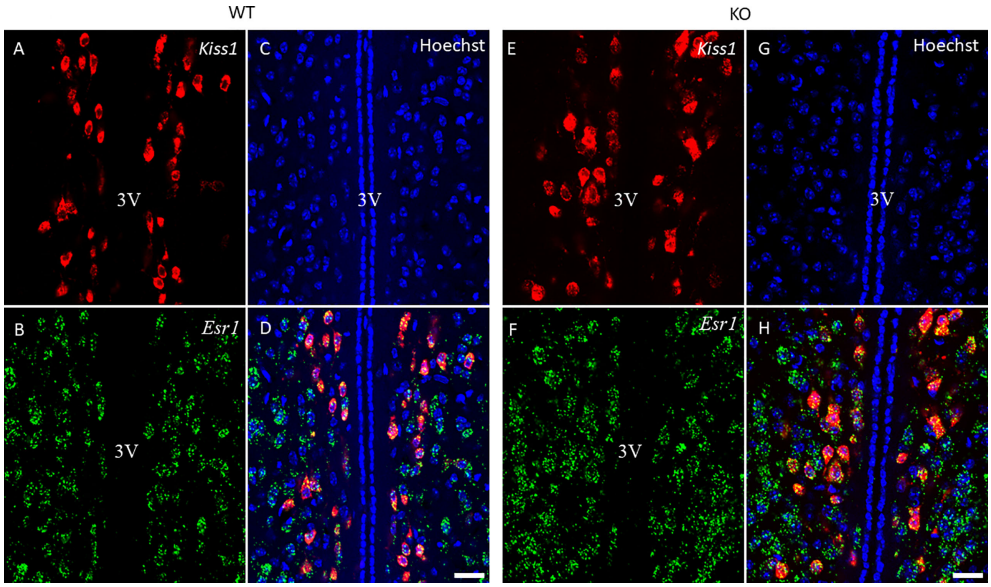

FIGURE 5
Kiss1 and *Esr1* mRNA expression in the RP3V of wild-type and PACAP KO female mice. Representative confocal fluorescence images depict the expression of *Kiss1* mRNA in the RP3V region (panels **A, E**) and *Esr1* mRNA-positive cells in the RP3V (panels **B, F**) of WT and PACAP KO mice. Nuclear counterstain with Hoechst33342 is presented in panels **(C, G)** while the merged image is shown in panels **D, H**. 3V, third ventricle. Images were taken with a 20× plan apochromat objective (scale bar: 100 μm).

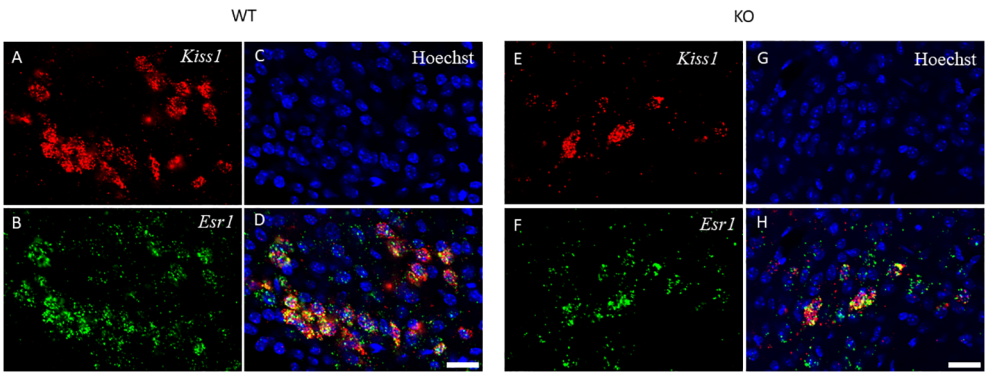

FIGURE 6
Kiss1 and *Esr1* mRNA expression in the ARC of wild-type and PACAP KO female mice. The expression of *Kiss1* (panels **A, E**) and *Esr1* (panels **B, F**) mRNAs in the ARC of WT and PACAP KO mice is depicted in representative confocal images. Nuclear counterstain with Hoechst33342 and the merged image are presented in panels **C, G** and **D, H** respectively. 20× magnification, scale bar: 25 µm.

regulating fertility. However, the central mechanism and site of action of PACAP have not been entirely revealed. There are hardly any data on how the key regulator of reproduction, namely, the kisspeptin–GnRH system, is coordinated by PACAP. Therefore, we first investigated the organization of GnRH neurons in the PACAP-KO female mice. We detected no significant difference in GnRH-ir and the number of GnRH neurons when we compared PACAP KO female mice with their wild-type littermates. Although we could not demonstrate any effect of PACAP deletion on these two parameters of GnRH organization, other characteristics such as synaptic density or targets of their projections could not be excluded. Although some reports suggest that there might be a direct effect of PACAP on GnRH neuronal activity, there is no clear-cut evidence to date that supports this theory. Nevertheless, it has recently been shown that the main upstream regulator of the GnRH neuronal network, the kisspeptin system, is influenced by PACAP. A subset of kisspeptin neurons located in the RP3V and

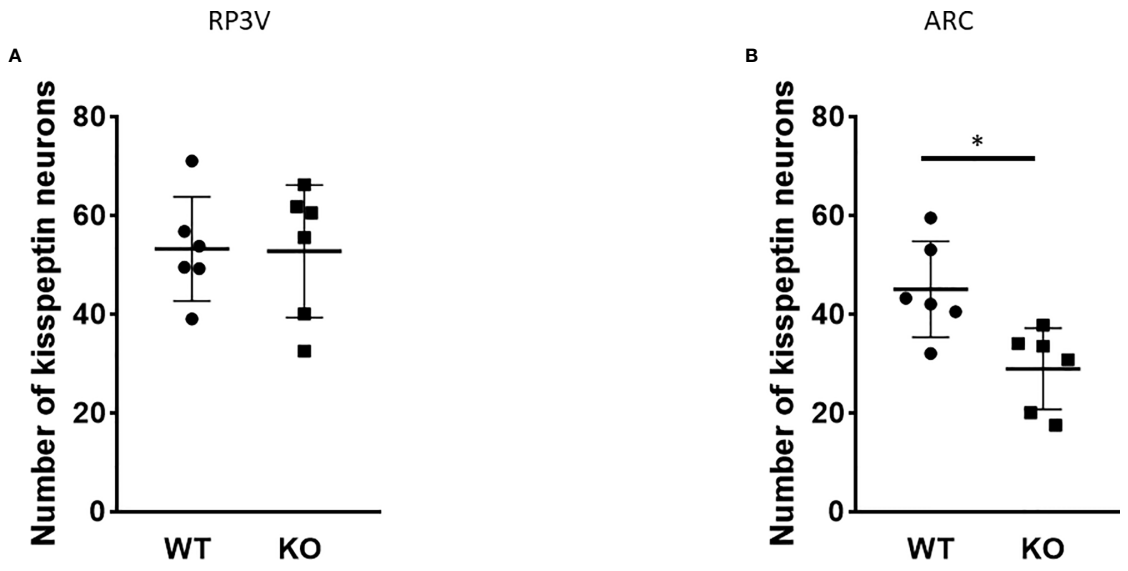

FIGURE 7
Number of *Kiss1* mRNA-positive neurons in the RP3V and ARC in wild-type and PACAP KO female mice. Summarized data of RNAscope *in situ* hybridization experiments are shown in dot plots. The number of *Kiss1* mRNA-positive cells is shown in RP3V **(A)** and ARC **(B)** from wild-type and PACAP KO female mice (two slices per animal, six animals in both groups). Data are presented as mean ± SD, $*p < 0.05$.

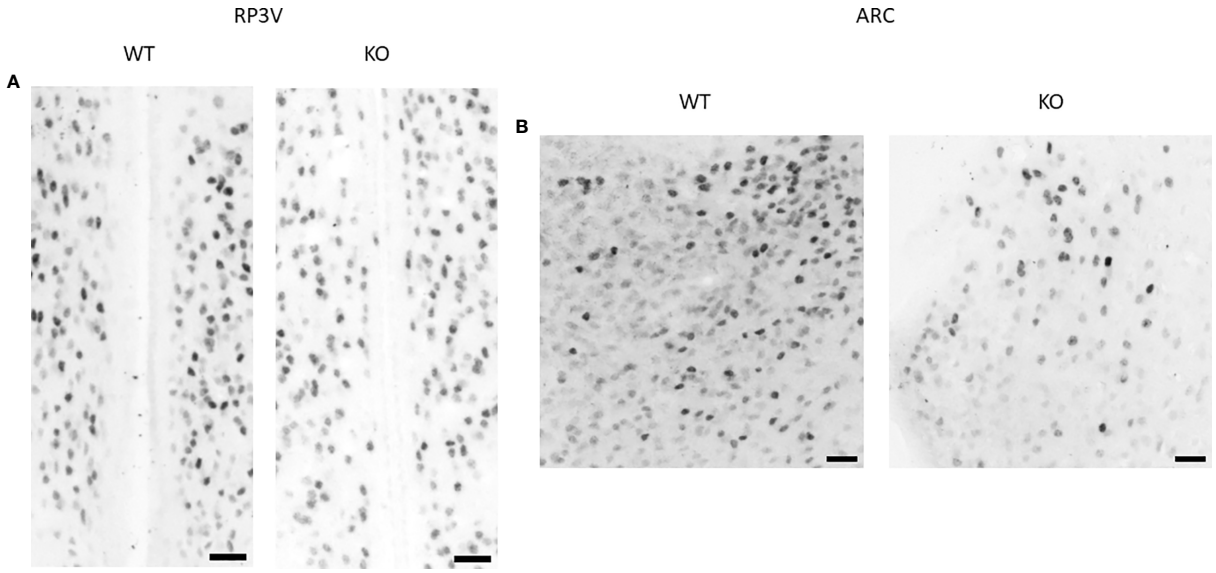

FIGURE 8
ERα protein expression in the RP3V and ARC in wild-type and PACAP KO female mice. Representative brightfield images show the expression of ERα protein in the RP3V **(A)** and ARC **(B)** of a WT and a PACAP KO female mouse. 20× magnification, scale bar: 25 μm.

ARC receives direct input from PACAP-expressing neurons residing in the ventral premammillary nucleus (24) and are involved in both pulsatile and surge-like release of GnRH. Therefore, we also examined the *Kiss1* mRNA expression levels in the RP3V and ARC and found that the number of *Kiss1* mRNA-positive cells decreased in the ARC, but not in the RP3V, of PACAP mutant female mice compared to their wild-type littermates. As kisspeptin neurons found in the ARC play a role in the regulation of pulsatile GnRH release, the decreased number of *Kiss1* mRNA-positive cells in the ARC can lead to the observed estrous cycle irregularity in PACAP KO female mice. PACAP has been shown to induce *Kiss1* expression in an immortalized neuronal cell line obtained from the ARC (28). This is in accordance with our data, because we found that PACAP deletion has the opposite effect, causing a decrease in the number of kisspeptin neurons in the ARC. Furthermore, our data indicate that PACAP deletion has a region-specific effect on kisspeptin neurons, as the number of kisspeptin-immunoreactive cells was not altered in RP3V.

Because ERα plays an important role in transmitting the stimulatory and inhibitory effects of circulating estradiol on GnRH neurons that drive the estrous cycle (5, 29–32), the number of ERα-immunoreactive cells is a good indicator of hypothalamic sensitivity to E2. In addition, as GnRH neurons do not express ERα (33), estradiol feedback is presumably conveyed to GnRH neurons *via* the afferents of ERα-expressing cells.

Therefore, we investigated whether the number of ERα-immunoreactive cells changed in the RP3V and ARC regions of PACAP KO female mice. We detected a decrease in the number of ERα-immunoreactive cells in the ARC of the PACAP KO female mice. In R3PV cells, an increase in ERα expression was observed only at the mRNA level. In the ARC, ERα is abundantly expressed and crucial for maintaining the regular estrous cycle (8, 34). We assumed that the decrease in ERα expression in the ARC may further explain the changes observed in the estrous cycle of PACAP KO mice. This assumption is supported by experiments showing that selective knockdown of ERα in arcuate kisspeptin neurons leads to disrupted cyclicity (35). Although we could not detect a change in the percentage of *Esr1* mRNA expressing kisspeptin neurons in PACAP-deficient mice in the ARC, the reduced number of kisspeptin neurons itself can result in decreased sensitivity to estradiol since all kisspeptin neurons express *Esr1* mRNA [(2), own observation as well]. As kisspeptin neurons and other cell types expressing ERα also send afferents to GnRH neurons, we cannot exclude the possibility that decreased ERα expression in other cell types can also contribute to the estrous cycle irregularity found in PACAP KO mice.

Our finding that the expression of Esr1 mRNA transcripts was increased in the RP3V of PACAP-deficient female mice was not confirmed by immunohistochemistry. Nevertheless, the possibility that PACAP can contribute to the control of LH

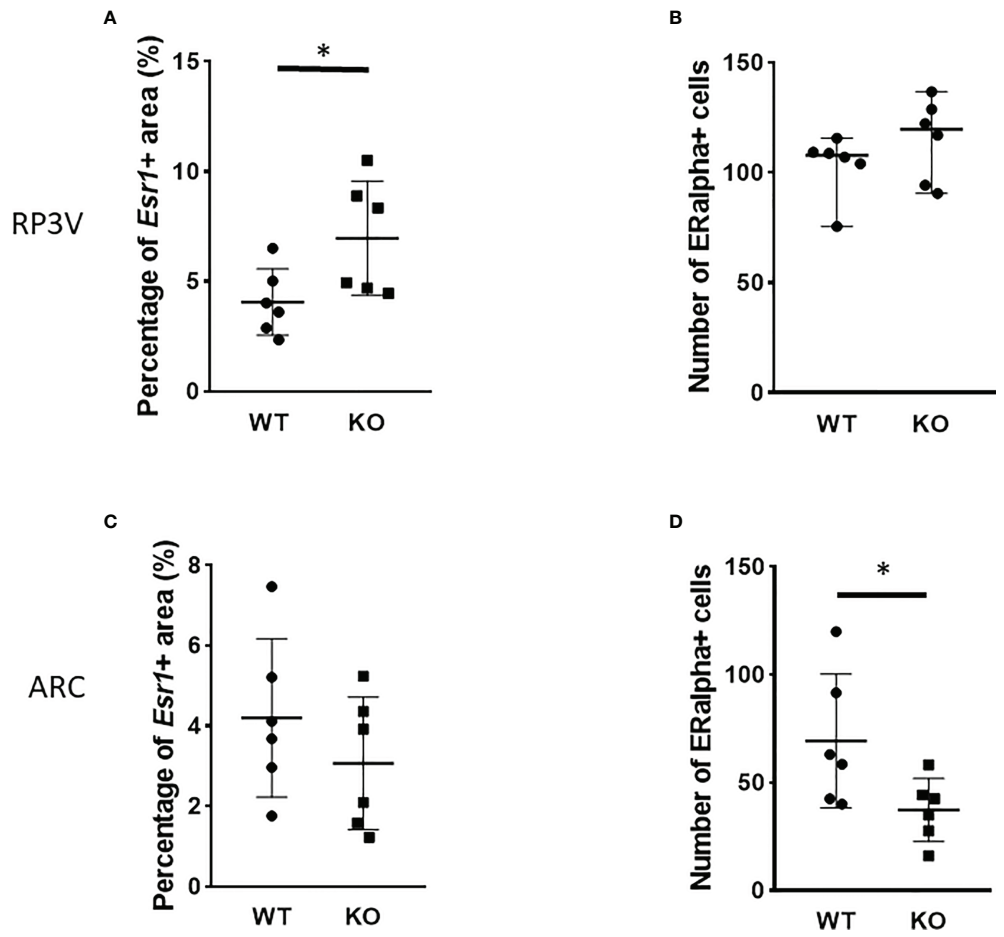

FIGURE 9
Number of ERα-immunoreactive cells in the RP3V and ARC in wild-type and PACAP KO female mice. Dot plots present the summarized data obtained by RNAscope *in situ* hybridization experiments showing *Esr1* mRNA expression in RP3V **(A)** and ARC regions **(C)**. Immunohistochemical staining demonstrating ERα protein expression in RP3V **(B)** and ARC regions **(D)**. n = 6–6 animals for each group with two slices per animal. Graphs show the mean ± SD for all panels, *$p < 0.05$.

surge by modulating the expression of other estrogen receptors in RP3V cannot be excluded.

In summary, we suggest that whole-body PACAP deletion causes irregular estrous cycles in mice. Our data suggest that the underlying mechanisms may include impaired central regulation of GnRH pulsatility due to reduced kisspeptin and ERα expression in the ARC. Further studies are required to determine whether the peripheral or central deletion of PACAP is responsible for the observed disruption of reproductive function in females.

Data availability statement

The original contributions presented in the study are included in the article. Further inquiries can be directed to the corresponding authors.

Ethics statement

All procedures were performed in accordance with the ethical guidelines approved by the University of Pécs (permission number: BA02/2000-24/2011).

Author contributions

KB: Conceptualization, Immunohistochemistry, Bright-field imaging, Image analysis, Writing, Supervision, GK: Conceptualization, Bright-field imaging, Confocal imaging, Image analysis, Statistical analysis, Supervision, VV: Estrous cycle evaluation, Immunohistochemistry, EK: Bright-field imaging, Image analysis, PF: RNAscope *in situ* hybridization, Bright-field imaging, Confocal imaging, IU: Perfusion,

Sectioning, Immunohistochemistry, RNAscope *in situ* hybridization, DP: Genotyping, Estrous cycle evaluation, DR: Conceptualization, Funding acquisition, Writing - Review and Editing, IÁ: Conceptualization, Funding acquisition, ZN: Conceptualization, Writing - Review and Editing. All authors contributed to the article and approved the submitted version.

Funding

This work was supported by the project TKP2021-EGA-16 that has been implemented with the support provided from the National Research, Development and Innovation Fund of Hungary, financed under the TKP2021-EGA funding scheme, the Hungarian Scientific Research Fund (NKFIH; 112807 and K135457), the Hungarian Brain Research Program (KTIA_NAP_13-2014-0001, 20017-1.2.1-NKP-2017-00002), MTA-TKI-14016 and the European Union and was co-financed by the European Social Fund under the following grants: EFOP-3.6.1.-16-2016-00004 (Comprehensive Development for Implementing Smart Specialization Strategies at the University of Pécs), EFOP 3.6.2-16-2017-00008 (The Role of Neuro-inflammation in Neurodegeneration: From Molecules to Clinics).

Acknowledgments

The research was performed in collaboration with the Nano-Bio-Imaging Core Facility at the Szentágothai Research Centre of the University of Pécs.

Conflict of interest

The authors declare that the research was conducted in the absence of any commercial or financial relationships that could be construed as a potential conflict of interest.

Publisher's note

References

1. Herbison AE. Control of puberty onset and fertility by gonadotropin-releasing hormone neurons. *Nat Rev Endocrinol* (2016) 12:452–66. doi: 10.1038/nrendo.2016.70

2. Smith JT, Cunningham MJ, Rissman EF, Clifton DK, Steiner RA. Regulation of Kiss1 gene expression in the brain of the female mouse. *Endocrinology* (2005) 146:3686–92. doi: 10.1210/en.2005-0488

3. Herbison AE. Estrogen positive feedback to gonadotropin-releasing hormone (GnRH) neurons in the rodent: The case for the rostral periventricular area of the third ventricle (RP3V). *Brain Res Rev* (2008) 57:277–87. doi: 10.1016/j.brainresrev.2007.05.006

4. Moenter SM, Chu Z, Christian CA. Neurobiological mechanisms underlying oestradiol negative and positive feedback regulation of gonadotrophin-releasing hormone neurones. *J Neuroendocrinol* (2009) 21:327–33. doi: 10.1111/j.1365-2826.2009.01826.x

5. Cheong RY, Czieselsky K, Porteous R, Herbison AE. Expression of ESR1 in glutamatergic and GABAergic neurons is essential for normal puberty onset, estrogen feedback, and fertility in female mice. *J Neurosci* (2015) 35:14533–43. doi: 10.1523/JNEUROSCI.1776-15.2015

6. Prashar V, Arora T, Singh R, Sharma A, Parkash J. Hypothalamic kisspeptin Neurons : Integral elements of the GnRH system. *Reprod Sci* (2022). doi: 10.1007/s43032-022-01027-5

7. Yip SH, Boehm U, Herbison AE, Campbell RE. Conditional viral tract tracing delineates the projections of the distinct kisspeptin neuron populations to gonadotropin-releasing hormone (GnRH) neurons in the mouse. *Endocrinol (United States)* (2015) 156:2582–94. doi: 10.1210/en.2015-1131

8. Uenoyama Y, Inoue N, Nakamura S, Tsukamura H. Kisspeptin neurons and estrogen–estrogen receptor α signaling: Unraveling the mystery of steroid feedback system regulating mammalian reproduction. *Int J Mol Sci* (2021) 22(17):9229. doi: 10.3390/ijms22179229

9. Reglodi D, Tamas A, Koppan M, Szogyi D, Welke L. Role of PACAP in female fertility and reproduction at gonadal level - recent advances. *Front Endocrinol (Lausanne)* (2012) 3:155. doi: 10.3389/fendo.2012.00155

10. Winters SJ, Moore JP. PACAP: A regulator of mammalian reproductive function. *Mol Cell Endocrinol* (2020) 518:110912. doi: 10.1016/j.mce.2020.110912

11. Köves K, Szabó E, Kántor O, Heinzlmann A, Szabó F, Csáki Á. Current state of understanding of the role of PACAP in the hypothalamo-hypophyseal gonadotropin functions of mammals. *Front Endocrinol (Lausanne)* (2020) 11:88. doi: 10.3389/fendo.2020.00088

12. Ha CM, Kang JH, Choi EJ, Kim MS, Park J-W, Kim Y, et al. Progesterone increases mRNA levels of pituitary adenylate cyclase-activating polypeptide (PACAP) and type I PACAP receptor (PAC1) in the rat hypothalamus. *Mol Brain Res* (2000) 78:59–68. doi: 10.1016/S0169-328X(00)00070-X

13. Nemeth J, Tamas A, Jozsa R, Horvath JE, Jakab B, Lengvari I, et al. Changes in PACAP levels in the central nervous system after ovariectomy and castration. *Ann N Y Acad Sci* (2006) 1070:468–73. doi: 10.1196/annals.1317.063

14. Oride A, Kanasaki H, Kyo S. Role of pituitary adenylate cyclase-activating polypeptide in modulating hypothalamic-pituitary system. *Reprod Med Biol* (2018) 17:234–41. doi: 10.1002/rmb2.12094

15. Jamen F, Rodriguez-Henche N, Pralong F, Jegou B, Gaillard R, Bockaert J, et al. PAC1 null females display decreased fertility. *Ann N Y Acad Sci* (2000) 921:400–4. doi: 10.1111/j.1749-6632.2000.tb07004.x

16. Li S, Grinevich V, Fournier A, Pelletier G. Effects of pituitary adenylate cyclase-activating polypeptide (PACAP) on gonadotropin-releasing hormone and somatostatin gene expression in the rat brain. *Mol Brain Res* (1996) 41:157–62. doi: 10.1016/0169-328X(96)00086-1

17. Hitoshi H, Norihito S, Kazuhiro T, Wakaba M, Megumi H, Toshio M, et al. Altered psychomotor behaviors in mice lacking pituitary adenylate cyclase-activating polypeptide (PACAP). *Proc Natl Acad Sci* (2001) 98:13355–60. doi: 10.1073/pnas.231094498

18. Caligioni CS. Assessing reproductive Status/Stages in mice. *Curr Protoc Neurosci* (2009) 48:A.4I.1–8. doi: 10.1002/0471142301.nsa04is48

19. Paxinos G, Franklin KBJ. *The mouse brain in stereotaxic coordinates. 2nd editio*. San Diego: Academic Press (2001).

20. Shintani N, Mori W, Hashimoto H, Imai M, Tanaka K, Tomimoto S, et al. Defects in reproductive functions in PACAP-deficient female mice. *Regul Pept* (2002) 109:45–8. doi: 10.1016/S0167-0115(02)00169-6

21. Sherwood NM, Adams BA, Isaac ER, Wu S, Fradinger EA. Knocked down and out: PACAP in development, reproduction and feeding. *Peptides* (2007) 28:1680–7. doi: 10.1016/j.peptides.2007.03.008

22. Isaac ER, Sherwood NM. Pituitary adenylate cyclase-activating polypeptide (PACAP) is important for embryo implantation in mice. *Mol Cell Endocrinol* (2008) 280:13–9. doi: 10.1016/j.mce.2007.09.003

23. Szabó F, Horváth J, Heinzlmann A, Arimura A, Köves K. Neonatal PACAP administration in rats delays puberty through the influence of the LHRH neuronal system. *Regul Pept* (2002) 109:49–55. doi: 10.1016/S0167-0115(02)00185-4

24. Ross RA, Leon S, Madara JC, Schafer D, Fergani C, Maguire CA, et al. PACAP neurons in the ventral premammillary nucleus regulate reproductive function in the female mouse. *Elife* (2018) 7:e35960. doi: 10.7554/eLife.35960

25. Moore JPJr., Burger LL, Dalkin AC, Winters SJ. Pituitary adenylate cyclase activating polypeptide messenger RNA in the paraventricular nucleus and anterior pituitary during the rat estrous Cycle1. *Biol Reprod* (2005) 73:491–9. doi: 10.1095/biolreprod.105.041624

26. Köves K, Molnár J, Kántor O, Görcs TJ, Lakatos A, Arimura A. New aspects of the neuroendocrine role of PACAPa. *Ann N Y Acad Sci* (1996) 805:648–54. doi: 10.1111/j.1749-6632.1996.tb17535.x

27. Heinzlmann A, Oláh M, Köves K. Intranasal application of PACAP and β-cyclodextrin before the "critical period of proestrous stage" can block ovulation. *Biol Futur* (2019) 70:62–70. doi: 10.1556/019.70.2019.08

28. Tumurbaatar T, Kanasaki H, Oride A, Okada H, Hara T, Tumurgan Z, et al. Effect of pituitary adenylate cyclase-activating polypeptide (PACAP) in the regulation of hypothalamic kisspeptin expression. *Gen Comp Endocrinol* (2019) 270:60–6. doi: 10.1016/j.ygcen.2018.10.006

29. Moenter SM, Caraty A, Karsch FJ. The estradiol-induced surge of gonadotropin-releasing hormone in the ewe*. *Endocrinology* (1990) 127:1375–84. doi: 10.1210/endo-127-3-1375

30. Wintermantel TM, Campbell RE, Porteous R, Bock D, Gröne HJ, Todman MG, et al. Definition of estrogen receptor pathway critical for estrogen positive feedback to gonadotropin-releasing hormone neurons and fertility. *Neuron* (2006) 52:271–80. doi: 10.1016/j.neuron.2006.07.023

31. Christian CA, Glidewell-Kenney C, Jameson JL, Moenter SM. Classical estrogen receptor α signaling mediates negative and positive feedback on gonadotropin-releasing hormone neuron firing. *Endocrinology* (2008) 149:5328–34. doi: 10.1210/en.2008-0520

32. Radovick S, Levine JE, Wolfe A. Estrogenic regulation of the GnRH neuron. *Front Endocrinol (Lausanne)* (2012) 3:52. doi: 10.3389/fendo.2012.00052

33. Hrabovszky E, Steinhauser A, Barabaís K, Shughrue PJ, Petersen SL, Merchenthaler I, et al. Estrogen receptor-β immunoreactivity in luteinizing hormone-releasing hormone neurons of the rat brain. *Endocrinology* (2001) 142:3261–4. doi: 10.1210/endo.142.7.8176

34. Yang JA, Mamounis KJ, Yasrebi A, Roepke TA. Regulation of gene expression by 17β-estradiol in the arcuate nucleus of the mouse through ERE-dependent and ERE-independent mechanisms. *Steroids* (2016) 107:128–38. doi: 10.1016/j.steroids.2016.01.003

35. Wang L, Vanacker C, Burger LL, Barnes T, Shah YM, Myers MG, et al. Genetic dissection of the different roles of hypothalamic kisspeptin neurons in regulating female reproduction. *Elife* (2019) 8:e43999. doi: 10.7554/eLife.43999

frontiers | Frontiers in Endocrinology

TYPE Original Research
PUBLISHED 27 October 2022
DOI 10.3389/fendo.2022.974788

OPEN ACCESS

EDITED BY
Kok-Min Seow,
Shin Kong Wu Ho-Su Memorial Hospital, Taiwan

REVIEWED BY
Marcelo Steiner,
Faculdade de Medicina do ABC, Brazil
Anna Piotrowska,
University School of Physical Education in Krakow, Poland

*CORRESPONDENCE
Dóra Zelena
dora.zelena@aok.pte.hu

SPECIALTY SECTION
This article was submitted to Reproduction, a section of the journal Frontiers in Endocrinology

RECEIVED 21 June 2022
ACCEPTED 10 October 2022
PUBLISHED 27 October 2022

CITATION
Barabás K, Makkai B, Farkas N, Horváth HR, Nagy Z, Váradi K and Zelena D (2022) Influence of COVID-19 pandemic and vaccination on the menstrual cycle: A retrospective study in Hungary. *Front. Endocrinol.* 13:974788. doi: 10.3389/fendo.2022.974788

Influence of COVID-19 pandemic and vaccination on the menstrual cycle: A retrospective study in Hungary

Klaudia Barabás[1,2], Bernadett Makkai[1], Nelli Farkas[3], Hanga Réka Horváth[1], Zsuzsanna Nagy[1], Kata Váradi[1,2] and Dóra Zelena[1,2]*

[1]Institute of Physiology, Medical School, University of Pécs, Pécs, Hungary, [2]Centre for Neuroscience, Szentágothai Research Centre, Pécs, Hungary, [3]Institute of Bioanalysis, Medical School, University of Pécs, Pécs, Hungary

Observations of women and clinicians indicated that the prevalence of menstrual cycle problems has escalated during the COVID-19 pandemic. However, it was not clear whether the observed menstrual cycle changes were related to vaccination, the disease itself or the COVID-19 pandemic-induced psychological alterations. To systematically analyze this question, we conducted a human online survey in women aged between 18 and 65 in Hungary. The menstrual cycle of 1563 individuals were analyzed in our study in relation to the COVID-19 vaccination, the COVID-19 infection, the pandemic itself and the mental health. We found no association between the COVID-19 vaccination, the vaccine types or the COVID-19 infection and the menstrual cycle changes. We also evaluated the menstrual cycle alterations focusing on three parameters of the menstrual cycle including the cycle length, the menses length and the cycle regularity in three pandemic phases: the pre-peak, the peak and the post-peak period in Hungary. Our finding was that the length of the menstrual cycle did not change in any of the periods. However, the menses length increased, while the regularity of the menstrual cycle decreased significantly during the peak of the COVID-19 pandemic when comparing to the pre- and post-peak periods. In addition, we exhibited that the length and the regularity of the menstrual cycle both correlated with the severity of depression during the post-peak period, therefore we concluded that the reported menstrual cycle abnormalities during the peak of COVID-19 in Hungary might be the result of elevated depressive symptoms.

KEYWORDS

COVID-19 vaccines, SARS-Cov-2 infection, COVID-19 pandemic, menstrual cycle, depression, human surveys

1 Introduction

Observations of women and clinicians implied that the incidence of menstrual cycle problems has increased during the COVID-19 pandemic. Concerns have been raised in the social media that COVID-19 vaccination may affect the menstrual cycle thereby causing infertility, which increased vaccine hesitancy. Many vaccine sceptics are reluctant to be vaccinated due to the fear from possible side effects of COVID-19 vaccines, hence it is crucial to understand the effects of vaccines – among others – on reproductive health. Since the mRNA vaccine technology is a revolutionary innovation, the least data was accumulated regarding its side-effects (1). Therefore, the new-generation mRNA vaccines were of particular interest in our study. A few reports have already been published investigating the impact of the COVID-19 vaccines on the menstrual cycle (2–4), but systematic analysis was missing at the beginning of our study.

In addition to the COVID-19 vaccines, SARS-CoV-2 infection has also been reported to cause menstrual cycle changes (5).

On the other hand, the COVID-19 crisis has exceedingly increased emotional distress, anxiety, and depression (6–9). It is well known that cortisol, the main stress hormone, inhibits the secretion of gonadotropin releasing hormone that governs the menstrual cycle by its pulsatile release (10). Therefore, the psychological stress experienced during the pandemic such as grief, fear of the virus, social isolation etc., might have contributed to menstrual cycle irregularities. All in all, it was not clear which factor - if any - might be responsible for the menstrual cycle changes.

To examine this question, we conducted an online survey in Hungary to collect information about the menstrual cycle pattern, the received vaccinations, the recognized infection, and the psychological burden of women aged between 18 and 65 during the pandemic. Our study might provide further evidence on the reproductive health safety of COVID-19 vaccines and might help to build trust in vaccines.

2 Materials and methods

2.1 Participants and study design

We conducted a retrospective analysis focusing on individual's mental state and menstrual cycle data using quantitative empirical methodology during three stages of the pandemic. We constructed a survey for women which was distributed online in social media using a google form. Thus, our participants were from the entire territory of Hungary. The questionnaire was generated in Hungarian and translated to English so that foreigners living in Hungary could also fill it in. We included the data of foreigners in our study as well because it did not change the outcome of our study.

Women aged between 18 and 65 were recruited between 1 September 2021 and 31 December 2021 to fill out the questionnaire. We collected information of 2429 individuals regarding 3 periods: January 2019 - September 2020 (1); October 2019 – March 2021 (2) and April 2021 – December 2021 (3). The first interval (referred to later as pre-peak) included a pre-pandemic period, the first wave of COVID-19 pandemic in Hungary (04.03.2020 – 17.07.2020.) and a temporary relief period in the summer of 2020. The epidemic curve of the first wave in Hungary was flat with low detected cases reaching the plateau on 4 May with 2055 cases and was mainly localized to hospitals and retirement homes in the capital, Budapest. The second interval (referred to later as peak) examined in our survey was basically the time of the second wave in Hungary (18.07.2020 – 16.02.2021.). The detected cases started to increase in September 2020 with a plateau of 198 785 active cases in December. This was also the time when the Hungarian government applied increasingly strict restrictive measures. The third probed interval (relief, referred to later as post-peak period) in our study coincided with the third wave in Hungary (17.02.2021- 11.06.2021.) that was due to the spreading of the "British variant". In March 2021 further restrictions were introduced by the government to reduce the risk of catching and spreading of COVID-19. Kindergartens, primary schools, and stores not selling fundamental items were closed for more than a month. However, from 6 April 2021 everyday life started to return to normal as coronavirus-related restrictions were gradually eased when the number of vaccinated Hungarians reached 2.5 million (11).

The questionnaire (available in the Supplementary Materials) consisted of questions divided into 84 (C1-84) categories and 6 main categories (I-VI). Some categories were further divided into subcategories (a-c). The first two questions were related to the information sheet. The first category (18 questions) covered demographics and other general data: age, body height, body weight, education, place of residence, employment status, financial situation, coffee, and alcohol consumption, smoking and physical activity. The second section (26 questions) collected information on mental health. The third category contained questions (9) about medication and chronic diseases: thyroid dysfunction, diabetes, high prolactin levels, high blood pressure. The fourth category dealt with female hormone-related questions (12): the time of first menstruation and/or menopause, the number of births, breastfeeding, contraception, menstrual cycle length (i.e., same number of days between the first day of bleeding across consecutive periods) and regularity, menses length (number of days with bleeding within a period), measured hormone levels due to menstrual cycle disturbances (if applicable). The fifth section was about pandemic-related questions (9): previous COVID-19 infection and its severity, vaccination (number of

vaccinations, vaccine types) and menstrual abnormalities after vaccination. The last question allowed participants to comment on any of the topics we did not ask for. (The analysis of sociodemographic data is not discussed in this paper.) The ethical approval of the questionnaire has been accepted by the Ethics Committee in Hungary (Medical Research Council; IV/ 7146- 1 /2021/EKU).

2.2 Measures

2.2.1 Mental health test

The overall mental health of the participants was evaluated by a mental health test (MHT) (13), which is based on a short questionnaire. MHT measures global well-being, which is associated with emotional, psychological, social, and spiritual well-being, resilience, coping and savoring capacity, as well as competencies and personality factors that ensure the sustainability of mental health, continuous improvement, and flexibility to adapt to changing conditions. Therefore, a comprehensive picture of the subject's mental health was determined by measuring five parameters: well-being, savoring, creative-executive efficiency, self-regulation, and resilience. The questionnaire included 17 questions. Responses were given on a 6-point Likert-type scale. The endpoints of the response options were 1 = not at all typical and 6 = very typical.

2.2.2 Shortened Beck Depression Inventory

The presence and the severity of depression symptoms were assessed by a Hungarian version of the shortened Beck Depression Inventory (BDI). This short form of BDI is a 9-item, self-rated scale that measures characteristic symptoms of depression (14, 15). It evaluates social withdrawal, indecisiveness, insomnia, fatigability, somatic preoccupation, work difficulty, pessimism, self-dissatisfaction, and self-accusation. In case of each item a sentence was stated that presented the most severe response such as "I have lost all interest in others." The participants chose the answer on a 4-point scale ranging from 1 to 4 (not at all typical to very typical) that best described their behavior the month before completing the test. A total score of 0-9 was interpreted "normal", 10-18 as mild mood disturbance, 19-25 as moderate depression and 26-36 as severe depression.

2.3 Statistical analysis

The categorical variables of the questionnaire were characterized with percentage distribution. To determine the connection between the variables Chi-squared test was applied. The variable BDI was treated as a continuous and its relationship with the MHT variables was analyzed using Spearman rank correlation. Significance level was set at 0.05. All calculation were made with SPSS statistical software (IBM Corp. Released 2020. IBM SPSS Statistics for Windows, Version 27.0. Armonk, NY: IBM Corp).

3 Results

3.1 Anthropometric and other general parameters

The participants were informed that the survey was anonymous and completely voluntary. 97.6 % of the respondents were Hungarian citizens and 2.4 % were foreigners living in Hungary. After excluding breastfeeding mothers and women using hormonal contraceptive methods, the menstrual cycle changes of 1563 individuals were analyzed. We have categorized the participants into age groups. Based on the database of the Hungarian Central Statistical Office (HCSO) the reproductive age of women is between 15-49 years in Hungary. The lower limit of the first age group was set to 18 years in our study because women between the age of 15 and 18 considered minors in Hungary. Women of reproductive age were further divided into three groups based on the consensus that under 25 years of age, an individual can be considered as young adult, while women between 36-50 years are older adults (16). In addition, one more group was included in the study: women over the reproductive age represented by women between age of 51 and 65. All age groups were represented in the study: 34.3 % of participants was between the age of 18-25, 23 % between the age of 26-35, 35.1 % between 36-50 and 7.6 % between the age of 51-65 (Figure 1A). Only the age group of 51-65 was under-represented in the investigation compared to the other age groups in the study, but as members of this group are usually already in menopause, their data was not the most relevant for studying the menstrual cycle parameters by any means. The individuals living in cities, villages, county seats and the capital were also equally represented (Figure 1B). However, 82.5 % of the participants was college educated (BSc/MSc or PhD) or undergraduate students (BSc/MSc in progress) meaning that the number of highly qualified individuals were over-represented in the survey (Figure 1C).

3.2 Association between menstrual cycle changes and COVID-19 vaccination

The majority of the participants, 87.5 % received at least one vaccination at the time of the examination, while 12.5 % did not receive any vaccination (Figure 2A). 62.2 % of the vaccine recipients received mRNA-based vaccine (56.3 % Pfizer-BioNTech, 5.9 % Moderna), 23.8 % received adenovirus vaccine (10.2 % Astra Zeneca, 12.4 % Sputnik, 1.2 % Janssen) and 8.5 % received the traditional, inactivated virus vaccine (Sinopharm), while 5.3 % received more than one type of vaccines (Figure 2B). Of the 87.5 %

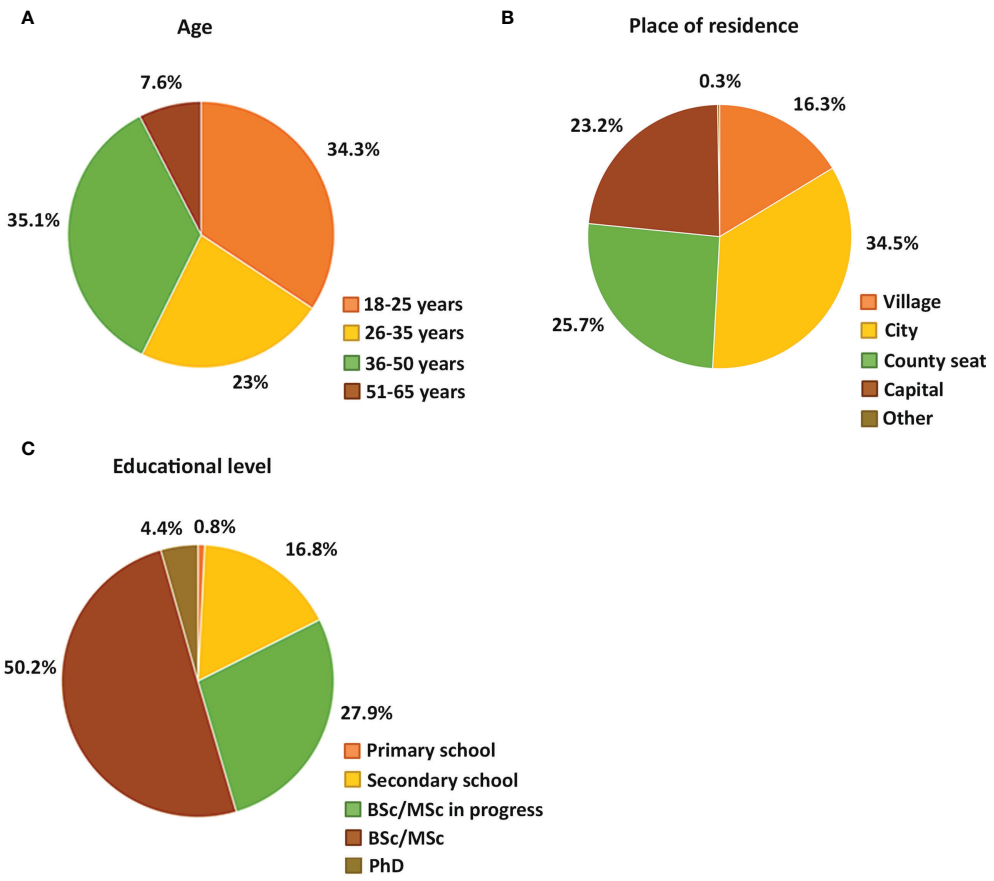

FIGURE 1
Pie charts show the percentage of different age groups **(A)**, different places of residence **(B)** and different educational background **(C)** of the female participants.

vaccinated individuals, 6.04 % was vaccinated once, 78.04 % was twice and 15.92 % was vaccinated three times.

Regarding the menstrual cycle changes, the menstrual cycle length, the menses length and the regularity of the menstrual cycle were taken into account. 40.4 % of vaccine recipients reported menstrual cycle disturbances after receiving COVID-19 vaccines (Figure 2C). Menstrual cycle disturbances were observed after the first and second vaccinations as well. 43.4 % of the participants receiving vaccine experienced menstrual problems after the first, while 41.3 % after the second shot of vaccine. 12.5 % reported menstrual cycle changes after both doses, 1.6 % encountered menstrual problems after the third vaccination only, and 1.2 % after different combinations of the vaccinations (after the first and third, after the second and third and after all vaccine shots) (Figure 2D).

Those who had menstrual problems post-vaccination, experienced various problems: both menstrual cycle length shortening (29.9 %) and prolongation (more than 7 days; 22.2 %) was reported. In addition, 13.9 % of female individuals had a missed period post-vaccination, while 7.8 % suffered from prolonged bleeding lasting for more than 2 weeks. The rest of the individuals (26.2 %) had other menstrual problems. The most frequently reported problems included the followings: irregular bleeding (12.2 %), heavier bleeding (4.3 %), strong menstrual cramps (2.8 %) and period reappearance (2 %).

Although a substantial number of vaccine recipients reported that they had experienced menstrual cycle disturbances after receiving vaccines, there was no association found between the vaccination and the menstrual cycle changes (pre-peak period: p=0.81; peak period: p=0.68; post-peak period: p=0.63) (data not shown).

Questions regarding menstruation have been ignored in most large-scale COVID-19 studies (including vaccine trials) (17), which was most critical in case of the newly introduced mRNA-based vaccines. Therefore, we also tested whether the type of vaccines (mRNA-based vaccine, adenovirus vaccine or the inactivated virus vaccine) influenced the occuring cycle changes differently but we did not find any change (pre-peak period: p=0.11; peak period: p=0.13; post-peak period: p=0.24) (Figure 2E).

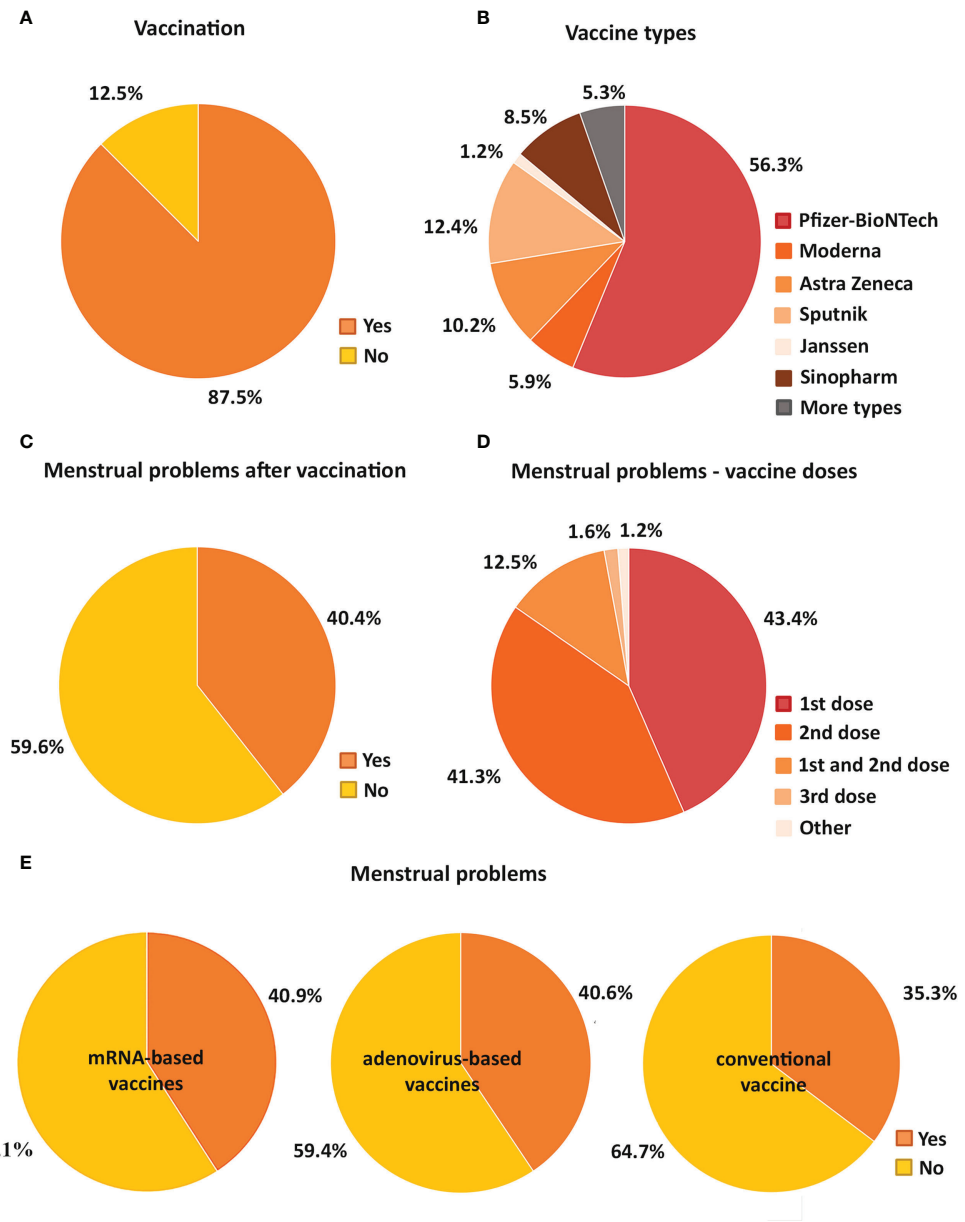

FIGURE 2
Pie charts demonstrate the percentage of vaccinated and unvaccinated individuals **(A)** and the proportion of the types of vaccines received in the vaccinated group **(B)**. The percentage of participants with and without menstrual cycle problems after vaccination is also shown **(C)**. It is also indicated how many doses of vaccine were given to those with menstrual cycle problems **(D)**. In addition, pie charts show how the proportion of individuals with menstrual problems and without menstrual problems varied for mRNA-based (Pfizer-BioNTech, Moderna), adenovirus-based (AstraZeneca, Sputnik, Janssen) and conventional vaccines (Sinopharm) **(E)**.

3.3 Association between menstrual cycle changes and SARS-CoV-2 infection: *Cross-sectional comparison*

Of those who surveyed, 73.4 % was unaware that they had SARS-CoV-2 infection, while 23.2 % was confirmed to have the infection (Figure 3A). Of those who reported to have SARS-CoV-2 infection, 3.4 % did not do a SARS-CoV-2 test but assumed they had the infection, 9.8 % were asymptomatic, 45 % had mild symptoms, 34.8 % had a moderate illness lasting for 7-14 days, 5.2 % had a severe illness lasting for more than two weeks and 1.8 % needed hospitalisation (Figure 3B).

We also compared the menstrual cycle changes of the group of women who had SARS-CoV-2 infection with the group who

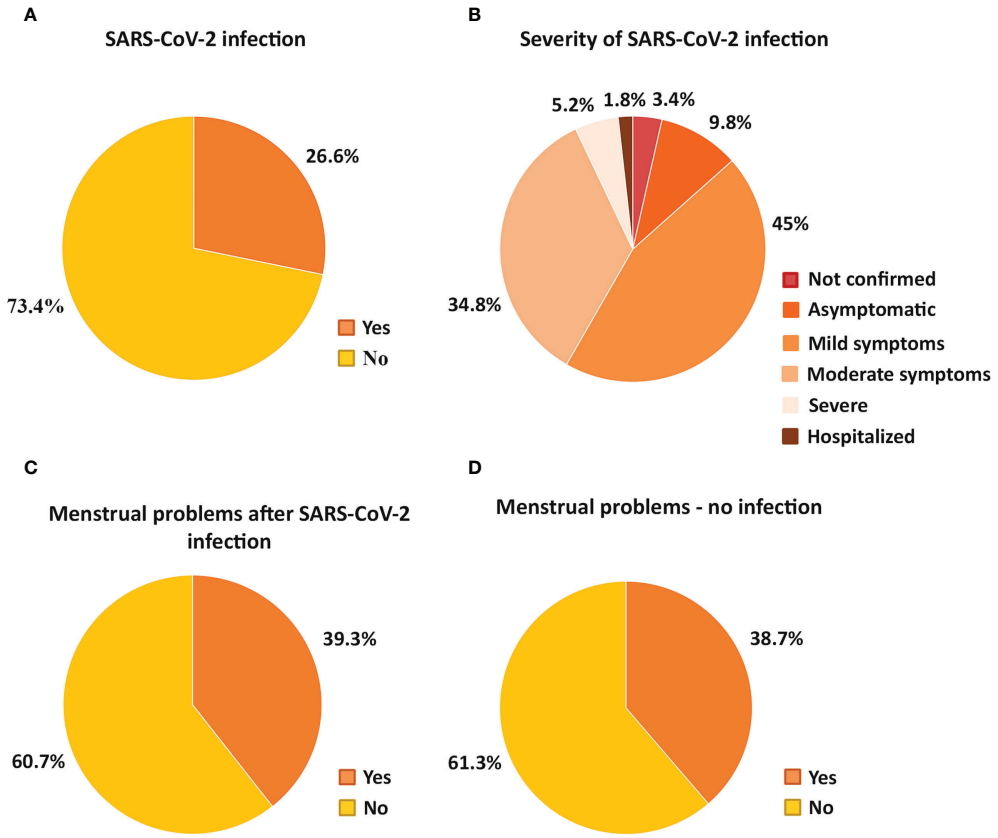

FIGURE 3
Pie charts show the percentage of participants who were or were not infected with SARS-CoV-2 **(A)**, detailing the proportion of infected individuals based on the severity of the infection **(B)**. The percentage of participants with and without menstrual cycle problems after SARS-CoV-2 infection **(C)** or no infection **(D)** is also demonstrated.

did not get the infection but we found no association between the measured parameters of the menstrual cycle and the SARS-CoV-2 infection (pre-peak period: p=0.37; peak period: p=0.55; post-peak period: p=0.89): the same proportion of individuals reported menstrual cycle problems regardless of SARS-CoV-2 infection (39.3 % of SARS-CoV infected and 38.7 % of uninfected respondents) (Figures 3C, D). We also analyzed whether the severity of the SARS-CoV-2 infection was in connection with the menstrual cycle changes but no interaction was uncovered (pre-peak period: p=0.65; peak period: p=0.58; post-peak period: p=0.11) (Table 1).

3.4 The effect of COVID-19 pandemic on the menstrual cycle: *Longitudinal comparison*

The menstrual cycle problems had also been assessed in the Hungarian population comparing 3 periods: in the pre-peak: January 2019 - September 2020; in the peak: October 2019 – March 2021 and in the post-peak period: April 2021 – December 2021.

We found that the length of the menstrual cycle did not change in any of the study-periods (Figure 4A). The vast majority (73-85 %) of female participants had an average cycle length of 24-38 days in all three periods, while shorter or longer menstrual cycles were less common. Interestingly, the menses length increased, while the regularity of the menstrual cycle decreased significantly during the peak of the pandemic compared to the pre- and postpeak periods (p<0.001) (Figures 4B, C). The average menses length was more than 7 days long in only 5.1 % of women during the pre-peak, while it lasted longer than 7 days in 81.4 % of women during the peak, then it was restored and only 7.5 % of women had longer period than 7 days during the post-peak period (Figure 4B). Although most women had regular periods in all three time periods, their menstrual cycle became more irregular during the peak compared to the pre-peak period and the irregularity further increased thereafter. The start of the period was unpredictable in 6.8 % of the individuals in the pre-peak period, which increased

10.3389/fendo.2022.974788

TABLE 1 Correlation between menstrual problems and SARS-CoV-2 infection.

SARS-CoV infection	Participants
Possibly	
Menstrual problems	1.40%
No menstrual problems	2.10%
Asymptomatic	
Menstrual problems	3.50%
No menstrual problems	6.30%
Mild symptoms	
Menstrual problems	16.30%
No menstrual problems	28.50%
Moderate symptoms	
Menstrual problems	13.80%
No menstrual problems	20.60%
Severe symptoms	
Menstrual problems	3.00%
No menstrual problems	2.10%
Hospitalized	
Menstrual problems	1.20%
No menstrual problems	0.70%

Table 1 summarizes the percentage of female participants with and without menstrual problems with SARS-CoV-2 infection of varying severity.

to 11.4 % at the peak and to 13.2 % thereafter. 58.6 % of the participants reported that their menstrual cycles were usually on time, with a maximum delay of 1-2 days (regular cycle) during the pre-peak, while 49.6 % addressed this during the peak and only 45.6 % during the post-peak period. 27.9 % of the respondents answered that they missed only one cycle 1-2 times a year, or there were 1–2-week delays 1-2 times per year in the pre-peak period (usually regular cycle). This proportion increased to 31.3 % at the peak of the pandemic and remained this high (31.7 %) after that as well. During the pre-peak 6.7 % of the participants reported that they had no regular cycle, which increased during the peak and the post-peak period to 7.9 % and 9.5 %, respectively (Figure 4C).

3.5 Association between menstrual cycle changes and depression

As the COVID-19 pandemic triggered the prevalence of depression and depressive symptoms (6) and it is well-known that depression inhibits the reproductive axis causing menstrual cycle alterations (10), we evaluated whether depressive symptoms developed during the pandemic could be responsible for the high number of noted menstrual cycle problems.

Data analysis with Chi-squared test showed that the menses length and the regularity of the menstrual cycle during the post-peak period changed with the severity of depression determined by the BDI. The average menses length (3-7 days) decreased with the severity of depression, while both shortened (1-2 days) and prolonged menses length (more than 7 days) became more frequent (Figure 5A). The regularity of the menstrual cycle decreased with the severity of depression (Figure 5B).

Although the measured parameters of the MHT (well-being, savoring, creative-executive efficiency, self-regulation, and resilience) did not display association with the surveyed parameters of the menstrual cycle in any of the observed periods, the five measured criteria of the MHT correlated with the result of the BDI. All parameters of the MHT showed negative correlation with the BDI. It means that the more severe the depression is based on the BDI, the lower the values are for the parameters of the MHT. (Tables 2A, B). We used Spearman's correlation for the analysis in this case, too.

4 Discussion

During the COVID-19 pandemic the prevalence of menstrual cycle problems has increased. The reason for this, however, is still not entirely revealed. The COVID-19 vaccines caused considerable concern because of a potential disruption of the menstrual cycle. In addition, growing evidence suggests that SARS-CoV-2 infection may have an impact on the menstrual cycle (5, 18). It is also clear that the COVID-19 pandemic put a great psychological burden on the society increasing the level of depression that can also influence the menstrual cycle (19). Thus, our survey aimed to explore whether the menstrual cycles of women between the age of 18-65 have been affected by the COVID-19 vaccines, SARS-CoV-2 infection, the COVID-19 pandemic, or psychological distress.

Human studies so far have shown that COVID-19 vaccines have a subtle and reversible effect on the menstrual cycle. Menstrual abnormalities such as menstrual irregularities, increase in the cycle length, menses length and heavier menstruation were observed post-vaccination. However, these changes were no greater than normal fluctuations and were restored within a few months (2–4, 20). Animal experiments also confirmed the lack of substantial vaccine effect on reproduction. No effects were found on fertility, or any studied ovarian and uterine parameters (12).

The occurrence of menstrual disturbances after COVID-19 vaccinations is not that surprising as vaccination has been linked to menstrual cycle changes earlier. It was published that the human papilloma virus vaccine had caused irregular and abnormal amount of menstrual bleeding (21). Such menstrual abnormalities can be the result of inflammatory reactions (22). Because of the severe symptoms and the rapid spread of SARS-CoV-2, the COVID-19 vaccines were developed and approved hastily. In addition, a new class of vaccines, the mRNA-based vaccines were also introduced against the SARS-CoV-2. The rapid development of vaccines has not allowed extensive studies

10.3389/fendo.2022.974788

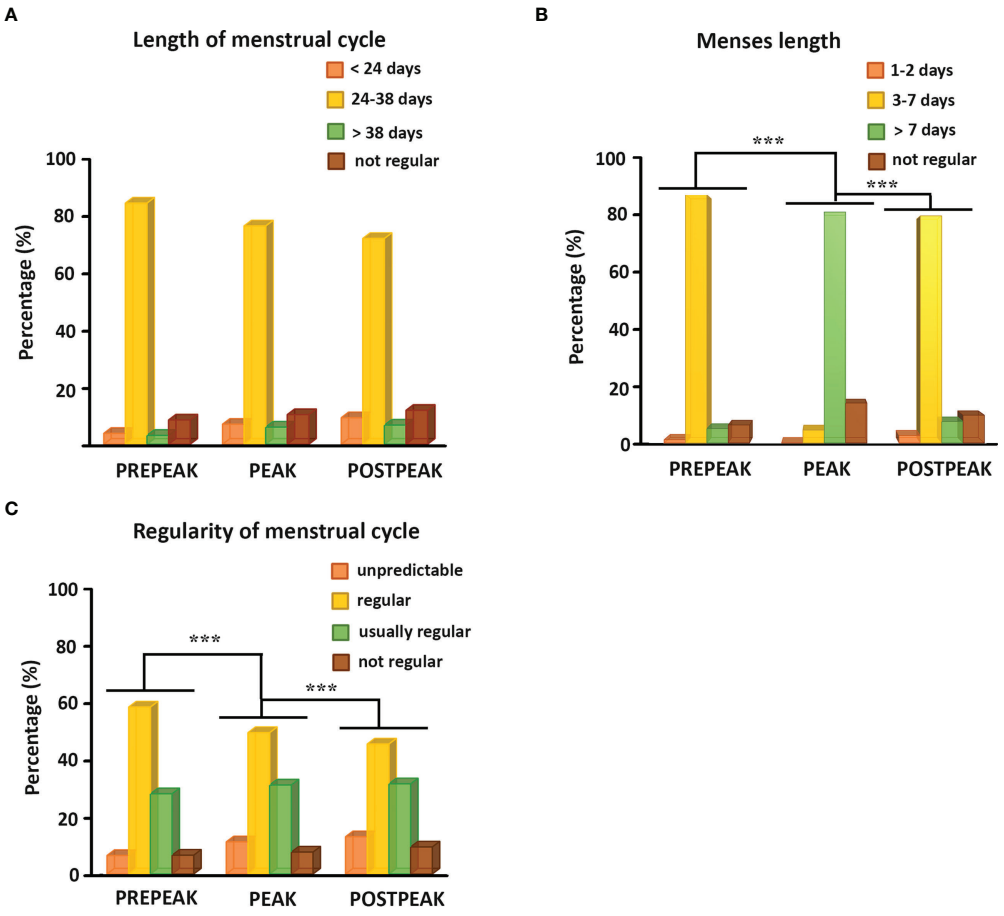

FIGURE 4
(A) Histograms show the percentage of female individuals bleeding more frequently than 24 days, between 24 and 38 days, less frequently than 38 days and having no regular menstrual bleeding during the pre-peak, the peak, and the post-peak period. **(B)** Histograms illustrate the percentage of female participants with menses length lasting for 1-2 days, 3-7 days, more than 7 days or having no regular bleeding during the pre-peak, the peak, and the post-peak period. **(C)** Histograms demonstrate the percentage of female respondents with unpredictable cycle, having regular cycle with a maximum delay of 1-2 days, usually regular cycle with 1-2 missed cycles or 1-2 weeks difference a year, or not regular menstrual cycle during the pre-peak, the peak, and the post-peak period. ***p≤0.001.

of all the side effects, especially for mRNA-based vaccines, which were not yet used before. Therefore, it was not assessed whether immunological reactions associated with vaccines may affect women's reproductive health. Lipid nanoparticles (LNPs) for instance that protect mRNA from degradation and help to deliver mRNA into the cells have been reported to be highly inflammatory in mice (23). Since the menstruation itself is associated with increased inflammation, we hypothesized that the LNPs being inflammatory and lipophilic molecules may interact with lipophilic sexual hormones and affect the menstrual cycle.

Our study demonstrated that 40.4 % of vaccine recipients had complained of menstrual cycle problems, particularly after the first and the second dose of COVID-19 vaccines. Despite of the fact that a large number of individuals reported menstrual cycle abnormalities, we found no correlation between the impact of vaccination and the menstrual cycle disturbances. According to our assumption we also tested whether the type of COVID-19 vaccines, especially the mRNA-based vaccines affected the menstrual cycle differently but we found no proof of that. However, we should mention that the slight and temporary menstrual cycle changes observed in previous studies (2–4, 20) could be masked by the over-representation of the highly qualified individuals (82.4 %) in our sample since the prevalence of irregular menstruation is increased in women with low educational levels (24). Also, menstrual cycle length variations occur more frequently with increasing age in women from lower social groups (25), whose representation was insufficient in our study.

SARS-CoV-2 infection may have also accounted for the observed menstrual cycle abnormalities during the pandemic (17). There is still relatively little scientific data available on how

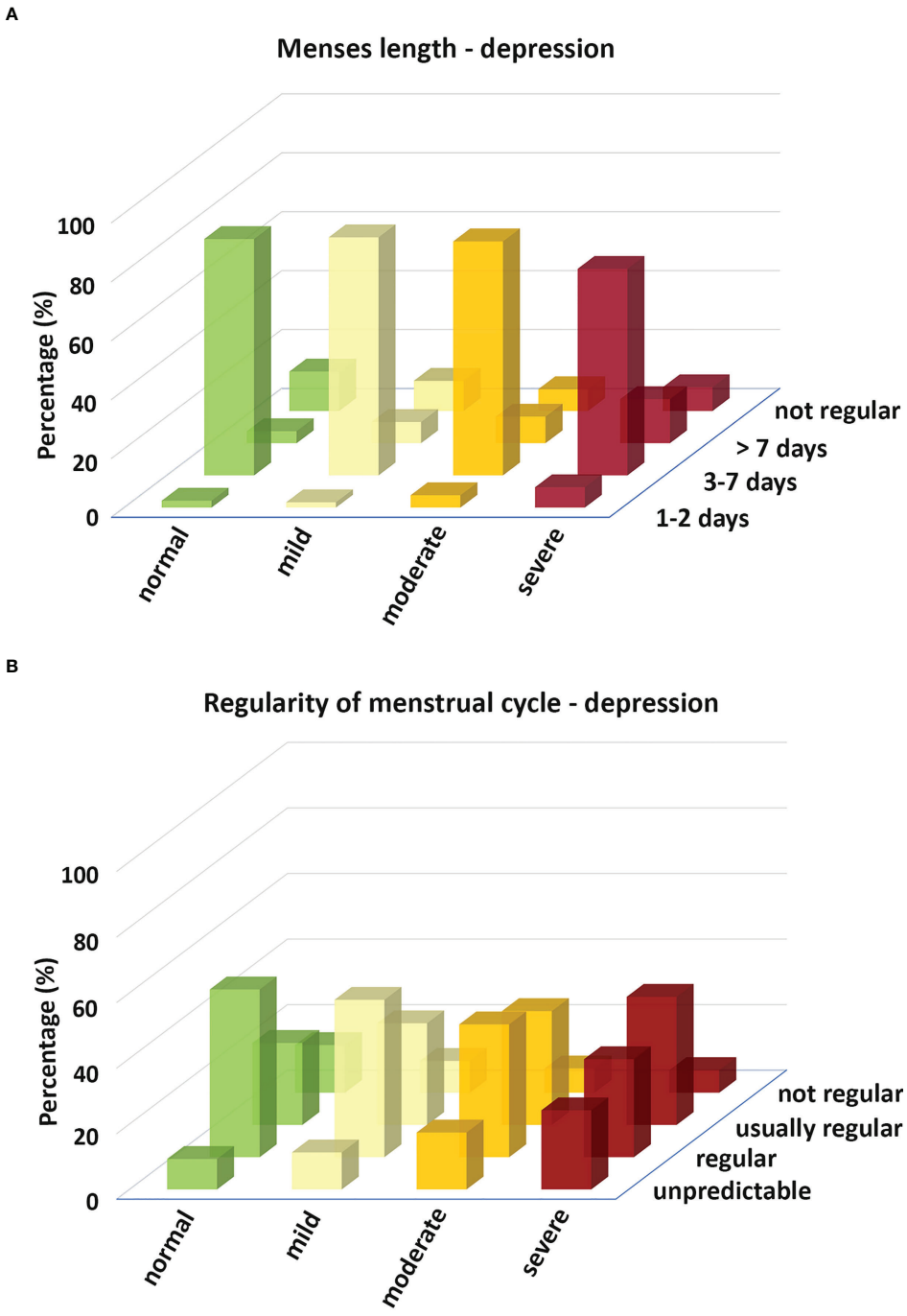

FIGURE 5
Histograms depict the menses length **(A)** and the regularity of the menstrual cycle **(B)** in relation to the severity of depression determined by the BDI.

and to what extent COVID-19 infection may affect the menstrual cycle. It has been published that women with severe COVID-19 symptoms are more likely to have menstrual cycle problems (5). Additionally, a case study reported that a 27-year-old female patient developed amenorrhea during and after a mild form of SARS-CoV-2 infection (26). SARS-CoV-2 infection could influence the menstrual cycle by influencing the hypothalamic-pituitary-gonad axis (17), but could also have a more specific effect on the reproductive system. The SARS-CoV-2 can bind to the angiotensin-converting enzyme ACE2, which acts as a viral receptor and is also expressed in the endometrium (27, 28). As ACE2 has a key role in regulating vasoconstriction of

TABLE 2A Cross-tabulation analysis between the menses length and BDI.

Depression \ Length	1-2 days	3-7 days	<7 days	Not regular	Participants
Normal	2.33%	80.23%	4.07%	13.37%	100% (172)
Mild	1.79%	80.80%	7.17%	10.24%	100% (948)
Moderate	4.18%	79.42%	9%	7.40%	100% (311)
Severe	6.90%	70.11%	14.94%	8.05%	100% (87)
		Chi-Square Tests			
Pearson Chi-Square	**Value**	**df**		**Asymptotic Significance (2-sided)**	
	27.023	9		0.001 ***	
		Symmetric Measures			
Cramer's V	**Value**			**Approximate Significance**	
	0.077			0.001	

TABLE 2B Cross-tabulation analysis between the regularity of the menstrual cycle and BDI.

Depression \ Regularity	Unpredictable	Regular	Usually regular	Not regular	Participants
Normal	9.3%	51.16%	25%	14.54%	100% (172)
Mild	11.29%	48%	31.01%	9.70%	100% (948)
Moderate	17.36%	40.51%	34.73%	7.40%	100% (311)
Severe	24.14%	29.89%	39.08%	6.89%	100% (87)
		Chi-Square Tests			
Pearson Chi-Square	**Value**	**df**		**Asymptotic Significance (2-sided)**	
	37.118	9		<0.001 ***	
		Symmetric Measures			
Cramer's V	**Value**			**Approximate Significance**	
	0.09			<0.001	

Table 2 shows the percentage distribution of women with different levels of depression in terms of menses length **(A)** or the regularity of the menstrual cycle **(B)**. The figures in the table show the percentage (and the number) of participants with different menses length and regularity of menstrual cycle. df=degree of freedom, ***p≤0.001.

the arteries that induces menstruation, the alteration of ACE2 may cause menstrual cycle abnormalities. Even though available data and scientific facts suggest that SARS-CoV-2 infection may alter the menstrual cycle, we found no connection between the SARS-CoV-2 infection or its severity and menstrual cycle disruptions.

Finally, we examined the effect of the pandemic itself on the menstrual cycle with its possible depression-inducing potential. Interestingly, the peak of the infection was associated with longer menses length and more irregularity in the menstrual cycle, which was normalized after the relief. Menstrual cycle characteristics such as cycle length, regularity, and menses length show strong association with psychiatric disorders including depression (29, 30).

Women during their reproductive years are nearly twice as likely to develop depression as men (31). In depression, the corticotropin-releasing hormone (CRH) levels, and consequently the cortisol levels are elevated resulting in the inhibition of the action of gonadotropin-releasing hormone (GnRH) neurons, gonadotrophs, and gonads (10). The COVID-19 pandemic increased the rate of depression (6) and exacerbated the existing mental health problems (7). Loneliness due to social distancing (8), elevated levels of fear of SARS-CoV-2 infection (9), or loss and grief during the pandemic became major factors contributing to the development of depressive symptoms. As a strong association between depression and menstrual cycle disorders was noted, we examined whether there was a connection between the depressive symptoms and the menstrual cycle disturbances.

We found an association between the BDI scores and the length and the regularity of the menstrual cycle during the post-peak period. The severity of the depression based on BDI positively correlated with the menses length changes (shortening and prolongation) and the irregularity of the menstrual cycle. Although the MHT did not show connection with the menstrual cycle changes, it exhibited negative correlation with the BDI. Individuals who scored lower in the MHT, which represents a general mental health state, had increased values in the BDI, which evaluated their mental health a month before completing the test. Although we could not measure, we assumed that the rate of depression might have been elevated during the peak of the pandemic. This suggests that the menstrual cycle problems

observed during the peak of infection, the significant increase in the menses length and the irregularity of the menstrual cycle, may be a consequence of depression.

Our survey has revealed a connection between depressive-like symptoms and menstrual cycle alterations but found no evidence of correlation between post-vaccination or SARS-CoV-2 infection and menstrual cycle changes. It suggests that depression may be a major factor causing menstrual cycle abnormalities during the COVID-19 pandemic.

5 Limitations

Our study has pitfalls and limitations. We should be cautious about drawing general conclusions from the gathered data as the questionnaire was completed voluntarily by female individuals online. Therefore, the collected data may contain some bias such as social acceptance error. Recall bias may also be a problem since the study was self-reporting and asked questions for an interval of more than one year. Furthermore, the over-representation of highly qualified individuals may also lead to bias as women's reproductive health is highly influenced by their socioeconomic status. Lower educational level for instance has been shown to act as a factor promoting irregular menstruation (24). Another drawback of our study is that we could not follow the level of depression of the female participants separately during the pre-peak, the peak, and the post-peak period. We could only assess their general mental health and the rate of depression at the end of the post-peak period. Therefore, we could only make assumptions that the depression level was the greatest during the peak period of the pandemic.

6 Conclusions

Our study provides evidence on the reproductive health safety of COVID-19 vaccines and indicates that the effect of COVID-19 vaccines and SARS-CoV-2 infection on the menstrual cycle may be negligible compared to the effect of depression.

Data availability statement

The original contributions presented in the study are included in the article/Supplementary Material. Further inquiries can be directed to the corresponding author.

Ethics statement

The ethical approval of the questionnaire has been accepted by the Ethics Committee in Hungary (Medical Research Council; IV/7146- 1 /2021/EKU).

Author contributions

DZ: Conceptualization, methodology, investigation. BM and NF: Statistical analysis. ZN: Conceptualization, clinical expertise. KB: Investigation, data assessment, writing. HH and KV: Visualization. All authors contributed to the article and approved the submitted version.

Funding

Project no. TKP2021-EGA-16 has been implemented with the support provided from the National Research, Development and Innovation Fund of Hungary, financed under the TKP2021-EGA funding scheme. This study was also supported by the National Research Development and Innovation Office of Hungary (grant numbers K141934, K138763, and K120311).

Conflict of interest

The authors declare that the research was conducted in the absence of any commercial or financial relationships that could be construed as a potential conflict of interest.

Publisher's note

Supplementary material

The Supplementary Material for this article can be found online at: https://www.frontiersin.org/articles/10.3389/fendo.2022.974788/full#supplementary-material

References

1. Anand P, Stahel VP. Review the safety of covid-19 mRNA vaccines: a review. *Patient Saf Surg* (2021) 15:1–9. doi: 10.1186/s13037-021-00291-9

2. Edelman A, Boniface ER, Benhar E, Han L, Matteson KA, Favaro C, et al. Association between menstrual cycle length and coronavirus disease 2019

(COVID-19) vaccination: A U.S. cohort. *Obstet Gynecol* (2022) 139:481–9. doi: 10.1097/AOG.0000000000004695

3. Laganà AS, Veronesi G, Ghezzi F, Ferrario MM, Cromi A, Bizzarri M, et al. Evaluation of menstrual irregularities after COVID-19 vaccination: Results of the MECOVAC survey. *Open Med (Warsaw Poland)* (2022) 17:475–84. doi: 10.1515/med-2022-0452

4. Muhaidat N, Alshrouf MA, Azzam MI, Karam AM, Al-Nazer MW, Al-Ani A. Menstrual symptoms after COVID-19 vaccine: A cross-sectional investigation in the MENA region. *Int J Womens Health* (2022) 14:395–404. doi: 10.2147/IJWH.S352167

5. Khan SM, Shilen A, Heslin KM, Ishimwe P, Allen AM, Jacobs ET, et al. SARS-CoV-2 infection and subsequent changes in the menstrual cycle among participants in the Arizona CoVHORT study. *Am J Obstet Gynecol* (2022) 226:270–3. doi: 10.1016/j.ajog.2021.09.016

6. Aguilar-Latorre A, Oliván-Blázquez B, Porroche-Escudero A, Méndez-López F, García-Gallego V, Benedé-Azagra B, et al. The impact of the COVID-19 lockdown on depression sufferers: a qualitative study from the province of zaragoza, Spain. *BMC Public Health* (2022) 22:780. doi: 10.1186/s12889-022-13083-2

7. Hager NM, Judah MR, Milam AL. Loneliness and depression in college students during the COVID-19 pandemic: the role of boredom and repetitive negative thinking. *Int J Cognit Ther* (2022) 15(2):134–52. doi: 10.1007/s41811-022-00135-z

8. Killgore WDS, Cloonan SA, Taylor EC, Miller MA, Dailey NS. Three months of loneliness during the COVID-19 lockdown. *Psychiatry Res* (2020) 293:113392. doi: 10.1016/j.psychres.2020.113392

9. Bakioğlu F, Korkmaz O, Ercan H. Fear of COVID-19 and positivity: Mediating role of intolerance of uncertainty, depression, anxiety, and stress. *Int J Ment Health Addict* (2021) 19:2369–82. doi: 10.1007/s11469-020-00331-y

10. Padda J, Khalid K, Hitawala G, Batra N, Pokhriyal S, Mohan A, et al. Depression and its effect on the menstrual cycle. *Cureus* (2021) 13:e16532. doi: 10.7759/cureus.16532

11. Uzzoli A, Kovács S, Páger Balázs ST. Regional inequalities in the waves of the COVID-19 pandemic in Hungary. *Területi Stat* (2021) 61:291–319. doi: 10.15196/TS610302

12. Bowman CJ, Bouressam M, Campion SN, Cappon GD, Catlin NR, Cutler MW, et al. Lack of effects on female fertility and prenatal and postnatal offspring development in rats with BNT162b2, a mRNA-based COVID-19 vaccine. *Reprod Toxicol* (2021) 103:28–35. doi: 10.1016/j.reprotox.2021.05.007

13. András V, Virág Z, Regina T, Attila O. Measuring well-being and mental health: The mental health test. *Mentalhig es Pszichoszomatika* (2020) 21:281–322. doi: 10.1556/0406.21.2020.014

14. Beck AT, Guth D, Steer RA, Ball R. Screening for major depression disorders in medical inpatients with the beck depression inventory for primary care. *Behav Res Ther* (1997) 35:785–91. doi: 10.1016/S0005-7967(97)00025-9

15. Rózsa S, Szádóczky E, Füredi J. Psychometric properties of the Hungarian version of the shortened beck depression inventory. *Psychiatr Hungarica* (2001) 16:384–402.

16. Schepis TS, Hakes JK. Age of initiation, psychopathology, and other substance use are associated with time to use disorder diagnosis in persons using opioids nonmedically. *Subst Abus* (2017) 38:407–13. doi: 10.1080/08897077.2017.1356791

17. Sharp GC, Fraser A, Sawyer G, Kountourides G, Easey KE, Ford G, et al. The COVID-19 pandemic and the menstrual cycle: research gaps and opportunities. *Int J Epidemiol* (2021), 51(3):691–700. doi: 10.1093/ije/dyab239

18. Li K, Chen G, Hou H, Liao Q, Chen J, Bai H, et al. Analysis of sex hormones and menstruation in COVID-19 women of child-bearing age. *Reprod BioMed Online* (2021) 42:260–7. doi: 10.1016/j.rbmo.2020.09.020

19. Demir O, Sal H, Comba C. Triangle of COVID, anxiety and menstrual cycle. *J Obstet Gynaecol (Lahore)* (2021) 41:1257–61. doi: 10.1080/01443615.2021.1907562

20. Maher M, O' Keeffe A, Phelan N, Behan LA, Collier S, Hevey D, et al. Female reproductive health disturbance experienced during the COVID-19 pandemic correlates with mental health disturbance and sleep quality. *Front Endocrinol (Lausanne)* (2022) 13:838886. doi: 10.3389/fendo.2022.838886

21. Suzuki S, Hosono A. No association between HPV vaccine and reported post-vaccination symptoms in Japanese young women: Results of the Nagoya study. *Papillomavirus Res (Amsterdam Netherlands)* (2018) 5:96–103. doi: 10.1016/j.pvr.2018.02.002

22. Berbic M, Ng CHM, Fraser IS. Inflammation and endometrial bleeding. *Climacteric* (2014) 17:47–53. doi: 10.3109/13697137.2014.963964

23. Ndeupen S, Qin Z, Jacobsen S, Bouteau A, Estanbouli H, Igyártó BZ. The mRNA-LNP platform's lipid nanoparticle component used in preclinical vaccine studies is highly inflammatory. *iScience* (2021) 24:103479. doi: 10.1016/j.isci.2021.103479

24. Kwak Y, Kim Y, Baek KA. Prevalence of irregular menstruation according to socioeconomic status: A population-based nationwide cross-sectional study. *PloS One* (2019) 14:e0214071. doi: 10.1371/journal.pone.0214071

25. Münster K, Schmidt L, Helm P. Length and variation in the menstrual cycle-a cross-sectional study from a Danish county. *Br J Obstet Gynaecol* (1992) 99(5):422–9. doi: 10.1111/j.1471-0528.1992.tb13762.x

26. Puca E, Puca E. Premature ovarian failure related to SARS-CoV-2 infection. *J Med cases* (2022) 13:155–8. doi: 10.14740/jmc3791

27. Carp-Veliscu A, Mehedintu C, Frincu F, Bratila E, Rasu S, Iordache I, et al. The effects of SARS-CoV-2 infection on female fertility: A review of the literature. *Int J Environ Res Public Health* (2022) 19:984. doi: 10.3390/ijerph19020984

28. Jing Y, Run-Qian L, Hao-Ran W, Hao-Ran C, Ya-Bin L, Yang G, et al. Potential influence of COVID-19/ACE2 on the female reproductive system. *Mol Hum Reprod* (2020) 26:367–73. doi: 10.1093/molehr/gaaa030

29. Barron ML, Flick LH, Cook CA, Homan SM, Campbell C. Associations between psychiatric disorders and menstrual cycle characteristics. *Arch Psychiatr Nurs* (2008) 22:254–65. doi: 10.1016/j.apnu.2007.11.001

30. Bromberger JT, Schott LL, Matthews KA, Kravitz HM, Randolph JFJr., Harlow S, et al. Association of past and recent major depression and menstrual characteristics in midlife: Study of women's health across the nation. *Menopause* (2012) 19:959–66. doi: 10.1097/gme.0b013e318248f2d5

31. Albert PR. Why is depression more prevalent in women? *J Psychiatry Neurosci* (2015) 40:219–21. doi: 10.1503/jpn.150205

frontiers | Frontiers in Endocrinology

TYPE Original Research
PUBLISHED 28 October 2022
DOI 10.3389/fendo.2022.939699

OPEN ACCESS

EDITED BY
Klaudia Barabas,
University of Pécs, Hungary

REVIEWED BY
Imre Farkas,
Institute of Experimental Medicine (MTA), Hungary
Honoo Satake,
Suntory Foundation for Life Sciences, Japan

*CORRESPONDENCE
Dong Hyu Cho
obgyn2001@jbnu.ac.kr
Seong Kyu Han
skhan@jbnu.ac.kr

†These authors have contributed equally to this work

SPECIALTY SECTION
This article was submitted to Reproduction, a section of the journal Frontiers in Endocrinology

RECEIVED 09 May 2022
ACCEPTED 14 October 2022
PUBLISHED 28 October 2022

CITATION
Rijal S, Jang SH, Cho DH and Han SK (2022) Hydrogen peroxide suppresses excitability of gonadotropin-releasing hormone neurons in adult mouse. *Front. Endocrinol.* 13:939699. doi: 10.3389/fendo.2022.939699

Hydrogen peroxide suppresses excitability of gonadotropin-releasing hormone neurons in adult mouse

Santosh Rijal[1], Seon Hui Jang[1], Dong Hyu Cho[2*†] and Seong Kyu Han[1*†]

[1]Department of Oral Physiology, School of Dentistry and Institute of Oral Bioscience, Jeonbuk National University, Jeonju, South Korea, [2]Department of Obstetrics and Gynecology, Jeonbuk National University Medical School, Institute of Clinical Medicine of Jeonbuk National University-Biomedical Research Institute for Medical Sciences, Jeonbuk National University Hospital, Jeonju, South Korea

It has been reported that reactive oxygen species (ROS) derived from oxygen molecule reduction can interfere with the cross-talk between the hypothalamic-pituitary-gonadal (HPG) axis and other endocrine axes, thus affecting fertility. Furthermore, ROS have been linked to GnRH receptor signaling in gonadotropes involved in gonadotropin release. There has been evidence that ROS can interfere with the HPG axis and gonadotropin release at various levels. However, the direct effect of ROS on gonadotropin-releasing hormone (GnRH) neuron remains unclear. Thus, the objective of this study was to determine the effect of hydrogen peroxide (H_2O_2), an ROS source, on GnRH neuronal excitabilities in transgenic GnRH-green fluorescent protein-tagged mice using the whole-cell patch-clamp electrophysiology. In adults, H_2O_2 at high concentrations (mM level) hyperpolarized most GnRH neurons tested, whereas low concentrations (pM to μM) caused slight depolarization. In immature GnRH neurons, H_2O_2 exposure induced excitation. The sensitivity of GnRH neurons to H_2O_2 was increased with postnatal development. The effect of H_2O_2 on adult female GnRH neurons was found to be estrous cycle-dependent. Hyperpolarization mediated by H_2O_2 persisted in the presence of tetrodotoxin, a voltage-gated Na^+ channel blocker, and amino-acids receptor blocking cocktail containing blockers for the ionotropic glutamate receptors, glycine receptors, and $GABA_A$ receptors, indicating that H_2O_2 could act on GnRH neurons directly. Furthermore, glibenclamide, an ATP-sensitive K^+ (K_{ATP}) channel blocker, completely blocked H_2O_2-mediated hyperpolarization. Increasing endogenous H_2O_2 by inhibiting glutathione peroxidase decreased spontaneous activities of most GnRH neurons. We conclude that ROS can act as signaling molecules for

regulating GnRH neuron's excitability and that adult GnRH neurons are sensitive to increased ROS concentration. Results of this study demonstrate that ROS have direct modulatory effects on the HPG axis at the hypothalamic level to regulate GnRH neuron's excitabilities.

KEYWORDS

hydrogen peroxide, gonadotropin-releasing hormone neurons, hypothalamic-pituitary-gonadal axis, patch-clamp, K_{ATP} channels, reactive oxygen species

Introduction

Reactive oxygen species (ROS) are chemically reactive molecules or free radicals formed when oxygen molecules are reduced. Mitochondria are primary cellular organelles responsible for the production of a large amount of ROS in cells (1, 2). External sources including pollution, radiation, physical stress, alcohol abuse, cigarette smoking and vaping, drug abuse, obesity, malnutrition, lifestyle modification, and endocrine-disrupting chemicals can intensify ROS production in cells (3, 4). At the cellular level, ROS at low concentrations operate as signaling molecules (5). However, excessive levels of ROS cause oxidative stress and cell death (6). Numerous enzymatic and non-enzymatic antioxidant systems can counteract increasing concentration of ROS in cells. Enzymes such as glutathione peroxidase (GPx), superoxide dismutase, and catalase (CAT) play an enzymatic role in the degradation of ROS, while scavengers such as vitamin C, vitamin E, glutathione, carotenoids, and ubiquinone play a non-enzymatic role in the detoxification of free radicals (7, 8).

Gonadotropin-releasing hormone (GnRH) neurons are key regulators of the hypothalamic-pituitary-gonadal (HPG) axis. They play a pivotal role in the regulation of fertility *via* release of gonadotropins in mammals (9). It has been shown that ROS produced by endogenous and exogenous sources can impair reproductive function, decrease gonadal hormones, and interfere with cross-talk between the HPG axis and other endocrine axes, eventually affecting fertility (3). Furthermore, ROS are connected to GnRH receptor signaling involved in gonadotropin release of gonadotropes (10). In contrast, endogenous gonadal hormones strongly influence ROS generation in brain mitochondria (11). An external source of ROS has now emerged as a leading cause of reproductive issues such as infertility and pregnancy complications (3, 12, 13).

ROS in the brain can act as potent signaling molecules at physiological concentration. Neurons can sense, convert, and transmit ROS into relevant intracellular signals and regulate peripheral tissue activities *via* the autonomous nervous system (14). New evidence has suggested that ROS play a signaling role in regulating hypothalamus activity. For example, ROS in the hypothalamus can regulate energy homeostasis (15) and maintain body fluid dynamics (16). ROS can also affect functions of hypothalamic neurons such as neuropeptide-Y (NPY)/agouti-related protein (AgRP) neurons, pro-opiomelanocortin (POMC)/cocaine-and-amphetamine responsive transcript (CART) neurons, and paraventricular nucleus (PVN) (17, 18). Hormones, peptides, neurotransmitters, and nutrients can also affect the release of ROS in the hypothalamus (14).

Studies mentioned above have shown that ROS can inhibit gonadotropin release at several levels of the HPG axis. However, the mechanism underlying how ROS impact GnRH neuronal activities remains unknown. Among various ROS, hydrogen peroxide (H_2O_2) is the most stable and long-lived ROS as it has a cellular half-life of 1 ms compared to other ROS such as superoxide anion radicals (1 μs), and hydroxyl radicals (1 ns) (19–21). Furthermore, Ledo et al. reported that the extracellular H_2O_2 in brain slices and *in vivo* has a half-life of 2.5 and 2.2 s respectively (22). Additionally, H_2O_2 is a highly diffusible and less toxic ROS that has emerged as a neuromodulator and an intercellular signaling molecule in the brain (19, 22). H_2O_2 perfusion on brain slices can influence neuronal excitabilities (18, 23–25), synaptic activity, and neurotransmitter release (26, 27). Thus, the objective of this study was to investigate the effect of membrane diffusible extracellular ROS source H_2O_2 on excitabilities of GnRH neurons in hypothalamic preoptic area (hPOA) brain slices using a whole-cell patch-clamp approach.

Materials and methods

Animals

C57BL/6 GnRH-green fluorescent protein-tagged (GnRH-GFP) mice (28) housed under stable room temperature (23-26 °C) and an automatic 12:12-h light-dark cycle (lights on at 07:00 h) with *ad libitum* access to food and water were sacrificed for the experiment. All animal care conditions and experimental procedures were in accordance with the Institutional Animal Care and Use Committee of Jeonbuk National University (CBNU 2020-0122). Estrous cycle stage of female mice was assessed by vaginal smear examination.

Preparation of brain slices

Coronal brain slices were prepared using the same procedure as described in a previous study (29). In brief, mice were beheaded between 10:00 and 12:00 p.m. UTC+09:00 (Universal Time Coordinated). Their brains were swiftly removed and immersed in ice-cold artificial cerebrospinal fluid (ACSF) containing 126 mM NaCl, 2.5 mM KCl, 2.4 mM $CaCl_2$, 1.2 mM $MgCl_2$, 11 mM D-glucose, 1.4 mM NaH_2PO_4, and 25 mM $NaHCO_3$ (pH value of 7.3 to 7.4 was maintained when bubbled with 95% O_2 and 5% CO_2). Coronal brain slices (180-270 µm thick) containing the preoptic hypothalamic area were prepared using a vibratome (VT1200S, Leica biosystem, Wetzlar, Germany) in ice-cold ACSF. For recovery, the brain slices were stored in oxygenated ACSF at room temperature for at least 1hour before being transferred to the recording chamber.

Electrophysiology

Before electrophysiological recording, brain slices were transferred to the recording chamber mounted on an upright microscope (BX51W1; Olympus, Tokyo, Japan). They were, entirely submerged, and continuously perfused (4~5 mL/min) with oxygenated ACSF. The view of the coronal slice was displayed on a video monitor. The hPOA region was identified under X10 objective magnification. Fluorescent GnRH neurons were identified under X40 objective magnification *via* brief fluorescence illumination. Identified GnRH neurons were patched under Nomarski differential interference contrast optics. Thin-wall borosilicate glass capillaries (PG52151-4, WPI, Sarasota, FL, USA) were pulled on a Flaming/Brown puller (P-97; Sutter Instruments Co., Novate, CA USA) to fabricate patch pipette. These pipettes typically displayed a tip resistance of 4 to 6 MΩ when filled with pipette solution filtered through a disposable 0.22-µM filter. The loaded pipette solution was composed of 140 mM KCl, 1mM $CaCl_2$, 1 mM $MgCl_2$, 10 mM HEPES, 10 mM EGTA, and 4 mM Mg-ATP (pH 7.3 with KOH). Pipette offset was set to zero before a high-resistance seal ("gigaseal") was achieved. After a giga seal was achieved between the pipette and the neuronal membrane, negative pressure by a short suction pulse was applied to make the whole cell.

Whole-cell recorded signals were amplified with an Axopatch 200B (Molecular Devices, San Jose, CA, USA) and filtered at 1 kHz with a Bessel filter before digitizing at a rate of 1 kHz. Membrane potential changes were sampled using a Digidata 1440A interface (Molecular Devices, San Jose, CA, USA). Signals were recorded and analyzed using an Axon pClamp 10.6 data acquisition program (Molecular Devices, San Jose, CA, USA). Neurons that showed changes in membrane potential of more than 2 mV after being exposed to H_2O_2 were considered to have responded. All recordings were made at room temperature.

Chemicals

Chemicals including hydrogen peroxide (H_2O_2), picrotoxin, strychnine hydrochloride (strychnine), glibenclamide, tetraethylammonium chloride (TEA), barium chloride (BaCl2), mercaptosuccinic acid (MCS), 3-amino-1,2,4-triazole (ATZ), and ACSF compositions were purchased from Sigma-Aldrich (St. Louis, MO, USA), except for CNQX disodium salt (CNQX), DL-AP5 (AP5), and tetrodotoxin citrate (TTX) which was bought from Tocris Bioscience (Avonmouth, Bristol, UK). Stocks were diluted (usually 1,000-fold) in ACSF to desired final concentrations before bath application. H_2O_2 of desired concentration was freshly prepared from stock by dripping directly to ACSF immediately before bath application.

Data and statistical analysis

For statistical analysis, Student's t-test and one-way ANOVA post-hoc Scheffe test were used to compare means of two and more than two experimental groups, respectively. All statistical analyses were performed using Origin 8 software (OriginLab Corp, Northampton, MA, USA). All numerical values are expressed as mean ± standard error of the mean. Results with p-value < 0.05 are considered to be statistically significant. Traces were plotted using Origin 8 software (OriginLab Corp, Northampton, MA, USA). Action potential firings were analyzed using a Mini-Analysis software (ver. 6.0.7; Synaptosoft Inc., Decatur, GA, USA).

Results

Hydrogen peroxide exposure induces variegated response in GnRH neurons

We used whole-cell current-clamp recordings to investigate the influence of H_2O_2 on membrane excitability in GnRH neurons and found that superfusion with 1 mM H_2O_2 elicited a variety of responses in adult GnRH neurons, including membrane hyperpolarization, depolarization, and no response as shown in Figure 1. Bath treatment with 1 mM H_2O_2 for 3 to 5 minutes produced responses in 70% of adult GnRH neurons, while 30% of adult GnRH neurons were unresponsive to H_2O_2 (Figure 1A). Among responding neurons, 10% generated an average membrane depolarization of 4.60 ± 0.65 mV (n = 15; Figure 1B) while 60% of neurons induced an average membrane

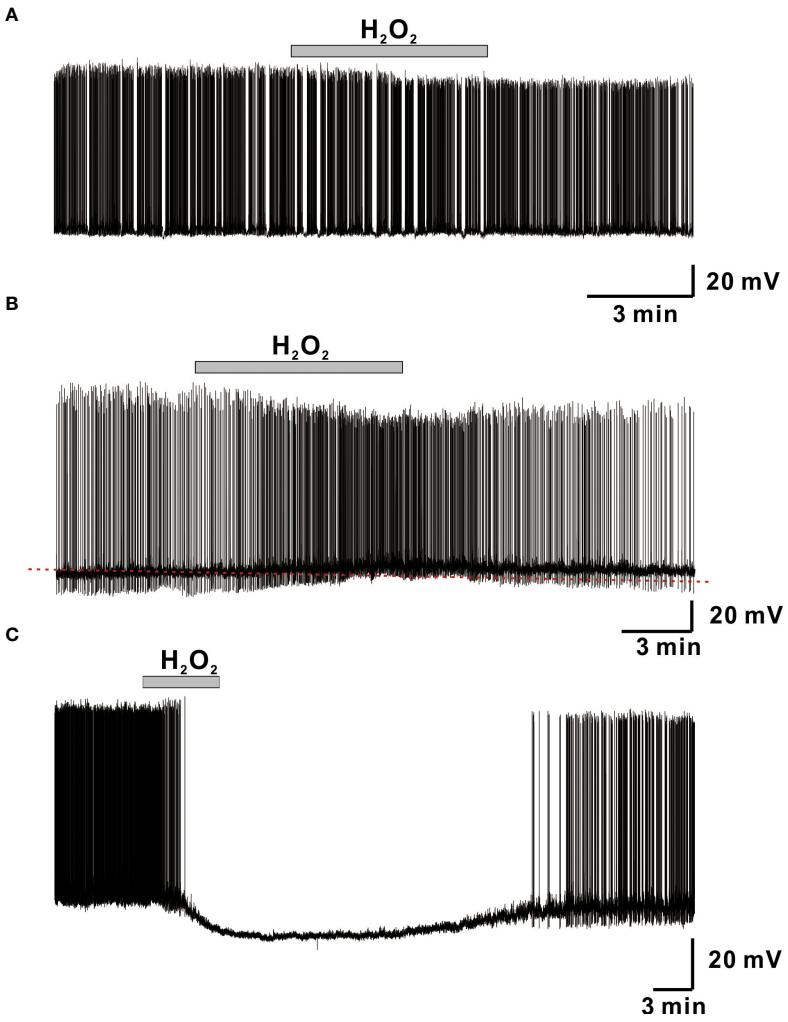

FIGURE 1
H_2O_2 induces variegated responses of adult male GnRH neurons. **(A–C)** Representative voltage traces from GnRH neurons showing no response, membrane depolarization, and membrane hyperpolarization, respectively, upon perfusion with 1 mM H_2O_2.

hyperpolarization of -14.6 ± 0.81 mV (n = 82; Figure 1C). Depolarized neurons showed a minor increase in spontaneous action potential firing in addition to membrane potential change. In contrast, hyperpolarized neurons showed partial and/or full cessation of spontaneous action potential firing. These alterations were reversed after more than 15-20 minutes of H_2O_2 washout.

According to previous studies, oxidative stress vulnerability increases with age, with adults being more vulnerable and juveniles being partially resistant (30, 31). In the present study, effects of 1 mM H_2O_2 on GnRH neurons were studied in three groups according to age: juvenile, 8 to 25 postnatal days (PND); peripubertal, 26 to 45 PND; and adults, more than 60 PND. In contrast with its hyperpolarization effect on most adult GnRH neurons, H_2O_2 depolarized most GnRH neurons 67% (8/12) in juveniles. On the other hand, H_2O_2 exposure elicited similar percentages of responses, 46% (5/11) for depolarization and 36% (4/11) for hyperpolarization in peripubertal mice as shown in Figures 2A, B. Furthermore, there was no significant difference in mean depolarization between juvenile and peripubertal. Similarly, GnRH neurons from both adult females and males responded equally to H_2O_2 exposure (females; 69%, 24/35: males; 69%, 73/106). In addition, the mean values for induced hyperpolarization (male; -14.9 ± 0.84 mV, n = 65: female; -12.5 ± 1.50 mV, n = 17, $p > 0.05$; unpaired *t*-test) and depolarization (male; 3.98 ± 0.46 mV, n = 8: female; 5.32 ± 1.3 mV, n = 7, $p > 0.05$; unpaired *t*-test) were not significantly different between adult females and males GnRH neurons as shown in Figure 2A. Similarly, there was no significant difference in the mean hyperpolarization among estrous phases in female mice (estrous; -11.1 ± 2.11mV, n = 5: diestrous; -15.4 ± 0.96 mV, n = 5: proestrous; -11.4 ± 3.23 mV, n = 7, $p > 0.05$; one-way ANOVA, Figure 2C). However, female GnRH

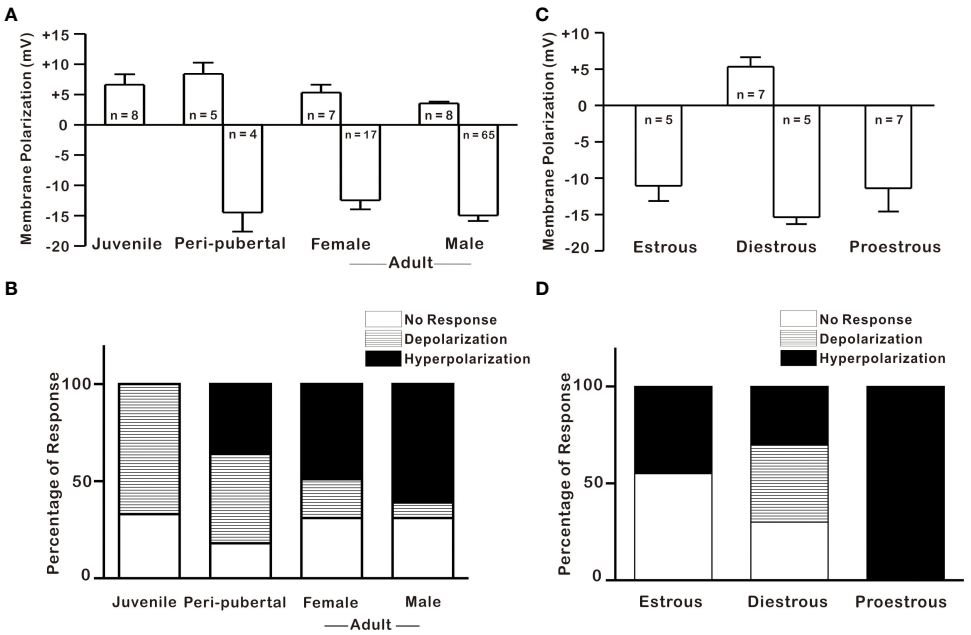

FIGURE 2
H_2O_2 effect on GnRH neurons across postnatal development and estrous cycle. **(A–C)** Histograms depicting H_2O_2-induced membrane polarization in GnRH neurons throughout the postnatal development and estrous cycle, respectively ($p > 0.05$; one-way ANOVA). **(B–D)** Histograms showing percentages of variegated responses of GnRH neurons by H_2O_2 exposure across postnatal development and at various estrous cycle stages in adult females, respectively.

neurons demonstrated estrous cycle-dependent variation in response percentage to H_2O_2 exposure. During H_2O_2 exposure, 100% of GnRH neurons from proestrous mice showed hyperpolarization, whereas only 45% of GnRH neurons from estrous mice responded to H_2O_2 with hyperpolarization. Similarly, 70% of GnRH neurons from diestrous mice responded to H_2O_2 treatment, accounting 30% for hyperpolarization and 40% for depolarization, as shown in Figure 2D.

Response of adult GnRH neurons to H_2O_2 exposure is concentration-dependent

After discovering that adult GnRH neurons were susceptible to 1 mM H_2O_2, we conducted a dose-dependent experiment in adult male GnRH neurons with low and high concentrations of H_2O_2. As demonstrated in Figure 3A, low concentrations of

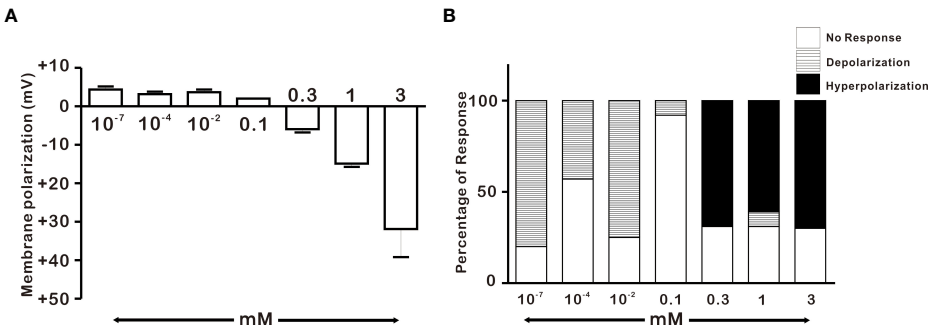

FIGURE 3
Concentration-dependent effect of H_2O_2 on GnRH membrane potential under whole-cell current clamp. **(A)** Histograms depicting H_2O_2-induced membrane polarization in response to various concentrations of H_2O_2 on GnRH neurons of adult males (one-way ANOVA post-hoc Scheffe test) **(B)** Histograms depicting percentage of variegated responses induced by various concentrations of H_2O_2 on GnRH neurons of adult males.

H_2O_2 caused minor membrane depolarization, whereas high concentrations of H_2O_2 caused membrane potential to become more hyperpolarized. Low concentrations of H_2O_2 (100 pm, 100 nM, and 10 µM) exhibited depolarization in the majority of GnRH neurons, corresponding to 80% (8/10), 43% (3/7), and 75% (3/4), respectively. In contrast, high concentrations of H_2O_2 (0.3, 1 and 3 mM) induced hyperpolarization in majority of GnRH neurons, corresponding to 69% (9/13), 61% (65/106), and 72% (13/18), respectively. However, 100 µM H_2O_2 induced depolarization in one of the fourteen neurons tested accounting 7% as shown in Figure 3B.

H_2O_2 acts on GnRH neurons postsynaptically

Hyperpolarization of GnRH neurons induced by 1 mM H_2O_2 recovered almost completely after more than 15 to 20 minutes of washout. Therefore, we determined whether H_2O_2 elicited repeatable responses of GnRH neurons. To access this, H_2O_2 was consecutively applied after the washout of the first application. On repeat application, H_2O_2 induced hyperpolarization with comparable amplitude to that of the first application. The mean hyperpolarization induced by H_2O_2 on the first application (-18.0 ± 4.84 mV, n = 8) was similar to that induced on the second application (-18.4 ± 4.8 mV, n = 8, $p > 0.05$; Figure 4A). Further, we aimed to examine whether H_2O_2 could act on GnRH neurons directly. For this, the hyperpolarization induced on bath application of H_2O_2 was recorded in the presence of TTX (0.5 µM), a sodium channel blocker known to block action potential-dependent transmission. Action potentials were promptly suppressed when recorded in the presence of TTX. However, the hyperpolarizing effect of H_2O_2 on GnRH neurons persisted. Average responses generated by H_2O_2 alone (-16.8 ± 2.2 mV, n = 8) and in the presence of TTX (-13.6 ± 1.7 mV, n = 8, p > 0.05; Figure 4B) were not significantly different.

Next, to assess the possible involvement of both pre- and post-synaptic GABA, glycine, and glutamate receptors in H_2O_2 mediated actions of GnRH neurons, H_2O_2-induced hyperpolarization was recorded in the presence of an amino acid receptor blocker cocktail (AARBC) containing picrotoxin (50 µM), AP5 (20 µM), CNQX (10 µM), and strychnine (2 µM). Under these circumstances, H_2O_2 still induced hyperpolarization of GnRH neurons. The average hyperpolarization induced by H_2O_2 alone was -17.0 ± 1.95 mV (n = 6), which was not significantly different from that induced by H_2O_2 in the presence of AARBC (-16.5 ± 2.57 mV, n = 6, p > 0.05; Figure 4C). As shown in Figure 4D, the average relative percentage of H_2O_2-induced hyperpolarization on the second application, TTX and AARBC compared to respective control were 101.3 ± 10.1% (n = 8, $p > 0.05$), 85.3 ± 8.9% (n = 8, $p > 0.05$), and 97.5 ± 13.3% (n = 6, p > 0.05), respectively. These findings imply that H_2O_2 directly acts on postsynaptic GnRH neurons to induce hyperpolarization effect.

H_2O_2-mediated hyperpolarization is due to activation of K_{ATP} channels

When exposed to exogenous H_2O_2, hyperpolarization and reduced excitation are hypothesized to be caused by the activation of potassium channels in various neuronal cells (18, 23). As a result, we examined hyperpolarization caused by H_2O_2 exposure in the presence of potassium channel blockers such as TEA, $BaCl_2$, and glibenclamide. Blocker concentrations utilized in this study have been shown to be able to inhibit potassium channels in brain slices (32–34). To confirm the involvement of potassium channels in the hyperpolarizing effect of H_2O_2, the response elicited by H_2O_2 was examined in the presence of non-specific K^+ channel blocker, TEA. The hyperpolarizing impact of H_2O_2 was maintained even in the presence of TEA (Figure 5A).

Next, hyperpolarization induced by H_2O_2 exposure was recorded in the presence of $BaCl_2$, a broad-spectrum potassium channel blocker. In the presence of $BaCl_2$, the hyperpolarization induced by H_2O_2 was partially suppressed (Figure 5B). Next, glibenclamide, K_{ATP} channel blocker, was coapplied with H_2O_2. After treatment with glibenclamide, five of nine GnRH neurons depolarized with increased firing frequency. Glibenclamide also prevented H_2O_2-elicited hyperpolarization of all neurons examined (Figure 5C). As shown in Figure 5D, average relative hyperpolarization percentages induced by H_2O_2 in the presence of TEA, $BaCl_2$ and glibenclamide compared to those by H_2O_2 alone were 91.0 ± 12.4% (n = 7, $p > 0.05$), 70.0 ± 6.04% (n = 7, $^{**}p < 0.01$), and 10.5 ± 1.52% (n = 9, $^{***}p < 0.001$), respectively. These findings imply a complete involvement of K_{ATP} channels in H_2O_2-mediated hyperpolarization of GnRH neurons.

Role of endogenous H_2O_2 in regulating excitability of GnRH neurons

In this study, exogenous H_2O_2 was identified as a possible regulator of GnRH neuron activity, influencing membrane potential and spontaneous firing activities. Next, we determined whether elevation in endogenously produced H_2O_2 could affect the activity of these cells. Recent studies have shown that endogenous H_2O_2 amplification can regulate neuronal excitability in distinct neuronal populations (23, 35).To explore the influence of endogenous H_2O_2 on GnRH neurons excitability, ATZ (1 mM), a CAT inhibitor, and MCS (1 mM), a GPx inhibitor, were bath applied. ATZ and MCS have been shown to increase the production of intracellular H_2O_2 in cells (23, 35). Using ATZ, we first examined the effect of CAT inhibition on GnRH neuronal activity. Except for one neuron that displayed depolarization of 19.7 mV, bath administration of 1mM ATZ had no significant effect on membrane potential or

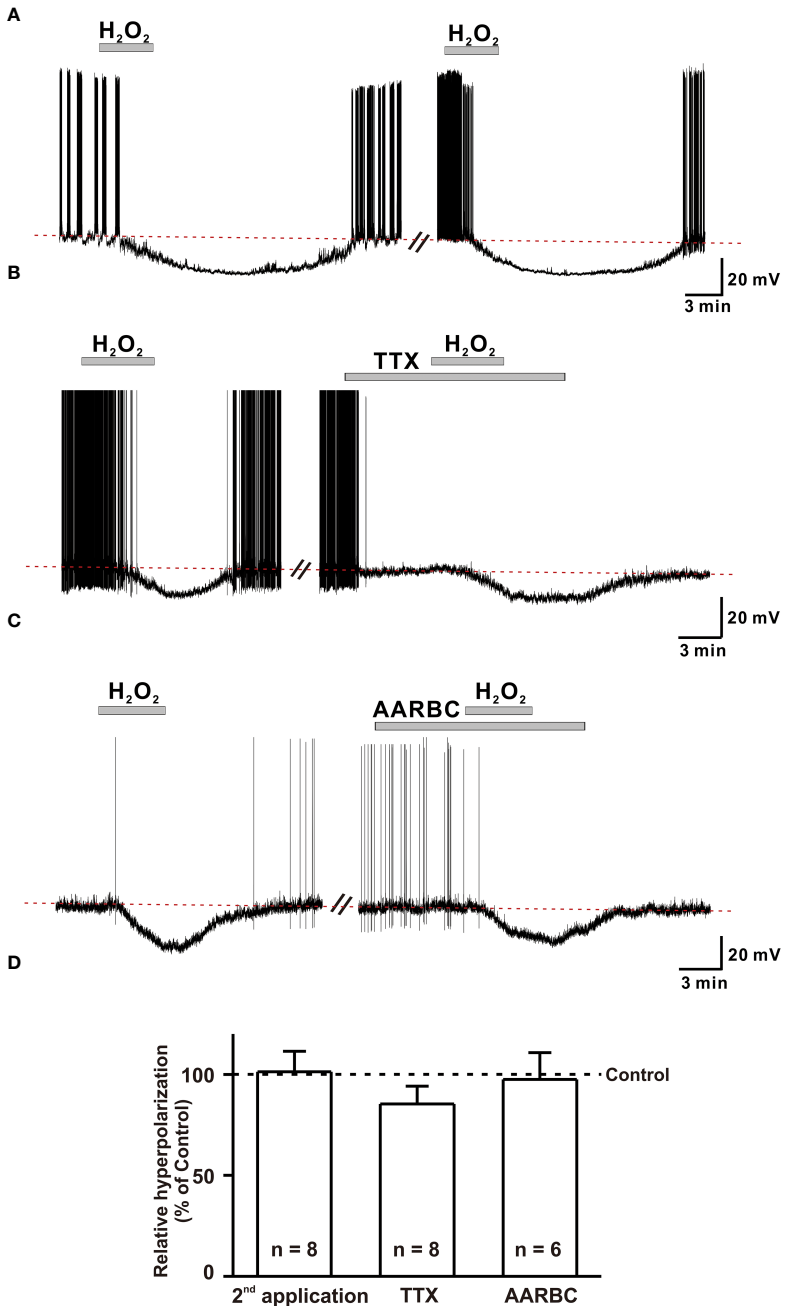

FIGURE 4
H_2O_2 acts on GnRH neurons post-synaptically. **(A)** A representative trace showing repeatable hyperpolarization induced by 1 mM H_2O_2 under a whole-cell current clamp. **(B, C)** Representative traces showing persistence of H_2O_2 induced hyperpolarization response in the presence of (TTX, 0.5 μM), the voltage-sensitive Na+ channel blocker and amino-acid receptor blocking cock-tail (AARBC), respectively. **(D)** A bar diagram showing mean relative values of hyperpolarization induced by 1 mM H_2O_2 on 2nd application, in the presence of TTX, and in the presence of AARBC ($p > 0.05$; paired *t*-test).

spontaneous activity of all GnRH neurons examined (Figure 6A). The frequency of spontaneous firing under ATZ treatment remained considerably unaltered compared to that of the control as shown in Figure 6B (Control: 1.68 ± 0.229, ATZ: 1.63 ± 0.22; n = 9; $p > 0.05$). Inhibiting GPx with MCS resulted in a partial cessation of spontaneous activity in most (13/17) GnRH neurons and a complete blockade in four neurons. In the presence of MCS, the spontaneous firing activity of GnRH neurons decreased from 1.90 ± 0.32 Hz to 0.80 ± 0.23 Hz (n = 17; $p < 0.05$; Figures 6C, D), with an average decrease of 66.2 ±

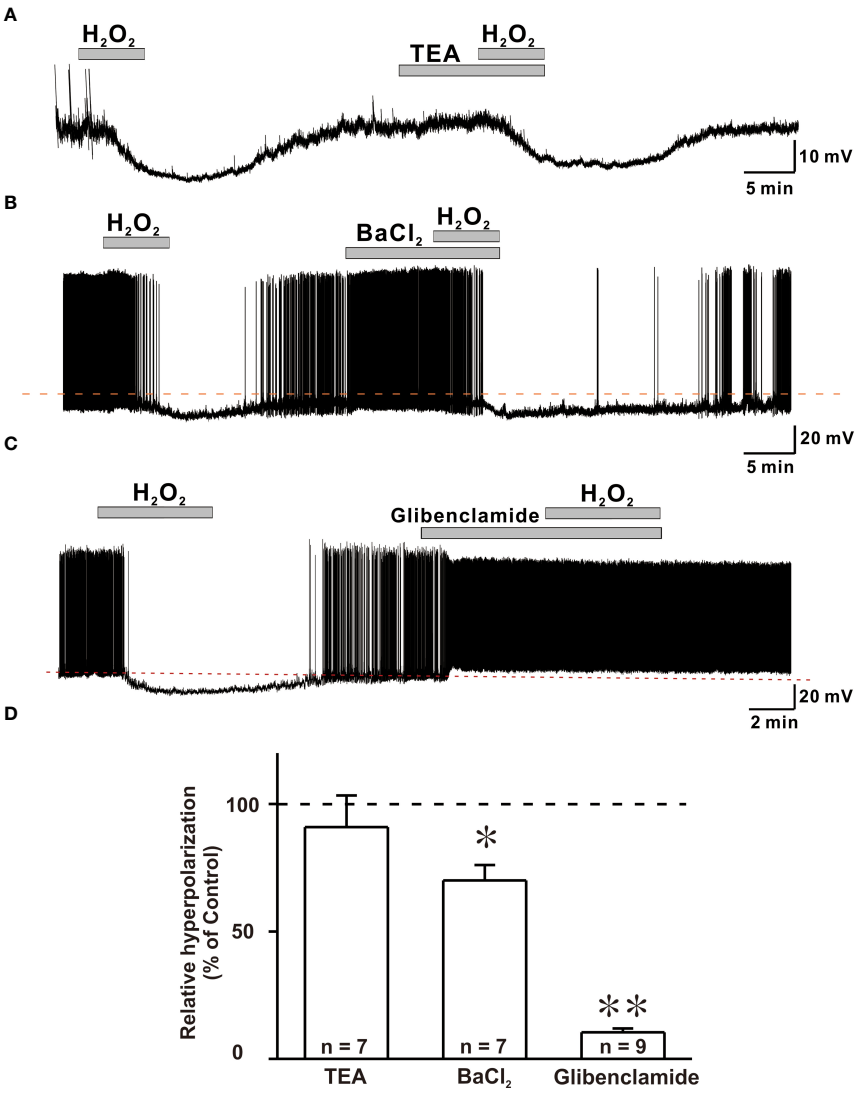

FIGURE 5
ATP-sensitive potassium channels (KATP) are susceptible to H2O2-induced hyperpolarization in GnRH neurons. **(A, B)** Representative traces showing persistence of H2O2-induced hyperpolarization response in the presence of TEA and BaCl2, respectively. **(C)** A representative trace showing complete blockade of hyperpolarization induced by 1mM H2O2 by KATP channel blocker glibenclamide under whole-cell current clamp. **(D)** A bar diagram depicting mean relative values of hyperpolarization caused by 1 mM H2O2 in the presence of various potassium channel blockers (TEA: n = 7, no significant; BaCl2: n = 7, *p < 0.05; glibenclamide: n = 9, **p < 0.01, paired t-test).

5.2%. In addition, MCS exposure resulted in membrane response in 9 of 17 GnRH neurons tested. Among them, seven neurons displayed a slight depolarization (3.75 ± 0.43 mV, n = 7), whereas the remaining two exhibited hyperpolarization of -3.70 ± 0.67 mV. All changes were reversible upon washout of MCS with ACSF.

Discussion

For the first time, this study shows that the majority of adult GnRH neurons are vulnerable to oxidative stress. This study aimed to determine the role of ROS H_2O_2 in modulating the GnRH neuronal activity. Our electrophysiological data demonstrated that exogenous H_2O_2 elicited post-synaptic inhibition of activities of most adult GnRH neurons *via* activation of K_{ATP} channels. Furthermore, immature GnRH neurons, unlike adult GnRH neurons, exhibited excitation upon H_2O_2 exposure. The vulnerability of GnRH neurons to H_2O_2 increased with postnatal development. H_2O_2 sensitivity to adult GnRH neurons was found to be highly dependent on H_2O_2 concentration and the estrous cycle of females. In addition, inhibiting GPx caused GnRH neurons to lose their spontaneous activity.

The hypothalamus is a predominant brain area that receives integrated information from multiple sources, including

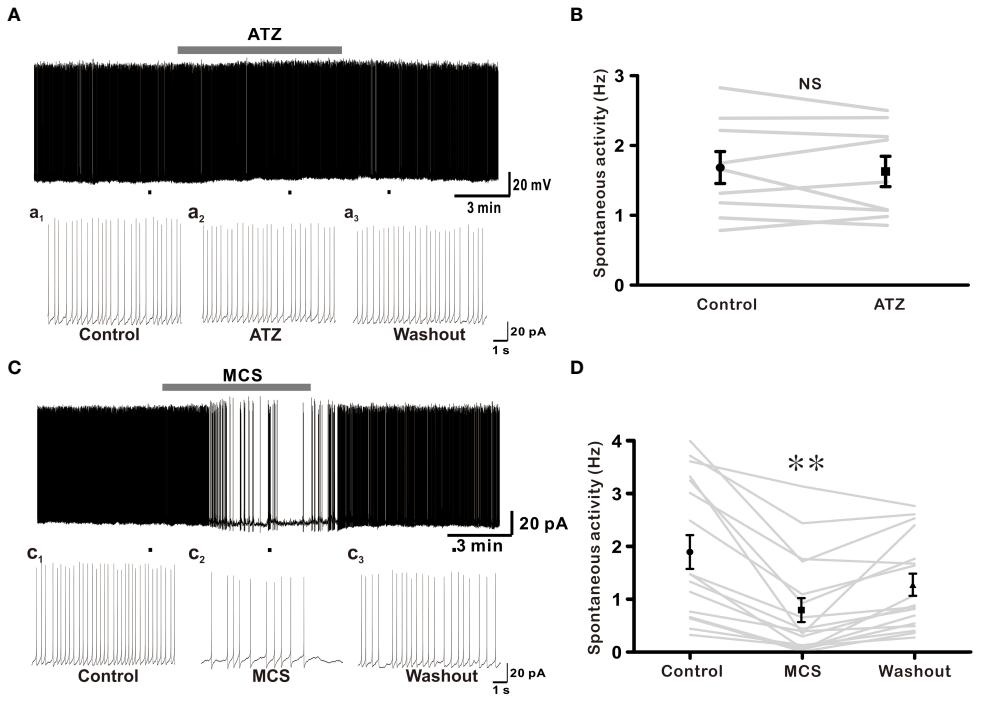

FIGURE 6
Glutathione peroxidase (GPx) inhibition suppresses excitability of GnRH neurons. **(A)** A representative current-clamp trace showing no effect of 1 mM ATZ (catalase inhibitor) on GnRH neurons. **(C)** A typical current-clamp trace showing a decrease of spontaneous activity of GnRH neurons after perfusion with 1 mM MCS, a GPx inhibitor. **(B, D)** Before and after plot showing effects of ATZ and MCS on mean spontaneous firing of GnRH neurons, respectively (**$p < 0.01$; one-way ANOVA).

hormones, neurotransmitters, and metabolites, to regulate homeostasis, energy metabolism, and hormone release (14, 36). Furthermore, the hypothalamus is highly susceptible to oxidative stress. In addition, NADPH oxidase, a neuronal enzyme that produces ROS, is found in the hypothalamus, especially in the arcuate nucleus (ARC), ventromedial (VMN), and PVN regions (14, 17). The ARC, PVN, and VMN are known to contain neuromodulators that affect fertility (37). NPY/AgRP and POMC/CART neurons in the ARC project directly onto GnRH neuron cell bodies and nerve terminals (38, 39). Neuropeptides released by these neurons can influence GnRH neuron activity (40, 41). Furthermore, cellular activity of the NPY/AgRP and POMC/CART neuronal population is directly controlled by intracellular ROS (17). In the case of GnRH neurons, ROS H_2O_2 appeared to influence neuronal activity across postnatal development in a concentration-dependent and estrous-cycle-dependent manner.

Our findings, revealed that 1 mM H_2O_2 inhibited adult GnRH neurons, consistent with previous studies on dopamine neurons (23), PVN (18), substantia nigra pars reticulate (SNr) GABAergic neurons (35), and intrinsic cardiac ganglia neurons (42). Most studies using adult experimental animals have shown that H_2O_2 can inhibit neuronal excitability (18, 23, 35, 42). However, unlike adults, most immature GnRH neurons were stimulated by the same concentration of H_2O_2. According to previous studies, oxidative stress vulnerability increase with age, with young rats being more resistant to ROS than adults (30). Furthermore, H_2O_2 has both excitatory and inhibitory effects on neuronal excitability depending on neuronal population and brain location (43).

In the present study, the responsiveness of adult female GnRH neurons to H_2O_2 exposure varied throughout the estrous cycle. Circulating gonadal hormones, which fluctuate during estrous phases (44), can significantly impact GnRH neuronal excitability (45). Some studies show that proestrus mice had higher GnRH neuronal activity than mice in other estrous phases (46, 47). On the other hand, *Piet et al.* have reported less GnRH neuronal activity in proestrus mice than in mice at diestrus stage (48). According to previous studies, estradiol appears to have a positive feedback effect on GnRH neuronal activity in proestrus mice (49), and a neuroprotective effect against oxidative stress (50). We found that GnRH neurons in proestrus mice were more vulnerable to oxidative stress than those in estrous and diestrous stages. There is no information on how circulating steroid hormones influence GnRH neurons during oxidative stress. This requires further investigation.

In mature GnRH neurons, H_2O_2 mainly caused hyperpolarization and action potential suppression. Such H_2O_2-mediated response was retained in the presence of voltage-gated Na^+ channel blocker TTX and AARBC,

indicating a post-synaptic effect of H_2O_2 on GnRH neurons. H_2O_2 has been previously shown to have a similar post-synaptic effect (18). Studies have shown that H_2O_2 can induce membrane potential depolarization and hyperpolarization *via* different mechanisms. H_2O_2 can activate transient receptor potential channels (35, 51) or inhibit inward-rectifying K^+ channels to induce depolarization (52). Opening of K_{ATP} channels leads to hyperpolarization (18, 23, 35). Activation of barium-sensitive potassium channels by H_2O_2 exposure has also been reported in a few studies (53). Similar to other studies, we observed the involvement of K_{ATP} and Ba^{2+} sensitive potassium channel in the hyperpolarization of GnRH neurons induced by H_2O_2.

The potassium channel plays a role in hormone and neurotransmitter release (54). Identifying signaling molecules that affect K^+ channels in GnRH neurons is of particular interest nowadays. Studies have shown that GnRH neurons are susceptible to metabolic stress, which activates K_{ATP} channels. Functional K_{ATP} channel subunits have been detected in GnRH neurons (55). When the ATP/ADP ratio falls, K_{ATP} channels, which govern resting membrane properties of neurons, will open, causing cells to hyperpolarize and provide neuroprotection (56). Aside from neuroprotection, K_{ATP} channels are involved in glucose homeostasis in the hypothalamus, including GnRH neurons (55, 57). Recently, H_2O_2 has been identified as a signaling molecule for K_{ATP} channel activation (23, 35). Furthermore, inhibiting GPx and CAT of antioxidant systems can increase endogenous H_2O_2 in midbrain dopamine neurons (23) and SNr GABAergic neurons (35), resulting in K_{ATP} channel activation.

GPx and CAT are two major enzymes involved in H_2O_2 detoxification. Therefore, antioxidant enzymes inhibitors ATZ and MCS were used to determine the effect of endogenous H_2O_2 on GnRH neuronal excitability in the present study. ATZ is a CAT inhibitor that elevates endogenous H_2O_2 (58). It has a similar effect as exogenous H_2O_2 on midbrain dopamine neurons (23). However, ATZ showed no effect on GnRH neuron excitability. On the other hand, inhibition of GPx, another antioxidant enzyme, caused GnRH neurons to lose their spontaneous activity. *Avshalumov et al.* have reported a similar result. They showed that MCS treatment caused most dopamine neurons in the midbrain to hyperpolarize and lose their spontaneous activity (23). CAT and GPx are endogenous antioxidant-active enzymes responsible for the enzymatic clearance of H_2O_2, changing H_2O_2 into H_2O and O_2 molecules (18, 59). GPx is a crucial enzyme in the cytosol that plays an important role in the host's defense against oxidative stress (60). Its principal antioxidant enzyme activity is to protect neurons against H_2O_2 toxicity (61). CAT is predominantly found in peroxisomes while GPx is distributed in the cytosol and mitochondria (61). Inhibiting GPx may cause H_2O_2 to accumulate in the cytosol, hence regulating neuronal excitability.

GnRH neurons not only can respond to hormonal, neurotransmitter, and neuropeptide inputs, but also can react directly to metabolic signals (55, 62, 63). The generation of reactive oxygen species is commonly linked to metabolic signals. In aging and pathologic situations, impairment in the antioxidant defense system becomes more noticeable, resulting in increased ROS generation (64, 65). The interaction between energy metabolism and ROS becomes more evident during aging, increasing the risk of age-related illnesses (66). Female reproductive disorders such as endometriosis, polycystic ovary syndrome, preeclampsia, and recurrent pregnancy loss can result from a pro-oxidant/antioxidant imbalance (12). Similarly, oxidative stress can affect sperm function in males, resulting in infertility (67). We demonstrated that H_2O_2 inhibited the majority of adult GnRH from both sex, which could reinforce the preexisting hypothesis about oxidative stress is linked to infertility. Furthermore, the direct impact of H_2O_2 on GnRH neuronal excitability *via* ion-channel mechanism could explain the cause of ROS disruption in the crosstalk of the HPG axis with another endocrine axis at hypothalamic levels and ROS-induced hormonal imbalance that leads to infertility.

In conclusion, current findings indicate that H_2O_2 can regulate K_{ATP} channels in adult GnRH neurons. Potassium channels can influence hormone and neurotransmitter release. Thus, oxidative stress regulating K_{ATP} channels in hypothalamic GnRH neurons could modulate pulsatile release of gonadotropins, impacting the reproductive axis.

Data availability statement

The raw data supporting the conclusions of this article will be made available by the authors, without undue reservation.

Ethics statement

The animal study was reviewed and approved by Institutional Animal Care and Use Committee of Jeonbuk National University (CBNU 2020-0122).

Author contributions

SR performed the experiments, analyzed the data, and wrote the draft. SJ contributed to reviewing and editing the draft. DC and SH conceptualized and design the study and completed the manuscript. All authors contributed to the article and approved the submitted version.

Funding

This research was supported by the National Research Foundation of Korea (NRF) grant funded by the Korean government (MSIT) (2021R1F1A1045406) and

(2021R1F1A1046123). The funders had no role in the design, analysis, or writing of this article.

Conflict of interest

The authors declare that the research was conducted in the absence of any commercial or financial relationships that could be construed as a potential conflict of interest.

Publisher's note

References

1. Beckhauser TF, Francis-Oliveira J, De Pasquale R. Reactive oxygen species: physiological and physiopathological effects on synaptic plasticity: supplementary issue: brain plasticity and repair. *J Exp Neurosci* (2016) 10:23–48. doi: 10.4137/JEN.S39887

2. Park A, Lee HI, Semjid D, Kim DK, Chun SW. Dual effect of exogenous nitric oxide on neuronal excitability in rat substantia gelatinosa neurons. *Neural Plast* (2014) 2014:628531. doi: 10.1155/2014/628531

3. Darbandi M, Darbandi S, Agarwal A, Sengupta P, Durairajanayagam D, Henkel R, et al. Reactive oxygen species and male reproductive hormones. *Reprod Biol Endocrinol* (2018) 16(1):87. doi: 10.1186/s12958-018-0406-2

4. Phaniendra A, Jestadi DB, Periyasamy L. Free radicals: properties, sources, targets, and their implication in various diseases. *Indian J Clin Biochem* (2015) 30 (1):11–26. doi: 10.1007/s12291-014-0446-0

5. Checa J, Aran JM. Reactive oxygen species: Drivers of physiological and pathological processes. *J Inflammation Res* (2020) 13:1057–73. doi: 10.2147/JIR.S275595

6. Chen Y, McMillan-Ward E, Kong J, Israels S, Gibson S. Oxidative stress induces autophagic cell death independent of apoptosis in transformed and cancer cells. *Cell Death Differ* (2008) 15(1):171–82. doi: 10.1038/sj.cdd.4402233

7. Kurutas EB. The importance of antioxidants which play the role in cellular response against oxidative/nitrosative stress: current state. *Nutr J* (2016) 15(1):71. doi: 10.1186/s12937-016-0186-5

8. Birben E, Sahiner UM, Sackesen C, Erzurum S, Kalayci O. Oxidative stress and antioxidant defense. *World Allergy Organ J* (2012) 5(1):9–19. doi: 10.1097/WOX.0b013e3182439613

9. Marques P, Skorupskaite K, George JT, Anderson RA. *Physiology of GnRH and gonadotropin secretion* (2000) MDText.com, Inc. Available at: http://www.ncbi.nlm.nih.gov/pubmed/25905297.

10. Terasaka T, Adakama ME, Li S, Kim T, Terasaka E, Li D. Et.al. reactive oxygen species link gonadotropin-releasing hormone receptor signaling cascades in the gonadotrope. *Front Endocrinol* (2017) 8:286. doi: 10.3389/fendo.2017.00286

11. Razmara A, Duckles SP, Krause DN, Procaccio V. Estrogen suppresses brain mitochondrial oxidative stress in female and male rats. *Brain Res* (2007) 1176:71–81. doi: 10.1016/j.brainres.2007.08.036

12. Agarwal A, Aponte-Mellado A, Premkumar BJ, Shaman A, Gupta S. The effects of oxidative stress on female reproduction: a review. *Reprod Biol Endocrinol* (2012) 10(1):1–31. doi: 10.1186/1477-7827-10-49

13. Barati E, Nikzad H, Karimian M. Oxidative stress and male infertility: Current knowledge of pathophysiology and role of antioxidant therapy in disease management. *Cell Mol Life Sci* (2020) 77(1):93–113. doi: 10.1007/s00018-019-03253-8

14. Drougard A, Fournel A, Valet P, Knauf C. Impact of hypothalamic reactive oxygen species in the regulation of energy metabolism and food intake. *Front Neurosci* (2015) 9:56. doi: 10.3389/fnins.2015.00056

15. Benani A, Troy S, Carmona MC, Fioramonti X, Lorsignol A, Leloup C, et al. Role for mitochondrial reactive oxygen species in brain lipid sensing: redox regulation of food intake. *Diabetes* (2007) 56(1):152–60. doi: 10.2337/db06-0440

16. St-Louis R, Parmentier C, Raison D, Grange-Messent V, Hardin-Pouzet H. Reactive oxygen species are required for the hypothalamic osmoregulatory response. *Endocrinology* (2012) 153(3):1317–29. doi: 10.1210/en.2011-1350

17. Gyengesi E, Paxinos G B, Andrews Z. Oxidative stress in the hypothalamus: the importance of calcium signaling and mitochondrial ROS in body weight regulation. *Curr Neuropharmacol* (2012) 10(4):344–53. doi: 10.2174/157015912804143496

18. Dantzler HA, Matott MP, Martinez D, Kline DD. Hydrogen peroxide inhibits neurons in the paraventricular nucleus of the hypothalamus *via* potassium channel activation. *Am J Physiol Regul Integr Comp Physiol* (2019) 317(1):R121–33. doi: 10.1152/ajpregu.00054.2019

19. Giniatullin A, Giniatullin R. Dual action of hydrogen peroxide on synaptic transmission at the frog neuromuscular junction. *J Physiol* (2003) 552(1):283–93. doi: 10.1113/jphysiol.2003.050690

20. Chen X, Song M, Zang B, Zang Y. Reactive oxygen species regulate T cell immune response in the tumor microenvironment. *Oxid Med Cell Longev* (2016) 2016:1580967. doi: 10.1155/2016/1580967

21. D'Autréaux B, Toledano MB. ROS as signalling molecules: mechanisms that generate specificity in ROS homeostasis. *Nat Rev Mol Cell Biol* (2007) 8(10):813–24. doi: 10.1038/nrm2256

22. Ledo A, Fernandes E, Salvador A, Laranjinha J, Barbosa R. *In vivo* hydrogen peroxide diffusivity in brain tissue supports volume signalling activity. *Redox Biol* (2022) 50:102250. doi: 10.1016/j.redox.2022.102250

23. Avshalumov MV, Chen BT, Koós T, Tepper JM, Rice ME. Endogenous hydrogen peroxide regulates the excitability of midbrain dopamine neurons *via* ATP-sensitive potassium channels. *J Neurosci* (2005) 25(17):4222–31. doi: 10.1523/JNEUROSCI.4701-04.2005

24. Ohashi M, Hirano T, Watanabe K, Shoji H, Ohashi N, Baba H, et al. Hydrogen peroxide modulates neuronal excitability and membrane properties in ventral horn neurons of the rat spinal cord. *Neuroscience* (2016) 331:206–20. doi: 10.1016/j.neuroscience.2016.06.033

25. Bal R, Ozturk G, Etem EO, Him A, Cengiz N, Kuloglu T, et al. Modulation of excitability of stellate neurons in the ventral cochlear nucleus of mice by ATP-sensitive potassium channels. *J Membr Biol* (2018) 251(1):163–78. doi: 10.1007/s00232-017-0011-x

26. Takahashi A, Mikami M, Yang J. Hydrogen peroxide increases GABAergic mIPSC through presynaptic release of calcium from IP3 receptor-sensitive stores in spinal cord substantia gelatinosa neurons. *Eur J Neurosci* (2007) 25(3):705–16. doi: 10.1111/j.1460-9568.2007.05323.x

27. Ohashi M, Hirano T, Watanabe K, Katsumi K, Ohashi N, Baba H, et al. Hydrogen peroxide modulates synaptic transmission in ventral horn neurons of the rat spinal cord. *J Physiol* (2016) 594(1):115–34. doi: 10.1113/JP271449

28. Spergel DJ, Krüth U, Hanley DF, Sprengel R, Seeburg PH. GABA-and glutamate-activated channels in green fluorescent protein-tagged gonadotropin-releasing hormone neurons in transgenic mice. *J Neurosci* (1999) 19(6):2037–50. doi: 10.1523/JNEUROSCI.19-06-02037.1999

29. Rijal S, Cho DH, Park SA, Jang SH, Ábrahám IM, Han SK. Melatonin suppresses the kainate receptor-mediated excitation on gonadotropin-releasing hormone neurons in female and Male prepubertal mice. *Int J Mol Sci* (2020) 21 (17):5991. doi: 10.3390/ijms21175991

30. Carrascal L, Gorton E, Pardillo-Díaz R, Perez-García P, Gómez-Oliva R, Castro C, et al. Age-dependent vulnerability to oxidative stress of postnatal rat pyramidal motor cortex neurons. *Antioxidants* (2020) 9(12):1307. doi: 10.3390/antiox9121307

31. Pardillo-Díaz R, Carrascal L, Ayala A, Nunez-Abades P. Oxidative stress induced by cumene hydroperoxide evokes changes in neuronal excitability of rat motor cortex neurons. *Neuroscience* (2015) 289:85–98. doi: 10.1016/j.neuroscience.2014.12.055

32. D'Ambrosio R, Gordon DS, Winn HR. Differential role of KIR channel and Na^+/K^+-pump in the regulation of extracellular k^+ in rat hippocampus. *J Neurophysiol* (2002) 87(1):87–102. doi: 10.1152/jn.00240.2001

33. Fujimura N, Tanaka E, Yamamoto S, Shigemori M, Higashi H. Contribution of ATP-sensitive potassium channels to hypoxic hyperpolarization in rat hippocampal CA1 neurons. *vitro J Neurophysiol* (1997) 77(1):378–85. doi: 10.1152/jn.1997.77.1.378

34. Bhattarai JP, Roa J, Herbison AE, Han SK. Serotonin acts through 5-HT_1 and 5-HT_2 receptors to exert biphasic actions on GnRH neuron excitability in the mouse. *Endocrinology* (2014) 155(2):513–24. doi: 10.1210/en.2013-1692

35. Lee CR, Witkovsky P, Rice ME. Regulation of substantia nigra pars reticulata GABAergic neuron activity by H_2O_2 *via* flufenamic acid-sensitive channels and K_{ATP} channels. *Front Syst Neurosci* (2011) 5:14. doi: 10.3389/fnsys.2011.00014

36. Cai D, Liu T. Hypothalamic inflammation: a double-edged sword to nutritional diseases. *Ann N Y Acad Sci* (2011) 1243(1):E1–E39. doi: 10.1111/j.1749-6632.2011.06388.x

37. Navarro VM. New insights into the control of pulsatile GnRH release: the role of Kiss1/neurokinin b neurons. *Front Endocrinol* (2012) 3:48. doi: 10.3389/fendo.2012.00048

38. Campbell RE, Cowley MA, Smith MS, Grove KL. Hypothalamic circuitry of neuropeptide y regulation of neuroendocrine function and food intake *via* the Y_5 receptor subtype. *Neuroendocrinology* (2001) 74(2):106–19. doi: 10.1159/000054676

39. Zheng SX, Bosch MA, Rønnekleiv OK. μ-opioid receptor mRNA expression in identified hypothalamic neurons. *J Comp Neurol* (2005) 487(3):332–44. doi: 10.1002/cne.20557

40. Klenke U, Constantin S, Wray S. Neuropeptide y directly inhibits neuronal activity in a subpopulation of gonadotropin-releasing hormone-1 neurons *via* Y1 receptors. *Endocrinology* (2010) 151(6):2736–46. doi: 10.1210/en.2009-1198

41. Roa J, Herbison AE. Direct regulation of GnRH neuron excitability by arcuate nucleus POMC and NPY neuron neuropeptides in female mice. *Endocrinology* (2012) 153(11):5587–99. doi: 10.1210/en.2012-1470

42. Whyte K, Hogg RC, Dyavanapalli J, Harper A, Adams DJ. Reactive oxygen species modulate neuronal excitability in rat intrinsic cardiac ganglia. *Auton Neurosci* (2009) 150(1-2):45–52. doi: 10.1016/j.autneu.2009.04.005

43. Lee CR, Patel JC, O'Neill B, Rice ME. Inhibitory and excitatory neuromodulation by hydrogen peroxide: translating energetics to information. *J Physiol* (2015) 593(16):3431–46. doi: 10.1113/jphysiol.2014.273839

44. Bell MR. Comparing postnatal development of gonadal hormones and associated social behaviors in rats, mice, and humans. *Endocrinology* (2018) 159(7):2596–613. doi: 10.1210/en.2018-00220

45. Radovick S, Levine JE, Wolfe A. Estrogenic regulation of the GnRH neuron. *Front Endocrin* (2012) 3:52. doi: 10.3389/fendo.2012.00052

46. Silveira MA, Burger LL, DeFazio RA, Wagenmaker ER, Moenter SM. GnRH neuron activity and pituitary response in estradiol-induced vs proestrous luteinizing hormone surges in female mice. *Endocrinology* (2017) 158(2):356–66. doi: 10.1210/en.2016-1771

47. Farkas I, Vastagh C, Sárvári M, Liposits Z. Ghrelin decreases firing activity of gonadotropin-releasing hormone (GnRH) neurons in an estrous cycle and endocannabinoid signaling dependent manner. *PloS One* (2013) 8(10):e78178. doi: 10.1371/journal.pone.0078178

48. Piet R, Dunckley H, Lee K, Herbison AE. Vasoactive intestinal peptide excites GnRH neurons in male and female mice. *Endocrinology* (2016) 157(9):3621–30. doi: 10.1210/en.2016-1399

49. Herbison AE. Estrogen positive feedback to gonadotropin-releasing hormone (GnRH) neurons in the rodent: the case for the rostral periventricular area of the third ventricle (RP3V). *Brain Res Rev* (2008) 57(2):277–87. doi: 10.1016/j.brainresrev.2007.05.006

50. Ozacmak VH, Sayan H. The effects of 17β estradiol, 17α estradiol and progesterone on oxidative stress biomarkers in ovariectomized female rat brain subjected to global cerebral ischemic. *Physiol Res* (2009) 58(6):909–12. doi: 10.33549/physiolres.931647

51. Bao L, Avshalumov MV, Rice ME. Partial mitochondrial inhibition causes striatal dopamine release suppression and medium spiny neuron depolarization *via* H_2O_2 elevation, not ATP depletion. *J Neurosci* (2005) 25(43):10029–40. doi: 10.1523/JNEUROSCI.2652-05.2005

52. Bychkov R, Pieper K, Ried C, Milosheva M, Bychkov E, Luft FC, et al. Hydrogen peroxide, potassium currents, and membrane potential in human endothelial cells. *Circulation* (1999) 99(13):1719–25. doi: 10.1161/01.cir.99.13.1719

53. Ostrowski TD, Hasser EM, Heesch CM, Kline DD. H_2O_2 induces delayed hyperexcitability in nucleus tractus solitarii neurons. *Neuroscience* (2014) 262:53–69. doi: 10.1016/j.neuroscience.2013.12.055

54. Yamada M, Inanobe A, Kurachi Y. G Protein regulation of potassium ion channels. *Pharmacol Rev* (1998) 50(4):723–57.

55. Zhang C, Bosch MA, Levine JE, Rønnekleiv OK, Kelly MJ. Gonadotropin-releasing hormone neurons express K_{ATP} channels that are regulated by estrogen and responsive to glucose and metabolic inhibition. *Neurosci* (2007) 27(38):10153–64. doi: 10.1523/JNEUROSCI.1657-07.2007

56. Sun HS, Feng ZP. Neuroprotective role of ATP-sensitive potassium channels in cerebral ischemia. *Acta Pharmacol Sin* (2013) 34(1):24–32. doi: 10.1038/aps.2012.138

57. Miki T, Liss B, Minami K, Shiuchi T, Saraya A, Kashima Y, et al. ATP-sensitive k^+ channels in the hypothalamus are essential for the maintenance of glucose homeostasis. *Nat Neurosci* (2001) 4(5):507–12. doi: 10.1038/87455

58. Zhang M, Qin DN, Suo YP, Su Q, Li HB, Miao YW, et al. Endogenous hydrogen peroxide in the hypothalamic paraventricular nucleus regulates neurohormonal excitation in high salt-induced hypertension. *Toxicol Lett* (2015) 235(3):206–15. doi: 10.1016/j.toxlet.2015.04.008

59. Leloup C, Magnan C, Benani A, Bonnet E, Alquier T, Offer G, et al. Mitochondrial reactive oxygen species are required for hypothalamic glucose sensing. *Diabetes* (2006) 55(7):2084–90. doi: 10.2337/db06-0086

60. Dede FÖ. Periodontal health and disease in glutathione peroxidase. In: *Glutathione system and oxidative stress in health and disease* London, United Kingdom: IntechOpen (2020), p. 83–96.

61. Desagher S, Glowinski J, Premont J. Astrocytes protect neurons from hydrogen peroxide toxicity. *J Neurosci* (1996) 16(8):2553–62. doi: 10.1523/JNEUROSCI.16-08-02553.1996

62. Spergel DJ. Modulation of gonadotropin-releasing hormone neuron activity and secretion in mice by non-peptide neurotransmitters, gasotransmitters, and gliotransmitters. *Front Endocrinol* (2019) 10:329. doi: 10.3389/fendo.2019.00329

63. Spergel DJ. Neuropeptidergic modulation of GnRH neuronal activity and GnRH secretion controlling reproduction: insights from recent mouse studies. *Cell Tissue Res* (2019) 375(1):179–91. doi: 10.1007/s00441-018-2893-z

64. Nita M, Grzybowski A. The role of the reactive oxygen species and oxidative stress in the pathomechanism of the age-related ocular diseases and other pathologies of the anterior and posterior eye segments in adults. *Oxid Med Cell Longev* (2016) 2016:3164734. doi: 10.1155/2016/3164734

65. Rybka J, Kupczyk D, Kędziora-Kornatowska K, Pawluk H, Czuczejko J, Szewczyk-Golec K, et al. Age-related changes in an antioxidant defense system in elderly patients with essential hypertension compared with healthy controls. *Redox Rep* (2011) 16(2):71–7. doi: 10.1179/174329211X13002357050897

66. Quijano C, Trujillo M, Castro L, Trostchansky A. Interplay between oxidant species and energy metabolism. *Redox Biol* (2016) 8:28–42. doi: 10.1016/j.redox.2015.11.010

67. Agarwal A, Virk G, Ong C, Du Plessis SS. Effect of oxidative stress on male reproduction. *World J Mens Health* (2014) 32(1):1–17. doi: 10.5534/wjmh.2014.32.1.1

frontiers | Frontiers in Endocrinology

TYPE Original Research
PUBLISHED 04 January 2023
DOI 10.3389/fendo.2022.993552

OPEN ACCESS

EDITED BY
Claus Yding Andersen,
University of Copenhagen, Denmark

REVIEWED BY
Erik Hrabovszky,
Institute of Experimental Medicine (MTA), Hungary
Vito Salvador Hernandez,
National Autonomous University of Mexico, Mexico

*CORRESPONDENCE
Gergely Kovács
gergely.kovacs@aok.pte.hu

SPECIALTY SECTION
This article was submitted to Reproduction, a section of the journal Frontiers in Endocrinology

RECEIVED 13 July 2022
ACCEPTED 12 December 2022
PUBLISHED 04 January 2023

CITATION
Kövesdi E, Udvarácz I, Kecskés A, Szőcs S, Farkas S, Faludi P, Jánosi TZ, Ábrahám IM and Kovács G (2023) 17β-estradiol does not have a direct effect on the function of striatal cholinergic interneurons in adult mice *in vitro*. *Front. Endocrinol.* 13:993552. doi: 10.3389/fendo.2022.993552

17β-estradiol does not have a direct effect on the function of striatal cholinergic interneurons in adult mice *in vitro*

Erzsébet Kövesdi[1,2], Ildikó Udvarácz[1,2], Angéla Kecskés[2,3], Szilárd Szőcs[1,3], Szidónia Farkas[1,2], Péter Faludi[1,2], Tibor Z. Jánosi[1,2], István M. Ábrahám[1,2] and Gergely Kovács[1,2]*

[1]Institute of Physiology, Medical School, University of Pécs, Pécs, Hungary, [2]Centre for Neuroscience, Szentágothai Research Centre, Pécs, Hungary, [3]Department of Pharmacology and Pharmacotherapy, Medical School, University of Pécs, Pécs, Hungary

The striatum is an essential component of the basal ganglia that is involved in motor control, action selection and motor learning. The pathophysiological changes of the striatum are present in several neurological and psychiatric disorder including Parkinson's and Huntington's diseases. The striatal cholinergic neurons are the main regulators of striatal microcircuitry. It has been demonstrated that estrogen exerts various effects on neuronal functions in dopaminergic and medium spiny neurons (MSN), however little is known about how the activity of cholinergic interneurons are influenced by estrogens. In this study we examined the acute effect of 17β-estradiol on the function of striatal cholinergic neurons in adult mice *in vitro*. We also tested the effect of estrus cycle and sex on the spontaneous activity of cholinergic interneurons in the striatum. Our RNAscope experiments showed that ERα, ERβ, and GPER1 receptor mRNAs are expressed in some striatal cholinergic neurons at a very low level. In cell-attached patch clamp experiments, we found that a high dose of 17β-estradiol (100 nM) affected the spontaneous firing rate of these neurons only in old males. Our findings did not demonstrate any acute effect of a low concentration of 17β-estradiol (100 pM) or show any association of estrus cycle or sex with the activity of striatal cholinergic neurons. Although estrogen did not induce changes in the intrinsic properties of neurons, indirect effects *via* modulation of the synaptic inputs of striatal cholinergic interneurons cannot be excluded.

KEYWORDS

17β-estradiol, cholinergic, striatum, RNAscope, estrogen receptor

1 Introduction

Basal ganglia are a group of deep subcortical nuclei in the brain that are essential for motor learning, formation of procedural memory and motor control. The striatum is the major input nucleus of the basal ganglia and is composed of two regions, the dorsal and the ventral striatum. In primates, the caudate nucleus and the putamen form the dorsal striatum, which corresponds to the dorsomedial (DMS) and dorsolateral (DLS) striatum in rodents, respectively. The DMS and the DLS receive inputs from different areas of the cortex, namely, afferents from the prefrontal and the associative cortex reach the DMS, whereas information from the sensorimotor area conveyed to the DLS (1, 2). Based on histochemical identification, the dorsal striatum is composed of two main compartments known as patches (striosomes) and matrix (3). The dorsal striatum is mostly involved in motor learning, action selection, execution and termination. The ventral striatum is composed of the nucleus accumbens and the olfactory tubercle, and is mainly engaged in goal-directed movement and reward-related behavior (2, 4).

Most of the striatal neurons are GABAergic medium spiny neurons (MSN) also known as spiny projection neurons (SPN). They form the sole output of the striatum (direct and indirect pathways). The remaining ~5% of the striatal neurons consist of different classes of aspiny interneurons including parvalbumin-positive, fast-spiking neurons, somatostatin-positive low-threshold spiking neurons, calretinin-positive neurons, and cholinergic interneurons (5).

Cholinergic neurons form a specific population of neurons in the brain that synthesize and release acetylcholine (ACh) as a neurotransmitter. Using specific markers for the intracellular metabolism of acetylcholine such as choline acetyl-transferase (CHAT), acetylcholine esterase (AChE), vesicular acetylcholine transporter (VAChT), or high-affinity choline transporter 1 (ChT1), cholinergic neurons were identified and localized in several discrete brain regions including the striatum (6). Although only ~1% of the striatal neurons are cholinergic interneurons, the highest levels of cholinergic markers are found in the striatum. Despite the fact that the somata of cholinergic interneurons are mostly located in the flanking region of the extrastriosomal matrix compartment of the striatum, cholinergic interneurons regulate and modulate the function of almost all striatal neurons in both striatosomes and the matrix compartment, innervating them with very extensive and massive axonal arborizations (3, 7). The identification of striatal cholinergic neurons (ChINs) is easy, based on the expression of the aforementioned specific neurochemical markers, their distinct morphological appearance (giant aspiny neurons with large (15-50 µm) soma), and unique electrophysiological parameters such as a relatively depolarized resting membrane potential, I_h current, prominent afterhyperpolarization and wide action potential (8). In addition, striatal ChINs act as autonomous pacemakers. Several studies suggest that *in vitro*, spontaneously firing ChINs most probably correspond to tonically active neurons (TANs) identified by *in vivo* recordings in the putamen (9). The ChINs express several receptors for different neurotransmitters as they play a central role in the striatal circuitry. They receive significant input from midbrain dopaminergic neurons (D2/D5 receptors), and other striatal ChINs (nAChR and mAChR). They also have extensive glutamatergic innervation from both the cortex and several thalamic nuclei (ionotropic and metabotropic glutamate receptors) and a variety of GABA-ergic inputs ($GABA_A$ receptors) (10, 11). On the other hand, besides modulating the activity of GABAergic and glutamatergic striatal afferents, striatal ChINs exert direct postsynaptic effects on MSN activity, which are the main output of the striatum, *via* primarily M1 subtypes of mAChRs (7).

In the nervous system estrogens play a role in sexual differentiation, synaptic plasticity, neuronal differentiation, and neuroprotection. Estrogens also modulate several striatal functions (12–14).

The cellular effects of estrogens are mediated by three different G protein-coupled receptors, namely ERα, ERβ, and G protein-coupled estrogen receptor 1 (GPER1 or GPR30). These receptors could reside in the nucleus (ERα and ERβ) or have an extranuclear localization. Although using *in situ* hybridization, a few groups (15, 16) detected no expression of ERα and ERβ mRNA in the striatum, the majority of previous studies showed that the expression of estrogen receptors in the rodent dorsal striatum was sparse and was weak to moderate even in positive cells (17–22). In addition, recent findings demonstrate that ERα and ERβ expression are high in mouse pups and decreases with time resulting in low or very low expression in adults (23, 24). Finally, ERα and GPER1 were detected in a small proportion of cholinergic interneurons using electron microscopy (17).

Striatal behavior as assessed using locomotor tests showed large differences between male and female animals under resting conditions or after psychostimulant administration (see (13) for review).

Estrogens have a wide variety of genomic and non-genomic effects on the dopaminergic system and MSN neurons in the striatum (see (12–14, 25) for reviews). Striatal cholinergic neurons have a pivotal role in the modulation and function of striatal microcircuitry interacting DA and MSN neurons among many others (10).

Although there is an extensive literature about the effect of estrogens on dopaminergic neurons there is not much information available about estrogens and striatal cholinergic neurons. Therefore, the aim of the present study was to examine how 17β-estradiol and sex affect the spontaneous activity of cholinergic interneurons *in vitro* in the murine dorsal striatum.

10.3389/fendo.2022.993552

2 Materials and methods

2.1 Animals

All animals (35 transgenic and 6 wild type C57Bl/6) were bred and kept in the temperature- and humidity-controlled animal facility of the Szentágothai Research Center under a 12-hour light/12-hour dark light cycle. The animals used in the experiments were fed with a standard chow and had access to water ad libitum. All experiments were performed on adult mice older than 3 months in accordance with the regulations of the European Community Council Directive and the Animal Welfare Committee of the University of Pécs. To generate ChAT-Cre-tdTomato transgenic mice ChAT-IRES-Cre knock in mice (B6,129S6-*Chat*$^{tm2(cre)Lowl}$/J) and the reporter mouse line B6,129S6-*Gt(ROSA)26Sor*$^{tm9(CAG-tdTomato)Hze}$/J were crossed.

2.2 Tissue fixation and slice preparation

Animals anaesthetized with 0.3-0.35 ml of 2.5% Avertin were transcardially perfusion-fixed with 4% paraformaldehyde (PFA) following perfusion with 0.9% physiological saline solution. Brains were removed and postfixed in 4% PFA overnight. Thereafter, samples were cryoprotected by incubating them in TBS (50 mM Tris, 150 mm NaCl, pH 7.4) containing 30% sucrose at +4°C for 8 hours. Next day, 50 µm sagittal sections kept on dry ice were cut for immunofluorescence staining using a sliding microtome (Leica SM2010 R), and the obtained slices were stored in anti-freeze solution (40 mM Na_2HPO_4, 6 mM NaH_2PO_4, 20% (v/v) glycerin, and 30% (v/v) ethylene glycol at –20°C until further processing. For RNAscope experiments, 30 µm coronal sections (Bregma +0.14 to +0.4 mm) were prepared from 3-3 male and female wild type C57Bl/6 animals as described above. In some cases, 50 µM sagittal slices were used.

2.3 Immunofluorescence and immunohistochemistry (IHC)

For immunofluorescence staining the cryoprotected slices were washed three times in TBS. Next, tissue permeabilization and blocking of non-specific antibody binding was performed by incubating the slices in 10% horse serum and 0.2% Triton X-100 containing TBS solution at room temperature for 2 hours followed by three washes in TBS. Thereafter, the slices were incubated with goat anti-CHAT (antibody registry number: AB 90650) or goat anti-parvalbumin primary antibody (antibody registry number: AB 2650496) at 1:1000 dilution in blocking solution (10% horse serum and 0.05% Triton X-100 containing TBS) at +4°C for 72 hours. Following three washes in TBS, slices were incubated in blocking solution containing donkey anti-goat secondary antibody conjugated to Alexa647 fluorophore (antibody registry number: AB 2340437) at room temperature for two hours. After three consecutive washes in TBS, nuclei were counterstained with Hoechst 33342 at 1:10000 dilution at room temperature for 5 minutes. Following the final three washes in TBS slices were mounted on microscope slides and covered with Prolong GOLD mounting medium.

We also performed NiDAB immunohistochemical staining for cholinergic neurons in some experiments. Here, following three consecutive 10-minute washes with TBS, the endogenous peroxidase activity was blocked by incubating the slices with 1% H_2O_2 in 10% methanol at room temperature for 15 minutes. The permeabilization, the blocking and the incubation step with goat anti-CHAT antibody (antibody registry number: AB 90650) was performed as described above. Thereafter, three consecutive washes with TBS were followed by incubation with biotinylated donkey anti-goat secondary antibody (antibody registry number: AB 2340397) diluted at 1:200 in blocking solution at room temperature for 2 hours. To detect the bound secondary antibodies, slices were incubated with avidin/peroxidase complex (Vectastain Elite ABC HRP kit, PK-6100, Vector Laboratories) diluted in blocking solution after three consecutive washes. Finally, NiDAB in 0.1 M acetate buffer was applied to cover the slices and the samples were developed until the desired color reaction could be observed by monitoring it with a brightfield microscope. Termination of development was achieved by rinsing the slides with Tris buffer. After drying the slices on slides, samples were dehydrated with an ascending concentration series of ethanol washes and mounted using DPX mounting medium.

IHC-stained and fluorescence slices were imaged with a Mantra Quantitative pathology workstation, or a Zeiss LSM 710 confocal laser scanning microscope system (Carl Zeiss, Jena, Germany) equipped with violet-diode (405 nm), multiline argon (457–517 nm), and solid-state (543, 561 nm and 633 nm) lasers, respectively. Images were taken with a 20x (N.A. 0.75) objective using ZEN 2.3 imaging software. Post-acquisition image processing was performed in Fiji software.

2.4 RNAscope and confocal laser scanning microscopy

In 30 µm thick, paraformaldehyde-fixed coronal brain sections mRNA transcripts of *estrogen receptors* (ERα, Erβ, and GPER1), and *choline acyltransferase* (CHAT), were visualized with a multiplex fluorescence RNAscope *in situ* hybridization assay (Advanced Cell Diagnostics, Newark, CA) (see Table 1). Following three consecutive washes in TBS free-floating sections were mounted on Superfrost Plus Gold adhesion slides (Thermo Scientific, 630-1324, VWR). The labeling of the selected transcripts was performed according to the manufacturer's instructions. Amplification and detection steps for the selected estrogen receptor and CHAT were

TABLE 1 Expression of estrogen receptor mRNAs in striatal cholinergic interneurons.

	Male			Female		
	Total CHAT neurons	ER+ CHAT neurons	% CHAT neurons expressing ER	Total CHAT neurons	ER+ CHAT neurons	% CHAT neurons expressing ER
ERα	286	28	8.71	167	37	21.85
ERβ	231	119	51.52	156	59	37.82
GPER1	184	26	14.13	153	11	7.19

Striatal cholinergic neurons were counted in fluorescently labeled RNAscope slices for each estrogen receptor type obtained from 3 male and 3 female mice. The percentage of the estrogen receptor expressing CHAT+ cells were calculated by dividing the number of ER+ cholinergic neurons with the total number of cholinergic neurons in one slice.

carried out sequentially. To ensure the specific staining of estrogen receptors transcripts, labeling of these mRNAs was performed before labeling CHAT mRNA. Nuclei were counterstained with Hoechst 33342, and stained sections were mounted with ProLong Diamond Antifade mountant. After 24 hours curing in the mounting medium, slices were sealed with nail polisher. 3-plex negative control probes for mouse tissue were used on two slices each time RNAscope labeling was performed.

Sections were imaged using a Nikon C2+ confocal laser scanning imaging system in less than one week later. During each imaging session a fluorescence, stitched, large overview image of the whole slice was taken first using a 10x objective (N.A. 0.45). Next, using high magnification objectives (60x or 100x, N.A. 1.4) 12-bit fluorescent images (512 x 512 pixels) were taken at a Nyquist sampling rate. Because the abundance of transcripts for estrogen receptors are low in the striatum, and somata of striatal cholinergic neurons are large, z-scans were carried out for the entire somata of individual cholinergic interneurons with 1 µm interslice distance, and a pinhole size less than one Airy unit. The laser power and the gain of the photomultiplier tube for each channel were set during imaging slices labeled with the 3-plex negative probes. All images were taken using the same imaging parameters during one imaging session. The localization of each imaged striatal cholinergic interneuron was saved on a superimposed, fluorescent overview image.

The image analysis of the obtained z-stacks was performed in Fiji software using the 3D object counter plug-in. The optimal size and intensity thresholds were selected analyzing slides labeled with negative control probes. The expression of estrogen receptors in striatal cholinergic interneurons were scored based on ACD scoring criteria: Score 0 (no expression): 0/cell, Score 1: 1-3 dots/cell, Score 2: 4-9 dots/cell.

2.5 Preparation of acute brain slices

ChAT-Cre-tdTomato transgenic mice under deep isoflurane anesthesia were decapitated, and the brain was removed from the skull. 300 µm thick, sagittal brain slices were cut with a vibratome (Leica VT1200s) in an ice-cold NMDG-ACSF solution composed of (in mM) 92 N-methyl-D-glucamine, 2.5 KCl, 30 NaHCO3, 20 HEPES, 25 glucose, 2 thiourea, 5 Na-ascorbate, 3 Na-pyruvate, 0.5 $CaCl_2{\cdot}2H_2O$, and 10 $MgSO_4{\cdot}7H_2O$. Upon finishing the cutting procedure, the slices were transferred into a pre-warmed (32°C) recovery vessel filled with NMDG-ACSF bubbled with 5% CO_2:95% O_2 gas mixture for 5-10 minutes. Finally, the slices were transferred into a long-term holding chamber filled with HEPES-ACSF solution consisting of (in mM): 92 NaCl, 2.5 KCl, 30 NaHCO3, 20 HEPES, 25 glucose, 2 thiourea, 5 Na-ascorbate, 3 Na-pyruvate, 2 $CaCl_2{\cdot}2H_2O$, and 2 $MgSO_4{\cdot}7H_2O$. The HEPES-ACSF holding solution was continuously bubbled with a gas mixture of 5% CO_2:95% O_2 and kept at room temperature. Slices were kept in holding solution for an additional one hour to recover. The pH of all solutions was adjusted to 7.4.

2.6 Electrophysiology

Electrophysiological experiments were performed on a Nikon Eclipse FN-1 upright microscope. Cells were visualized with infrared differential interference contrast (DIC) optics using a Nikon 40x NIR Apo N2 water dipping objective (N.A. 0.8). Cholinergic neurons expressing tdTomato fluorescent proteins were illuminated with an epifluorescence excitation light source (CoolLED pE-300). Fluorescence signals were detected with an Andor Zyla 5.5 sCMOS camera.

Patch pipettes were pulled from borosilicate glass capillaries with filament (O.D. 1.5 mm, I.D: 1.1 mm) using a Narishige vertical pipette puller. Pipette resistance was between 3-7 MΩ.

In all experiments acute brain slices were constantly superfused with standard artificial cerebrospinal fluid (ACSF) composed of (in mM): 124 NaCl, 2.5 KCl, 24 NaHCO3, 5 HEPES, 12.5 glucose, 2 $CaCl_2{\cdot}2H_2O$, and 2 $MgSO_4{\cdot}7H_2O$ with a pH adjusted to 7.4 and bubbled with a 95% O_2/5% CO_2 gas mixture. Experiments were carried out at 32°C. All drugs were applied into the bath solution *via* superfusion at least for 5 minutes. 17β-estradiol was dissolved in absolute ethanol to obtain 10 mM stock solution. 17β-estradiol stock solution was

diluted 1:100000 to reach 100 nM concentration, and further diluted 1:1000 to obtain 100 pM concentration.

In loose patch or cell-attached patch experiments patch pipettes were filled with the standard ACSF. The liquid junction potential was around zero because the composition of the solutions in the bath and the pipette was the same. Measurements were mostly carried out in current clamp mode using 0 mA holding current. In some tight cell-attached experiment recordings were made in voltage clamp mode using a command potential resulting in zero current passing across the patch. Under these conditions the spontaneous firing pattern is not affected (26). Signals were low pass filtered with 4kHz Bessel filter and digitized at 50 kHz (Digidata 1550B, Molecular Devices).

Offline data analysis was carried out using Clampfit 10.7 software (Molecular Devices). The average frequency of the neuronal action potential firing and the local variation of the interspike intervals over 5 minutes periods were. The local variation (27) was defined as:

$$L_v = \frac{3}{n-1}\sum_{i=1}^{n-1}\left(\frac{I_i - I_{i+1}}{I_i + I_{i+1}}\right)^2$$

As compared to the coefficient of variation, the local variation is a better firing metric, because it is insensitive to firing rate fluctuations and represents the instantaneous variability of interspike intervals more closely (28).

In cell-attached experiments with a pipette-cell seal resistance over 1 GΩ, the resting membrane potential could be recorded in current-clamp mode (26, 29).

2.7 Determination of estrous cycles by vaginal smear

Vaginal smears were taken from female mice by application of 100 µl of physiological saline solution into the vagina followed by aspiration of the flushed fluids. Samples were immediately placed and smeared on glass microscope slides and allowed to dry at room temperature. Dried smears were stained with methylene blue solution for 1 min and washed in tap water. The estrus state was determined using a light microscope with 10x objective (30).

2.8 Statistical analysis

For data analysis and graph generation Microsoft Excel 2018 and GraphPad Prism 8 software were used. Data are represented in figures either as sample median ± range or as individual data points. The normal distribution of the sample data was tested with the Shapiro-Wilk test. The obtained average firing rate and the local variation data of control and estrogen-treated groups were compared with Wilcoxon matched-pairs signed rank t-test. The comparison of non-paired experimental data was tested with Kolgomorov-Smirnov test (comparing two groups) or non-parametric Kruskal-Wallis test (comparing several groups). The sample size was based on reports in related literature and was not predetermined by calculation.

3 Results

3.1 Expression pattern of tdTomato fluorescent protein in the dorsal striatum of ChAT-Cre-tdTomato animals

First, we tested how many cells have ectopic expression tdTomato fluorescence protein in the dorsal striatum. The immunohistochemical staining for CHAT protein showed the well-known morphological characteristics of the giant, aspiny cholinergic interneurons (Figure 1A). As depicted in Figure 1B, the fluorescence image of the immunohistochemical staining revealed that only a negligible fraction of the tdTomato-positive cells was CHAT-negative. The only cell found to be non-cholinergic is marked with an arrow in Figure 1B. The morphology and expression pattern of the fluorescent, tdTomato-expressing cells in the fluorescent image of the dorsal striatum clearly resemble striatal cholinergic interneuron cells (Supplementary 1). Furthermore, immunofluorescent labeling of the CHAT protein showed almost complete colocalization whereas absolutely no colocalization was observed between parvalbumin- and CHAT-positive neurons (Figure 2). Our data showed that 97.72% of the tdTomato-expressing cells were cholinergic interneurons (927 of 939 cells n = 5 animals).

3.2 Expression of ERα, ERβ, and GPER1 mRNA in the cholinergic interneurons of the dorsal striatum

Using RNAscope *in situ* hybridization we found that many cholinergic neurons express no detectable ERα mRNA (Figure 3) in either sex. A smaller fraction of cholinergic interneurons (8.71% in males, and 21.85% in females), showed weak ERα positivity (Table 1). We have to note that there were some non-cholinergic cells that expressed a moderate amount of ERα mRNA (Figure 3). Weak ERβ mRNA expression was detected in 51.52% and 37.82% of cholinergic interneurons in males and females, respectively (Figure 4 and Table 1). The plasma membrane estrogen receptor (GPER1) mRNA was found in small amounts in some cholinergic interneurons in both sexes (Figure 5 and Table 1).

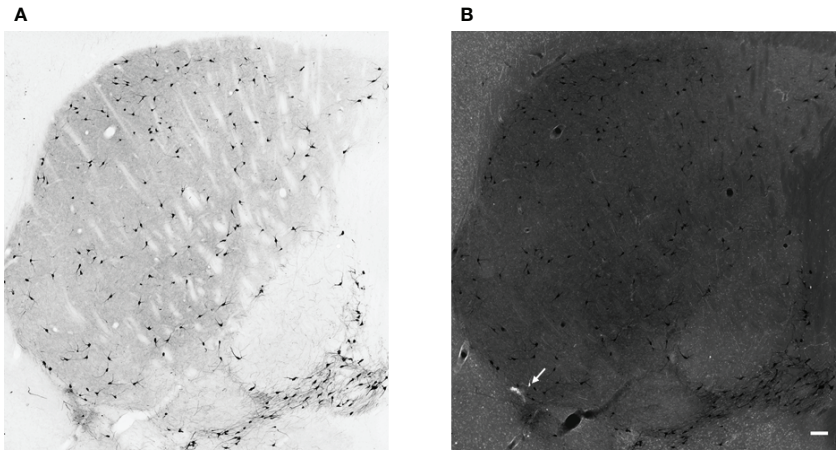

FIGURE 1
Cholinergic neurons in the striatum. Representative images of DAB immunohistochemistry for CHAT in the striatum from adult female ChAT-Cre-tdTomato transgenic mouse (Panel **A**, brightfield image, and Panel **(B)**, fluorescence image). In panel **B** the white cell represents non-cholinergic but tdTomato-positive cells (white arrow), whereas cholinergic, CHAT-positive interneurons are black in both panels. 10x magnification, scale bar represents 100 µm.

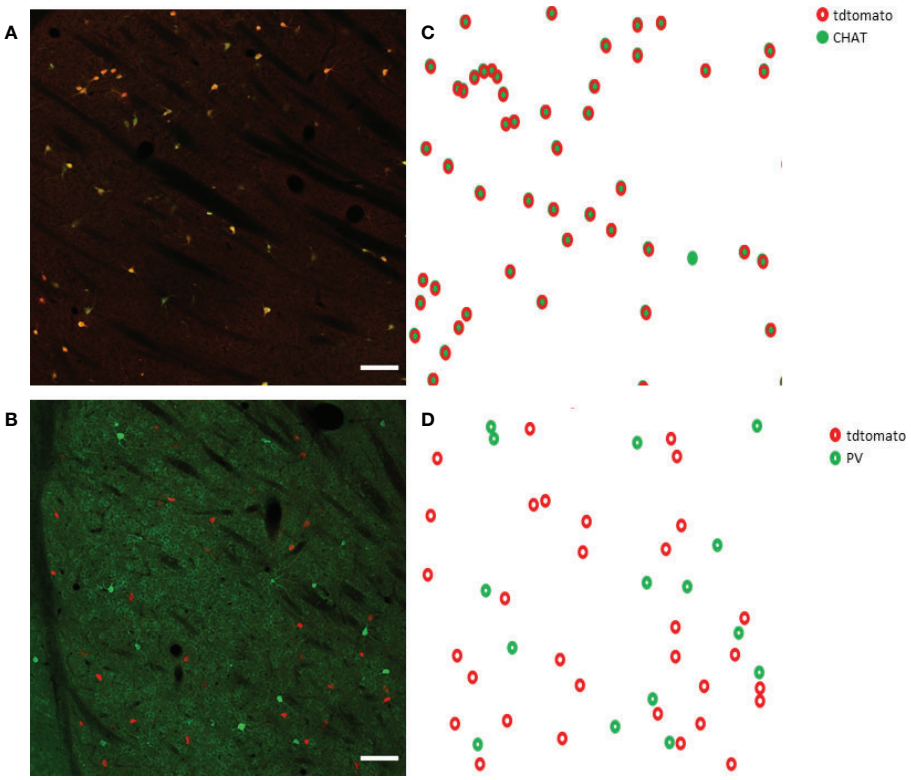

FIGURE 2
CHAT and parvalbumin (PV) staining in the striatum from a ChAT-Cre-tdTomato transgenic adult female mouse. Representative images show CHAT- and PV-positive cells in green in a sagittal section of the striatum in Panels **(A, B)** respectively. TdTomato-expressing cells are presented in red. CHAT+ cells are marked with filled circles in Panel **(C)**, while open green circles represent PV+ cells in Panel **(D)**. TdTomato-expressing cells are marked with open red circles in both Panels **(C, D)**. 20x magnification, scale bar presents 100 µm.

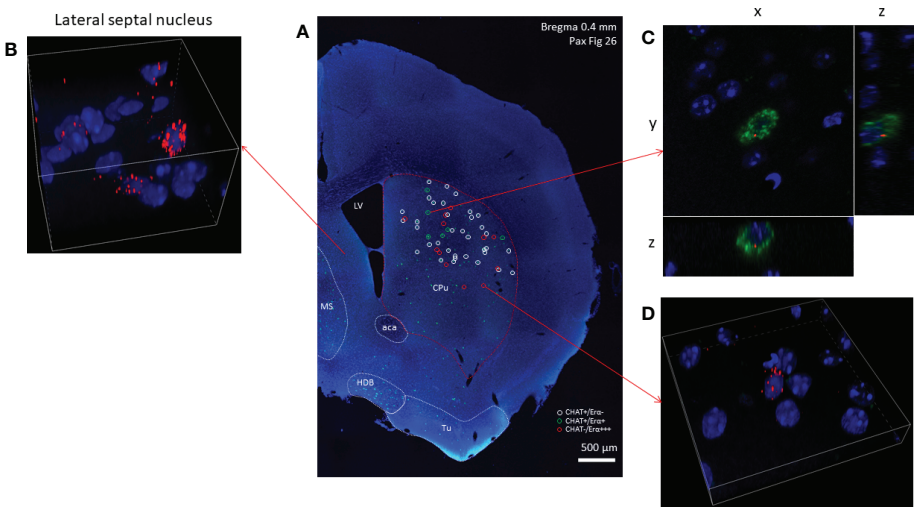

FIGURE 3
Estrogen receptor alpha mRNA expression in striatal cholinergic neurons. Overview image of the right side of a coronal section obtained from an adult male mouse brain is presented in Panel **(A)** (10x). Green fluorescence labeling show cholinergic cells expressing CHAT mRNA (Panel **A**). White and green circles mark ERα-negative and ERα-positive striatal cholinergic neurons, respectively. Non-cholinergic cells with strong ERα positivity are highlighted with red circles. Cells expressing ERα at high level in the lateral septum are depicted in Panel **(B)** (60x). A representative ERα-positive striatal cholinergic neuron is shown in Panel **(C)** (blue: nuclei, green: CHAT mRNA, red: ERα mRNA, 60x). In Panel **(D)**, one non-cholinergic cell with abundant expression of ERα mRNA is presented (60x). CPu, caudate-putamen; aca, anterior limb of anterior commissure; MS, medial septum; HDB, horizontal limb of the diagonal band of Broca; Tu, olfactory tubercle; LV, lateral ventricle.

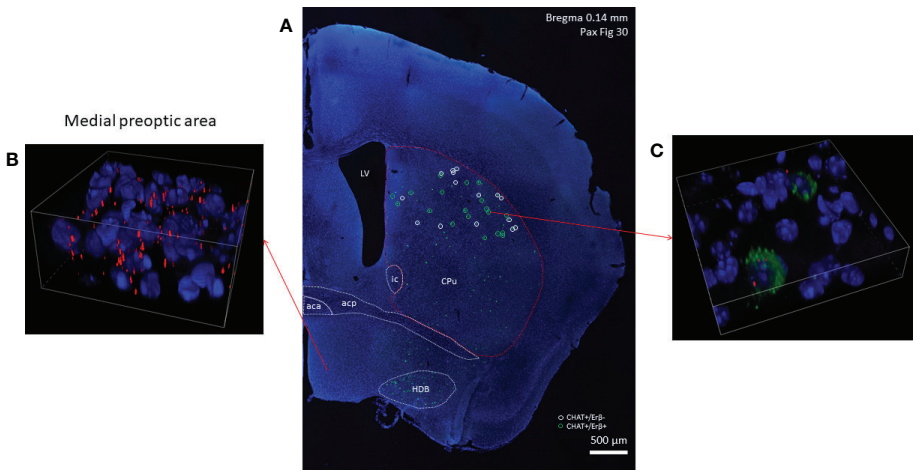

FIGURE 4
Estrogen receptor beta mRNA expression in striatal cholinergic neurons. CHAT mRNA-positive cells showing green fluorescence labeling in the right side of a coronal section are depicted in Panel **(A)** (10x). In the dorsal striatum white and green circles mark ERβ-negative and ERβ-positive cholinergic interneurons, respectively. Cells with high ERβ mRNA expression in the medial preoptic area are presented in Panel **(B)** Representative confocal image shows the expression of ERβ mRNA in 2 cholinergic interneurons in the dorsal striatum (blue: nuclei, green: CHAT mRNA, red: ERα mRNA, 60x) (Panel **C**). CPu, caudate-putamen; aca, anterior limb of anterior commissure; acp, posterior limb of anterior commissure; HDB, horizontal limb of the diagonal band of Broca; LV, lateral ventricle.

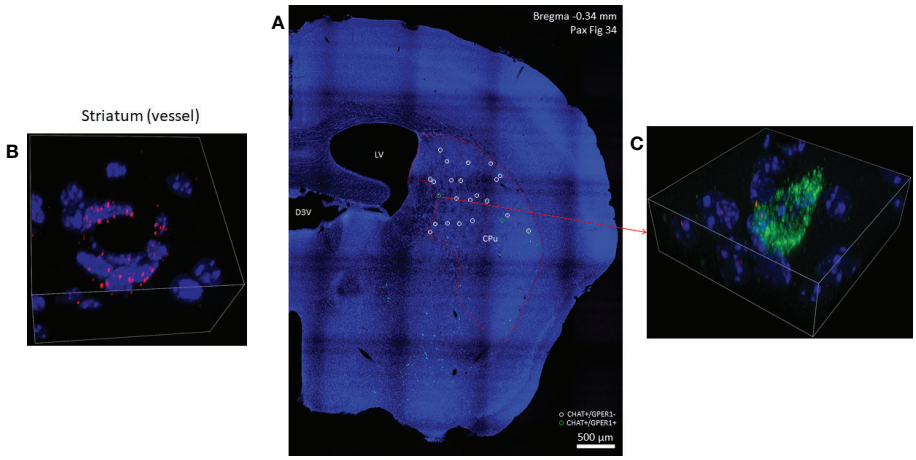

FIGURE 5
GPER1 (GPR30) mRNA expression in striatal cholinergic neurons. In one half of a coronal section cholinergic neurons marked with green, fluorescent probes used against CHAT mRNA are depicted in Panel **(A)** (10x). GPER1-positive striatal cholinergic interneurons are marked with green open circles while white open circles show cholinergic neurons with no GPER1 mRNA expression in the dorsal striatum. In Panel **(B)**, endothelial cells of a small vessel abundantly expressing GPER1 mRNA are depicted (60x). One GPER1-positive striatal cholinergic interneuron is shown in Panel **(C)** (blue: nuclei, green: CHAT mRNA, red: ERα mRNA, 60x). CPu, caudate-putamen; LV, lateral ventricle; D3V, third ventricle.

3.3 Effect of sex and age on spontaneous firing of cholinergic interneurons in the dorsal striatum in male and female mice

Dorsal striatal cholinergic interneurons are pacemaker cells that are able to fire spontaneously in the absence of any synaptic input (Figure 6A). The rate and variation of the spontaneous firing of these interneurons were measured between 10 and 15 minutes after a seal was established in order not to confound the results due to mechanical disturbance of seal formation. Nearly half of the patched neurons showed spontaneous activity at higher than 0.1% Hz frequency in both sexes (97/215 in males, 94/191 in females, respectively).We found no difference in the number of spontaneous active cells between sexes in old animals (age > 15 month), as 54.39% (31/57) of the patched striatal cholinergic neurons were active in females, and 54.10% (33/61) in males. The resting membrane potential measured in cells monitored in cell-attached mode (seal resistance is greater than 1 GΩ) in 61, 58, 12 and 10 neurons obtained from adult male and female, as well as old male and female animals, respectively. No significant difference was found among the different groups (-68.31 mV ± 4.90 in adult males vs -64.72 mV ± 5.63 in adult females, -63.05 mV ± 2.68 in old males vs -61.84 mV ± 8.26 in old females) (Figure 6B). We also did not observe any difference in frequency between sexes or detect any effect of age (1.26 Hz ± 1.09 in adult males vs 1.11 Hz ± 1.00 in adult females, p = 0.6754, 1.34 Hz ± 1.33 in old males vs 1.42 ± 1.04 in old females, p = 0.9984) (Figure 6C). In addition, local variation in spontaneous firing was not affected by either sex or age (0.43 ± 0.27 in adult males vs 0.44 ± 0.24 in adult females, p = 0.957, 0.382 ± 029 in old males vs 0.38 ± 0.20 in old females, p = 0.958) (Figure 6D). In female mice, both frequency and local variation were unaffected by the phase of estrous cycle (Figures 7A, B).

3.4 Rapid effect of 17β-estradiol on spontaneous firing activity of cholinergic interneurons

To test the rapid effect of 17β-estradiol superfused into bath, we measured the frequency and the local variation of the spontaneous firing of striatal cholinergic neurons over the first 5 minutes after the administration of 17β-estradiol. 17β-estradiol at 100 pM concentration did not affect neither frequency nor the local variation of spontaneous firing in any of the examined groups (Figures 8A, 9A). In addition, 100 nM 17β-estradiol had no effect on local variation in adult or old females (Figures 8B, 9B). Interestingly, when we compared the adult (younger than 15 month) with the old (older than 15 month) male animals, 100 nM 17β-estradiol significantly lowered the local variation only in the old animals (from 0.235 ± 0.118 to 0.178 ± 0.085, n = 8, p = 0.0184) but not in the adult animals (from 0.316 ± 0.210 to 0.252 ± 0.157, n = 15, p = 0.1326).

4 Discussion

Sex and gonadal hormones can influence many neural functions to a large extent in different brain regions. Estrogens evoke two kinds of effect that are different in many ways. The

10.3389/fendo.2022.993552

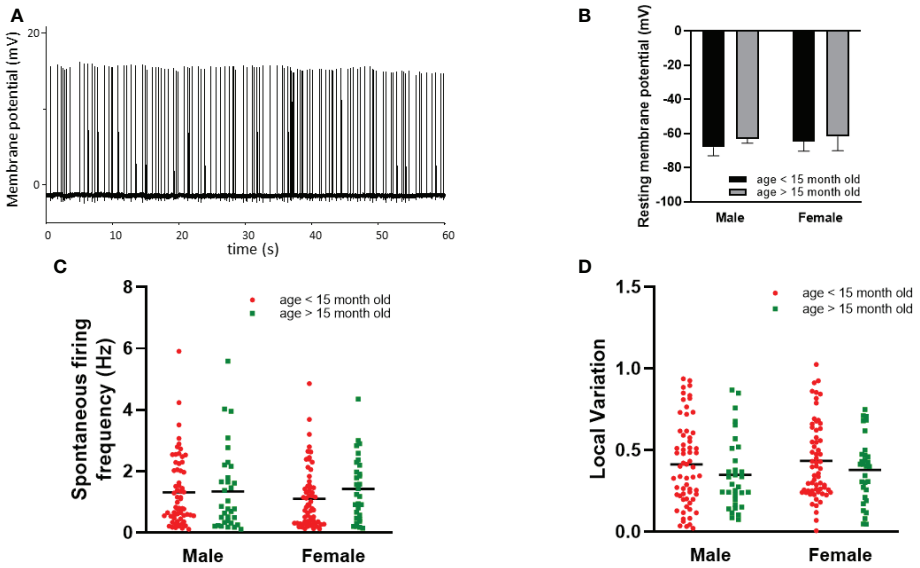

FIGURE 6
Effect of age and sex on intrinsic properties of striatal cholinergic interneurons. Representative, loose patch recording of spontaneous activity obtained from a striatal cholinergic neuron is depicted in Panel **(A)**. The resting membrane potential, the frequency, and the local variation of spontaneous firing activity in males and females is presented in Panels **(B-D)**, respectively. Data in one gender were further divided based on age.

rapid effects can be evoked in seconds or minutes, and they do not activate the transcription of any target genes. The underlying mechanisms are non-genomic and mediated by extranuclear, mostly membrane-bound estrogen receptors such as ERα and GPER1. Various intracellular signaling pathways including phosphatidylinositol 3-kinase (PI3K)/Akt pathway, mitogen-activated protein kinase (MAPK)/extracellular regulated kinase (ERK) pathway, protein kinase A, and protein kinase C pathways are involved in rapid, non-genomic effects (31). Because estrogens are synthesized also in the brain and modulate many neuronal and glial cellular functions *via* non-genomic effects, they are considered as neurosteroids (32). In contrast, the genomic effects develop in hours to days, but they are long lasting because changes in gene transcription and protein synthesis are involved. The genomic effects of estrogens are mediated by the nuclear estrogen receptors ERα and ERβ. Estrogens form a complex with estrogen receptors and that complex binds to the estrogen response element (ERE) in

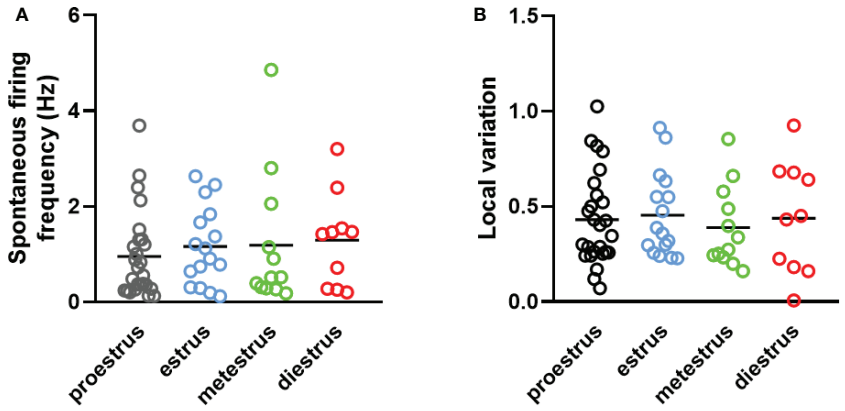

FIGURE 7
The effect of estrous cycle on spontaneous firing of striatal cholinergic interneurons in adult female mice. The frequency and the local variation of spontaneous activity in cholinergic interneurons in different phases of estrous cycle are presented in Panels **(A, B)**, respectively.

10.3389/fendo.2022.993552

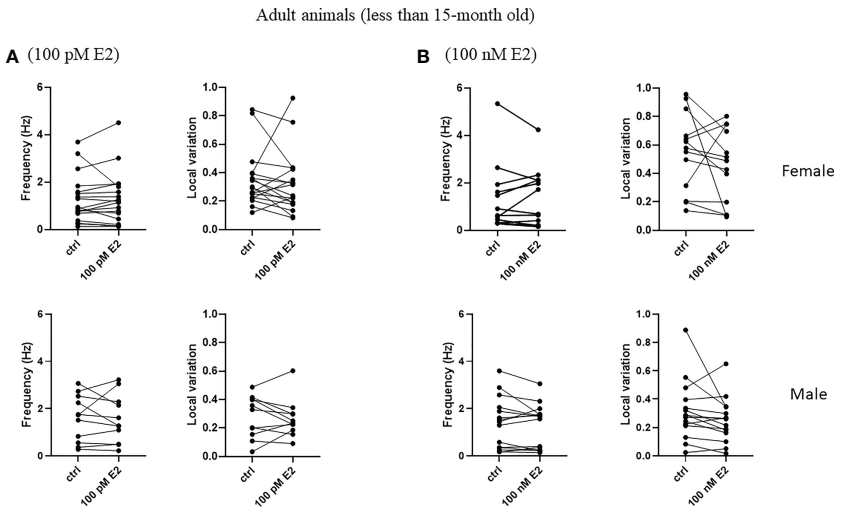

FIGURE 8
Rapid effect of 17β-estradiol on spontaneous activity of cholinergic interneurons in adult animals. The acute effect of 100 pM or 100 nM 17β-estradiol on spontaneous activity of cholinergic interneurons are shown in Panels **(A, B)**, respectively.

the promoter region of the target genes resulting in the modulation of the transcriptional activity.

It is well documented that there are large sex-related differences in nigrostriatal and mesolimbic dopaminergic pathways (12, 13, 25). Ligand binding studies of striatal D1 and D2 dopaminergic receptors that indicate changes in expression and/or binding affinity showed clear sex differences in rodents (12, 13, 33). Studies performed on ovariectomized female rats showed that ovariectomy decreased both D1 and D2 ligand binding, which was prevented by administration of 17β-estradiol (33–37). Administration of 17β-estradiol increased the binding to striatal D1 receptors in male mice after 6 days, but not at earlier timepoints after the treatment (38, 39). In contrast, binding to D2 receptors were decreased in both male and female mice after 24 hours (38). In non-human primates, D2 receptor availability was reported to be higher in the luteal phase as compared to the follicular phase, and the number of D1-D2 heteromeric complex expressing neurons and the density of D1-

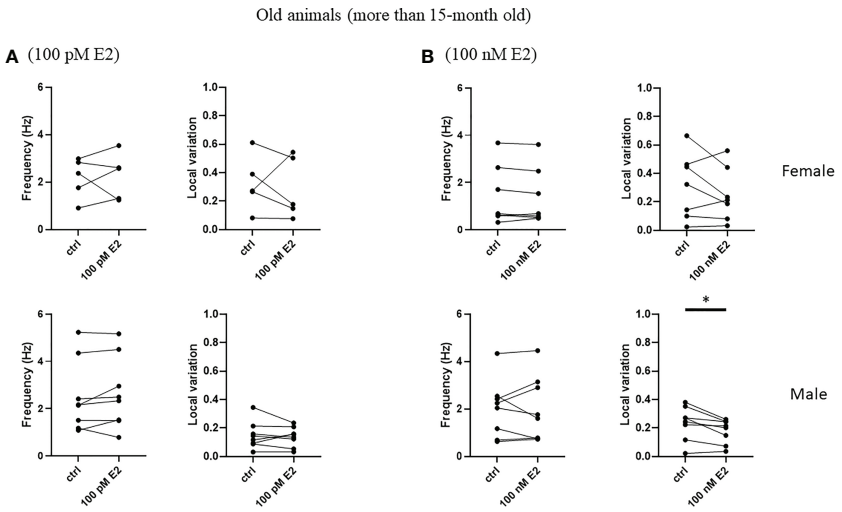

FIGURE 9
Rapid effect of 17β-estradiol on spontaneous activity of cholinergic interneurons in old animals.The effect of 100 pM or 100 nM 17β-estradiol in 5 minutes on spontaneous activity of cholinergic interneurons are shown in Panels **(A, B)**, respectively. *p< 0.05.

D2 complexes were higher in females (40, 41). Besides the changes in dopamine receptor function by estrogens in the striatum, dopamine turnover is also greatly affected by estradiol. The expression of the dopamine transporter (DAT) was lower in males than females and the level of DAT was dependent on estrous cycle phase and greatly reduced by ovariectomy (40, 42–45).

Estrous cycle phases were also clearly associated with the level of extracellular dopamine concentrations in the striatum (highest in proestrus lowest in metestrus/diestrus). In addition, 17β-estradiol rapidly enhanced K^+- or amphetamine-induced dopamine release in the striatum suggesting underlying non-genomic mechanisms (see (12, 25) for reviews).

Dopaminergic input has a large effect on striatal cholinergic neurons. The predominant, D2-mediated, inhibitory effect is achieved by modulating the I_h current and enhancing the slow inactivation of voltage-gated Na^+ channels. The synaptic input is reduced by inhibition of high-voltage-activated Ca^{2+}channels. Dopamine enhances ACh release from striatal cholinergic neurons by promoting the opening of non-selective cation channels and the closure of K^+ channels (see (7, 10) for reviews).

A rapid decrease in L-type calcium current and cAMP responsive-element-binding protein (CREB) phosphorylation induced by 17β-estradiol *via* estrogen receptor alpha (ERα), estrogen receptor beta (ERβ) and mGluR was demonstrated in striatal MSN (46, 47).

Therefore, the main goal of the present study was to examine the rapid effect of 17β-estradiol and the influence of sex on the spontaneous activity of striatal cholinergic interneurons. First, we examined the expression of estrogen receptors on cholinergic interneurons in the dorsal striatum. Because of the lack of specific antibodies, we performed RNAscope *in situ* hybridization to detect estrogen receptor mRNA in CHAT-positive cells. Our data showed that subpopulations of cholinergic interneurons express at least one of the estrogen receptors at low levels. In addition, we found sex differences in estrogen receptor-positive populations of cholinergic interneurons. Here, we also observed some non-cholinergic cells that strongly express ERα mRNA. These data are in accordance with previously published data demonstrating the expression of estrogen receptors at low level in the dorsal striatum (17, 20–22). In addition, using electron microscopy, Almey et al. reported that ERα and GPER1 protein labeling is associated with axons and terminals of striatal cholinergic neurons (17). Furthermore, GABAergic medium spiny neurons, which innervate cholinergic interneurons, also express estrogen receptors (18). These data suggest that either directly or indirectly through MSN afferents, estrogens could modulate the activity of cholinergic interneurons.

To test this hypothesis we measured two parameters, namely frequency and local variation of spontaneous activity of cholinergic interneurons. We found that none of these parameters were affected by sex or the phase of the estrous cycle *in vitro* under resting conditions. There was also no difference in resting membrane potential between males and females. These data suggest that the locally produced endogenous estrogens do not have any influence on basal pacemaker activity of cholinergic interneurons. However, the mRNA expression of CHAT, the enzyme that synthesizes acetylcholine, fluctuates during the course of the estrous cycle in different regions of rat basal forebrain including the striatum (48). It was also reported that CHAT mRNA significantly increased in response to OVX (48). Although mRNA abundance might not correlate with the protein abundance, the basal acetylcholine release can be different between sexes and can be dependent on estrogen levels at the same spontaneous firing rate.

We also investigated whether 17β-estradiol can alter the spontaneous activity of cholinergic interneurons in a rapid, non-genomic way. We used 17β-estradiol at two different concentrations, namely 100 pM and 100 nM, that was used before in neuronal patch-clamp studies to investigate the rapid, non-genomic effect of 17β-estradiol on neuronal activity (49–52). Administration of 100 pM, the so called "physiological concentration" of 17β-estradiol, did not influence the frequency or the local variation of basal firing of cholinergic neurons in either sex. In addition, a large "pharmacological 100 nM dose" of 17β-estradiol did not induce any changes in females in 5 minutes. However, we found that while in adult animals there was only a tendency for a decrease in the local variation of spontaneous firing activity of ChINs induced by 100 nM 17β-estradiol, in old animals it was clearly demonstratable. It should be noted that the physiological concentration of endogenous 17β-estradiol in the brain is still not known, so the physiological and the pharmacological concentrations refers to blood levels.

The information encoded in neuronal firing can occur in two ways: in the rate (rate coding) or in the temporal distribution (temporal coding) of spiking activity (53). The rapid effect of large dose of 17β-estradiol on the variation of spiking activity in males suggest that estrogen can rapidly modulate the striatal output *via* MSN activity by altering the regulatory function of cholinergic interneurons. The interpretation of this finding in the context of locomotor responses in rodents needs further investigation. Nevertheless, our data are consistent with blocking the production of endogenous estrogens, as aromatase inhibition did not alter the firing pattern discharge, the current-voltage relationship parameter, or the EPSC amplitude of cholinergic interneurons in male rats (54). On the other hand, long-term potentiation (LTP) induced by a high-frequency stimulation protocol was completely prevented by aromatase inhibition which was restored by the dopamine receptor 1 (D1R) agonist SKF-82958 (54). In addition, the increase in striatal acetylcholine level induced by the dopamine agonist apomorphine was significantly attenuated by moxestrol, a potent estrogen (55). These data suggest that cholinergic activity can be modulated by

17β-estradiol indirectly *via* dopaminergic afferents under certain circumstances.

In summary, we found that sex has no effect on basal activity of striatal cholinergic neurons, while a rapid, non-genomic effect of 17β-estradiol at a pharmacological dose was observed on firing variability only in old males. Our data suggest that underlying mechanisms of sex differences in striatal behavior does not include differences in basal intrinsic electrophysiological properties of striatal cholinergic neurons. However, the possibility that E2 regulates ChINs indirectly *via* acting on its afferent cannot be excluded.

Data availability statement

The raw data supporting the conclusions of this article will be made available by the authors, without undue reservation.

Ethics statement

The animal study was approved by the Local Animal Care Committee of the University of Pécs (BAI/35/51-141/2016 University of Pécs, Hungary).

Author contributions

EK: design of the study, writing, data analysis. IU: perfusion, sectioning, immunohistochemistry, RNAscope *in situ* hybridization. AK: RNAscope *in situ* hybridization, validation, data analysis. SS: bright-field imaging, image analysis, data analysis and interpretation. SF: data analysis and interpretation. PF: RNAscope *in situ* hybridization, bright-field imaging, confocal imaging, data analysis and interpretation. TJ: data analysis. IÁ: conceptualization, funding acquisition. GK: design and supervision of the study, writing, critical reading, editing, and revising the manuscript. All authors were involved in the critical revision of the manuscript. All authors read and approved the final manuscript.

Funding

This work was supported by the Research Grant of Medical School, University of Pécs (KA-2020-11), the project TKP2021-EGA-16 that has been implemented with the support provided from the National Research, Development and Innovation Fund of Hungary, financed under the TKP2021-EGA funding scheme, the Hungarian Scientific Research Fund (OTKA; 112807), the Hungarian Brain Research Program (KTIA_NAP_13-2014-0001, 20017-1.2.1-NKP-2017-00002), and the European Union and was co-financed by the European Social Fund under the following grants: EFOP-3.6.1.-16-2016-00004 (Comprehensive Development for Implementing Smart Specialization Strategies at the University of Pécs), EFOP 3.6.2-16-2017-00008 (The Role of Neuro-inflammation in Neurodegeneration: From Molecules to Clinics).

Acknowledgments

The authors thank Prof. Catherine M Fuller (University of Alabama at Birmingham, AL, USA) for careful editing the manuscript for English language, grammar, and overall style. The research was performed in collaboration with the Nano-Bio-Imaging core facility and the animal facility at the Szentágothai Research Centre of the University of Pécs.

Conflict of interest

The authors declare that the research was conducted in the absence of any commercial or financial relationships that could be construed as a potential conflict of interest.

Publisher's note

Supplementary material

The Supplementary Material for this article can be found online at: https://www.frontiersin.org/articles/10.3389/fendo.2022.993552/full#supplementary-material

SUPPLEMENTARY 1
TdTomato-expressing cells in a sagittal section of the striatum from adult ChAT-Cre-tdTomato mouse. Red fluorescent cells representing striatal cholinergic interneurons are shown in Panel **A**. Nuclear counterstaining and merged image are presented in Panels **B** and **C**, respectively. 10x magnification, scale bar presents 100 µm.

References

1. Lanciego JL, Luquin N, Obeso JA. Functional neuroanatomy of the basal ganglia. *Cold Spring Harb Perspect Med* (2012) 2:1–21. doi: 10.1101/cshperspect.a009621

2. Cataldi S, Stanley AT, Miniaci MC, Sulzer D. Interpreting the role of the striatum during multiple phases of motor learning. *FEBS J* (2022) 289:2263–81. doi: 10.1111/febs.15908

3. Brimblecombe KR, Cragg SJ. The striosome and matrix compartments of the striatum: A path through the labyrinth from neurochemistry toward function. *ACS Chem Neurosci* (2017) 8:235–42. doi: 10.1021/acschemneuro.6b00333

4. Florio TM, Scarnati E, Rosa I, Di Censo D, Ranieri B, Cimini A, et al. The basal ganglia: More than just a switching device. *CNS Neurosci Ther* (2018) 24:677–84. doi: 10.1111/cns.12987

5. Kreitzer AC. Physiology and pharmacology of striatal neurons. *Annu Rev Neurosci* (2009) 32:127–47. doi: 10.1146/annurev.neuro.051508.135422

6. Oda Y, Nakanishi I. The distribution of cholinergic neurons in the human central nervous system. *Histol Histopathol* (2000) 15:825–34. doi: 10.14760/HH-15.825

7. Bonsi P, Cuomo D, Martella G, Madeo G, Schirinzi T, Puglisi F, et al. Centrality of striatal cholinergic transmission in basal ganglia function. *Front Neuroanat* (2011) 5:6. doi: 10.3389/fnana.2011.00006

8. Gonzales KK, Smith Y. Cholinergic interneurons in the dorsal and ventral striatum: Anatomical and functional considerations in normal and diseased conditions. *Ann N Y Acad Sci* (2015) 1349:1–45. doi: 10.1111/nyas.12762

9. Apicella P. The role of the intrinsic cholinergic system of the striatum: What have we learned from TAN recordings in behaving animals? *Neuroscience* (2017) 360:81–94. doi: 10.1016/j.neuroscience.2017.07.060

10. Lim SAO, Kang UJ, McGehee DS. Striatal cholinergic interneuron regulation and circuit effects. *Front Synaptic Neurosci* (2014) 6:22. doi: 10.3389/fnsyn.2014.00022

11. Tanimura A, Pancani T, Lim SAO, Tubert C, Melendez AE, Shen W, et al. Striatal cholinergic interneurons and parkinson's disease. *Eur J Neurosci* (2018) 47:1148–58. doi: 10.1111/ejn.13638

12. Yoest KE, Quigley JA, Becker JB. Rapid effects of ovarian hormones in dorsal striatum and nucleus accumbens. *Horm Behav* (2018) 104:119–29. doi: 10.1016/j.yhbeh.2018.04.002

13. Meitzen J, Meisel RL, Mermelstein PG. Sex differences and the effects of estradiol on striatal function. *Curr Opin Behav Sci* (2018) 23:42–8. doi: 10.1016/j.cobeha.2018.03.007

14. Krentzel AA, Meitzen J. Biological sex, estradiol and striatal medium spiny neuron physiology: A mini-review. *Front Cell Neurosci* (2018) 12:492. doi: 10.3389/fncel.2018.00492

15. Kanaya M, Higo S, Ozawa H. Neurochemical characterization of neurons expressing estrogen receptor β in the hypothalamic nuclei of rats using *in situ* hybridization and immunofluorescence. *Int J Mol Sci* (2020) 21. doi: 10.3390/ijms21010115

16. Shughrue PJ, Lane MV, Merchenthaler I. (1997) 525:507–25. @ of Estrogen Receptor- _ and - NL mRNA.

17. Almey A, Filardo EJ, Milner TA, Brake WG. Estrogen receptors are found in glia and at extranuclear neuronal sites in the dorsal striatum of female rats: Evidence for cholinergic but not dopaminergic colocalization. *Endocrinology* (2012) 153:5373–83. doi: 10.1210/en.2012-1458

18. Almey A, Milner TA, Brake WG. Estrogen receptor α and G-protein coupled estrogen receptor 1 are localized to GABAergic neurons in the dorsal striatum. *Neurosci Lett* (2016) 622:118–23. doi: 10.1016/j.neulet.2016.04.023

19. Enterria-Morales D, López-López I, López-Barneo J, De Tassigny XDA. Striatal GDNF production is independent to circulating estradiol level despite pan-neuronal activation in the female mouse. *PloS One* (2016) 11:1–17. doi: 10.1371/journal.pone.0164391

20. Küppers E, Beyer C. Expression of estrogen receptor-α and β mRNA in the developing and adult mouse striatum. *Neurosci Lett* (1999) 276:95–8. doi: 10.1016/S0304-3940(99)00815-0

21. Mitra SW, Hoskin E, Yudkovitz J, Pear L, Wilkinson HA, Hayashi S, et al. Immunolocalization of estrogen receptor β in the mouse brain: Comparison with estrogen receptor α. *Endocrinology* (2003) 144:2055–67. doi: 10.1210/en.2002-221069

22. Ghiglieri V, Napolitano F, Pelosi B, Schepisi C, Migliarini S, Di Maio A, et al. Rhes influences striatal cAMP/PKA-dependent signaling and synaptic plasticity in a gender-sensitive fashion. *Sci Rep* (2015) 5:1–17. doi: 10.1038/srep10933

23. Krentzel AA, Willett JA, Johnson AG, Meitzen J. Estrogen receptor alpha, G-protein coupled estrogen receptor 1, and aromatase: Developmental, sex, and region-specific differences across the rat caudate–putamen, nucleus accumbens core and shell. *J Comp Neurol* (2021) 529:786–801. doi: 10.1002/cne.24978

24. Drzewiecki CM, Sellinger EP, Juraska JM. Impact of pubertal onset on region-specific Esr2 expression. *J Neuroendocrinol* (2021) 33. doi: 10.1111/jne.13029

25. Zachry JE, Nolan SO, Brady LJ, Kelly SJ, Siciliano CA, Calipari ES. Sex differences in dopamine release regulation in the striatum. *Neuropsychopharmacol Off Publ Am Coll Neuropsychopharmacol* (2021) 46:491–9. doi: 10.1038/s41386-020-00915-1

26. Perkins KL. Cell-attached voltage-clamp and current-clamp recording and stimulation techniques in brain slices. *J Neurosci Methods* (2006) 154:1–18. doi: 10.1016/j.jneumeth.2006.02.010

27. Shinomoto S, Shima K, Tanji J. Differences in spiking patterns among cortical neurons. *Neural Comput* (2003) 15:2823–42. doi: 10.1162/089976603322518759

28. Shinomoto S, Kim H, Shimokawa T, Matsuno N, Funahashi S, Shima K, et al. Relating neuronal firing patterns to functional differentiation of cerebral cortex. *PloS Comput Biol* (2009) 5. doi: 10.1371/journal.pcbi.1000433

29. Mason MJ, Simpson AK, Mahaut-Smith MP, Robinson HPC. The interpretation of current-clamp recordings in the cell-attached patch-clamp configuration. *Biophys J* (2005) 88:739–50. doi: 10.1529/biophysj.104.049866

30. Caligioni CS. Assessing reproductive status/stages in mice. *Curr Protoc Neurosci* (2009) Appendix 4:Appendix 4I. doi: 10.1002/0471142301.nsa04is48

31. Lai YJ, Yu D, Zhang JH, Chen GJ. Cooperation of genomic and rapid nongenomic actions of estrogens in synaptic plasticity. *Mol Neurobiol* (2017) 54:4113–26. doi: 10.1007/s12035-016-9979-y

32. Reddy DS. Neurosteroids. endogenous role in the human brain and therapeutic potentials. *Prog Brain Res* (2010) 186:113–37. doi: 10.1016/B978-0-444-53630-3.00008-7

33. Lévesque D, Gagnon S, Di Paolo T. Striatal D1 dopamine receptor density fluctuates during the rat estrous cycle. *Neurosci Lett* (1989) 98:345–50. doi: 10.1016/0304-3940(89)90426-6

34. Lévesque D, Di Paolo T. Effect of the rat estrous cycle at ovariectomy on striatal d-1 dopamine receptors. *Brain Res Bull* (1990) 24:281–4. doi: 10.1016/0361-9230(90)90216-m

35. Tonnaer JADM, Leinders T, van Delft AML. Ovariectomy and subchronic estradiol-17β administration decrease dopamine D1 and D2 receptors in rat striatum. *Psychoneuroendocrinology* (1989) 14:469–76. doi: 10.1016/0306-4530(89)90046-2

36. Le Saux M, Morissette M, Di Paolo T. ERβ mediates the estradiol increase of D2 receptors in rat striatum and nucleus accumbens. *Neuropharmacology* (2006) 50:451–7. doi: 10.1016/j.neuropharm.2005.10.004

37. Landry M, Lévesque D, Di Paolo T. Estrogenic properties of raloxifene, but not tamoxifen, on D2 and D3 dopamine receptors in the rat forebrain. *Neuroendocrinology* (2002) 76:214–22. doi: 10.1159/000065951

38. Ferretti C, Blengio M, Vigna I, Ghi P, Genazzani E. Effects of estradiol on the ontogenesis of striatal dopamine D1 and D2 receptor sites in male and female rats. *Brain Res* (1992) 571:212–7. doi: 10.1016/0006-8993(92)90657-U

39. Hruska RE, Nowak MW. Estrogen treatment increases the density of D1 dopamine receptors in the rat striatum. *Brain Res* (1988) 442:349–50. doi: 10.1016/0006-8993(88)91523-5

40. Hasbi A, Nguyen T, Rahal H, Manduca JD, Miksys S, Tyndale RF, et al. Sex difference in dopamine D1-D2 receptor complex expression and signaling affects depression-and anxiety-like behaviors. *Biol Sex Differ* (2020) 11:7–10. doi: 10.1186/s13293-020-00285-9

41. Czoty PW, Riddick NV, Gage HD, Sandridge M, Nader SH, Garg S, et al. Effect of menstrual cycle phase on dopamine D2 receptor availability in female cynomolgus monkeys. *Neuropsychopharmacology* (2009) 34:548–54. doi: 10.1038/npp.2008.3

42. Bossé R, Rivest R, Di Paolo T. Ovariectomy and estradiol treatment affect the dopamine transporter and its gene expression in the rat brain. *Mol Brain Res* (1997) 46:343–6. doi: 10.1016/S0169-328X(97)00082-X

43. Chavez C, Hollaus M, Scarr E, Pavey G, Gogos A, van den Buuse M. The effect of estrogen on dopamine and serotonin receptor and transporter levels in the brain: An autoradiography study. *Brain Res* (2010) 1321:51–9. doi: 10.1016/j.brainres.2009.12.093

44. Dluzen DE, McDermott JL. Sex differences in dopamine- and vesicular monoamine-transporter functions: Implications for methamphetamine use and neurotoxicity. *Ann N Y Acad Sci* (2008) 1139:140–50. doi: 10.1196/annals.1432.010

45. Morissette M, Di Paolo T. Sex and estrous cycle variations of rat striatal dopamine uptake sites. *Neuroendocrinology* (1993) 58:16–22. doi: 10.1159/000126507

46. Grove-Strawser D, Boulware MI, Mermelstein PG. Membrane estrogen receptors activate the metabotropic glutamate receptors mGluR5 and mGluR3 to bidirectionally regulate CREB phosphorylation in female rat striatal neurons. *Neuroscience* (2010) 170:1045–55. doi: 10.1016/j.neuroscience.2010.08.012

47. Mermelstein PG, Becker JB, Surmeier DJ. Estradiol reduces calcium currents in rat neostriatal neurons *via* a membrane receptor. *J Neurosci Off J Soc Neurosci* (1996) 16:595–604. doi: 10.1523/JNEUROSCI.16-02-00595.1996

48. Gibbs RB. Fluctuations in relative levels of choline acetyltransferase mRNA in different regions of the rat basal forebrain across the estrous cycle: Effects of estrogen and progesterone. *J Neurosci* (1996) 16:1049–55. doi: 10.1523/jneurosci.16-03-01049.1996

49. Wartenberg P, Farkas I, Csillag V, Colledge WH, Hrabovszky E, Boehm U. Sexually dimorphic neurosteroid synthesis regulates neuronal activity in the murine brain. *J Neurosci* (2021) 41:9177–91. doi: 10.1523/JNEUROSCI.0885-21.2021

50. Herbison AE. Rapid actions of oestrogen on gonadotropin-releasing hormone neurons; from fantasy to physiology? *J Physiol* (2009) 587:5025–30. doi: 10.1113/jphysiol.2009.179838

51. Romanò N, Lee K, Ábrahám IM, Jasoni CL, Herbison AE. Nonclassical estrogen modulation of presynaptic GABA terminals modulates calcium dynamics in gonadotropin-releasing hormone neurons. *Endocrinology* (2008) 149:5335–44. doi: 10.1210/en.2008-0424

52. Chu Z, Andrade J, Shupnik MA, Moenter SM. Differential regulation of gonadotropin-releasing hormone neuron activity and membrane properties by acutely applied estradiol: Dependence on dose and estrogen receptor subtype. *J Neurosci* (2009) 29:5616–27. doi: 10.1523/JNEUROSCI.0352-09.2009

53. Kuebler ES, Thivierge J-P. Spiking variability: Theory, measures and implementation in matlab. *Quant Methods Psychol* (2014) 10:131–42. doi: 10.20982/tqmp.10.2.p131

54. Tozzi A, de Iure A, Tantucci M, Durante V, Quiroga-Varela A, Giampà C, et al. Endogenous 17β-estradiol is required for activity-dependent long-term potentiation in the striatum: Interaction with the dopaminergic system. *Front Cell Neurosci* (2015) 9:192. doi: 10.3389/fncel.2015.00192

55. Euvrard C, Labrie F, Boissier JR. Effect of estrogen on changes in the activity of striatal cholinergic neurons induced by DA drugs. *Brain Res* (1979) 169:215–20. doi: 10.1016/0006-8993(79)90392-5

frontiers | Frontiers in Neuroinformatics

TYPE Original Research
PUBLISHED 08 March 2023
DOI 10.3389/fninf.2023.1005936

OPEN ACCESS

EDITED BY
Gyorgy Vamosi,
University of Debrecen, Hungary

REVIEWED BY
Nela Durisic,
The University of Queensland, Australia
Deepak Prakash Srivastava,
King's College London, United Kingdom

*CORRESPONDENCE
Tibor Z. Janosi
✉ tzjanosi@gamma.ttk.pte.hu

RECEIVED 02 August 2022
ACCEPTED 21 February 2023
PUBLISHED 08 March 2023

CITATION
Makkai G, Abraham IM, Barabas K, Godo S, Ernszt D, Kovacs T, Kovacs G, Szocs S and Janosi TZ (2023) Maximum likelihood-based estimation of diffusion coefficient is quick and reliable method for analyzing estradiol actions on surface receptor movements. *Front. Neuroinform.* 17:1005936. doi: 10.3389/fninf.2023.1005936

Maximum likelihood-based estimation of diffusion coefficient is quick and reliable method for analyzing estradiol actions on surface receptor movements

Geza Makkai[1,2], Istvan M. Abraham[1,3], Klaudia Barabas[1,3], Soma Godo[1,3], David Ernszt[1,3], Tamas Kovacs[1,3], Gergely Kovacs[1,3], Szilard Szocs[1] and Tibor Z. Janosi[1,2]*

[1]Institute of Physiology, Medical School, University of Pécs, Pécs, Hungary, [2]Nano-Bio-Imaging Core Facility at the Szentágothai Research Centre of the University of Pécs, Pécs, Hungary, [3]Centre for Neuroscience, Szentágothai Research Centre, University of Pécs, Pécs, Hungary

The rapid effects of estradiol on membrane receptors are in the focus of the estradiol research field, however, the molecular mechanisms of these non-classical estradiol actions are poorly understood. Since the lateral diffusion of membrane receptors is an important indicator of their function, a deeper understanding of the underlying mechanisms of non-classical estradiol actions can be achieved by investigating receptor dynamics. Diffusion coefficient is a crucial and widely used parameter to characterize the movement of receptors in the cell membrane. The aim of this study was to investigate the differences between maximum likelihood-based estimation (MLE) and mean square displacement (MSD) based calculation of diffusion coefficients. In this work we applied both MSD and MLE to calculate diffusion coefficients. Single particle trajectories were extracted from simulation as well as from α-amino-3-hydroxy-5-methyl-4-isoxazolepropionic acid (AMPA) receptor tracking in live estradiol-treated differentiated PC12 (dPC12) cells. The comparison of the obtained diffusion coefficients revealed the superiority of MLE over the generally used MSD analysis. Our results suggest the use of the MLE of diffusion coefficients because as it has a better performance, especially for large localization errors or slow receptor movements.

KEYWORDS

diffusion coefficient, maximum likelihood, mean square displacement, MLE, receptor movements

Introduction

The diffusion coefficient is the most frequently defined parameter used to characterize receptor movements (De Keijzer et al., 2011; Knight and Falke, 2009; Knight et al., 2010; Matsuoka et al., 2009; Michalet and Berglund, 2012; Michalet, 2010; Pinaud and Dahan, 2011; Qian and Sheetz, 1991; Sahl et al., 2010; Schütz et al., 1997; Weigel et al., 2011).

The derivation of diffusion coefficient from mean square displacement (MSD) curve fitting (Matysik and Kraut, 2014) is a basic and frequently used method because it provides

consistent results despite of the statistical shortcomings of MSD analysis (Saxton, 1997). The main problem with MSD analysis is that the overlapping time-averaging calculations in MSD curves from a single trajectory generate complex noise characteristics (Grebenkov, 2011; Qian and Sheetz, 1991). This resulted in an asymmetric distribution of the estimated diffusion constant around the true value that makes the interpretation of the results difficult (Yu, 2016). Another problem is that MSD cannot handle the uncertainty of the localization properly, in other words, the MSD requires the real coordinates of the particle to provide correct results. However, this is not the case in practice, because observed trajectories are compromised with both the localization error (Martin et al., 2002) and the motion blur effect (Savin and Doyle, 2005).

Maximum likelihood-based estimation (MLE) has already been successfully applied to estimate diffusion coefficients from single-particle tracking experiments (Shuang et al., 2013). The MLE is one of the most frequently used method in statistics to estimate arbitrary parameters of theoretical models describing the observed event by using recorded data. Changing the model's parameters will alter the probability of the recorded dataset. MLE is an optimization method, that estimates a set of parameters that provides the maximal probability of the observed data. The MLE has asymptotically optimal properties, it determines the correct distribution of diffusion coefficients for a homogenous set of particles localized within a finite camera integration time and in the presence of localization error (Zacks, 1971). A comprehensive study on detailed comparison of MSD and MLE methods was recently published (Bullerjahn and Hummer, 2021), which concluded several advantages of the maximum likelihood estimator compared to other diffusion coefficient calculating methods.

There is a clear relation between the movement of cell surface receptors and their signal transduction activity. There are several single molecule detection (SMD) techniques to investigate this relationship. Events that result in clear changes, such as receptor ligand interactions can be studied by previously widely used analytical methods such as MSD curve analysis. However, for biological effects that cause only small variations in receptor movements but result in biologically significant changes, conventional methods can no longer be used for reliable investigation.

The reliability of the MSD and MLE methods were tested on simulated datasets as well as on data derived from live-cell experiments. For the live-cell measurements we detected changes in the surface movement of α-amino-3-hydroxy-5-methyl-4-isoxazolepropionic acid (AMPA) receptors after estradiol exposure.

The gonadal steroid 17β-estradiol (E2) is a powerful molecule playing a key role in learning and memory formation by influencing glutamatergic neurotransmission and synaptic plasticity (Kramár et al., 2009; Ledoux et al., 2009; Lu et al., 2019; Murakami et al., 2018; Teyler et al., 1980; Vierk et al., 2014; Wong and Moss, 1992). Besides its well-known classical actions, E2 can influence gene expression indirectly by rapidly altering the functions of membrane receptors and the activity of second messenger molecules. These are referred to as the non-classical effects of E2 (Rudolph et al., 2016). Although ample data have been accumulated on the rapid effects of E2 on learning and memory (Phan et al., 2015; Taxier et al., 2020), the molecular mechanisms are still largely unknown. Single-molecule tracking studies showed that the lateral diffusion of membrane receptors determine the activation state of membrane receptors and consequently the downstream signaling events (Kusumi et al., 2014).

The surface movement of glutamate receptors including AMPA receptors is pivotal in glutamatergic neurotransmission and synaptic plasticity (Babayan and Kramar, 2013; Penn et al., 2017).

Accordingly, measuring the diffusion parameters of the AMPARs can provide a better understanding of the non-classical E2 effects on learning and memory processes (Godó et al., 2021). Therefore, it is crucial to improve currently available methods to analyze membrane receptor movements.

Recent studies (Barabas et al., 2021; Godó et al., 2021) on lateral movement of receptors in the plasma membrane have demonstrated the value of the data extracted from SMD. SMD is a technique that can identify individual molecules and create the trajectories of these particles for detailed analysis. This allows deeper insights into the function of the receptors and helps us to understand the underlying mechanisms of different agents actions such as E2.

When examining the effect of E2 on the movement of AMPA receptors, because of the shortness of the detected trajectories and the larger localization error due to the specificity of the labeling, the MLE method has been proven to be more accurate in determining the diffusion coefficient of the AMPA receptors.

In this current manuscript we found that MLE method is better to analyze single molecule receptor movements by comparing the MSD and the MLE analysis of simulated and real, live-cell datasets.

Materials and methods

Simulated trajectories

A Matlab script was applied to generate sets of trajectories for two dimensional Brownian-diffusion with different characteristics. Besides the number of desired trajectories, the script allows the user to define the diffusion coefficient, the Gaussian localization error, the exposure time, the pixel size, the number of frames in each individual trajectory to customize the output according to the requirements. Moreover, there is an additional option that allows the user to turn the motion blur effect on or off.

Measured trajectories

To collect trajectories of real immobilized and diffusing molecules we performed single-molecule imaging using total internal reflection fluorescence microscopy (TIRFM). Single-molecule imaging was carried out on an Olympus (Tokyo, Japan) IX81 fiber TIRF microscope equipped with Z-drift compensation (ZDC2) stage control, a plan apochromat objective (100X, NA 1.49, Olympus), and a humidified chamber heated to 37°C and containing 5% CO_2. The dish containing dPC12 was mounted in the humidified chamber of the TIRF microscope immediately after *in vivo* labeling. A 491 nm diode laser (Olympus) was used to excite ATTO 488, and emission was detected above the 510 nm emission wavelength range. The angle of the excitation laser beam was set to reach a 100 nm penetration depth of the evanescent wave.

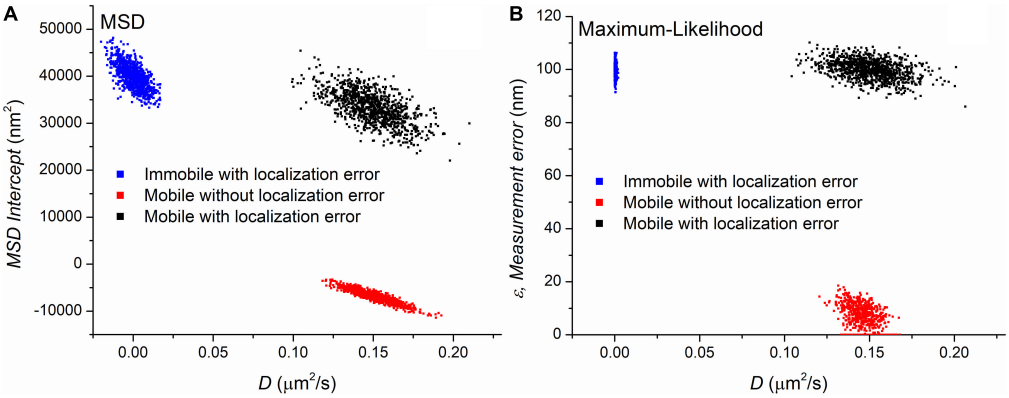

FIGURE 1
The parameters extracted by mean square displacement (MSD) **(A)** and maximum likelihood-based estimation (MLE) **(B)** based parameter estimation on three set of simulated trajectories. Each point on the graphs represents a set of parameters calculated from a trajectory. The value of diffusion coefficients is shown on the *x*-axis of both graphs. The *y*-axis represents another parameters provided by the diffusion coefficient's estimation, namely they are the *y*-intercept of the linear fitting and the extracted localization error for the MSD and MLE graph, respectively. The number of trajectories is 1,000 in each group.

A Hamamatsu 9100-13 electron-multiplying charge-coupled device (EMCCD) camera and Olympus Excellence Pro imaging software were used for image acquisition by TIRF microscopy. Image series were captured with 10-s sampling intervals and 33-ms acquisition times. Single-molecule tracking of labeled particles was performed with custom-made software written in C++ (WinATR, Kusumi Lab, Membrane Cooperativity Unit, OIST). The center of each particle was localized by two-dimensional Gaussian fitting, and the trajectory for each signal was created by a minimum step size linking algorithm that connected the localized dots in subsequent images. The trajectories were individually checked, and artifacts or tracks shorter than 15 frames were excluded from further analysis.

Immobilized particles

To measure immobilized particles, we dried a droplet of ATTO 488-labeled antibodies directed against the extracellular N-terminal domain of rat GluR2 (1:1,000 in PBS, Alomone Labs) onto a glass bottomed dish. The dried dyes were covered with Prolong Gold Antifade Mountant (P10144, Thermo Fisher, Waltham, MA, USA). After 24 h, image series of immobilized ATTO-488 dyes were collected and analyzed as described above.

AMPARs in live dPC12 cells

To detect GluR2-AMPAR molecules in the plasma membranes of differentiated PC12 (dPC12) (Godó et al., 2021), live-cell immunofluorescent labeling was performed. Before single-molecule imaging, dPC12 were incubated with ATTO 488-labeled antibodies directed against the extracellular N-terminal domain of rat GluR2 (1:100, Alomone Labs Cat #: AGC-005-AG) in dRPMI cell culture medium at 37°C for 6 min. During the measurement period of ATTO 488-GluR2-AMPAR, 20–30 image series were recorded. 17β-estradiol was applied immediately before imaging the dPC12 in dRPMI in 100 pM and 100 nM concentration dissolved in vehicle (EtOH).

Calculation of diffusion coefficients

Mean square displacement curve (MSD) for each trajectory was calculated by the following equation (Matysik and Kraut, 2014; Yu, 2016):

$$\mathrm{MSD}\left(m\Delta T\right) = \frac{1}{N-m}\sum_{i=1}^{N-m}\left(\left(x_{i+m}-x_i\right)^2+\left(y_{i+m}-y_i\right)^2\right)$$

where x_i and y_i are the observed coordinates of tracked particle, ΔT: time interval between two consecutive frames, N: total number of frames, and m as an independent variable represents the time delay (in frames) applied for the particular point of the MSD curve. The calculation of diffusion coefficients was implemented by three points linear fitting on the MSD curve. The parameters extracted from the MSD fitting are also provided by the Matlab script available in the **Supplementary material**.

In order to obtain the corresponding D value by MLE, the MLE was applied as previously described (Berglund, 2010). Δx_k and Δy_k represent the observed displacements ($\Delta x_k = x_{k+1} - x_k$ and $\Delta y_k = y_{k+1} - y_k$) arranged in N-component column vectors, where the total number of frames is equal to N+1. x_n and y_n are the coordinates of the signal's center on the nth frame, as usual. The $N \times N$ covariance matrix (Σ) is defined by the following equation:

$$\Sigma_{ij} = \begin{cases} 2D\Delta t - 2\left(2DR\Delta t - \sigma^2\right), & \text{if i} = \text{j} \\ 2DR\Delta t - \sigma^2, & \text{if i} = \text{j} \pm 1 \\ 0, & \text{otherwise} \end{cases}$$

where D is the diffusion coefficient, Δt is frame integration time, σ is the static localization noise, i and j are the row and column indexes in the covariance matrix and R summarizes the motion blur effect.

$$R = \frac{1}{T}\int_0^T S\left(t\right)\left[1 - S\left(t\right)\right]dt \text{ where } S(t) = \int_0^t s\left(t'\right)dt'$$

where $s\left(t\right)$ is the shutter function, in our case, R = 1/6 as a consequence of continuous illumination.

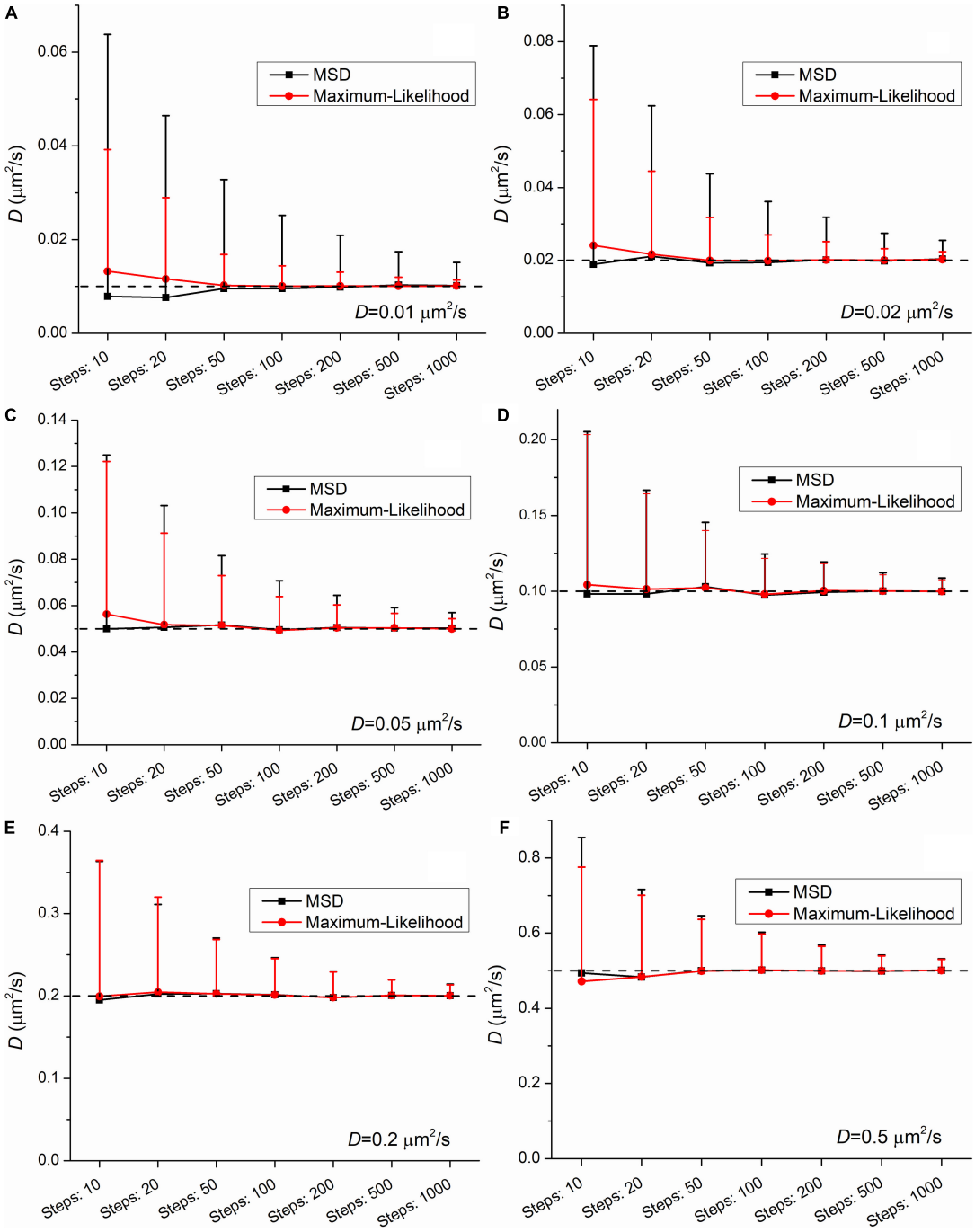

FIGURE 2
Mean and standard deviation (SD) values of diffusion coefficients extracted from a set of trajectories (N = 1,000) simulated with the following diffusion coefficients: **(A)** 0.01$\mu m^2/s$, **(B)** 0.02$\mu m^2/s$, **(C)** 0.05$\mu m^2/s$, **(D)** 0.1$\mu m^2/s$, **(E)** 0.2$\mu m^2/s$, **(F)** 0.5$\mu m^2/s$ as a function of the length of trajectories. The diffusion coefficients were extracted by both the mean square displacement (MSD) (black) and maximum likelihood-based estimation (MLE) (red) method.

The likelihood was defined by the following function:

$$L\left(\Delta x, \Delta y\right) = -log\left|\Sigma\right| - \frac{1}{2}(\Delta x)^T \Sigma^{-1}(\Delta x) - \frac{1}{2}(\Delta y)^T \Sigma^{-1}(\Delta y)$$

The D and σ which provides the maximal likelihood is the estimated diffusion coefficient and static localization noise, respectively. The calculation of the determinant and the inverse of covariance matrix at each step of the optimization method can be a severe computational difficulty at high value of N. An approximation (Gray, 2005) based on the theory of circulant matrices is applicable (Berglund, 2010). In the script we defined a constant for the limit to switch between the direct and the simplified calculation method. Based on our experience we set the value of this constant to 1,001. When the number of frames exceeds 1,000 this simplified likelihood function is used for the global optimization, otherwise the direct likelihood function was

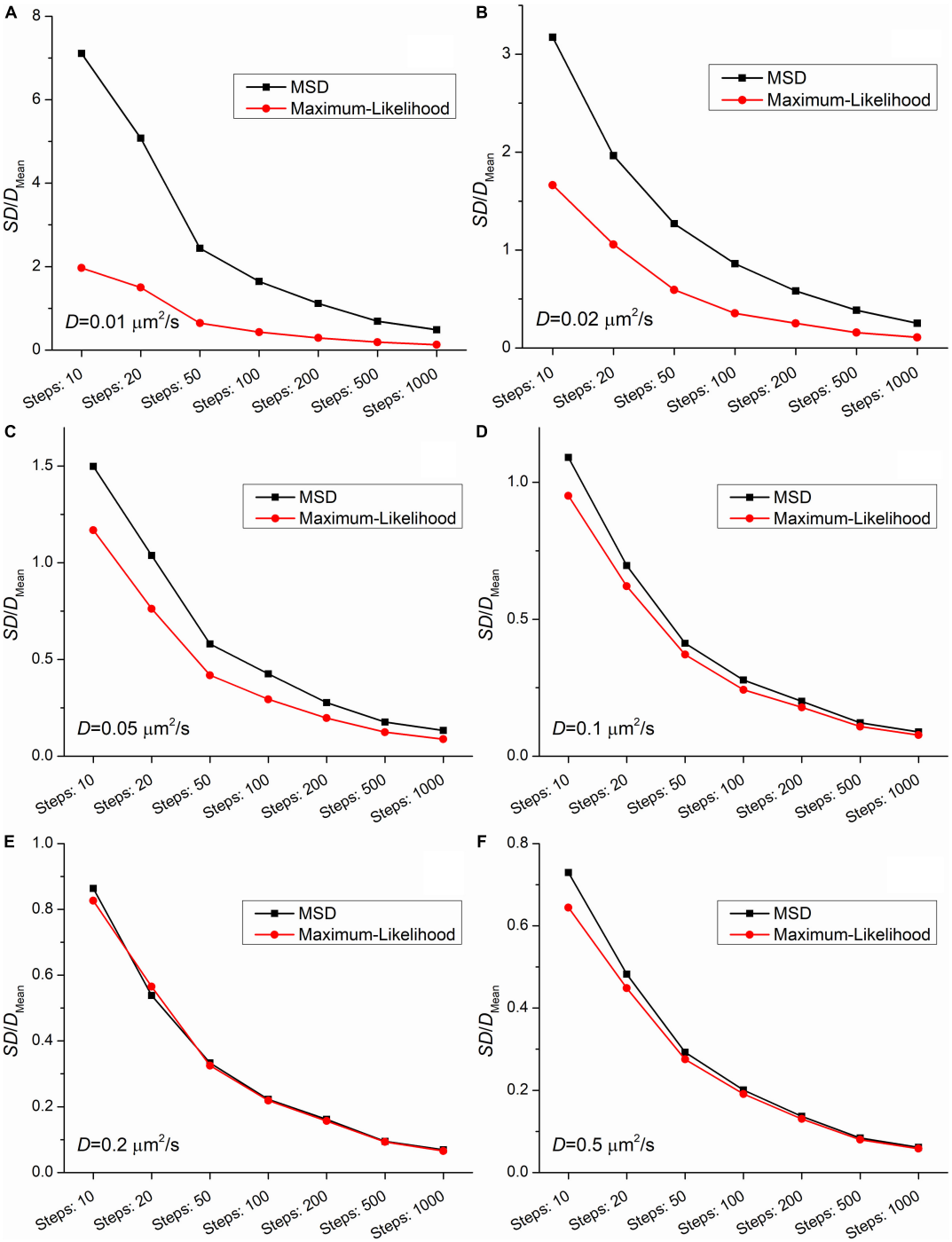

FIGURE 3
The coefficients of variation (the ratio of the SD and the mean from Figure 2) as a function of the length of trajectories. The diffusion coefficients for the simulation were: **(A)** 0.01$\mu m^2/s$, **(B)** 0.02$\mu m^2/s$, **(C)** 0.05$\mu m^2/s$, **(D)** 0.1$\mu m^2/s$, **(E)** 0.2$\mu m^2/s$, **(F)** 0.5$\mu m^2/s$.

applied. In this study the maximal length of trajectories was 1,000 frames, so the script applied the direct method for each trajectory. To estimate the area of molecule trajectories the convex hull for each trajectory was created by a Matlab script. Area of the molecule trajectory was defined as the area of this convex hull.

The Matlab script for the MLE based estimation of diffusion coefficient is available as a zip file available in the Supplementary material.

Results

Simulated trajectories

Three sets of trajectories were generated with MSD and MLE estimations assuming the presence of the blur effect due to continuous recording. Each set containing 1,000 trajectories with a length of 501 frames differed in the values of the

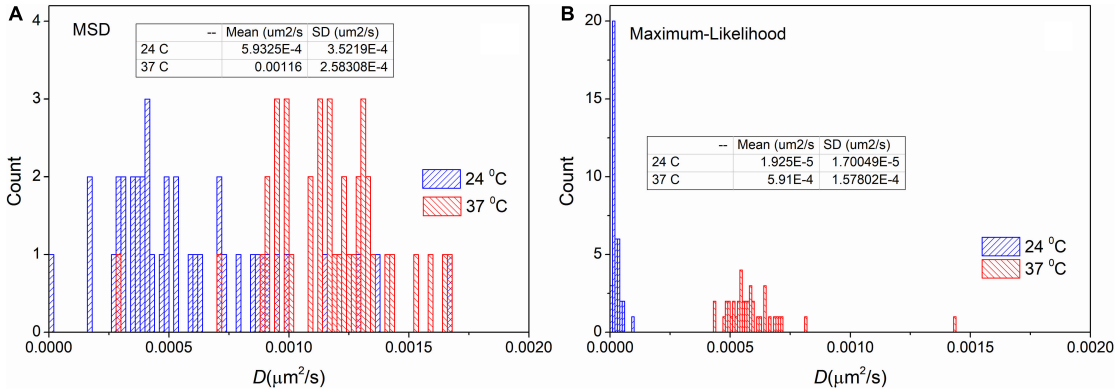

FIGURE 4
Distribution of diffusion coefficients derived from trajectories recorded on immobile particles. The measurement was carried out on different temperatures and the extracted trajectories were analyzed by the mean square displacement (MSD) **(A)** and the maximum likelihood-based estimation (MLE) **(B)** method. The inserted table shows the mean and SD values for each group, respectively.

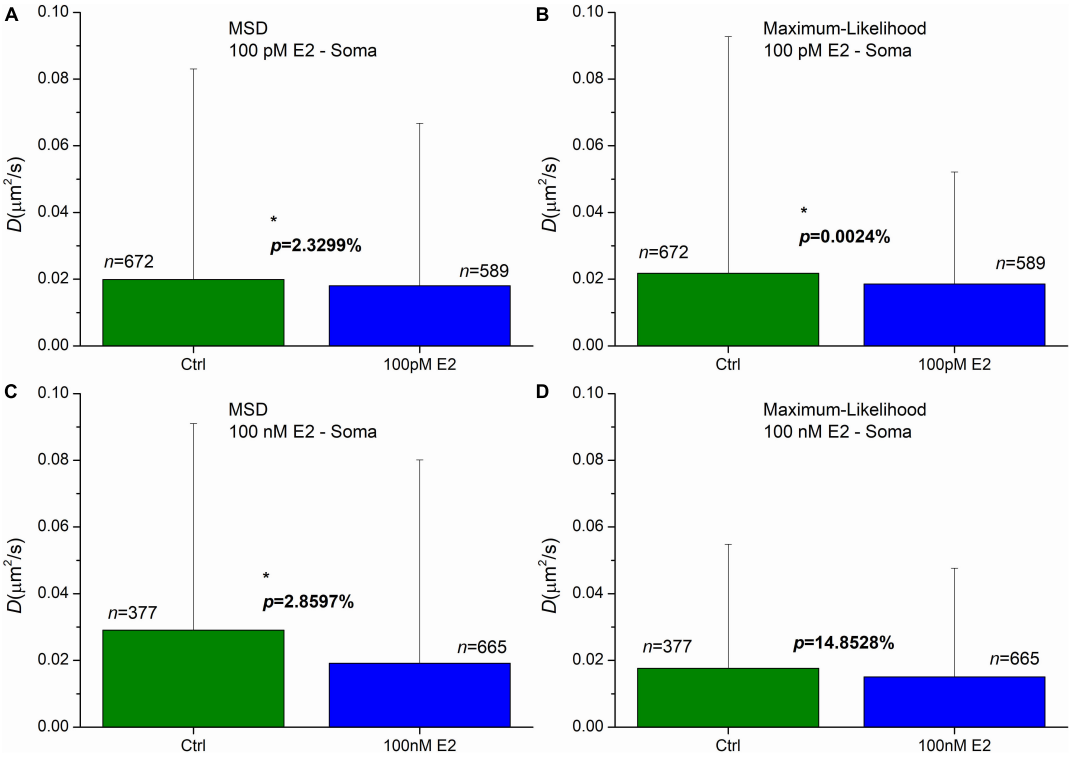

FIGURE 5
The effect of E2 treatment on the diffusion coefficient of GluR2-AMPAR molecules in the soma's plasma membranes of dPC12, live-cell. The E2 treatments were carried out by the concentration of 100 pM **(A,B)** and 100 nM **(C,D)**. Both the mean square displacement (MSD) **(A,C)** and the maximum likelihood-based estimation (MLE) **(B,D)** methods were used for further analysis to obtain the diffusion coefficients from the recorded trajectories. The graphs represent the groups as mean and SD values. The probability values of significant differences calculated by Kolmogorov–Smirnov test (*$p < 0.05$) and the number of trajectories in each group are also shown.

diffusion coefficient and the localization error. The first group contained immobile ($D = 0\mu m^2/s$) trajectories in the presence of $\varepsilon = 100\ nm$ localization uncertainty. The second set contained mobile ($D = 0.15\mu m^2/s$) trajectories without any localization error ($\varepsilon = 0\ nm$). The last group simulated trajectories recorded on moving particles ($D = 0.15\mu m^2/s$) with $\varepsilon = 100\ nm$ measurement error. Figure 1 shows the parameters provided by the MSD and MLE.

Figure 1 demonstrates that both methods clearly separate the distinct sets of trajectories. The MLE reliably provides the expected parameters while diffusion coefficients provided by the MSD method are in good agreement with the theoretical values. A minor difference between the two methods is observed between the distribution of diffusion coefficients from the mobile trajectories with no localization error. The MLE estimates the diffusion coefficients with less standard deviation (SD). However,

this observation has no significance in the single molecule imaging because the lack of localization error is a purely theoretical category. The main difference between the two sets of data is the distribution of diffusion coefficients extracted from the immobile trajectories. While the MSD based diffusion coefficients show some variability around the group's average of 0 $\mu m^2/s$, the distribution of the same parameter in the same group provided by the MLE is much narrower. Since this scenario can easily happen if we observe slow particles, this finding has a great importance, and we went further to investigate it in detail.

To investigate this phenomenon, another set of trajectories were created and analyzed. While the localization error was constant ($\varepsilon = 100\ nm$), both the length of trajectories and the diffusion coefficients were altered. The length was altered from 11 to 1,001 frames. The diffusion coefficients had the following values: $0.01\mu m^2/s$, $0.02\mu m^2/s$, $0.05\mu m^2/s$, $0.1\mu m^2/s$, $0.2\mu m^2/s$, and $0.5\mu m^2/s$. The number of randomly created trajectories in each group was 1,000. The set of raw simulated data is available in the Supplementary material.

The group means provide satisfactory estimation of the diffusion coefficient when the number of steps (i.e., the number of frames minus one) is equal or above 20. At the shortest trajectories (length is equal to 10 steps) some uncertainty is present independently of the applied method. In this case the mean values slightly differ from the expected ones. This finding confirms the legitimacy of the general practice that in studies with single-molecule tracking the trajectories below the length of 15 steps are omitted from further analysis.

Figures 2, 3 demonstrate that the SD and coefficient of variation (CoV) of diffusion coefficients derived by MSD are larger than the corresponding values extracted by MLE. In the two slowest group of trajectories ($D = 0.01\mu m^2/s$ and $D = 0.02\mu m^2/s$) both the CoV and SD parameters provided by the two analyses differ to a large extent and this difference is independent of the trajectory length. The values of CoV of the MSD based diffusion coefficients for the slowest trajectories ($D = 0.01\mu m^2/s$) are approximately three times higher than the corresponding values extracted by the MLE. In the case of the slightly faster group ($D = 0.02\mu m^2/s$) the application of the MSD method provides two times higher CoV values for the diffusion coefficients than the MLE based analysis. In the group simulated with $D = 0.05\mu m^2/s$ the MSD provided values of CoV for the diffusion coefficients exceed the same values from MLE based calculation by 30%. This difference between the values of SD and CoV diminish slowly with the increasing diffusion coefficient. The values of SD and CoV are crucial in several types of statistical test, and a broader distribution can easily disguise a slight but a real difference between the investigated groups. While the provided mean values calculated by the MLE as well as the MSD method are in good agreement with the expected values, the distribution of the group's diffusions coefficients are narrower in each set of trajectories proving a better performance of MLE based calculation on simulated data.

Measured immobile particles

To test the usability of MLE on measured trajectories we carried out an analysis on trajectories recorded on immobile particles at different temperatures. However, the investigated particles are named "immobile" some movement is always present. For these particles diffusion coefficients are approximately two orders of magnitude smaller than receptor's diffusion coefficients. We expected more intense movement at elevated temperature. The trajectories are available in the Supplementary material.

Figure 4 shows the distribution of diffusion coefficients measured at different temperatures on immobile samples. These distributions confirm the result derived from the simulated data. There is a shift in the mean values $5.9{\cdot}10^{-4}\mu m^2/s$ and $3.0{\cdot}10^{-5}\mu m^2/s$ for the trajectories measured at 24°C. As it was expected the mean values are higher ($1.2{\cdot}10^{-3}\mu m^2/s$ and $6.1{\cdot}10^{-4}\mu m^2/s$) at 37°C. More importantly, the values of SD are significantly decreased by applying the MLE. While provided values of SD by the MSD method are $3.5{\cdot}10^{-4}\mu m^2/s$ and $2.6{\cdot}10^{-4}\mu m^2/s$, the distributions from MLE based analysis are significantly narrower (the corresponding SD values are: $2.7{\cdot}10^{-5}\mu m^2/s$ and $1.7{\cdot}10^{-4}\mu m^2/s$). These findings match the results of our previous *in silico* experiments.

Trajectories measured on live dPC12 cells

Analysis performed on simulated data and immobile particles showed that the MLE had remarkable performance which occasionally exceeded the abilities of MSD based method. To compare the two approaches also in live-cell experiments, we tested their usability and reliability in an experimental model that has been routinely used in our laboratory. Therefore, comprehensive analysis was carried out on AMPA receptor (GluR2-AMPAR) trajectories measured in live dPC12 cells after E2 or vehicle treatment.

Administration of 100 pM E2 induced a significant decrease of diffusion coefficients in AMPAR in soma in the first 20 min after the treatment. The means were decreased to 0.018 $\mu m^2/s$ and 0.019 $\mu m^2/s$, while the control's mean values were 0.020 $\mu m^2/s$ and 0.022 $\mu m^2/s$ for the MSD and MLE, respectively (Figures 5A, B). The probability of significance was $p = 2.33\%$ and less than 0.01% for the MSD and MLE method, respectively. The application of 100 nM E2 highlighted the difference between the two calculation methods. While analysis conducted by the MLE (Figure 5D) showed no effect ($p = 14.85\%$) after E2 administration, the MSD method provided a significant decrease of the diffusion coefficients (Figure 5C). In this case the mean of diffusion coefficients was 0.019 $\mu m^2/s$, which was significantly lower (probability of significance is $p = 2.86\%$) than the same value in the control group 0.029 $\mu m^2/s$.

The result of MLE can be surprising as the lower E2 concentration (100 pM) evoked a significant decrease of the diffusion coefficients, while the administration of the higher dose of E2 (100 nM) did not induce any change. This effect was previously investigated (Godó et al., 2021) and it was revealed that the difference may be the consequence of GPER1 internalization in the soma induced by 100 nM E2. It was also demonstrated that both ERβ and GPER1 are required for the effect of E2. The higher dose of E2 induced elimination of GPER1 preventing E2 to cause decrease of the diffusion coefficient.

In soma, the 100 nM E2 treatment has distinct effect, based on the two calculation methods. On one hand, the MLE does not reveal

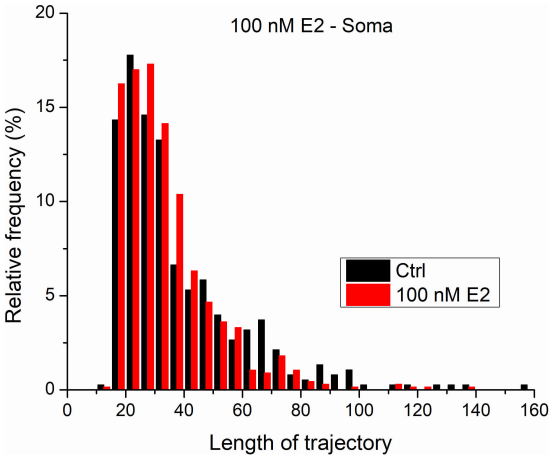

FIGURE 6
The trajectories length distribution from GluR2-AMPAR molecules in the soma's plasma membranes of dPC12, live-cell in control state and after administration of 100 nM E2.

any significant effect due to E2 treatment, on the other hand the application of E2 significantly decreases the diffusion coefficients based on statistics on the MSD results. Previous study (Godó et al., 2021) has shown that GPER1 internalization depletes the GPER1 which is crucial for the effectiveness of E2 in soma, indicating the propriety of MLE based result.

Figure 6 shows the distribution length distribution of trajectories measured on GluR2-AMPAR molecules in the somatic plasma membrane of living dPC12 cells both in control state and after the administration of 100 nM E2. The vast majority of trajectories are shorter than 50 steps. Our previous results on simulated trajectories proved that MLE provides more reliable result on trajectories characterized with similar parameters ($D = 0.02\mu m^2/s$ and the length are less or equal to 100 steps). Based on this we think that in this case we can acknowledge the MLE provided results and statistical statement.

Discussion

The focus of the current study was to examine in depth the differences between MLE and MSD-based methods. First, we used simulated trajectories, which are suitable to detect localization errors. Our results show that while the obtained group averages of the diffusion coefficients perfectly corresponded to the expected values regardless of the computational methods, the SD values of the diffusion coefficients were significantly lower for the $D = 0\mu m^2/s$ (immobile trajectories with localization error) group using the MLE method. This difference between the distribution of the diffusion coefficient values is the consequence of the fundamental difference between the two methods. On one hand the MSD based calculation does not constrain the sign of the diffusion coefficient, therefore the D values, especially for slow or immobile trajectories, often have a negative sign, which is difficult to interpret. On the other hand, the MLE method does not provide sub-zero diffusion coefficients, so the distribution of D values is much narrower.

Secondly, the reliability of the methods was investigated, also using simulated trajectories to compare mean and SD values for low diffusion coefficients. The length of the trajectories and expected diffusion coefficients characterized the randomly generated trajectories in these groups. The analysis of the set of simulated trajectories showed no difference between the two methods in terms of mean values. Both analyses provided good estimates of the expected values. These results were consistent with our previous finding, namely that the MLE method gave more accurate estimation of diffusion coefficients. The SD value of diffusion coefficients from MSD method exceeded the SD provided by MLE based calculation when the value of D was less than $0.2\mu m^2/s$. In addition, both mean and SD values were identical when the diffusion coefficient was greater or equal to $0.2\mu m^2/s$. The analysis following numerical simulation showed that the MLE outperforms the MSD as a data analysis tool.

Regarding measured immobile trajectories at different temperatures, the two methods provided similar values for the average of the diffusion coefficient in any analyzed groups. According to the expectations, the higher temperature evoked a more intense movement, which was reflected in increased diffusion coefficients. The experiment clearly confirmed that the distribution of diffusion coefficients provided by the MLE is much narrower than the distribution calculated by the MSD approach. The reason for this difference is the following: in contrast to MLE method MSD is less effective in separating the static localization noise from the diffusion generated displacement, which causes increased uncertainty in the calculated diffusion coefficients. This phenomenon is pronounced when the localization error exceeds the expected displacement by diffusion (i.e., in the case of so-called immobile particles).

Finally, the two methods were tested on trajectories collected from live dPC12 cells. The effect of E2 on the movement of GluR2-AMPAR molecules was investigated in somata of dPC12 cells. On the one hand, the 100 pM E2 treatment significantly decreased the mean value of diffusion coefficients by applying either the MSD or the MLE method. On the other hand, the two calculation methods resulted in conflicting results when comparing the effect of 100 nM E2 in the soma. The MSD method showed a significant alteration in the diffusion coefficients of GluR2-AMPAR molecules, while the MLE demonstrated no effect. The result of MLE is consistent with the previously reported ineffectiveness of 100 nM E2 in the soma, due to GPER1 internalization. The investigation of length distribution of the trajectories and the results gained from simulated trajectories reveals that for this set of trajectories the MLE provides more reliable diffusion coefficients. So, the statistical result extracted from MLE based calculation seems to be more reliable and accurate in this particular case.

Conclusion

The performed analysis conducted on simulated trajectories revealed that the provided mean values of diffusion coefficients are in good agreement with the theoretical values, regardless of the applied method. The superiority of MLE based calculation over MSD was shown by examination of the coefficients of variation (ratio of SD and the mean) for the distribution of the estimated

diffusion coefficients. The CoV is remarkably lower by using MLE based method instead of the application of MSD based in the case of slow particle movement.

The results of simulation were confirmed by the results extracted from immobile trajectories measured at different temperatures. The distribution of diffusion coefficients is undoubtedly narrower in the case of MLE making the interpretation of obtained results easier.

Moreover, our findings were tested on AMPA receptor trajectories measured in live dPC12 cells after estradiol-treatment. The two calculation methods provided conflicting results when comparing the effect of 100 nM E2 in the soma.

On the one hand, MSD is less reliable for short trajectories or trajectories characterized with small diffusion coefficients. Moreover, MSD does not effectively separate the localization error from diffusion. On the other hand, MLE is applicable on short and slow trajectories, and it does separate the localization error from the movement. The superiority of the MLE method was demonstrated on simulated as well as on measured trajectories in live cells.

These results indicate that MLE method is one of the first recommended approach to analyze data obtained in single-molecule imaging measurements.

Data availability statement

The original contributions presented in this study are included in the article/**Supplementary material**, further inquiries can be directed to the corresponding author.

Author contributions

IA, KB, and TJ contributed to conception and design of the study. DE, TK, and SG were involved in sample preparation for the TIRF measurements. SG performed the TIRF measurements. KB, SG, and GK extracted trajectories from measured videos. TJ created the Matlab script for analyzing trajectories. SS and GM checked and optimized the script. GM and TJ performed the statistical analysis and wrote the first draft of the manuscript. KB, DE, TK, GK, and SG wrote sections of the manuscript. All authors contributed to manuscript revision, read, and approved the submitted version.

Funding

TKP2021-EGA-16 has been implemented with the support provided from the National Research, Development and Innovation Fund of Hungary, financed under the TKP2021-EGA funding scheme. DE was supported by the únkp-21-4-II new national excellence program of the ministry for innovation and technology from the source of the National Research, Development and Innovation Fund. SS acknowledges the support of National Research, Development and Innovation Fund of Hungary (TKP-2021-EGA-16).

Acknowledgments

The research was performed in collaboration with the Nano-Bio-Imaging Core Facility at the Szentágothai Research Centre of the University of Pécs. We thank Prof. Akihiro Kusumi and Prof. Takahiro Fujiwara for providing the WinATR software.

Conflict of interest

The authors declare that the research was conducted in the absence of any commercial or financial relationships that could be construed as a potential conflict of interest.

Publisher's note

Supplementary material

The Supplementary Material for this article can be found online at: https://www.frontiersin.org/articles/10.3389/fninf.2023.1005936/full#supplementary-material

References

Babayan, A. H., and Kramar, E. A. (2013). Rapid effects of oestrogen on synaptic plasticity: Interactions with actin and its signaling proteins. *J. Neuroendocrinol.* 25, 1163–1172. doi: 10.1111/jne.12108

Barabas, K., Kobolak, J., Godo, S., Kovacs, T., Ernszt, D., Kecskes, M., et al. (2021). Live-cell imaging of single neurotrophin receptor molecules on human neurons in Alzheimer's disease. *Int. J. Mol. Sci.* 22, 1–15. doi: 10.3390/ijms222413260

Berglund, A. J. (2010). Statistics of camera-based single-particle tracking. *Phys. Rev. E Stat. Nonlin. Soft Matter Phys.* 82:011917. doi: 10.1103/PhysRevE.82.011917

Bullerjahn, J. T., and Hummer, G. (2021). Maximum likelihood estimates of diffusion coefficients from single-particle tracking experiments. *J. Chem. Phys.* 154:234105. doi: 10.1063/5.0038174

De Keijzer, S., Galloway, J., Harms, G. S., Devreotes, P. N., and Iglesias, P. A. (2011). Disrupting microtubule network immobilizes amoeboid chemotactic receptor in the plasma membrane. *Biochim. Biophys. Acta Biomembr.* 1808, 1701–1708. doi: 10.1016/j.bbamem.2011.02.009

Godó, S., Barabás, K., Lengyel, F., Ernszt, D., Kovács, T., Kecskés, M., et al. (2021). Single-molecule imaging reveals rapid estradiol action on the surface movement of AMPA receptors in live neurons. *Front. Cell Dev. Biol.* 9:708715. doi: 10.3389/fcell.2021.708715

Gray, R. M. (2005). *Toeplitz and Circulant Matrices: A Review*. Norwell, MA: Now publishers.

Grebenkov, D. S. (2011). Probability distribution of the time-averaged mean-square displacement of a Gaussian process. *Phys. Rev. E Stat. Nonlin. Soft Matter Phys.* 84, 1–14. doi: 10.1103/PhysRevE.84.031124

Knight, J. D., and Falke, J. J. (2009). Single-molecule fluorescence studies of a PH domain: New insights into the membrane docking reaction. *Biophys. J.* 96, 566–582. doi: 10.1016/j.bpj.2008.10.020

Knight, J. D., Lerner, M. G., Marcano-Velázquez, J. G., Pastor, R. W., and Falke, J. J. (2010). Single molecule diffusion of membrane-bound proteins: Window into lipid contacts and bilayer dynamics. *Biophys. J.* 99, 2879–2887. doi: 10.1016/j.bpj.2010.08.046

Kramár, E. A., Chen, L. Y., Rex, C. S., Gall, C. M., and Lynch, G. (2009). Estrogen's place in the family of synaptic modulators. *Mol. Cell Pharmacol.* 1, 258–262. doi: 10.4255/mcpharmacol.09.31

Kusumi, A., Tsunoyama, T. A., Hirosawa, K. M., Kasai, R. S., and Fujiwara, T. K. (2014). Tracking single molecules at work in living cells. *Nat. Chem. Biol.* 10, 524–532. doi: 10.1038/nchembio.1558

Ledoux, V. A., Smejkalova, T., May, R. M., Cooke, B. M., and Woolley, C. S. (2009). Estradiol facilitates the release of neuropeptide y to suppress hippocampus-dependent seizures. *J. Neurosci.* 29, 1457–1468. doi: 10.1523/JNEUROSCI.4688-08.2009

Lu, Y., Sareddy, G. R., Wang, J., Wang, R., Li, Y., Dong, Y., et al. (2019). Neuron-derived estrogen regulates synaptic plasticity and memory. *J. Neurosci.* 39, 2792–2809. doi: 10.1523/JNEUROSCI.1970-18.2019

Martin, D. S., Forstner, M. B., and Kas, J. A. (2002). Apparent subdiffusion inherent to single particle tracking. *Biophys. J.* 83, 2109–2117. doi: 10.1016/S0006-3495(02)73971-4

Matsuoka, S., Shibata, T., and Ueda, M. (2009). Statistical analysis of lateral diffusion and multistate kinetics in single-molecule imaging. *Biophys. J.* 97, 1115–1124. doi: 10.1016/j.bpj.2009.06.007

Matysik, A., and Kraut, R. S. (2014). TrackArt: The user friendly interface for single molecule tracking data analysis and simulation applied to complex diffusion in mica supported lipid bilayers. *BMC Res. Notes* 7:274. doi: 10.1186/1756-0500-7-274

Michalet, X. (2010). Mean square displacement analysis of single-particle trajectories with localization error: Brownian motion in an isotropic medium. *Phys. Rev. E Stat. Nonlin. Soft Matter Phys.* 82(Pt 1):041914. doi: 10.1103/PhysRevE.82.041914

Michalet, X., and Berglund, A. J. (2012). Optimal diffusion coefficient estimation in single-particle tracking. *Phys. Rev. E Stat. Nonlin. Soft Matter Phys.* 85(Pt 1):061916. doi: 10.1103/PhysRevE.85.061916

Murakami, G., Hojo, Y., Kato, A., Komatsuzaki, Y., Horie, S., Soma, M., et al. (2018). Rapid nongenomic modulation by neurosteroids of dendritic spines in the hippocampus: Androgen, oestrogen and corticosteroid. *J. Neuroendocrinol.* 30:e12561. doi: 10.1111/jne.12561

Penn, A. C., Zhang, C. L., Georges, F., Royer, L., Breillat, C., Hosy, E., et al. (2017). Hippocampal LTP and contextual learning require surface diffusion of AMPA receptors. *Nature* 549, 384–388. doi: 10.1038/nature23658

Phan, A., Suschkov, S., Molinaro, L., Reynolds, K., Lymer, J. M., Bailey, C. D. C., et al. (2015). Rapid increases in immature synapses parallel estrogen-induced hippocampal learning enhancements. *Proc. Natl. Acad. Sci. U.S.A.* 112, 16018–16023. doi: 10.1073/pnas.1522150112

Pinaud, F., and Dahan, M. (2011). Targeting and imaging single biomolecules in living cells by complementation-activated light microscopy with split-fluorescent proteins. *Proc. Natl. Acad. Sci. U.S.A.* 108, E201–E210. doi: 10.1073/pnas.1101929108

Qian, H., and Sheetz, M. P. (1991). Single particle tracking. Analysis of diffusion and flow in two-dimensional systems. *Biophys. J.* 60, 910–921. doi: 10.1016/S0006-3495(91)82125-7

Rudolph, L. M., Cornil, C. A., Mittelman-Smith, M. A., Rainville, J. R., Remage-Healey, L., Sinchak, K., et al. (2016). Actions of steroids: New neurotransmitters. *J. Neurosci.* 36, 11449–11458. doi: 10.1523/JNEUROSCI.2473-16.2016

Sahl, S. J., Leutenegger, M., Hilbert, M., Hell, S. W., and Eggeling, C. (2010). Fast molecular tracking maps nanoscale dynamics of plasma membrane lipids. *Proc. Natl. Acad. Sci. U.S.A.* 107, 6829–6834. doi: 10.1073/pnas.0912894107

Savin, T., and Doyle, P. S. (2005). Static and dynamic errors in particle tracking microrheology. *Biophys. J.* 88, 623–638. doi: 10.1529/biophysj.104.042457

Saxton, M. J. (1997). Single-particle tracking: The distribution of diffusion coefficients. *Biophys. J.* 72, 1744–1753. doi: 10.1016/S0006-3495(97)78820-9

Schütz, G. J., Schindler, H., and Schmidt, T. (1997). Single-molecule microscopy on model membranes reveals anomalous diffusion. *Biophys. J.* 73, 1073–1080. doi: 10.1016/S0006-3495(97)78139-6

Shuang, B., Byers, C. P., Kisley, L., Wang, L. Y., Zhao, J., Morimura, H., et al. (2013). Improved analysis for determining diffusion coefficients from short, single-molecule trajectories with photoblinking. *Langmuir* 29, 228–234. doi: 10.1021/la304063j

Taxier, L. R., Gross, K. S., and Frick, K. M. (2020). Oestradiol as a neuromodulator of learning and memory. *Nat. Rev. Neurosci.* 21, 535–550. doi: 10.1038/s41583-020-0362-7

Teyler, T. J., Vardaris, R. M., Lewis, D., and Rawitch, A. B. (1980). Gonadal steroids: Effects on excitability of hippocampal pyramidal cells. *Science (80)* 209, 1017–1018. doi: 10.1126/science.7190730

Vierk, R., Brandt, N., and Rune, G. M. (2014). Hippocampal estradiol synthesis and its significance for hippocampal synaptic stability in male and female animals. *Neuroscience* 274, 24–32. doi: 10.1016/j.neuroscience.2014.05.003

Weigel, A. V., Simon, B., Tamkun, M. M., and Krapf, D. (2011). Ergodic and nonergodic processes coexist in the plasma membrane as observed by single-molecule tracking. *Proc. Natl. Acad. Sci. U.S.A.* 108, 6438–6443. doi: 10.1073/pnas.1016325108

Wong, M., and Moss, R. L. (1992). Long-term and short-term electrophysiological effects of estrogen on the synaptic properties of hippocampal CA1 neurons. *J. Neurosci.* 12, 3217–3225. doi: 10.1523/jneurosci.12-08-03217.1992

Yu, J. (2016). Single-molecule studies in live cells. *Annu. Rev. Phys. Chem.* 67, 565–585. doi: 10.1146/annurev-physchem-040215-112451

Zacks, S. (1971). *Theory of Statistical Inference*. New York, NY: John Wiley & Sons Inc.

frontiers | Frontiers in Endocrinology

TYPE Opinion
PUBLISHED 14 June 2023
DOI 10.3389/fendo.2023.1144417

OPEN ACCESS

EDITED BY
Erik Hrabovszky,
Institute of Experimental Medicine (MTA), Hungary

REVIEWED BY
Imre Kalló,
Institute of Experimental Medicine (MTA), Hungary
Zsolt Liposits,
Institute of Experimental Medicine (MTA), Hungary

*CORRESPONDENCE
Zsuzsanna Nagy
zsuzsanna.nagy69@gmail.com
Klaudia Barabas
klaudia.barabas@aok.pte.hu
Gergely Kovacs
gergely.kovacs@aok.pte.hu

†These authors have contributed equally to this work and share first authorship

RECEIVED 14 January 2023
ACCEPTED 26 May 2023
PUBLISHED 14 June 2023

CITATION
Nagy Z, Barabas K and Kovacs G (2023) Obituary: Prof. István M. Ábrahám. *Front. Endocrinol.* 14:1144417. doi: 10.3389/fendo.2023.1144417

Obituary: Prof. István M. Ábrahám

Zsuzsanna Nagy*†, Klaudia Barabas*† and Gergely Kovacs*†

Institute of Physiology, Medical School, University of Pécs, Pécs, Hungary

KEYWORDS

estrogen, neurodegenaration, fertility, classical way, non-classical way

The authors dedicate this special issue in Frontiers in Endocrinology to Prof. István Ábrahám, on the occasion of his passing away in April 2021.

Prof. Dr. István Miklós Ábrahám

(1967-2021)

István Ábrahám graduated *summa cum laude* from the University Medical School Pécs, in 1993. As a student, he began research at the Institute of Physiology, Neurophysiology Research Group of the Hungarian Academy of Sciences, under the guidance of Professor László Lénárd. During his undergraduate years, Professor Ábrahám achieved outstanding results for which he was awarded the Fellowship of the Republic in sequentially three times. Additionally, he was awarded a Demonstrator Fellowship in the Department of Physiology, and in 1993, he was awarded the prestigious Pro Scientia Gold Medal.

Uniquely, in 1993, he presented two lectures at the National Conference of the Undergraduate Research Society, for which he received one First and one Second Prize.

Following graduation, he continued his PhD studies at the Institute of Experimental Medicine in Budapest, under the supervision of Dr. Krisztina Kovács. During this time, he broadened his professional knowledge in the research group of world-renowned neuroendocrinologist Béla Bohus, at the University of Groningen in the Netherlands. He defended his PhD thesis *summa cum laude* at the School of PhD Studies, Semmelweis University of Medicine in Budapest in 1998.

After earning his PhD, he spent two more years at the Molecular Neuroendocrinology Research Group of the Institute of Experimental Medicine, where his research focused on stress-related neuronal networks.

Between 2000 and 2002, he was a Marie Curie Fellow in Prof. Allan Herbison's laboratory at the Babraham Institute in Cambridge, England, where he developed a lifelong professional relationship with Professors Allan Herbison and Seong Kyu Han. He studied the concentration dependent action of glucocorticoids on neuronal cell viability and cell survival in the brain. His interest then shifted towards studying the non-genomic effects of estrogen in the brain.

Following his return home, he became one of the leading researchers in the Neurobiology Research Group of the Hungarian Academy of Sciences at the Eötvös Loránd University (Budapest) for a 4-year period, in which he continued studying the effects of estrogen in the brain. During this time, two PhD students obtained their doctoral degrees under his professional supervision.

In 2007, he was offered the opportunity to set up and manage his own research group at the University of Otago in New Zealand, where he achieved considerable professional success. During the six years he spent in New Zealand, two other students completed their PhD studies under his guidance. While in Otago, he developed a close collaboration with Professor Akihiro Kusumi in the field of single molecule detection. It was this collaboration which gradually shifted his interest towards super-resolution microscopy.

Despite his success abroad, his heart always remained in Hungary, where he envisioned a future for his children and his family. Eventually, he returned to his Alma Mater in 2011, where he started to work in part time.

With the support of the Albert Szent-Györgyi Scholarship, among others, Professor Ábrahám began implementing his innovative ideas in 2013. Following his appointment as Professor at the Department of Phyiology, he founded the Molecular Neuroendocrinology Research Group, which has consistently undergone expansion, and evolved into a professionally diverse and exceptionally cohesive group in the following years. In 2013, an academic research doctorate was also awarded to him.

He was instrumental in founding and chairing the first Centre for Neuroscience in the country, at the University of Pécs. Professor Ábrahám served on several editorial boards of international scientific journals and scientific societies. In early 2021, he was elected President of the Hungarian Neuroscience Society.

Following his appointment as Director of the Institute of Physiology in 2019, István immersed himself into the task of reforming the institute with his characteristic drive and determination. Additionally, he exerted immense energy in seeing one of his greatest dreams take flight, which was the creation of a facility accommodating a wide range of super-resolution and advanced fluorescence microscopes. In Spring 2021, the equipment was about to be set up at its new premises, designed by Professor Árbahám; but tragically, he never saw this completed. The centre was launched at its final location and named István Ábrahám Nano-Bio-Imaging Core Facility in December 2021.

István had an excellent scientific carrier with many fruitful professional collaborations. Besides being an outstanding scientist, he was an excellent leader, a great teacher, and a very good friend. We all miss him.

Author contributions

All authors listed have made a substantial, direct, and intellectual contribution to the work and approved it for publication.

Funding

Obituary articles are fully waived

Conflict of interest

The authors declare that the research was conducted in the absence of any commercial or financial relationships that could be construed as a potential conflict of interest.

Publisher's note

Frontiers in Endocrinology

Explores the endocrine system to find new therapies for key health issues

The second most-cited endocrinology and metabolism journal, which advances our understanding of the endocrine system. It uncovers new therapies for prevalent health issues such as obesity, diabetes, reproduction, and aging.

Discover the latest Research Topics

See more →

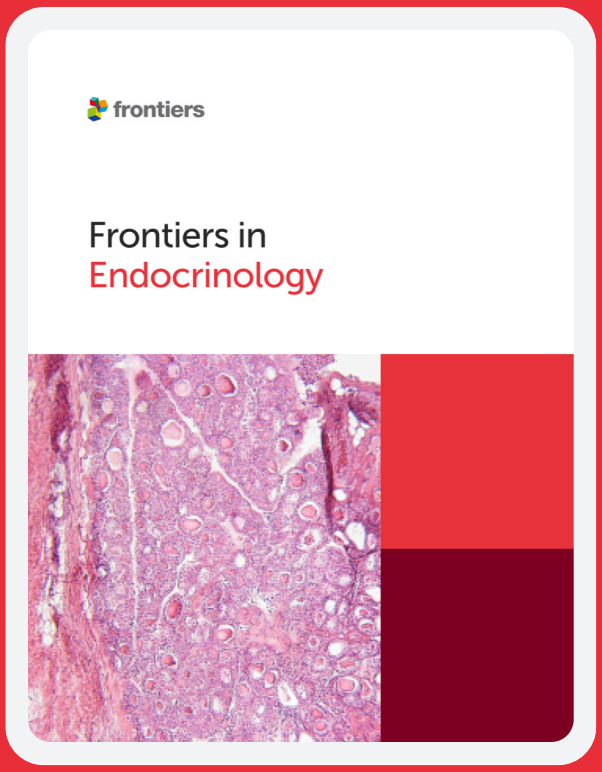

Frontiers

Avenue du Tribunal-Fédéral 34
1005 Lausanne, Switzerland
frontiersin.org

Contact us

+41 (0)21 510 17 00
frontiersin.org/about/contact